

**STRUCTURAL AND FUNCTIONAL REGULATIONS
BY MODULES IN GLOBIN PROTEINS**

Kenji Inaba

*Department of Molecular Engineering,
Graduate School of Engineering,
Kyoto University*

1998

PREFACE

Recent investigations of eukaryotic genes have demonstrated that many have mosaic structures, in which expressed sequences (exon) of DNA are separated from intervening non-coding sequences (intron). The existence of the exons and introns suggests that proteins could have been produced by bringing together structural segments encoded by exons with recourse to a joint of intron. That is, the mosaic structure in the gene can be thought to be reflected in the protein structure. Using diagonal plots of all the distances between α -carbon atoms of proteins, Go has demonstrated that there are statistically correlations between protein structures and the exon patterns, and found that the protein "modules", constructing a compact structural unit, correspond to the exons. Based on such correspondence of the modules to the exons, it has been hypothesized that the modules may have behaved as structural/functional units to produce novel proteins by combining various modules through the mechanism of exon shuffling. Thus, it seems biologically significant to investigate structural and functional properties of the modules in many proteins, but very few experimental studies on the modules have been attempted so far.

This thesis contains the collected papers and discussions of the author's study at Department of Molecular Engineering, Graduate School of Engineering, Kyoto University during 1993-1998. The aim of this thesis is to elucidate the structural and functional roles of the modules in globin proteins and to provide insights into the module-based design of novel functional hemoproteins. This thesis is composed of five parts. Part I contains a survey of module structure in globin proteins and affords sufficient background and significance of these studies. Part II deals with the characterization of module substituted hemoglobin subunits. Particularly, the author focuses upon structural alterations induced by the module substitutions. In Part III, structural and functional effects by substitutions of "non-modules" in hemoglobin subunits and myoglobin are also examined and compared with those by the module substitutions. The author chooses the "pseudo-module" as the non-module, of which boundaries are located at the centers of the modules. In this part, it is proposed that each of the conventional modules in globins would be further divided into two sub-modules at its center. In Part IV, the author confirms structural and functional roles of the newly proposed sub-modules by preparing new chimeric globins, where the sub-modules are substituted in hemoglobin α -, β -subunits and myoglobin. Finally, summary and general aspects of the present work are discussed in Part V.

ACKNOWLEDGMENTS

It is author's pleasure to acknowledge profound indebtedness to Professor Isao Morishima for his continual guidance, criticism, and encouragement. The author also wishes to express sincere gratitude to Associate Professor Koichiro Ishimori, Dr. Satoshi Takahashi and Professor Yoshihito Watanabe for their guidance and fruitful discussions throughout the course of this study.

It should be emphasized that the studies in this thesis have required the cooperation with some investigators. Grateful acknowledgment is dedicated to Dr. Tsuyoshi Shirai (x-ray crystal structure analysis and computer modelling studies), Dr. Kiyohiro Imai (oxygen equilibrium curve measurements), Dr. Takashi Konno (x-ray small angle scattering measurements), Dr. Hirokazu Tamamura (circular dichroism measurements), Professor Teizo Kitagawa (resonance Raman measurements), Dr. Kei Yura and Professor Mitiko Go (information about the modular structure of globin proteins and exciting discussions).

This work would not have been achieved without help of colleagues in Molecular Design Group. In particular, grateful acknowledgment is made to Dr. Keisuke Wakasugi for his many advices on this work. Collaborations by Michihiro Izuta, Jin Nakatani, Masahiro Izuta, Syuji Akiyama and Shino Kondo are also greatly appreciated. The author is indebted to Drs. Shinji Ozawa, Shingo Nagano and Keisuke Wakasugi and Messrs. Masaaki Aoki, Kenji Machii, Eigo Sakamoto, Takeshi Uchida, Tatsuya Murakami, Motomasa Tanaka, Yoshio Goto, Taroh Ichikawa, Michihiro Izuta, Takai Hatsui, Shiro Yoshioka, Jin Nakatani, Masahiro Yamada, Yoichi Sugiyama, Hirotaka Kataoka, Atsushi Morimoto, Masaki Ihara, Mitsuru Murata, Syuzi Akiyama, Shino Kondo, Haruto Ishikawa, Yoshiaki Furukawa, Norihiro Maeda, Akihiro Tanioka, Jun Inoue, Satoshi Nakano, Manabu Teramoto and Yoko Imai. He is also grateful to Mr. Haruyuki Harada for assistance in the NMR measurements.

Finally, the author express his gratitude to his family for their unfailing understanding and affectionate encouragement.

January, 1998

Kyoto

Kenji Inaba

LIST OF PUBLICATIONS

PART II

CHAPTER 1: "Structural and Functional Roles of Modules in Hemoglobin -SUBSTITUTION OF MODULE M4 IN HEMOGLOBIN SUBUNITS-" Inaba, K., Wakasugi, K., Ishimori, K., Konno, T., Kataoka, M. and Morishima, I. (1997) *J. Biol. Chem.* **272**, 30054-30060

CHAPTER 2: "Design, construction, crystallization and preliminary X-ray studies of a fine-tuning mutant (F133V) of module substituted chimera hemoglobin" Shirai, T., Inaba, K., Fujikake, M., Yamane, T., Ishimori, K. and Morishima, I. (1998) *Proteins* in Press

PART III

CHAPTER 3: "Structural and Functional Effects of Pseudo-Module Substitution in Hemoglobin Subunits -NEW STRUCTURAL AND FUNCTIONAL UNITS IN GLOBIN STRUCTURE-" Inaba, K., Ishimori, K., Imai, K. and Morishima, I. (1998) *J. Biol. Chem.* in Press

CHAPTER 4: "Structural and Functional Effects of Implantation of Pseudo-Module from Hemoglobin α -Subunit into myoglobin " Inaba, K., Ishimori and Morishima, I. submitted for publication (*J. Biol. Chem.*)

PART IV

CHAPTER 5: "Structural and Functional Roles of Heme Binding Module in Globin Proteins -IMPLANTATION OF HEME BINDING MODULE FROM HEMOGLOBIN α -SUBUNIT INTO MYOGLOBIN-" Inaba, K., Ishimori, K. and Morishima, I. submitted for publication (*J. Mol. Biol.*)

CHAPTER 6: "Structural and Functional Roles of Heme Binding Module in Globin Proteins -IMPLANTATION OF HEME BINDING MODULE FROM HEMOGLOBIN α -SUBUNIT INTO β -SUBUNIT-" Inaba, K., Ishimori, K. and Morishima, I. submitted for publication (*J. Mol. Biol.*)

Other Publications:

"Module Substitutions among Myoglobin, Hemoglobin α - and β -subunits" Wakasugi, K., Inaba, K., Ishimori, K. and Morishima, I. (1997) *Biophys. Chem.* in press

CONTENTS

| | |
|---|----------|
| PREFACE | (i) |
| ACKNOWLEDGMENTS | (ii) |
| LIST OF PUBLICATIONS | (iii) |
| CONTENTS | (iv) |
| I. GENERAL INTRODUCTION | -----1 |
| II. EFFECTS OF MODULE SUBSTITUTION ON GLOBIN STRUCTURE AND FUNCTION | |
| 1. Substitution of module M4 in hemoglobin α - and β -subunits ($\alpha\beta$ (M4)- and $\beta\alpha$ (M4)-subunits) | -----13 |
| 2. X-ray Crystallographic Study on a Fine-tuning Mutant (F133V) of the Module Substituted $\beta\alpha$ (M4)-Subunit | -----35 |
| III. EFFECTS OF PSEUDO-MODULE SUBSTITUTION ON GLOBIN STRUCTURE AND FUNCTION | |
| 3. Substitution of pseudo-module PM3 in hemoglobin α - and β -subunits ($\beta\alpha$ (PM3)-subunit) | -----61 |
| 4. Substitution of pseudo-module PM3 in hemoglobin α -subunit and myoglobin (Mb α (PM3)-subunit) | -----87 |
| IV. EFFECTS OF SUB-MODULE SUBSTITUTION ON GLOBIN STRUCTURE AND FUNCTION | |
| 5. Substitution of sub-module m6 in hemoglobin α -subunit and myoglobin (Mb α (m6)-subunit) | -----109 |
| 6. Substitution of sub-modules m6 and m7 in hemoglobin α - and β -subunits ($\beta\alpha$ (m6)- and $\beta\alpha$ (m7)-subunits) | -----141 |
| V. SUMMARY AND GENERAL CONCLUSIONS | -----167 |

PART I

GENERAL INTRODUCTION

The structure of a protein consists of a mosaic of globular structural units such as domains or super-secondary structures (1). These structural units also serve as functional units that play crucial roles in protein activity. Immunoglobulin and DNA binding proteins represent clear examples of the mosaic structure of proteins; these proteins have conservative antigen or nucleotide binding domains for common activity and involve various additional domains that bear specific activity for each protein (2-5). The mosaic structure of proteins might be a trace of the evolutionary history in which they were developed by adding or removing the structural units (2, 6,7).

The geometrically determined "module" is one of such structural units (8-12). The module is defined as a continuous local peptide segment that folds into a compact globular conformation in protein structure. Of particular interest is that the modules correspond to exons in several genes. According to the hypothesis by Gilbert and Blake, the correspondence of the modules to the exons is thought to be a relic of protein evolution in which recombination or shuffling of exons has played an important role in the creation of the current variety of proteins (7, 8). That is, modules would have a crucial factor in molecular evolution.

If modules are an evolutionary unit as stated above, they should have structurally stable element. First of all, the modules retain compactness. In addition, boundaries of modules exist in interior of proteins and are not located far from all the other residues. On the basis of these criteria of the modules, an algorithm for module identification has been established. One of the algorithms is a distance map, on which are marked the pairs of amino acid residues separated by more than a certain distance as illustrated in Fig. 1 (8). That is, non-marked region on this map represents a structural block within which residues are close to each other.

According to this algorithm, globin structures of the α - and β -subunits in vertebrate hemoglobins are found to be made up of four modules M1, M2+M3 and M4 as shown in Fig. 2 (8). Apparently, each module could be called a compact structural unit and they are encoded by an exon with the exception of the large central exon comprising two modules M2 and M3. Here, it is notable that on the basis of the analysis of hemoglobin function in terms of its modular structure, the amino acid residues associated with the heme contacts and the $\alpha_1\beta_2$ contacts are concentrated in the central modules (M2+M3), and the $\alpha_1\beta_1$ interaction region, which is most contributing to the subunit association, is mainly located in the module M4 (Fig. 3) (13). Based on such relationship

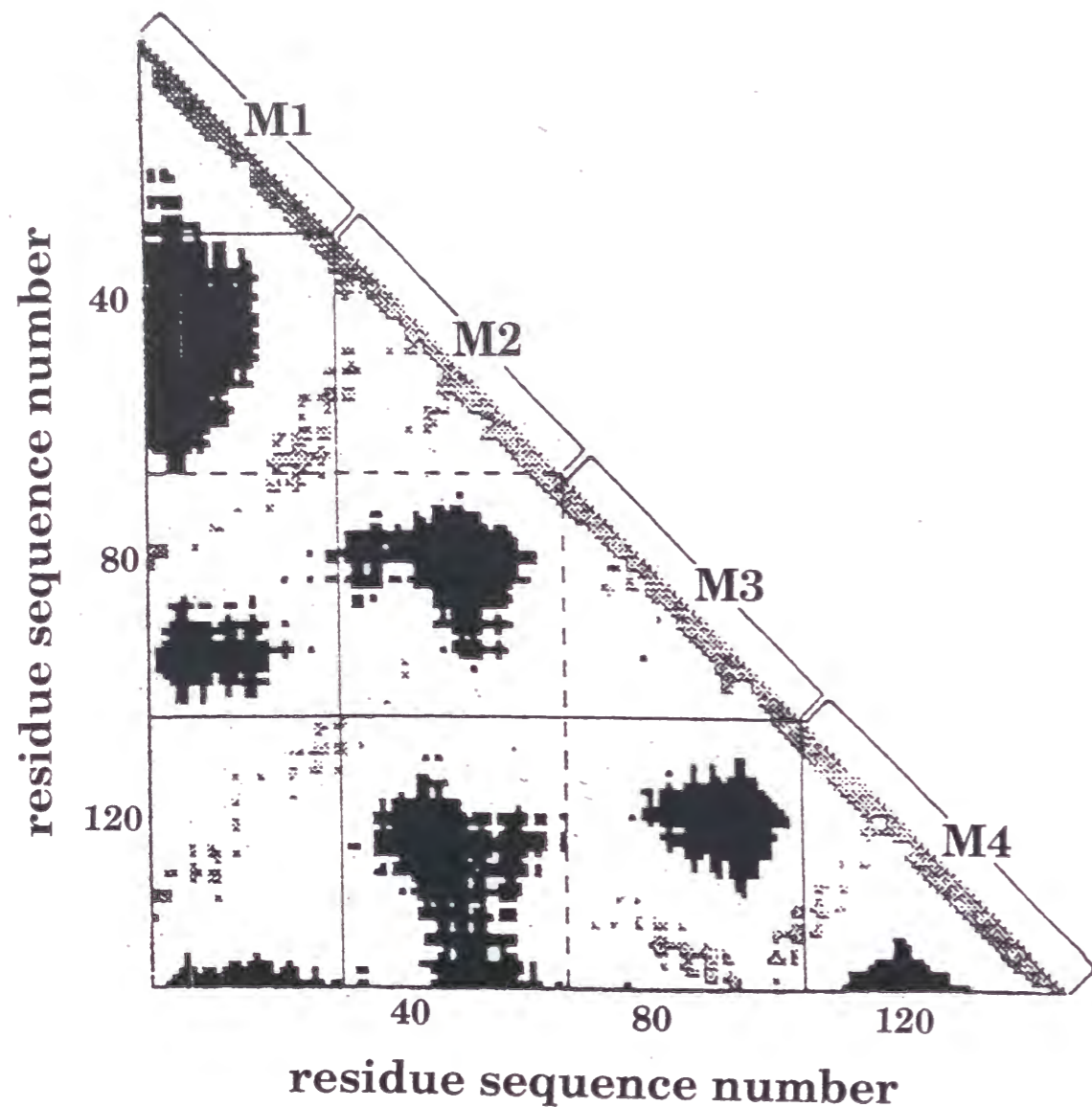


Figure 1 Plot of the distances between α -carbon atoms in the hemoglobin β -subunit. Distances between pairs of atoms greater than 27 Å appear as dark regions. Solid lines are drawn at the joints between polypeptide segments (M1, M2+M3 and M4) encoded by different exons. Note that these lines scarcely cross the dark regions. In the gene of leghemoglobin from soybean, an additional intron was found at the boundary of the modules M2 and M3, which is shown by a broken line.

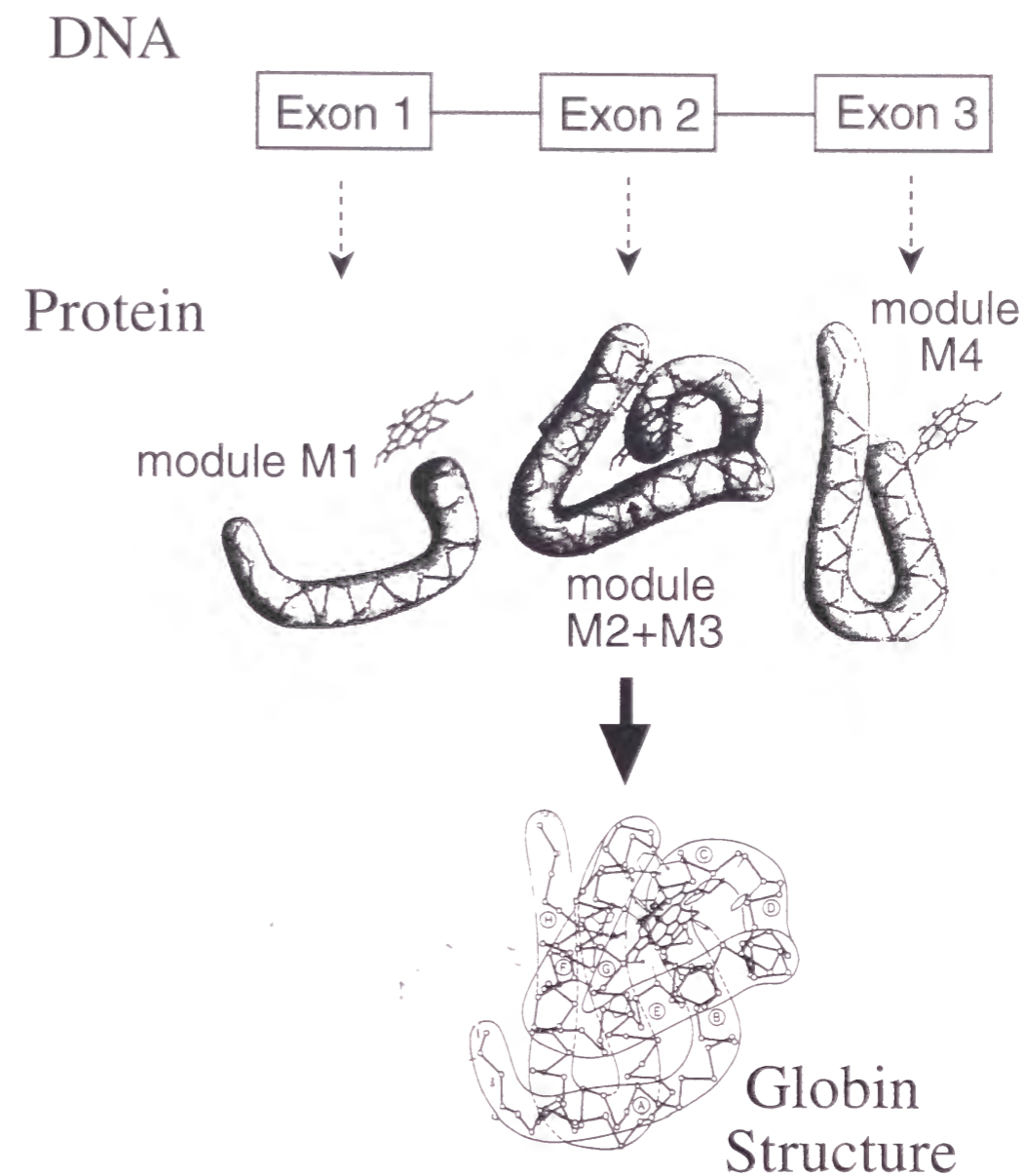


Figure 2 Correlations between the modules of globin and the exons in its gene. The exons 1, 2 and 3 of globins correspond to the modules M1, M2+m3 and M4, respectively.

between modules and functions, a few experimental approaches to test the module as a structural/functional unit have been performed (14-18).

Wakasugi et al., have so far prepared many kinds of module-substituted globin subunits, where each of the modules M1-M4 is replaced between hemoglobin α - and β -subunits or between myoglobin and hemoglobin subunits (14, 15). For the chimeric $\beta\alpha(M4)$ -subunit, in which the module M4 of the β -subunit is replaced by that of the α -subunit, its heme environmental structure were quite similar to those of the β -subunit (14). On the contrary, the chimeric

subunit preferentially bound to the native β -subunit to form a heterotetramer, $(\beta\alpha)_2(\beta)_2$, not to the native α -subunit and showed an association property of the α -subunit type (14). Such chimeric properties for the $\beta\alpha(M4)$ -subunit indicate that the module M4 behave as a structural/functional unit regulating the heme environmental structure and subunit assembly in hemoglobin α - and β -subunits. In sharp contrast to the case for the $\beta\alpha(M4)$ -subunit, however, substantial structural destabilization was encountered for many other module substituted globins, resulting in failure of their functional conversion (15). These results suggest that it is necessary to reconsider the structural and functional significance of the modules in globin proteins.

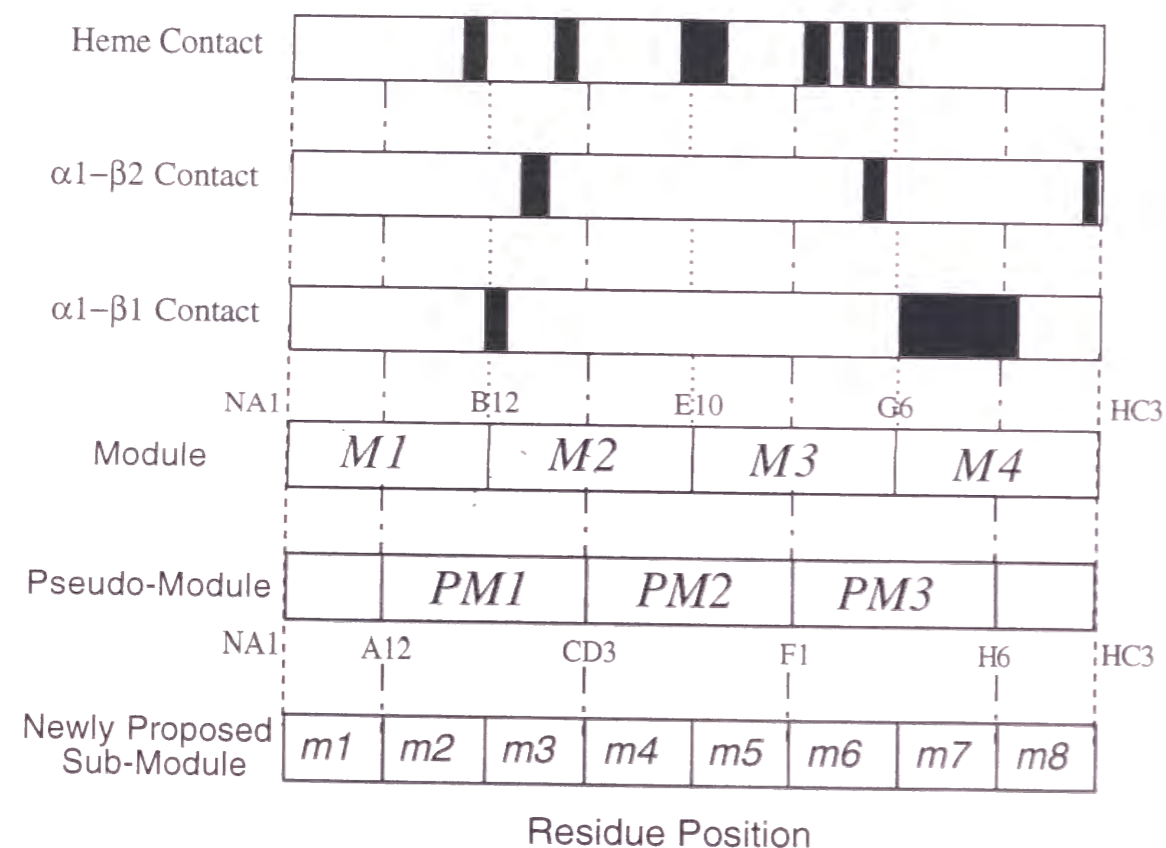


Figure 3 Module, pseudo-module, sub-module boundaries and residues with well defined functional roles in human hemoglobin proposed by Eaton. Residues that are involved in particular functions are marked by heavy lines

In this thesis, accordingly, the author investigates structural and functional effects of the module substitutions in more detail compared to the previous studies. Furthermore, the author believes that thorough comparisons between "module" and "non-module" substituted globins provide further inspections on the properties of the modules, since the modules are

supposed to be a unique structural/functional unit in globin proteins (13, 14). In chapter 1 of Part II, to confirm the functional role of the module M4 in regulation of subunit assembly, the author has prepared and characterized the chimeric $\alpha\beta(M4)$ -subunit, which is the "reversed" chimeric subunit of the $\beta\alpha(M4)$ -subunit. Moreover, in chapter 2 of Part II, he has tried x-ray crystal structure analysis of the chimeric $\beta\alpha(M4)$ -subunit to completely elucidate structural alterations induced by the module M4 substitution, in which F133V mutation is introduced for the crystallization.

In Part III, to re-examine the structural and functional significance of the modular structures in globins, we have studied effects of "non-module" substitution on globin structure and function. In particular, the author has focused upon a pseudo-module substitution. The pseudo-modules are defined as a segment starting at a center of one module and ending at the center of the following one and supposed not to form a compact structural unit in sharp contrast to the modules (12). Furthermore, since the pseudo-modules do not statistically coincide with exons, they would not have evolutionary meanings unlike the modules (19). On the basis of their structural and functional contrasts to the modules, comparison between module and pseudo-module substitutions would provide many insights into structural and functional significance of the modules. In chapter 3 of Part III, the author has engineered the $\beta\alpha(PM3)$ -subunit, in which the pseudo module PM3 of the hemoglobin β -subunit is replaced by that of the α -subunit, and compared its structural and functional characters with those of the $\beta\alpha(M4)$ -subunit. In chapter 4, the author implanted the pseudo-module PM3 from the α -subunit into myoglobin besides the β -subunit and compared the pseudo-module substituted myoglobin, $Mb\alpha(PM3)$, with the module substituted myoglobin, $Mb\alpha(M4)$. Based on the fact that homology of the amino acid sequence between myoglobin and the α -subunit (20%) is much lower than that between the α - and β -subunits (40%), it can be inferred that the implantation of the pseudo-module PM3 from the α -subunit into myoglobin causes other effects on the globin structure and function than the implantation into the β -subunit. Therefore, the study for the $Mb\alpha(PM3)$ as well as the $\beta\alpha(PM3)$ -subunit would provide more general informations on structural/functional significance of the modules or pseudo-module PM3. Interestingly, it is proposed in this part that the conventional modules M1-M4 can be further divided into sub-modules at their center as illustrated in Fig. 3, and the sub-modules are probably a new structural/functional unit regulating heme proximal structure or subunit assembly in globin proteins.

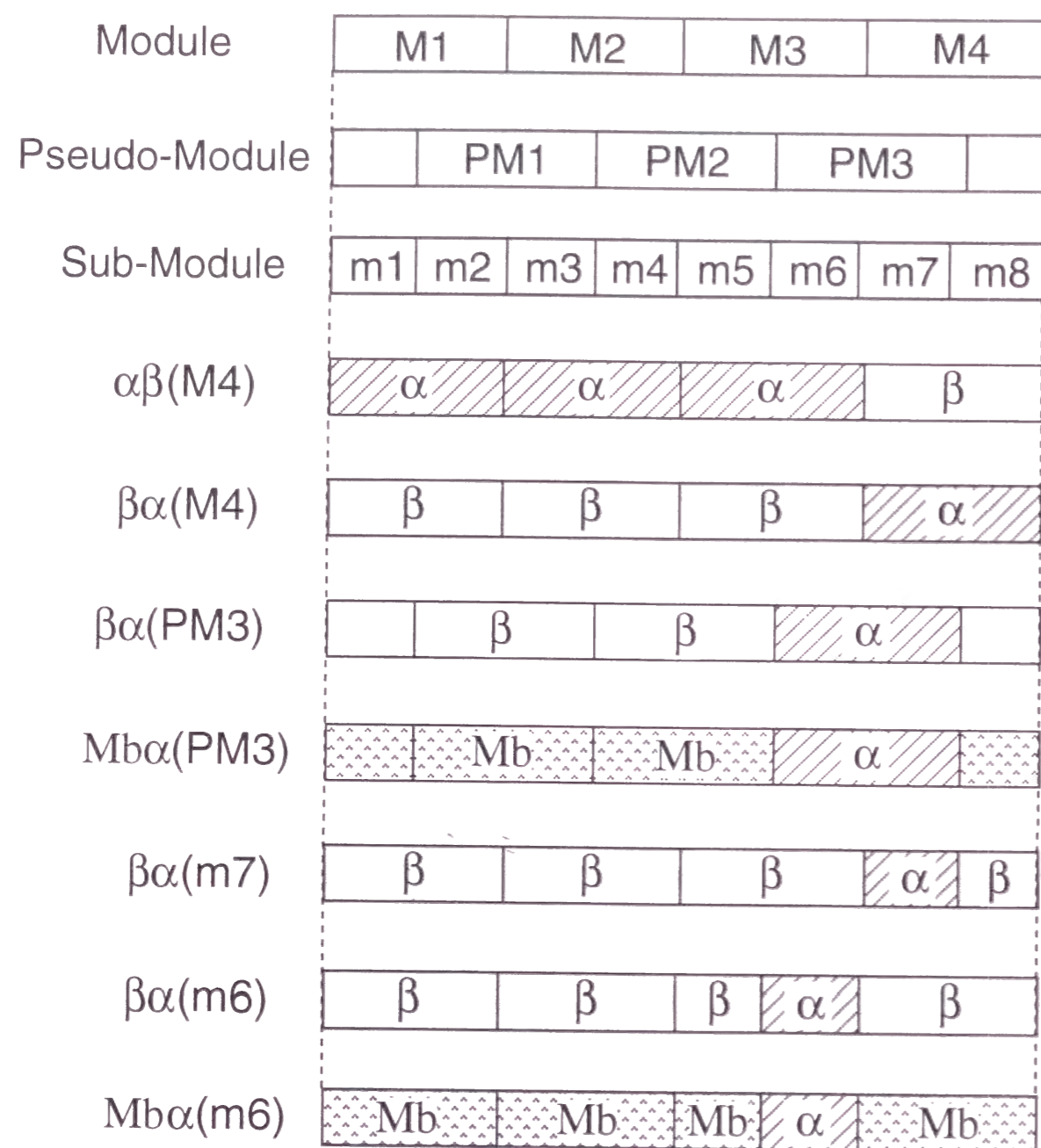


Figure 4 List of the artificial chimeric globins synthesized in this study

In part IV, the author tried to examine the structural and functional significance of the sub-modules by characterizing the sub-module substituted globins. Particularly, since the amino acid residues contributing to heme contacts and the α 1- β 1 subunit contacts are concentrated in the sub-modules m6 and m7 respectively, the functional roles of these sub-modules have been studied here. In Chapter 5, he has prepared the $Mb\alpha(m6)$, where the sub-module m6 of myoglobin was replaced by that of the α -subunit, and inspected

changes of its heme vicinity to the α -subunit one. In addition, he has prepared and characterized the $\beta\alpha(m6)$ - and $\beta\alpha(m7)$ -subunits in Chapter 6, where the sub-modules m6 and m7 of the β -subunit are respectively exchanged with those of the α -subunit. Here, the author has been concerned with whether or not the heme proximal structure of the $\beta\alpha(m6)$ -subunit is altered into the α -subunit-like structure as the case for the $Mb\alpha(m6)$ and whether or not the $\beta\alpha(m7)$ -subunit exhibits the association property of the α -subunit just as do the $\beta\alpha(M4)$ - and $\beta\alpha(PM3)$ -subunits. From these experimental results, it has been shown that the conventional module assignment in globin proteins needs to be revised and the novel functional modules are proposed.

In summary, the author has artificially shuffled the modules, pseudo-modules or newly proposed sub-modules among the hemoglobin subunits and myoglobin (Fig. 4), and characterized the structure and function of these artificial globins. In the present study, he has been especially concerned with the following three points.

- i) What effects on globin structure and function are caused by the module substitution ?
- ii) Are the conventional modules M1-M4 unique structural and functional units in globin proteins ?
- iii) Is the conventional module assignment of globin proteins right ?

The author has answered these questions in this thesis and believes that the present findings may help not only to understand the regulation mechanism of globin structure and function by the modules but also to develop the effective module-based design of novel functional proteins.

REFERENCE

1. Richardson, J. S. (1981) *Adv. Protein Chem.* **34**, 167-339
2. Tonegawa, S., Maxam, A. M., Tizard, R., Bernard, O. and Gilbert, W. (1978) *Proc. Natl. Acad. Sci. U. S. A.* **75**, 1485-1989
3. Sakano, H. (1979) *Nature* **277**, 627-633
4. Rossmann, M. G., Lilijas, A., Branden, C. I. and Banaszak, L. J. (1975) *The Enzymes* Vol. XI (Boyer P. D. eds) Academic Press, New York, 62-102
5. Cusack, S. (1995) *Nature Struct. Biol.* **2**, 824-831
6. Gilbert, W. (1978) *Nature* **271**, 501
7. Blake, C. C. F. (1979) *Nature* **277**, 598
8. Go, M. (1981) *Nature* **291**, 90-92
9. Go, M. (1983) *Proc. Natl. Acad. Sci. U. S. A.* **80**, 1964-1968
10. Go, M. (1985) *Adv. Biophys.* **19**, 91-131

11. Go, M. and Nosaka, M. (1987) *Cold Spring Harbor Symp. Quant. Biol.* **52**, 915-924
12. Noguti, T., Sakakibara, H. and Go, M. (1993) *Proteins* **16**, 357-363
13. Eaton, W. A. (1980) *Nature* **284**, 183-185
14. Wakasugi, K., Ishimori, K., Imai, K., Wada, Y., and Morishima, I. (1994) *J. Biol. Chem.* **269**, 18750-18756
15. Waksugi, K., Inaba, K., Ishimori, K. and Morishima, I. (1997) *Biophys. Chem.* in press
16. Yanagawa, H., Yoshida, K., Torigoe, C., Park, J. S., Sato, K., Shirai, T. and Go, M. (1993) *J. Biol. Chem.* **268**, 5861-5865
17. Ikura, T., Go, N., Kohda, D., Inagaki, F., Yanagawa, H., Kawabata, M., Kawabata, S., Iwanaga, S., Noguti, T. and Go, M. (1993) *Proteins* **16**, 341-356
18. Yaoi, T., Miyazaki, K., Oshima, T., Komukai, Y. and Go, M. (1996) *J. Biochem.* **119**, 1014-1018
19. Go, M. and Noguti, T. (1995) *Tracing Biological Evolution in Protein and Gene Structures* (eds Go, M. and Scimmel, P) Elsevier, Amsterdam, 229-235.

PART II

EFFECTS OF MODULE SUBSTITUTION ON GLOBIN STRUCTURE AND FUNCTION

Chapter 1

Substitution of module M4 in hemoglobin α - and β -
subunits ($\alpha\beta$ (M4)- and $\beta\alpha$ (M4)-subunits)

ABSTRACT

The α - and β - subunits of human hemoglobin consist of the modules M1, M2 + M3, and M4, which correspond to the exons 1, 2, and 3, respectively [Go, M. (1981) *Nature* 291, 90-92]. To gain further insight into functional and structural significance of the modules, we designed two kinds of chimeric hemoglobin subunits (chimeric $\alpha\beta$ (M4)- and $\beta\alpha$ (M4)-subunits), in which the module M4 was replaced by the partner subunits. CD spectra in far UV region showed that the secondary structure of the chimeric $\alpha\beta$ (M4)-subunit drastically collapsed, while the chimeric $\beta\alpha$ (M4)-subunit conserved the native globin structure [Wakasugi, K. *et al.*, (1994) *J. Biol. Chem.* 269, 18750-18756]. SAXS data also suggested partially disordered structure of the chimeric $\alpha\beta$ (M4)-subunit. Based on tryptophan fluorescence spectra and computer modelling from x-ray structures of native globins, steric constraint between 14 Trp and 125 Tyr would be induced in the $\alpha\beta$ (M4) chimeric subunit, which would perturb the packing of the A- and H-helices and destabilize the globule structure. On the other hand, such a steric constraint was not found between the modules M1 and M4 in the counterpart chimeric subunit, $\beta\alpha$ (M4) subunit. The different stabilities of these module substituted globins implies that modules would not be always stable "structural" units and interactions between modules are crucial to construct stable globin subunits.

Recent structural studies on proteins have revealed that some are constructed by "modules", which are compact structural units (1, 3). The exon shuffling in protein evolution with the correspondence of the "module" to the exon on the gene structure strongly suggested that the "module" structure is one of the key factors in evolution of structure and function of protein (4, 5). The "module" structure was first identified in the globin family (1) and their diagonal plots have clearly shown that both of the Hb¹ subunits (α - and β -subunits) consist of the four modular structures, the modules M1, M2, M3 and M4 (1), each of which is coded by an exon with the exception of the large central exon comprising two compact units.

The analysis of hemoglobin functions elucidated that the amino acid residues associated with the heme contacts are concentrated in the central modules (M2 + M3) as illustrated in Fig. 1 (6). In 1980, by using a protease, Craik *et al.* isolated the central region of the β -subunit, which corresponds to the module M2 + M3 and is coded by the central exon of the β -subunit (7, 8). They showed that the fragment from the central region bound heme stoichiometrically and tightly, generating a characteristic strong Soret absorption band as found for the intact subunits. De Sanctis *et al.* also prepared "mini-myoglobin" which is constructed by the peptide fragment from 32 (Leu) to 139 (Asn) of horse heart Mb (9, 10, 11, 12). The heme binding property of the "mini-myoglobin" peptide was almost the same as that of the intact Mb, and the heme binding induced the recovery of secondary structure of the mini-myoglobin. They concluded that the removal of the peptide fragments from amino- and carboxyl-terminus has little effect on the heme binding to the apoprotein. These experimental results from the limited proteolysis of globins indicate that the module M2 + M3 can be a structural and functional unit to bind heme.

In order to obtain further insight into the modular structure in globins, we have focused on the "module" substitution by use of the cassette mutagenesis (2). Our previous results have revealed that the heme environmental structure and ligand binding property of the chimeric $\beta\alpha(M4)$ -subunit, in which the module M4 of the β subunit was replaced by that of the α -subunit, were quite similar to those of the β -subunit, while the chimeric subunit preferentially bound to the native β -subunit to form a heterotetramer, $(\beta\alpha(M4))_2(\beta\beta)_2$, not to the native α -subunit. The conversion of the association property indicates that the module M4 is a key module in specific binding of the α -subunit to the β -subunit. This conclusion also corresponds to the

distribution of the amino acid residues responsible for the formation of the $\alpha 1$ - $\beta 1$ subunit interface as shown in Fig. 1.

In the present study, we prepared the "reversed" chimeric subunit, $\alpha\beta(M4)$ -subunit, in which the module M4 of the α -subunit is replaced by that of the β -subunit, to clarify structural and functional roles of the module M4 in more detail. We examined here the contributions of the modular structure to stability of globular proteins and their functional roles in regulating the association property by comparing structural and functional properties of the chimeric $\alpha\beta(M4)$ - and $\beta\alpha(M4)$ -subunits.

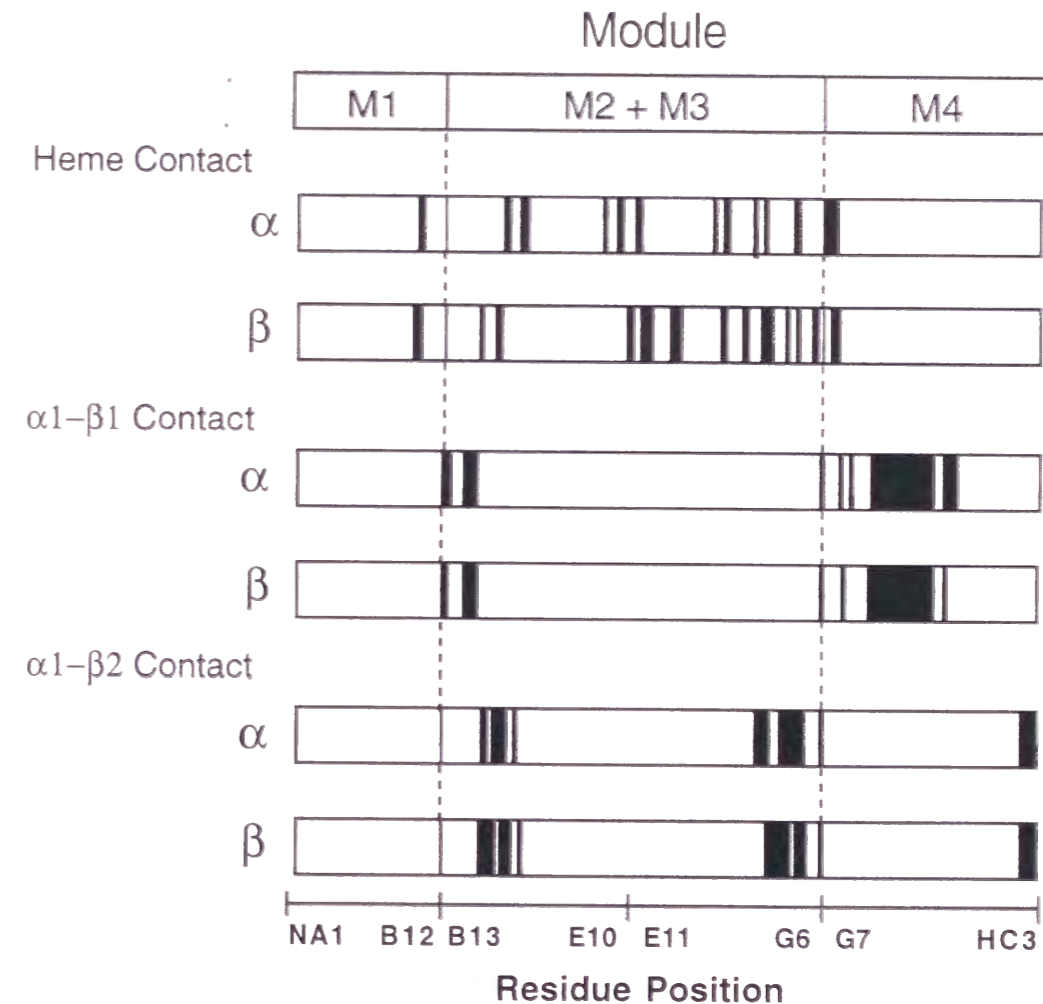


Fig.1. Module boundaries and residues with well defined functional roles in human hemoglobin proposed by Eaton (1980). Black bands represent residues with well defined functional roles for each subunit.

EXPERIMENTAL PROCEDURES

Expression Vector Construction – To construct the mutated gene for the chimeric $\alpha\beta$ (M4)-subunit, the phage vector M13mp18 containing the α -subunit gene was digested with *Hind* III and *Nde* I (13). Since the native β subunit gene has no *Hind* III site at the corresponding position, a *Hind* III site was introduced at the position FG3 in the β -subunit gene on M13mp18 cII FX β -subunit (14, 15, 16) without changing the encoded amino acid residue (2). The *Hind* III - *Nde* I fragment of the α -subunit and the *Hind* III - *Hind* III fragment of the mutant β -subunit were purified on agarose gel. The fragments were ligated into the *Hind* III - *Nde* I fragment of M13mp18 to form M13mp18 cII FX chimeric $\alpha\beta$ (M4)-subunit². The ligated fragment was then cloned into the *Hind* III - *Nde* I fragment of the T7 expression vector.

Protein Preparation – The prepared gene encoding the chimeric subunits were transformed into an *Escherichia coli* strain (BL21), which was grown at 37 °C in 2xTY culture containing ampicillin (100 μ g/ml) overnight. This culture was centrifuged by 5,000 r.p.m. and the cell pellets were lysed with lysozyme (100 mg per 10 g of pellets) to get the crude chimeric subunits. By purification processes with gel chromatography (Sephacryl-200) and ion-exchanged column (CL-6B), we obtained chimeric subunit purity of more than 90 % as estimated on SDS gels. Fast atom bombardment mass spectroscopy on trypsin digested proteins (17) showed no unexpected mutations in the chimeric subunits (data not shown).

Heme Titration and Electron Absorption Spectra – Heme titration was monitored by the absorbance change at 413 nm (Hitachi U-3210). In order to estimate the concentration of the chimeric subunits, we used the extinction coefficient at 280 nm, which was determined to be 8.8 $\text{mM}^{-1}\text{cm}^{-1}$ for the $\alpha\beta$ (M4) chimeric subunits and 13.2 $\text{mM}^{-1}\text{cm}^{-1}$ for the $\beta\alpha$ (M4) chimeric subunits by the number of the aromatic residues, tryptophan ($\epsilon_{280} = 5.5 \text{ mM}^{-1}\text{cm}^{-1}$) and tyrosine ($\epsilon_{280} = 1.1 \text{ mM}^{-1}\text{cm}^{-1}$) (18). The carbon monoxide derivative was prepared by adding dithionite to the ferric chimeric subunits under CO atmosphere. No endogenous ligand-bound derivative was gained with recourse to substituting N_2 for CO. Absorption spectra were recorded with a Hitachi U-3210 spectrophotometer.

Circular Dichroism Spectra – CD spectra of the chimeric and native subunits in far UV and Soret region were measured at 20 °C with a JASCO J-760 spectrometer. Concentration of the sample was 10 μ M and the buffer was 50 mM Tris, 0.1 M NaCl, 10 mM NaCN and 1 mM Na_2EDTA , pH 7.4. The

path lengths for the measurements in far UV and Soret region were 1 mm and 10 mm, respectively. The mean residue α -helical contents were estimated with the deconvolution method by Greenfield and Fasman (19), where the chimeric globin subunits are assumed to contain only α -helical and random coil structure since the native globin subunits have no β -strand.

Tryptophan Fluorescence Spectra – Tryptophan fluorescence spectra were measured with a Perkin Elmer LB50 emission spectrometer. The samples were excited at 280 nm, and the emission spectra were measured between 300 and 400 nm. We used a crystal cuvette for the fluorescence measurements and the path length was 10 mm. The concentration of the samples was 5 μ M on the heme basis, and the buffer was the same as used in the CD measurements.

Urea Denaturation Curves - Reaction solutions contained 50 mM Na-phosphate (pH 7.4), 1 mM NaCN and various concentrations of urea. Changes in ellipticity at 222 nm, $[\theta]_{222}$ were monitored with Jasco J-760 CD spectrophotometer after several hours equilibration at room temperature. The fractional population of denatured form (f_D) in each condition was estimated by the following equation:

$$f_D = ([\theta]_{222, N} - [\theta]_{222, D}) / ([\theta]_{222, N} - [\theta]_{222, D})$$

where $[\theta]_{222, N}$ and $[\theta]_{222, D}$ represent ellipticities at 222 nm in the native and denatured state, respectively (20).

Solution X-ray scattering measurement. – Solution X-ray scattering experiments on native Hb and the chimeric globin subunits were carried out at the solution scattering station (SAXS camera) installed at BL-10C, the Photon Factory, Tsukuba, Japan (21, 22). The sample-to-detector distance was about 90 cm for measurements of SAXS, calibrated by meridional diffraction of dried chicken collagen. The wave length of the X-ray was 1.488 Å. The sample cell was 50 μ l in volume with 15- μ m-thick quartz windows, and had a 1 mm X-ray pathlength. The temperature of the sample was controlled at 25 °C by circulating the temperature-controlled water. The protein concentrations were varied within the range of 3 to 10 mg/ml, and the measurement time for each scattering experiment was 10 minutes. The scattering from the solution containing no protein was measured to subtract background scattering.

Analysis of SAXS data – Data processing was carried out with Macintosh (Apple) personal computers. The scattering curve at infinite dilution was obtained from a series of scattering data with different protein concentrations (23). X-ray scattering intensities at the small-angle region are given as

$$I(Q) = I(0) \exp(-Rg^2 \cdot Q^{2/3}) \quad (1)$$

where Q and $I(0)$ are the momentum transfer and the intensity at 0 scattering angle, respectively (24). Q is defined by $Q = 4\pi\sin\theta / \lambda$, where 2θ and λ are the scattering angle and the wavelength of the X-ray, respectively. The radius of gyration (R_g) was obtained from the slope of the Guinier plot, a plot of $\ln[I(Q)]$ against Q^2 (25).

Gel Chromatogram - Measurements were performed by gel filtration on a Sephacryl S-200 HR column (0.8 cm-d x 62 cm-l) at 4°C. The buffer used for the chromatography was 50 mM Tris, 0.1 M NaCl, and 1 mM Na₂EDTA, pH 7.4 and the flow rate was 5 ml/h. Sample concentration was 15 μM, and eluted fractions were monitored at the Soret absorption band.

RESULTS

Heme Titration and Absorption Spectra - The spectrophotometric titration of heme to the αβ(M4)- and βα(M4)-chimeric subunits showed that the chimeric subunits bound heme stoichiometrically (figure not shown). The absorption spectra of the carbonmonoxy chimeric subunits were identical to that of native subunit as illustrated in Fig. 2(A). However, the deoxygenated chimeric αβ(M4)-subunit exhibited a quite different spectrum from that of deoxy native subunit (Fig. 2(B)), while the chimeric βα(M4)-subunit showed the deoxy-type spectrum as found for native subunit (2). In the deoxygenated form, the absorption maxima were observed at 531 and 559 nm in the Q-band of the chimeric αβ(M4)-subunit, whereas native subunit (α subunit) and the chimeric βα(M4)-subunit have a single and broad peak at 555 nm. The peak position of the Soret band also showed a blue-shift for the deoxy chimeric αβ(M4)-subunit. This spectral pattern is characteristic of the hemochromogen-type hemoprotein, in which the distal histidine as well as the proximal histidine is coordinated to iron(II) (26).

Circular Dichroism Spectra - In Fig. 3A, the far-UV CD spectra of the cyanomet native and chimeric subunits are shown. The native α- and β-subunits exhibited two negative broad peaks around 222 and 208 nm (27). In the spectra of the chimeric subunits, remarkable decrease in the negative ellipticity around 222 nm was observed and a new negative peak around 206 nm appeared. Based on the deconvolution method by Greenfield and Fasman (19), the α-helical content of the αβ(M4)-chimeric subunit was estimated as 30 %, which is much lower than that of the native subunits (70 %) and the chimeric βα(M4)-subunit (68 %). In the Soret region, the CD spectrum of hemoprotein has also provided some information of the heme environmental structure (28).

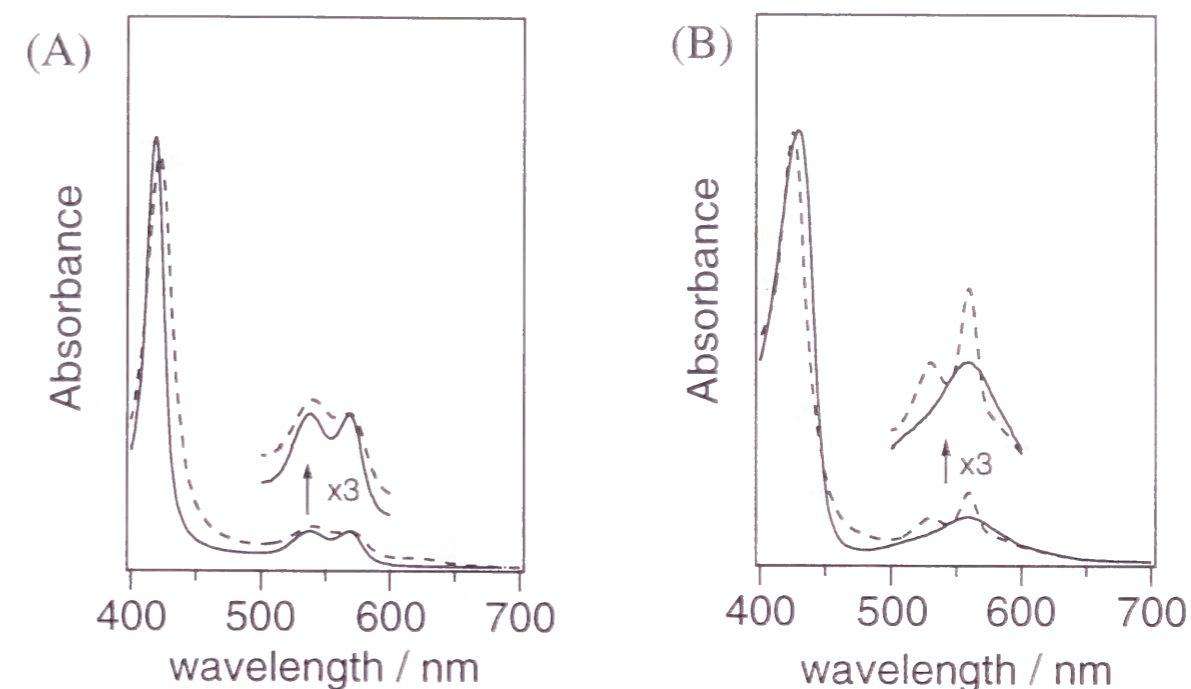


Fig.2. Electron absorption spectra of a carbon monoxide derivative (A) and a non-ligand derivative (B). Concentration of each subunit was 10 μM. Spectra of native subunit (α-subunit) and the chimeric αβ(M4)-subunit are expressed by solid and broken lines, respectively. The Q bands from 500 to 600 nm are enlarged by three times on the perpendicular axis.

As shown in Fig. 3B, the CD spectra in Soret region for cyano-met native and chimeric βα(M4)-subunits exhibit maxima around 420 nm, which is characteristic Cotton effect in hemoproteins (28). In sharp contrast to the large Cotton effect in native and chimeric βα(M4)-subunits, the CD spectra of the αβ(M4)-subunit shows a small maximum at 417 nm, suggesting that the substitution of the module M4 induced large structural changes in the heme environment of the chimeric αβ(M4)-subunit, but not so much of the βα(M4)-subunit.

Tryptophan Fluorescence Spectra - Fig. 4 illustrates the fluorescence spectra of the α-, β-, chimeric αβ(M4)- and βα(M4)-subunits. The α-subunit showed a small peak around 310 nm originated from tyrosines (²⁴Tyr, ⁴²Tyr and ¹⁴⁰Tyr) (29), while the fluorescence peak of the β-subunit around 335 nm is characteristic of ³⁷Trp (30). In the chimeric proteins, the αβ(M4)-subunit indicated a large peak around 345 nm, in addition to the peak at 310 nm, although the chimeric subunit contains only one tryptophan (¹⁴Trp) in the A-helix. In the spectra of the chimeric βα(M4)-subunit, a broad peak appeared

around 335 nm with a shoulder at 310 nm as observed for the β -subunit, but the intensity is larger than that of the β -subunit.

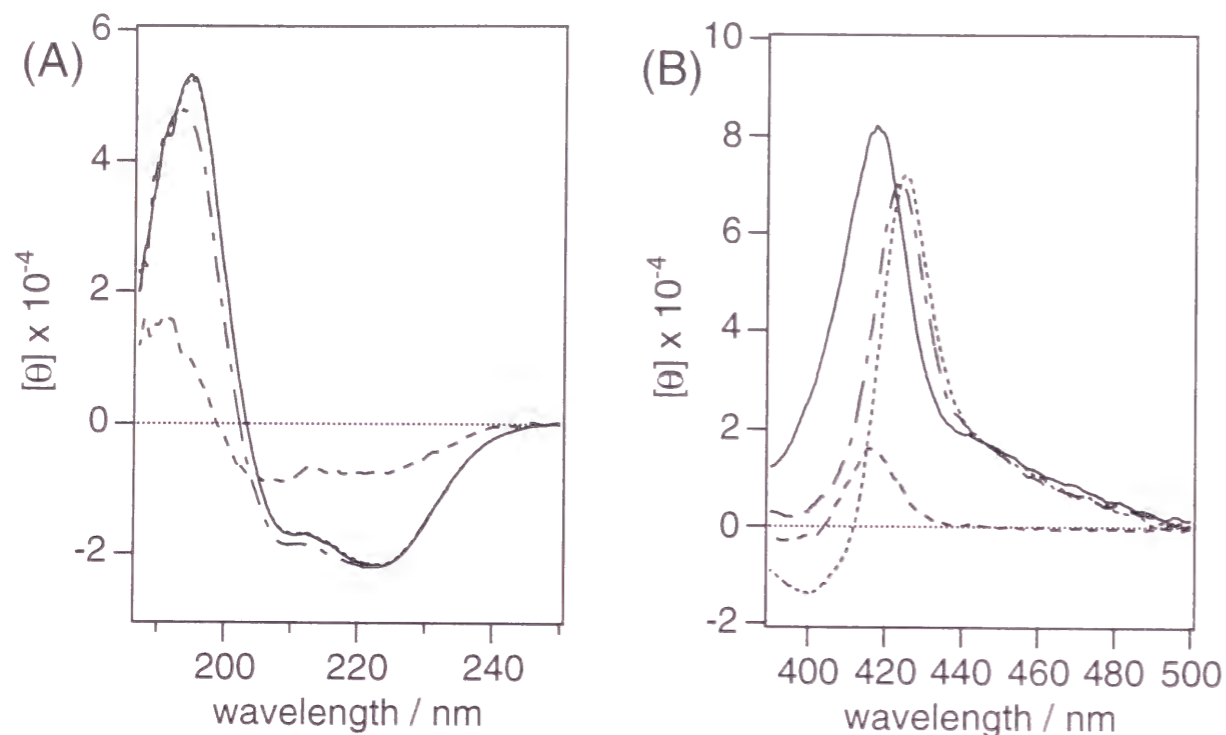


Fig.3. CD spectra in far UV region (A) and Soret region (B) Lines correspond to α -subunit (—), β -subunit (·····), chimeric $\alpha\beta$ (M4)-subunit (---), chimeric $\beta\alpha$ (M4)-subunit (-·-·).

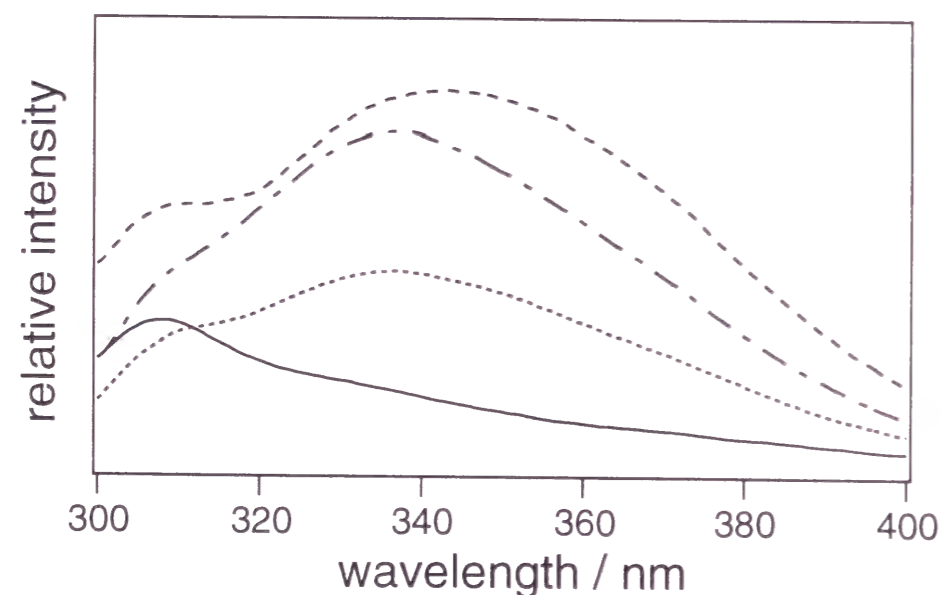


Fig. 4. Tryptophan fluorescence spectra Lines correspond to α -subunit (—), β -subunit (·····), chimeric $\alpha\beta$ (M4)-subunit (---), chimeric $\beta\alpha$ (M4)-subunit (-·-·).

Urea Denaturation Curves - The structural stability of the chimeric $\alpha\beta$ (M4)- and $\beta\alpha$ (M4)-subunits was examined by urea denaturation³. Urea denaturation curves for Hb tetramer, native α -, β -, chimeric $\alpha\beta$ (M4)- and $\beta\alpha$ (M4)-subunits are shown in Figure 5. As clearly shown in the figure, the transition curve for the chimeric $\alpha\beta$ (M4)-subunit largely shifted to the left side and did not show cooperativity, which implies large destabilization caused by the substitution of the module M4. On the other hand, the denaturation curve for the chimeric $\beta\alpha$ (M4)-subunit was cooperative and similar to those of native subunits, indicating that structural stability is not perturbed by the module substitution in the chimeric $\beta\alpha$ (M4)-subunit.

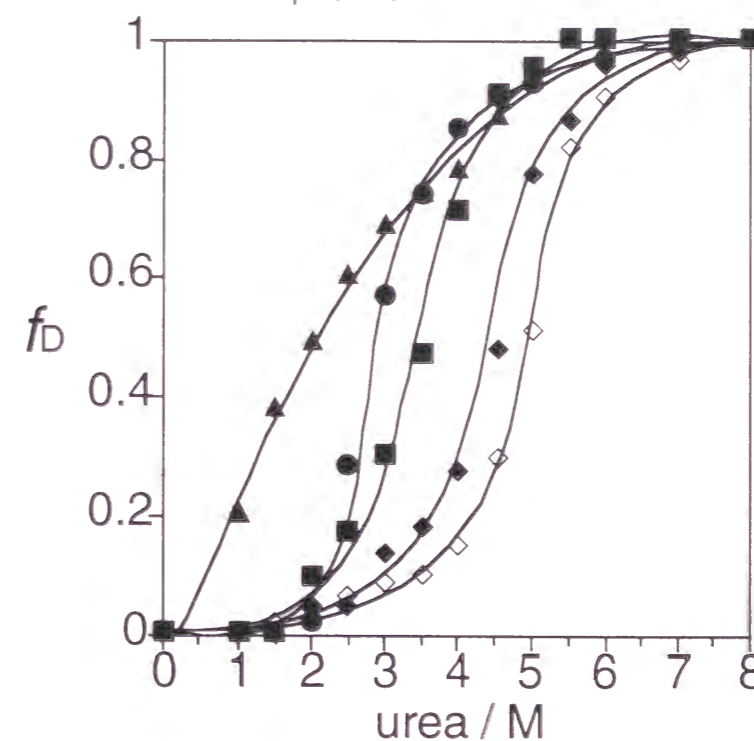


Fig.5. Denaturation curves of the subunits by urea Symbols correspond to hemoglobin(\diamond), α -subunit (\blacksquare), β -subunit (\bullet), chimeric $\alpha\beta$ (M4)-subunit (\blacktriangle), chimeric $\beta\alpha$ (M4)-subunit (\blacklozenge). Molecular ellipticities at 222 nm in a native state and a completely denatured state were calibrated to 0 and 1, respectively.

Solution X-ray scattering measurement Fig. 6 (A) shows Guinier plots of SAXS data for native Hb and the chimeric $\beta\alpha$ (M4)- and $\alpha\beta$ (M4)-subunits. The curves for Hb and the chimeric $\beta\alpha$ (M4)-subunit are well approximated by a straight line in the small-angle region (the Guinier region) (25). Their R_g values were deduced from the slopes of the regression lines within the Guinier region, defined as $R_g \cdot Q < 1.3$ in the present study (31). The R_g value for the chimeric $\beta\alpha$ (M4)-subunit is 25.9 Å, which is slightly larger than that for Hb

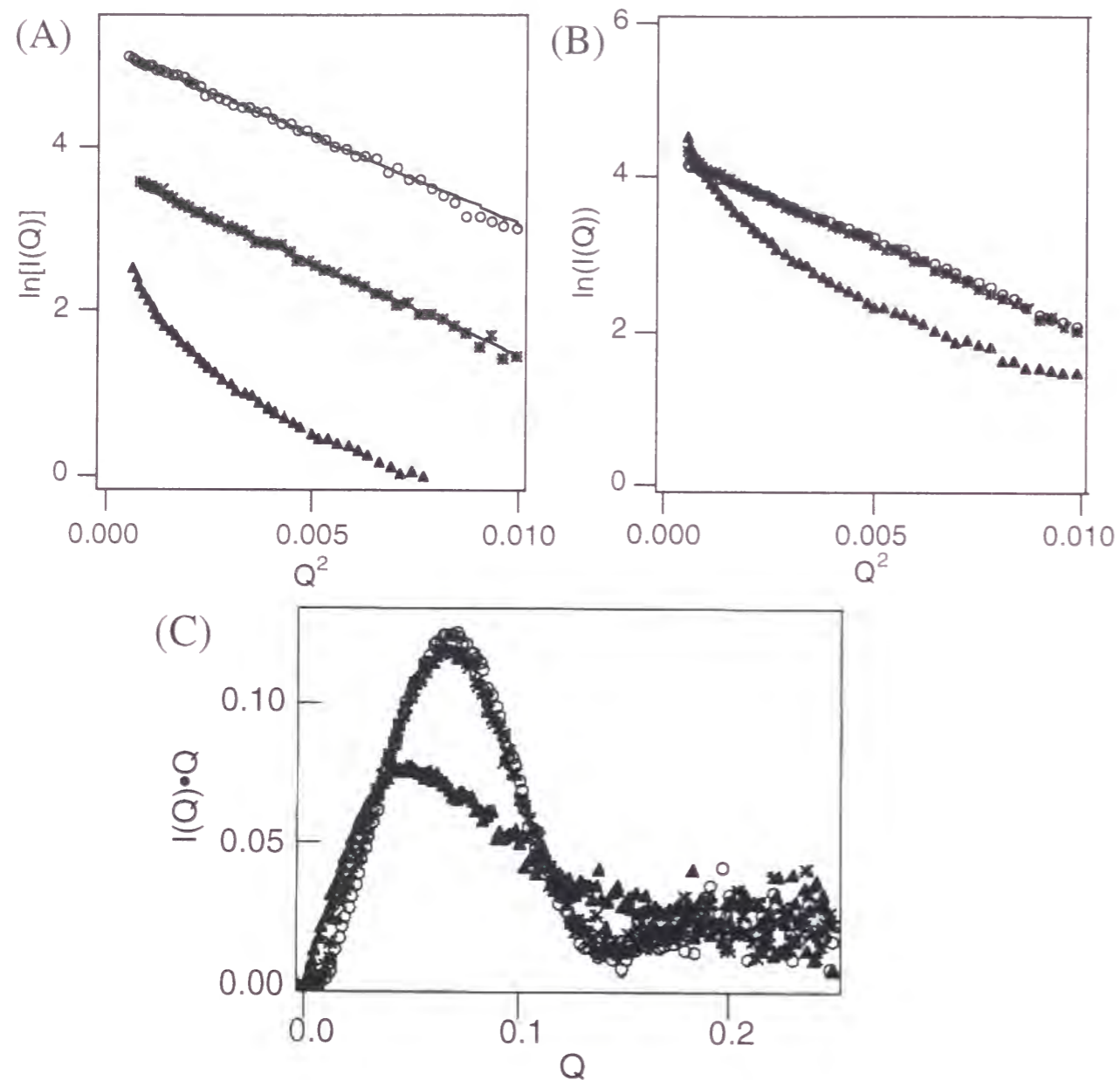


Fig. 6. Solution X-ray scattering (A) Guinier plots of hemoglobin (○), $\beta\alpha(M4)$ (✱) and $\alpha\beta(M4)$ (▲) subunits at 25 °C. The proteins are dissolved in the buffer solution with 10 mM Tris (pH 7.4), 10 mM NaCN. Each plot was obtained by the extrapolation to zero protein concentration of the data for four different protein concentrations (Kataoka et al., 1989). For clarity, each plot is shifted on the $\ln[I(Q)]$ axis. The regression lines were fitted to the data within $R_g \cdot Q < 1.3$. (B) The non-shifted Guinier plots of each subunit. Symbols are the same as Panel (A). In this panel, the extrapolation to zero protein concentration of the data was not performed. The protein concentration is 8 mg/ml for all the profiles. (C) Kratky plot of hemoglobin (○), $\beta\alpha(M4)$ (✱) and $\alpha\beta(M4)$ (▲) subunits. The protein concentration is kept at 10 mg/ml for all the profiles.

tetramer (25.3 Å). By the linear fitting analysis, the almost identical values of the intensity at 0 scattering angle, $I(0)$, was obtained for Hb tetramer (2.18 ± 0.03 arbitrary unit) and the chimeric $\beta\alpha(M4)$ -subunit (2.18 ± 0.06 arbitrary unit). Assuming the same specific volumes for Hb tetramer and the chimeric $\beta\alpha(M4)$ -subunit, these results on the $I(0)$ values suggest the same molecular mass of Hb and the chimeric $\beta\alpha(M4)$ -subunit. On the other hand, some oligomerizations were observed for the chimeric $\alpha\beta(M4)$ -subunit solutions. Although the accurate R_g and $I(0)$ values of $\alpha\beta(M4)$ -subunit could not be determined due to the deviation from the regression line, the $I(0)$ value can be larger than those of Hb and the chimeric $\beta\alpha(M4)$ -subunit (Fig. 6B), probably due to aggregation and/or unstable tertiary fold.

The Kratky plots of Hb and the chimeric subunits were shown in Fig. 6C. Hb indicated a clear peak fitted to a quadratic function, which is typical for a rigidly folded globular protein. The plot pattern for the chimeric $\beta\alpha(M4)$ -subunit is almost identical to that of Hb, implying that the global conformation of the chimeric $\beta\alpha(M4)$ -subunit is essentially the same as that of Hb. For the chimeric $\alpha\beta(M4)$ -subunit, however, the peak intensity in the Kratky plot highly decreased. The smaller descent, or larger slope, toward larger values of Q suggests partly disordered structure of the chimeric $\alpha\beta(M4)$ -subunit, since this plot pattern is clearly different from that of completely denatured proteins (24).

Gel Chromatography - Gel chromatograms of the carbonmonoxy chimeric $\alpha\beta(M4)$ -subunit in the presence and absence of native subunits are shown in Fig. 7. Under the condition applied here, the mixture of native α - and β -subunits formed tetramers, whereas the α -subunit still remains in a monomer (32). The β -subunit was in the equilibrium between monomers and tetramers (32). As shown in the figure, the elution peak for the chimeric $\alpha\beta(M4)$ -subunit was observed at the position for a tetrameric globin, which indicates that the chimeric $\alpha\beta(M4)$ -subunit forms the homo-tetrameric protein, $(\alpha\beta(M4))_4$, by the self-association. In the chromatogram of the mixture of the chimeric $\alpha\beta(M4)$ - and α -subunits, two peaks were observed, which coincided with the peaks for the isolated chimeric $\alpha\beta(M4)$ - and α -subunit. On the other hand, the peak for the mixture of the chimeric $\alpha\beta(M4)$ - and β -subunits was twice as high as that for the isolated chimeric $\alpha\beta(M4)$ -subunit, implying that the chimeric $\alpha\beta(M4)$ -subunit associates with the β -subunit to form a heterotetramer, not with the α -subunit. These association properties were independent of the sample concentration from 1 μ M to 50 μ M.

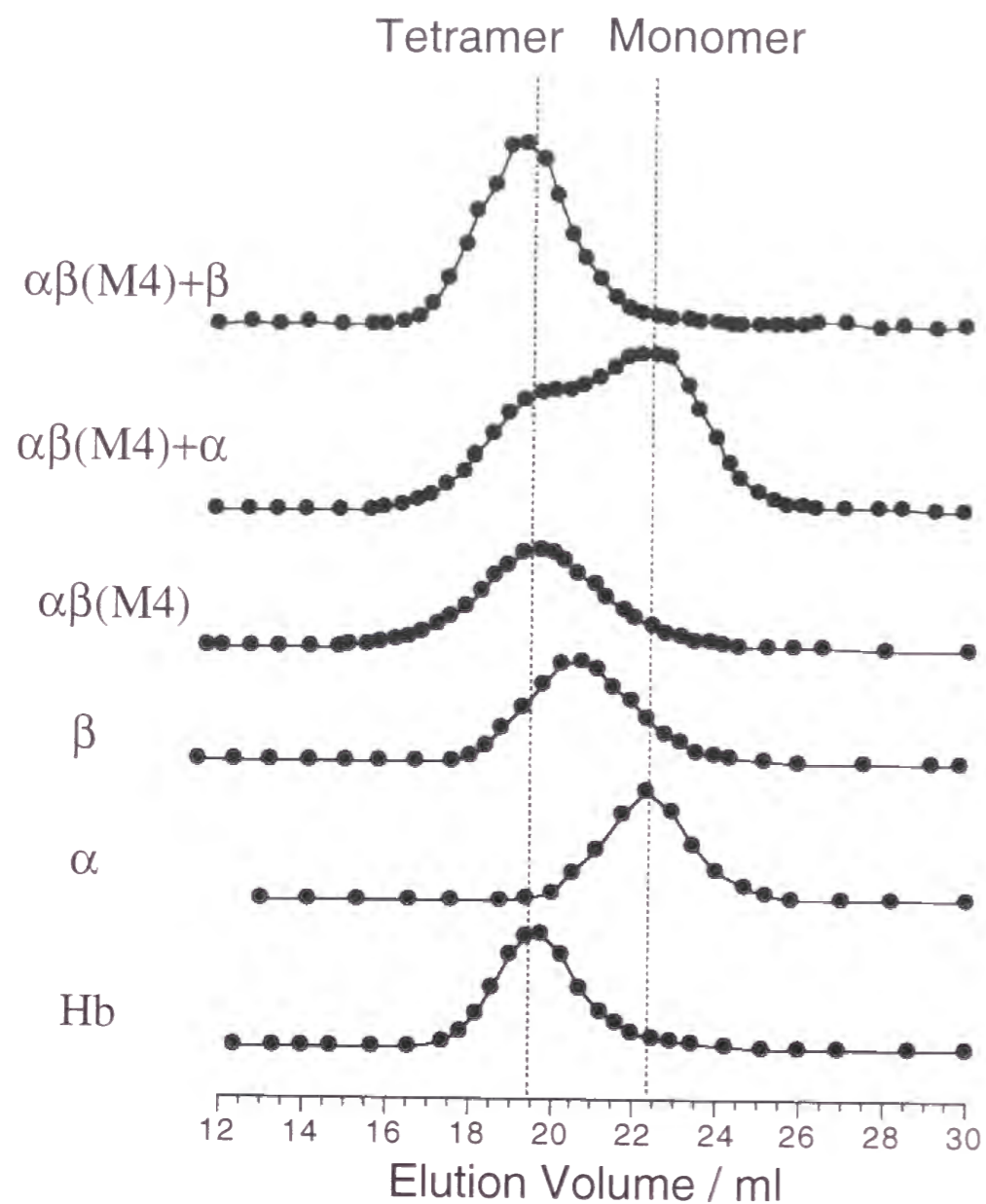


Fig.7. Gel chromatography of carbonmonoxide derivatives of the subunits on a Sephacryl S-200 HR column Perpendicular axis represents absorbance of each sample at Soret band, and sample concentration was 15 μ M.

We also examined salt effects on the association property of the chimeric globins by the gel chromatography in the presence of NaCl (up to 1 M). Previous studies have shown that the addition of NaCl drastically increases dissociation of Hb tetramer, whereas the tetrameric β -subunit (β_4) is relatively insensitive to salt or slightly stabilized in salt. These different response to the addition of salt were attributed to the different intersubunit interactions

between the two tetrameric globins (32, 33). The elution pattern of the chimeric $\alpha\beta$ (M4)-subunit was almost insensitive to NaCl (data not shown), suggesting that the subunit interactions in the $\alpha\beta$ (M4)-subunit are different from both of the native tetrameric globins.

DISCUSSION

Structure of the Chimeric Subunits. Although the heme titration clearly showed that the chimeric-subunits stoichiometrically bound heme as found for the native subunit, the hemochromogen-type spectrum was observed for the deoxygenated $\alpha\beta$ (M4)-chimeric subunit (Fig. 2). Since the hemochromogen-type spectrum is one of the characteristics for the denatured or partially unfold hemoproteins (26), the heme environmental structure of the chimeric $\alpha\beta$ (M4)-subunit was significantly perturbed upon the substitution of the module M4. The perturbation to the globin structure by the module substitution is also manifested in the CD spectra as illustrated in Fig. 3. The decreased Cotton effect in the Soret region for the chimeric $\alpha\beta$ (M4)-subunit can be interpreted as large structural changes in its heme vicinity and the small negative ellipticity around 222 nm in the chimeric $\alpha\beta$ (M4) indicates that the module substitution also induced global structural changes in the chimeric protein⁴. Since the mean residue ellipticity at 222 nm depends on the dynamic motion of the protein and the precise conformation of helical residues (34), the lower helical content implies that the structure of the chimeric $\alpha\beta$ (M4)-subunit would not be a "rigid" globular conformation as found in native globins, and that the fragmentation of long helices might be induced by the module substitution of the module M4 in the α -subunit.

Tryptophan fluorescence spectra also strengthen the suggestion of a partially unfolded structure of the chimeric $\alpha\beta$ (M4)-subunit. In the native α -subunit, since ¹⁴Trp is fully buried near the center of the molecule, the fluorescence of ¹⁴Trp is quenched due to resonance energy transfer to the heme moiety and low intensity (30). By the substitution of the module M4, the remarkable increase in the intensity of the fluorescence peak around 345 nm is observed in the chimeric $\alpha\beta$ (M4)-subunit, suggesting drastic changes in the microenvironment of ¹⁴Trp and heme moiety. The large peak at 345 nm implies that ¹⁴Trp is located in a hydrophilic and exposed environment (35), which leads us to speculate that protein structure around ¹⁴Trp does not completely fold in the chimeric $\alpha\beta$ (M4)-subunit as found in denatured proteins (35).

Partially unfolded structure in the chimeric $\alpha\beta$ (M4)-subunit is confirmed by the SAXS measurements. Large $I(0)$ value in the Guinier plot for the chimeric $\alpha\beta$ (M4)-subunit suggests aggregation, corresponding to many fluctuations and/or partial exposure of hydrophobic residues in the chimeric $\alpha\beta$ (M4)-subunit. In the Kratky plot, the peak for the chimeric $\alpha\beta$ (M4)-subunit is low and asymmetric, which is also characteristic of partially denatured globular structure (24). Together with these spectral data, the chimeric $\alpha\beta$ (M4)-subunit does not fold as does the native subunit and some parts of the chimeric protein appear to remain unfolded and largely fluctuate. Such large fluctuation would be related with the destabilization for the chimeric $\alpha\beta$ (M4)-subunit as suggested in the urea denaturation experiment, where melting of the secondary structure was observed in the chimeric $\alpha\beta$ (M4) subunit at the lower urea concentration than in the native β subunit. The non-cooperative denaturation of the chimeric $\alpha\beta$ (M4)-subunit also implies that its folded structure is different from the α - and β -subunits of native globin.

On the other hand, as our previous studies have shown, the structure of the $\beta\alpha$ (M4)-subunit is quite similar to that of the β -subunit (2). In the present study, the spectral features in the CD spectra of the chimeric $\beta\alpha$ (M4)-subunit are typical of the globin proteins, indicating the heme environment and secondary structure are retained despite this module substitution. Also, based on the fluorescence spectra, ^{37}Trp and ^{15}Trp of the chimeric $\beta\alpha$ (M4)-subunit are located in the similar environment to those of the β -subunit. The stable globin structure in the $\beta\alpha$ (M4)-subunit is manifested in the SAXS and urea denaturation measurements. The R_g and $I(0)$ values for the chimeric $\beta\alpha$ (M4)-subunit were estimated to be the same as those of native Hb tetramer. The denaturation curve for the chimeric $\beta\alpha$ (M4)-subunit is similar to that of Hb.

It is quite interesting that the chimeric $\alpha\beta$ (M4)- and $\beta\alpha$ (M4)-subunits exhibited remarkable differences in their structure and stability. Based on the computer modelling of the $\alpha\beta$ (M4)-subunit, the side chains of ^{125}Tyr (in the module M4 in the β -subunit) would be located around the indole group of ^{14}Trp (in the module M1 of the α -subunit), which might induce some steric constraint between the two side chains. Since Jennings and Wright showed that the packing between the A (M1), G (M4), and H helices (M4) are formed in the first step of the folding process in apo Mb (36), and these helices are crucial in protein folding of globins, the steric hindrance between the side chains of ^{125}Tyr (M4) and ^{14}Trp (M1) could interfere with the packing of the modules M1 and M4, thereby resulting in the destabilization of the globular structure of the

chimeric $\alpha\beta$ (M4)-subunit. The fluorescence spectra for the chimeric $\alpha\beta$ (M4)-subunit also indicates that the micro-environment around ^{14}Trp is much different from that in the native α -subunit. Such steric hindrance cannot be found between modules M1 and M4 of the $\beta\alpha$ (M4)-chimeric subunit, which leads to the formation of the stable packing between the helices of the modules M1 and M4. Although the quantitative analysis and comparison of the effects of the module substitution on the globin structure between the two chimeric globins have not yet been done due to lack of their structural information, it can be safely said that prominent steric hindrance is less in the $\beta\alpha$ (M4)-subunit than in the $\alpha\beta$ (M4)-subunit.

In our previous paper, we suggested that the modules are structural and functional units that have the advantage of producing stable functional proteins by their combinations (2). However, the large structural changes and destabilization for the chimeric $\alpha\beta$ (M4)-subunit, which were never observed in the chimeric $\beta\alpha$ (M4)-subunit, indicate that the simple substitutions of the modules are not enough to construct stable globins. The steric constraint between side chains exerted by the module substitution would prevent the chimeric globin from forming the stable globular structure as discussed above, suggesting that interactions between modules are essential to stabilize the globular structure.

Association Properties of Chimeric Subunits - Schematic representation for the subunit interactions in the mixture of the chimeric and native subunits is illustrated in Fig. 8 (6). In the chimeric $\alpha\beta$ (M4)-globin, the module substitution would create some interactions between the modules M2 + M3 and M4 of the two chimeric $\alpha\beta$ (M4)-subunits and also between their modules M4, which are not found for the α -subunits. These new subunit interactions formed by the substitution of the module M4 would lead to the formation of homotetramer, $(\alpha\beta\text{(M4)})_4$. Although the elution peak for the chimeric $\alpha\beta$ (M4)-subunit appeared at the position of the tetrameric globin, the broad elution peak for the chimeric $\alpha\beta$ (M4)-subunit suggests the formation of oligomeric globins other than the tetrameric globin. Such a broad peak was also encountered for unstable protein solution, in which the protein has a high molecular dispersity (37). The Guinier plot for the chimeric $\alpha\beta$ (M4)-subunit shows negative steep gradient in the small Q region, which is also suggestive of the existence of several oligomeric globins. We cannot also rule out the possibility of the elongated dimer formation in the chimeric $\alpha\beta$ (M4)-subunit. Previous studies on the molten-globule state of apomyoglobin and cytochrome c pointed out that

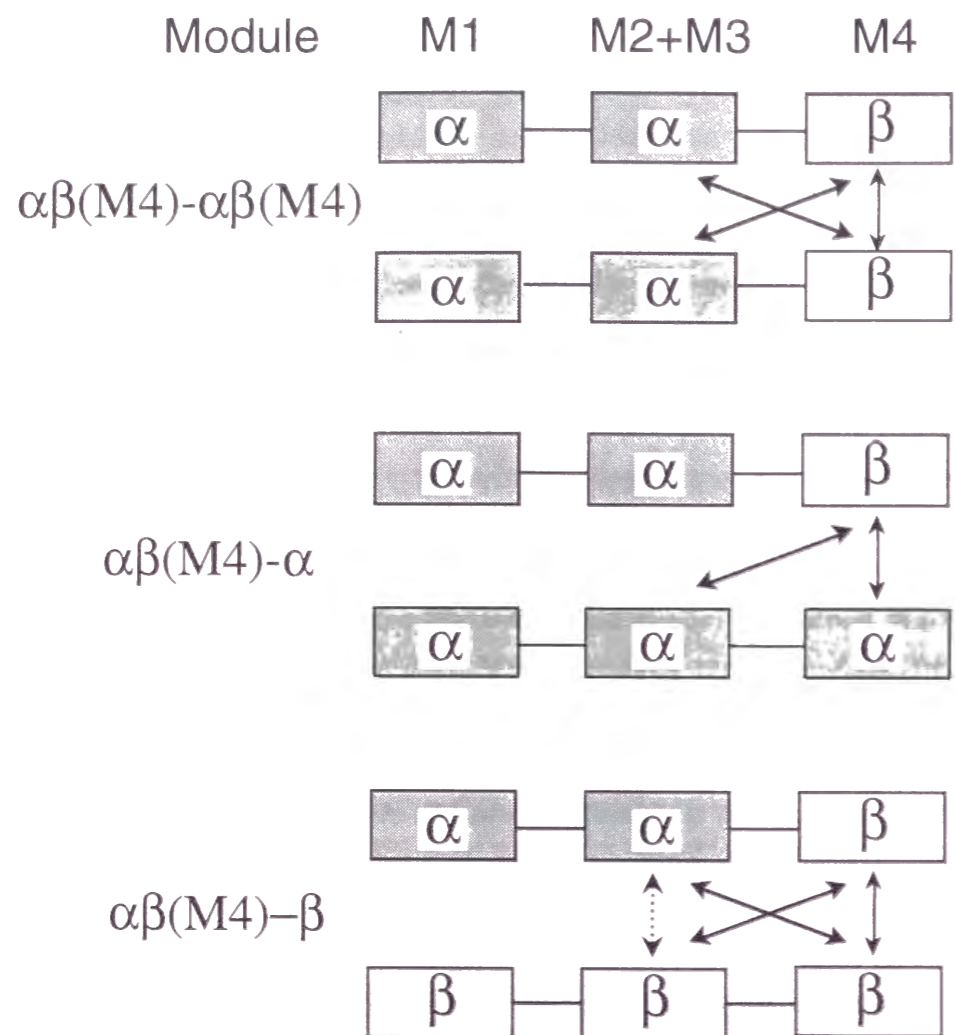


Fig.8. Interactions between the modules of the chimeric $\alpha\beta(M4)$ -subunits and those of the native subunits Predicted interactions at the α_1 - β_1 (solid line) and α_1 - β_2 (dotted line) contacts in native and module-substituted globin subunits are expressed as arrows.

the molecular radius of a partly unfolded dimer state could be enlarged as much as that of a stable tetramer in the native state (38, 39) so that it is possible that the elution volume of the chimeric $\alpha\beta(M4)$ -subunit coincides with that of native tetrameric Hb in the gel chromatogram.

The unstable structure in the associated chimeric $\alpha\beta(M4)$ -subunit can be interpreted in terms of the differences of the subunit interfaces between the chimeric and native subunits. As the CD and fluorescence spectra show, it is unlikely that the structure of the interface in the tetrameric chimeric globins

was conserved as found for the native subunit, which is also supported by the effects of NaCl on the association property. In the native Hb tetramer, the addition of NaCl facilitates its dissociation into dimers, due to perturbation of the salt bridges and hydrogen bonds which play a crucial role in α_1 - β_2 subunit interface (40). The negligible effect of NaCl on the association property of the chimeric $\alpha\beta(M4)$ -subunit suggests that electrostatic interactions such as hydrogen bonds and salt bridges would not be essential in the interface of the associated chimeric globin. Based on the remarkable dispersity of the associated states for the chimeric $\alpha\beta(M4)$ -subunit (Figs. 6 and 7), the structural disorder would induce unspecified interactions between the exposed hydrophobic residues, which might be responsible for the association in the chimeric $\alpha\beta(M4)$ -subunit.

In the presence of the native β -subunit, the elution pattern indicated that the homotetramer of the chimeric $\alpha\beta(M4)$ -subunits dissociates and an $(\alpha\beta(M4))_2\beta_2$ heterotetramer forms. Since the crystallographic study of the native β -subunit showed that the module M4 of the β -subunits interacts with the module M4 of the other β -subunits (33, 41, 42), it is plausible that there are many interactions between the chimeric $\alpha\beta(M4)$ - and the native β -subunit to form the stable heterotetramer as shown in Fig. 8.

On the other hand, addition of the α -subunit did not induce the dissociation of the tetrameric $\alpha\beta(M4)$ -subunit and the formation of the heterotetramer was never observed. Due to weak interactions between the two α -subunits (32), interactions for formation of the heterotetramer between the native α - and chimeric $\alpha\beta(M4)$ -subunits are only formed between the module M4 of the chimeric $\alpha\beta(M4)$ -subunit and the modules M2 + M3 and M4 of the α -subunit (Fig. 8), which would be much weaker than those of the homotetramer, $(\alpha\beta(M4))_4$.

CONCLUSION

In summary, the substitution of the module M4 in the α -subunit for that of the β -subunit induces structural alterations in the heme vicinity as well as in the global structure of globins. The resulting structural defects would originate from the failure of the stable packing of the helices in the modules M1 and M4. Comparison with our previous results of the chimeric $\beta\alpha(M4)$ -subunit suggests that the module cannot be a structural unit without the stable and proper interactions between the modules. Thus, we can conclude that, although module substitution would be useful in the first step to design novel

functional proteins, structural collapse must be considered in module-based protein design and fine tuning by site-directed or random mutagenesis is required to recover protein structure and optimize function.

ACKNOWLEDGMENTS

Grateful acknowledgment is dedicated to Dr. Yoshinao Wada for fast atom bombardment mass spectrometry. We are very indebted to the referee for many suggestions on our study.

REFERENCES

1. Go, M. (1981) *Nature* **291**, 90-92
2. Wakasugi, K., Ishimori, K., Imai, K., Wada, Y., and Morishima, I. (1994) *J. Biol. Chem.* **269**, 18750-18756
3. Go, M. (1983) *Proc. Natl. Acad. Sci. U.S.A.* **80**, 1964-1968
4. Gilbert, W. (1978) *Nature* **271**, 501
5. Blake, C. C. F. (1979) *Nature* **277**, 598
6. Eaton, W. A. (1980) *Nature* **284**, 183-185
7. Craik, C.S., Buchman, S. R., and Beychok, S. (1980) *Proc. Natl. Acad. Sci. U.S.A.* **77**, 1384-1388
8. Craik, C.S., Buchman, S. R., and Beychok, S. (1981) *Nature* **291**, 87-90
9. De Sanctis, G., Falcioni, G., Giardina, B., Ascoli, F., and Brunori, M. (1986) *J. Mol. Biol.* **188**, 73-76
10. De Sanctis, G., Falcioni, G., Giardina, B., Ascoli, F., and Brunori, M. (1988) *J. Mol. Biol.* **200**, 725-733
11. De Sanctis, G., Falcioni, G., Grelloni, F., Desideri, A., Polizio, F., Giardina, B., Ascoli, F., and Brunori, M. (1991) *J. Mol. Biol.* **222**, 637-643
12. Di Iorio, E.E., Yu, W., Calonder C., Winterhalter, K. H., Sanctis, G. D., Falcioni, G., Ascoli, F., Giardina, B., and Brunori, M. (1993) *Proc. Natl. Acad. Sci. U. S. A.* **90**, 2025-2029
13. Tame, J., Shih, D., Pagnier, J., Fermi, G., and Nagai, K. (1991) *J. Mol. Biol.* **218**, 761-767
14. Nagai, K., and Thøgerson, H.C. (1984) *Nature* **309**, 810-812
15. Nagai, K., and Thøgerson, H.C. (1987) *Methods Enzymol.* **153**, 461-481
16. Nagai, K., Perutz, M. F., and Poyart, C. (1985) *Proc. Natl. Acad. Sci. U.S.A.* **82**, 7252-7257
17. Wada, Y., Fujita, T. Hayashi, A., Sakurai, T., and Matsuo, T. (1989) *Biomed. Environ Mass Spectrom.* **18**, 563-565
18. Fasman C. D. (1976) *Handbook of Biochemistry Molecular Biology*, 3rd ed., A Proteins, vol. 1. CRC Press, Ohio
19. Greenfield, N. and Fasman, G. D. (1969) *Biochemistry* **8**, 4108
20. Konno, T. and Morishima, I. (1993) *Biochim. Biophys. Acta.* **1162**, 93-98
21. Ueki, T., Hiragi, Y., Kataoka, M., Inoko, Y., Amemiya, Y., Izumi, Y., Tagawa, H., and Muraga, Y. (1985) *Biophys. Chem.* **23**, 115-124
22. Kataoka, M., Head, J. F., Persechini, A., Kretsinger, R. H. and Engleman, D.M. (1991) *Biochemistry* **30**, 1188-1192
23. Kataoka, M., Head, J. F., Seaton, B. A. and Engleman, D. M. (1989) *Proc. Natl. Acad. Sci. U. S. A.* **86**, 6944-6948
24. Glatter, O. and Kratky, O. (1982) *Small Angle X-ray Scattering*, Academic Press, New York
25. Guinier, A. and Fournet, B. (1955) *Small Angle Scattering of X-rays*, John Wiley, New York
26. Rachmilewitz, E. A., Peisach, J., and Blumberg, W. E. (1971) *J. Biol. Chem.* **246**, 3356-3366
27. Beychok, S., Tyuma, I., Benesch, R. E., and Benesch, R. E. (1967) *J. Biol. Chem.* **242**, 2460-2462
28. Hsu, M. and Woody, R. W. (1971) *J. Am. Chem. Soc.* **93**, 3515-3525
29. Hirsh, R. E. and Peisach, J. (1986) *Biochim. Biophys. Acta.* **872**, 147-153
30. Hirsch, R. E., Zukin, R. S. and Nagel, R. L. (1980) *Biochem. Biophys. Res. Commun.* **93**, 432-439
31. Olah, G. A., Trakhanov, S., Trehwella, J. and Quioco, F. A. (1993) *J. Biol. Chem.* **268**, 16241-16247
32. Valdes, R. Jr., and Ackers, G. K. (1977) *J. Biol. Chem.* **252**, 74-81
33. Tainsky M. and Edelstein J. (1973) *J. Mol. Biol.* **75**, 735-739
34. Jonathan, D. H., and Charles, L. B. III (1994) *J. Mol. Biol.* **243**, 173-178
35. Burstein, E. A., Vedenkina, N. S. and Ivkova, M. N. (1973) *Photochem. Photobiol.* **18**, 263-279
36. Jennings, P. A., and Wright, P. E. (1993) *Science* **262**, 892-896
37. Wakasugi, K., Inaba, K., Ishimori, K. and Morishima, I. (1997) *Biophys. Chem.* in press
38. Kataoka, M., Hagihara, Y., Mihara, K. and Goto, Y. (1993) *J. Mol. Biol.* **229**, 591-596
39. Kataoka, M., Kuwajima, K., Tokunaga, F. and Goto, Y. (1997) *Protein Sci.* **6**, 422-430
40. Fermi, G. (1975) *J. Mol. Biol.* **97**, 237-256

41. Gloria, E. O., Borgstahl, Paul, H. R., and Arthur, A. (1994) *J. Mol. Biol.* **236**, 817-830
42. Gloria, E.O., Borgstahl, Paul, H. R., and Arthur, A. (1994) *J. Mol. Biol.* **236**, 831-843

FOOTENOTES

¹Abbreviations: Hb; hemoglobin, Mb; myoglobin

²In this study, we prepared the chimeric $\alpha\beta$ (M4)-subunit by connecting the α -subunit with the α -subunit at the position of FG 3. On the other hand, module M3 and module M4 are separated at the position between G6 and G7 (Go, 1981), which is 8 amino acids downstream from the connection site. The homology between the α - and β -subunits in this region is very high, and the different amino acids are located at only three positions, FG4 (Arg(α), His(β)), G3 (Val(α), Glu(β)) and G6 (Lys(α), Arg(β)). The substitutions at the FG4 and G6 retain the hydrophathy index of the amino acid residues at these positions. On the basis of the crystallography, no direct interactions through the G3 position were observed in the α 1- β 2 intersubunit. Consequently, it is unlikely that the shift of the connection site causes serious complexities in interpreting structure and function of the chimeric subunit.

³In this denaturation experiments, we used cyano-met derivatives of the samples to prevent aggregation of dissociated heme for the reversible denaturation. In this condition, however, the reversibility was about 50 % probably due to irreversible loss of heme. The incomplete reversibility was also encountered for the previous study on the denaturation of myoglobin (Konno *et al.*, (1993) *Biochim. Biophys. Acta.* **1162**, 93-98).

⁴We have examined effects of addition of small percentage (5, 10, 15 and 20 %) of TFE on structure for the chimeric $\alpha\beta$ (M4)-subunit to recover the α -helical contents and stabilize the globin structure. The α -helical content were recovered from 30 to 50 % by the addition of TFE. However, no significant changes was detected for the CD spectrum in the Soret region, indicating that heme environmental structure is still highly perturbed in the $\alpha\beta$ (M4)-subunit in the presence of TFE. We have also tried to stabilize the chimeric $\alpha\beta$ (M4)-subunit by addition of other chemicals such as glycerol and D-sorbitol, but no significant stabilization effects were observed for the CD spectra in far UV and Soret region.

Chapter 2

X-ray Crystallographic Study on a Fine-tuning Mutant (F133V) of the Module Substituted $\beta\alpha$ (M4)-subunit

ABSTRACT

In order to elucidate the structure of the module substituted globin, $\beta\alpha(\text{M4})$ -subunit, in detail, we have tried x-ray crystal structure analysis of the subunit in a carbonmonoxy form. We have succeeded in the crystallization of the $\beta\alpha(\text{M4})$ -subunit by removing a steric hindrance between ^{71}Phe and ^{133}Phe with recourse to a site-directed mutagenesis, ^{133}Phe to Val (F133V). In the crystal structure analysis, it was found that tertiary structure of the $\beta\alpha(\text{F133V})$ -subunit are not completely superimposed on that of the β -subunit. The segment corresponding to the module M4 in the $\beta\alpha(\text{F133V})$ -subunit remarkably moves from the original position to close to that of the α -subunit, strongly suggesting that the module M4 is a quasi-indepent structural unit in globin structure. However, the substitution of the module M4 simultaneously caused structural perturbations on some other regions through the intramolecular interactions between the modules. On the other hand, although the homotetramer structure $[\beta\alpha(\text{F133V})]_4$ are quite similar to that of the native β_4 , the $\beta\alpha(\text{F133V})_1$ - $\beta\alpha(\text{F133V})_3$ and $\beta\alpha(\text{F133V})_1$ - $\beta\alpha(\text{F133V})_2$ interface structures are different from the β_1 - β_2 and β_1 - β_3 ones. Of particular interest is that two salt bridges between ^{97}Arg and ^{43}Glu and between ^{99}Asp and ^{40}Arg in the $\beta\alpha(\text{F133V})_1$ - $\beta\alpha(\text{F133V})_3$ interface, which would be crucial for the tetramer formation of the $\beta\alpha(\text{F133V})$ -subunit. Thus, the module substitution caused substantial alterations in structure and function of hemoglobin subunit, which reflects structural and functional significance of the modules and the modular interactions in globin proteins.

INTRODUCTION

Go's geometrically determined modules are supposed to be a compact structural unit relevant to function in proteins (1, 2). On the basis of this concept for the modules, their structural and functional significance should be reflected in many proteins. Hemoglobin is one of such proteins. Hemoglobin α - and β -subunits are composed of the modules M1-M4 (Fig. 1), and M4 is particularly noted as a functional module regulating subunit assembly. In fact, the module substituted globin, $\beta\alpha$ (M4)-subunit, where the module M4 of hemoglobin β -subunit is replaced by that of the α -subunit, exhibited the α -subunit like association property, which strongly suggests that the module M4 in hemoglobin is a functional unit dominant in subunit assembly.

On the contrary to functional significance of the module M4, its structural meaning is still unclear. NMR measurements revealed that the heme environmental structure of the $\beta\alpha$ (M4)-subunit remains to be β -subunit like (3), but structural informations on the other regions including the module M4 have not yet been obtained at all. Furthermore, tetramer structure the $\beta\alpha$ (M4)-subunit constructs and its self-association mechanism have not been exactly investigated. Does the implanted module M4 in the $\beta\alpha$ (M4)-subunit conserve tertiary structure of the α -subunit? How does the implanted module M4 contribute to formation of the homo-tetramer $[\beta\alpha$ (M4)]₄. Acquisition of these structural insights would allow us to evaluate the structural significance of the module M4.

We have herewith conducted a x-ray crystallographic study of the $\beta\alpha$ (M4)-subunit. However, the crystallization of the $\beta\alpha$ (M4)-subunit did not proceed smoothly because of substantial aggregation. Based on a computer modelling technique, the side chain of ¹³³Phe in the $\beta\alpha$ (M4)-subunit is distorted because of collision with that of ⁷¹Phe, which might cause enhancement in local fluctuation, resulting in the failure of the crystallization. Accordingly, a site-directed mutagenesis (F133V) was introduced to remove the provable collision between side-chains of ¹³³Phe and ⁷¹Phe. With recourse to the mutation, we have performed x-ray crystal structure analysis of the $\beta\alpha$ (M4)-subunit with a resolution of 2.5 Å. In this study, we are especially concerned about the structure of the implanted module M4 and subunit interface structure of the homo-tetramer $[\beta\alpha$ (M4)]₄. The present study would provide further insights into structural and functional properties of the module M4. In addition, of note is that this is the first crystal structure analysis of module substituted proteins and one of yet few structure analyses of heavily engineered proteins.

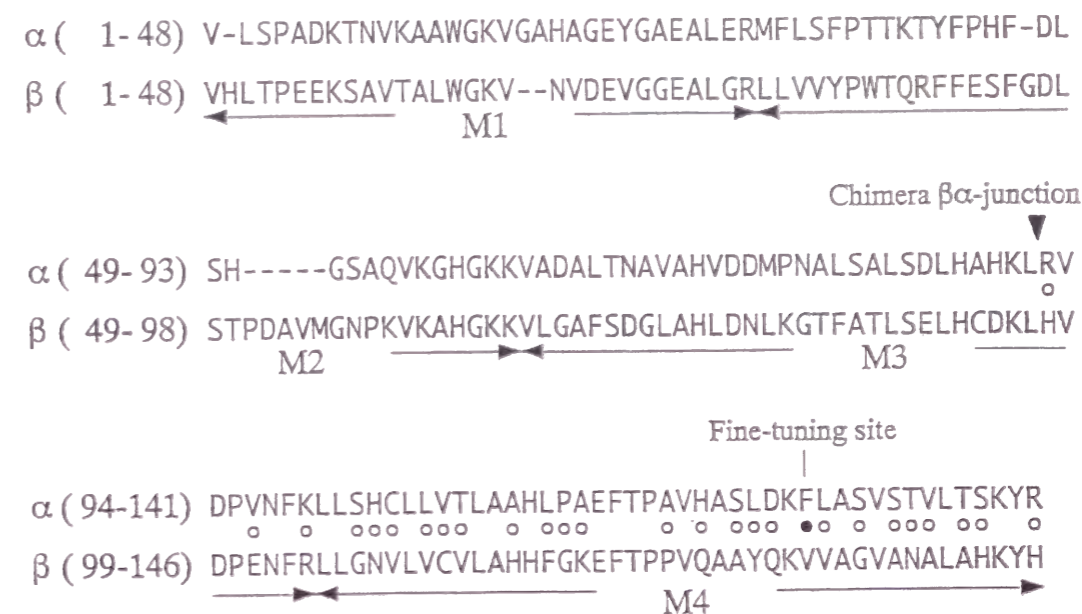


Fig. 1 Amino acid sequence comparison between α - and β -subunits of human hemoglobin. The regions of modules M1-M4 are indicated below the sequences. The position, at which the sequences of the two subunits are interchanged from β to α in chimera $\beta\alpha$ (M4)-subunit, is indicated by the downward arrowhead. There is eight residues discrepancy between the chimera junction and the border of modules M3 and M4. The residue sites that are different between α - and β -subunits in the module M4 are indicated by open circles. The filled circle indicates the position of the F133V mutant.

EXPERIMENTAL PROCEDURES

Computer aided design of a $\beta\alpha$ (F133V)-subunit - A residue site of the $\beta\alpha$ (M4)-subunit for a target of fine-tuning mutagenesis was determined by using the method of computer modeling. A molecular model of the $\beta\alpha$ (M4)-subunit was constructed on the basis of the crystal structure of human hemoglobin A (BNL code 1HGB) as follows: (1) C α atoms of residues 92-141 of the α -subunit was superimposed on the corresponding C α atoms (residues 97-146) of the β -subunit to minimize their root mean square deviation (R. M. S. D.). (2) The portion of the β -subunit was replaced with the superimposed structure of the α -subunit. (3) Leu96 (the C-terminal residue of β -subunit region) and His92 of the α -subunit (the N-terminal residue of the region from the subunit) was connected by a peptide bond with arbitrary geometry. The numbering system of the chimeric subunit was coordinated with that of the β -subunit so that His92 of the α -subunit corresponds to His97 of the chimeric subunit and so on (Fig. 1a). (4) The total energy of the model was minimized in order to reduce hindrance of atoms and correct the arbitrary peptide bond at the $\beta\alpha$ -junction.

The program insight II (Molecular Simulations Inc.) was used for the molecular modeling and the program X-PLOR was used for the energy calculation (4).

Site-directed Mutagenesis - Site-directed mutagenesis of the Phe133 in the chimeric $\beta\alpha$ (M4)-subunit was carried out by using the polymerase chain reaction (PCR) technique with T7 $\beta\alpha$ (M4)-subunit as a template (3), where the methionine residue was introduced to the N-terminal to initiate the peptide elongation for the module substituted subunit. The synthetic oligonucleotide 5'-CTG GAC AAG GTA CTG GCT TCT GTG AGC ACC-3' was used as a primer to multiply double-stranded DNA fragments bearing mutation (Phe133 --> Val). The mutated DNA fragments were then ligated into the plasmid at 16 °C for 1 hour by utilizing the *Hind* III - *Hind* III restriction enzyme sites in the T7 $\beta\alpha$ (M4)-subunit vector. We used *E. coli* strain BL 21 to transform the ligation mixture with ampicillin resistance. Introduction of the mutation was verified by double-stranded DNA sequence analysis (373 DNA sequencer, Applied Biosystems).

Protein Preparation - The chimeric $\beta\alpha$ (F133V)-subunit was purified as previously reported for recombinant Hb (3, 6-9). We confirmed the expression of the desired subunit by fast atom bombardment mass spectroscopy (data not shown) (5) and no additional mutations were detected.

Crystallization of [CO- $\beta\alpha$ (F133V)]₄ - The $\beta\alpha$ (F133V)-subunit tetramer was crystallized in carbonmonoxy form¹. The crystal was prepared with the hanging drop vapor diffusion method. Preliminary crystallization conditions were determined with the sparse-matrix sampling method (10). The optimized condition for [CO- $\beta\alpha$ (F133V)]₄ was 1 ml of 25% (w/v) PEG4000 solution in 0.1 M K₂HPO₄-NaH₂PO₄ buffer (pH 6.5) for a reservoir, a 10 ml mixture of equal volumes of the reservoir solution and a 600 μ M protein solution in 50mM sodium phosphate buffer (pH 7.0) for a hanging drop. The crystal grew in one week at 18 °C under each condition.

X-ray diffraction data collection and processing - X-ray diffraction data of a [CO- $\beta\alpha$ (F133V)]₄ crystal were collected with the oscillation method using Cu K α radiation ($\lambda = 1.54 \text{ \AA}$) from Rigaku RU-300 generator, operating at 45 kV x 80 mA, with a double-mirror monochromator. The reflections were collected by DIP100 imaging plate detector (MAC Science Co., Ltd.). The frame images were processed into sets of intensity data using the programs DENZO and SCALEPACK (11)

Crystallographic Refinement - The atomic model of [CO- $\beta\alpha$ (F133V)]₄ was constructed on the basis of a β -subunit tetramer (12, 13). The crystallographic refinement was executed by recurrently applying conjugate-gradient positional

refinement, B-factor refinement with the program X-PLOR (4) and manual model adjustments with the program turbo-FRODO (14). The model was refined against a total of 15212 reflections ($F > 3\sigma F$) between 8.0 and 2.5 \AA resolution, saving 5 % of the observed reflections for a test set. Side chains and carbonmonoxy heme groups were built into the 2F_o-2F_c electron density map. Non-crystallographic symmetry (NCS) constraint was introduced when the crystallographic R-factor became 0.152 (free-R = 0.251). Two monomers, β_1 - and β_3 -subunits which correspond to α_1 and β_2 -subunits in hemoglobin tetramer, respectively, were selected as the NCS asymmetric unit and the two-fold symmetry between dimers $\beta_1\beta_3$ and $\beta_2\beta_4$ was used for the NCS operator. Initial NCS parameters were obtained from a superposition of C α atoms between the dimers, and they were refined in later stage by map averaging using the program DM (15). The refinement was continued applying cycles of NCS operator refinement, simulated annealing, B-factor refinement and manual manipulations of the model. Six side chains, Arg40, Arg97 and His 108 in β_1 -subunit and their equivalents in the β_3 -subunit were modeled as multiple conformers at this stage. The refinement converged at a crystallographic R-factor of 0.181 (free-R = 0.244). The crystallographic parameters, data collection and refinement statistics are summarized in Table I.

NMR Measurements - ¹H NMR spectra at 500 MHz were recorded on BRUKER Avance DRX 500 spectrometer equipped with the Indy workstation (silicon Graphics). In order to measure proton resonances in the diamagnetic region, we used a water gate pulse sequence with 50 μ s pulse and 33 K data points over 13-kHz spectral width and minimized the water signal in the sample. The probe temperature was controlled at 290 \pm 0.5 K by a temperature control unit of the spectrometer. The volume of the NMR sample was 600 μ l and the concentration was 1 mM on the heme basis. Proton shifts were referenced with respect to the proton resonance of 2, 2,-dimethyl-2-silapentane-5-sulfonate (DSS).

Oxygen Equilibrium Curves and Analysis - Oxygen equilibrium curves were measured by using an improved version (16, 17) of an auto-oxygenation apparatus (18). The wavelength of the detection light was 560 nm. The temperature of the sample in the oxygenation cell was constant at 25 \pm 0.05 °C. Sample concentration was 60 μ M on the heme basis, and the sample volume was 6 ml. The hemoglobin reductase system (19) was added to the sample before each measurement to reduce oxidized subunits. To minimize the autooxidation of the sample during the measurements, catalase and superoxide dismutase were added to the sample and the concentration was 0.1

μM (20, 21). The oxygenation data were acquired by use of a micro-computer (model PC-98XA, Nippon Electric Co., Tokyo), which was interfaced to the oxygenation apparatus (22).

RESULTS AND DISCUSSIONS

Designing a fine-tuned $\beta\alpha(\text{F133V})$ -subunit for crystallization - In an initial attempt for crystallization of chimeric $\beta\alpha(\text{M4})$ -subunit, it was found that the proteins heavily precipitated under conditions in which native β -subunits did not. Presumably, the module substitution would lead to perturbations on the intramolecular interactions between the module M4 and the other regions. Then we decided to introduce a site-directed mutation to the subunit for recovery of the interactions. A computer-aided modeling work was carried out to design the position and pattern of the point mutation.

It was assumed that some of the improper atomic contacts at the interface of implanted module M4 and other modules were the main cause of the perturbations. A molecular model of the chimeric $\beta\alpha(\text{M4})$ -subunit was constructed as written in Materials and Methods and applied for an energy minimization to identify the amino acid residues in aberrant contact (4). The initial total energy of the model was disparately high (> 103 kcal/mol) due to atomic overlap at the module interface, but finally it has converged at -4.5 kcal/mol. The root mean square deviation between 146 C^α atoms of the initial and final models was 1.3 \AA , which corresponds to a presumed structural transition induced by the implantation of the module M4 from the α -subunit.

From an inspection of the structural difference between the initial and final models in this energy minimization process, a drastic dislocation of atoms was found at the position where three aromatic side chains of Trp15, Phe71 and Phe133 were in contact (Fig. 2). The side chain of Phe71 was repelled outward upon the energy minimization process, which suggested existence of an intramolecular collision between side chains of Phe71 and Phe133 in the $\beta\alpha(\text{M4})$ -subunit. Accordingly, in order to reduce this steric hindrance, Phe133, the contact partner of Phe71 on module M4, was determined to be replaced with a valine residue, which has high hydrophobicity but smaller volume than Phe (23). This site-directed mutagenesis was expected to locally regain the intramolecular packing in the $\beta\alpha(\text{M4})$ -subunit.

X-ray characterization of crystals - Crystals of $[\text{CO-}\beta\alpha(\text{F133V})]_4$ were grown in pillar or plate shapes. A crystal ($0.9 \times 0.1 \times 0.1 \text{ mm}^3$) was used for a X-ray diffraction experiment. The diffraction data were collected around two

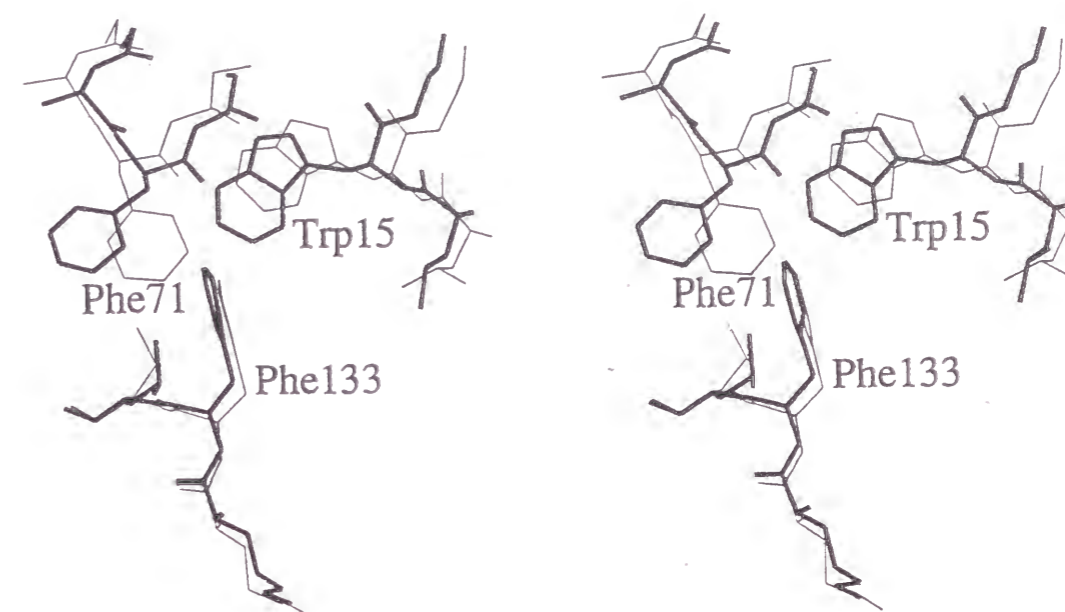


Fig. 2 Comparison of the molecular models of chimeric $\beta\alpha(\text{F133V})$ -subunit before (thin lines) and after (thick lines) energy minimization. Only the portion is presented, where a large shift of side chain (Phe71) has been observed.

different rotation axes from the crystal. The crystal reflections were processed to a resolution of 2.5 \AA . The higher angle reflections were rather weak in final stage of the diffraction experiment possibly due to radiation damage. Here, it should be noted here that the crystallographic parameters of $[\text{CO-}\beta\alpha(\text{F133V})]_4$ crystals were close to those of the β -subunit tetramer crystals (Table I). This strongly suggests that the quaternary structure and the crystal packing of the subunits are similar in those crystals. The similar crystal packing of $[\text{CO-}\beta\alpha(\text{F133V})]_4$ to that of the native β -subunit tetramer might be explained in that a majority of the residues, which are dissimilar in the α - and β -subunits on the module M4, are buried inside the tetramer.

Globin Structure of $\beta\alpha(\text{F133V})$ -subunit - As described in Experimental Procedures, the refinement of the crystal structure for the chimeric $\beta\alpha(\text{F133V})$ -subunit has been performed. Fig. 3 illustrates the back-bone structures of the native α -, β - and chimeric $\beta\alpha(\text{F133V})$ -subunits, where they are superimposed to minimize R. M. S. D. in their modules M4. As clearly shown in the figure, their tertiary structures are quite similar except for the loss of D-helix in the α -subunit, confirming that there are no substantial collapse in the tertiary structure of the $\beta\alpha(\text{F133V})$ -subunit. However, it should be noted here that the back-bone structure of the $\beta\alpha(\text{F133V})$ -subunit subtly but significantly deviates

Table I Crystallographic parameters and data collection

| | [CO- $\beta\alpha$ (F133V)] ₄ | [CO- β_4]* |
|-----------------------------|--|-------------------|
| Crystallographic parameters | | |
| Space Group | P2 ₁ | P2 ₁ |
| Unit cell dimensions | | |
| a(Å) | 62.9 | 63.3 |
| b(Å) | 81.3 | 82.4 |
| c(Å) | 55.1 | 53.7 |
| β (°) | 91.0 | 90.1 |
| Asymmetric unit | tetramer | tetramer |
| Data collection statistics | | |
| Resolution limit (Å) | 2.5 | 1.8 |
| No. of unique ref. | 17766 | 52563 |
| R _{sym} (%) | 8.8 | 4.75 |
| Completeness (%) | 91 | 94 |
| Refinement statistics | | |
| Model contents | | |
| NCS asymmetric unit | dimer | – |
| No. amino acid residues | 292 | 584 |
| No. non-H atom | 2320 | 4620 |
| No. water mol. | 22 | 132 |
| Working R-factor | 0.181 | 0.177 |

*Borgstahl et al. (1994)

from that of the β -subunit in some local parts. In Fig. 4, the perpendicular axis represents the difference in the distance between one C $^{\alpha}$ atom of the α -subunit and the corresponding one of the $\beta\alpha$ (F133V)-subunit, $d[\alpha - \beta\alpha(\text{F133V})]$, and the distance between the C $^{\alpha}$ atom of the β -subunit and the corresponding one of the $\beta\alpha$ (F133V)-subunit, $d[\beta - \beta\alpha(\text{F133V})]$. That is, a negative value of the difference implies that the position of the C $^{\alpha}$ atom in the $\beta\alpha$ (F133V)-subunit is similar to that in the α -subunit, and a positive value reflect that the position of the C $^{\alpha}$ atom in the $\beta\alpha$ (F133V)-subunit remains to be close to that of the β -subunit. Interestingly, this value is negative in the region of residue number 100-140 approximately corresponding to the module M4, which suggests that back-bone structure of the module m4 in the $\beta\alpha$ (F133V)-subunit is rather similar to that in the α -subunit. Consequently, the module M4 is considered to

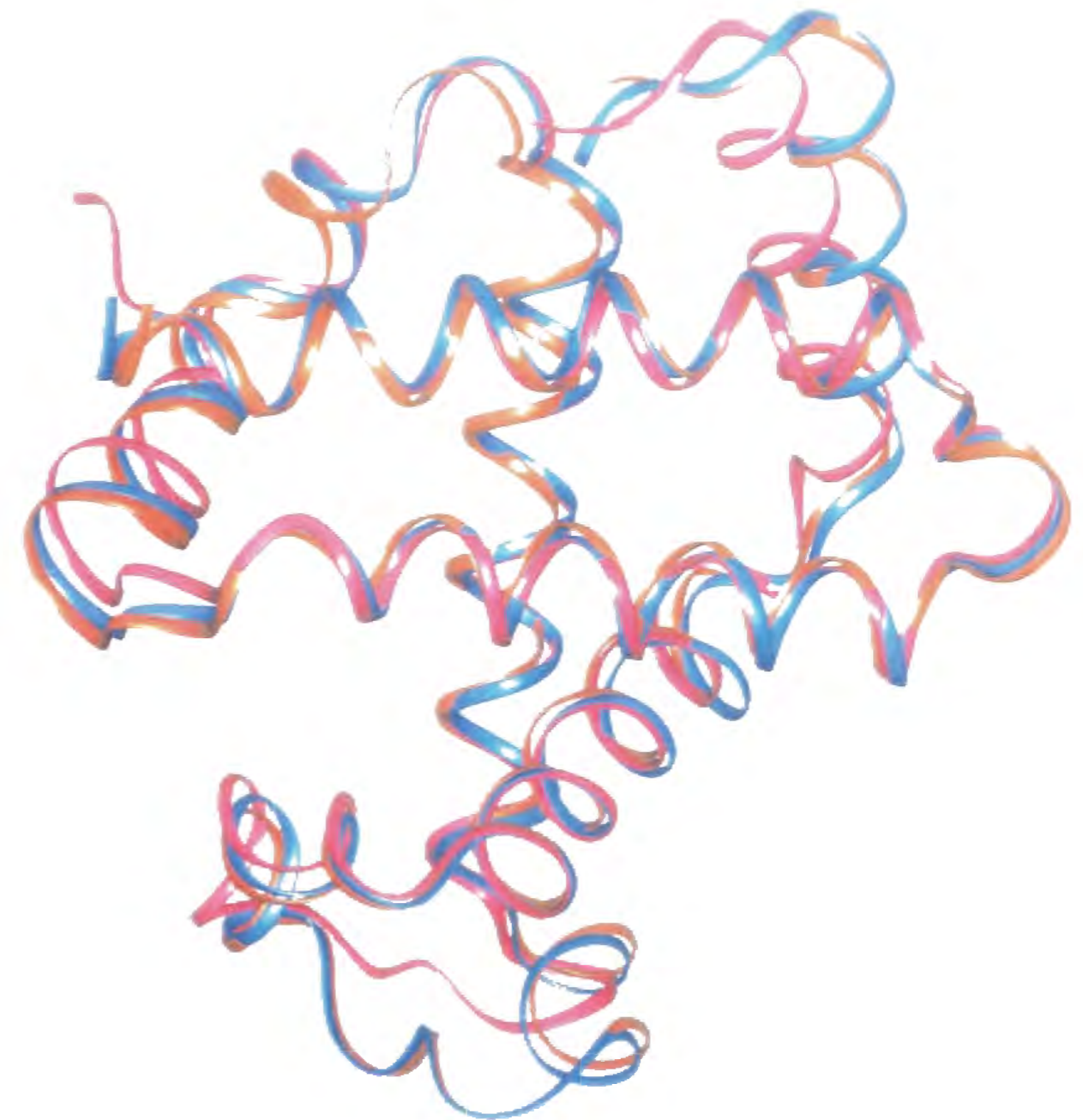


Fig. 3 Back-bone structures of the hemoglobin α -, β - and chimeric $\beta\alpha$ (F133V)-subunits. Ribbon represents main chains of the subunits. Colors correspond to the α -subunit (red), β -subunit (yellow) and $\beta\alpha$ (F133V)-subunit (blue).

behave as a quasi-independent structural unit in hemoglobin subunit. However, it is not negligible that structural conversion into the α -subunit type is also found in the segments from 25 to 40 and from 70 to 85, which reflects that the module M4 substitution causes structural alteration in these regions. Here, observations of intramolecular interactions in globin structure could provide some insights into such structural alterations. According to the inspection on the globin structure by Lesk and Chothia, the major interhelix contacts are A/H, B/E, B/G, F/H and G/H (24). Nevertheless, the module M4 includes both the G- and H-helices and homology of amino acid sequence between the α - and β -subunits is quite low (less than 40%), so that the substitution of the module M4 should accompany perturbations on most of those helix contacts. In fact, since the segment from 25 to 40, constructing most parts of the B-helix, is considerably relevant to the B/G packing, it would

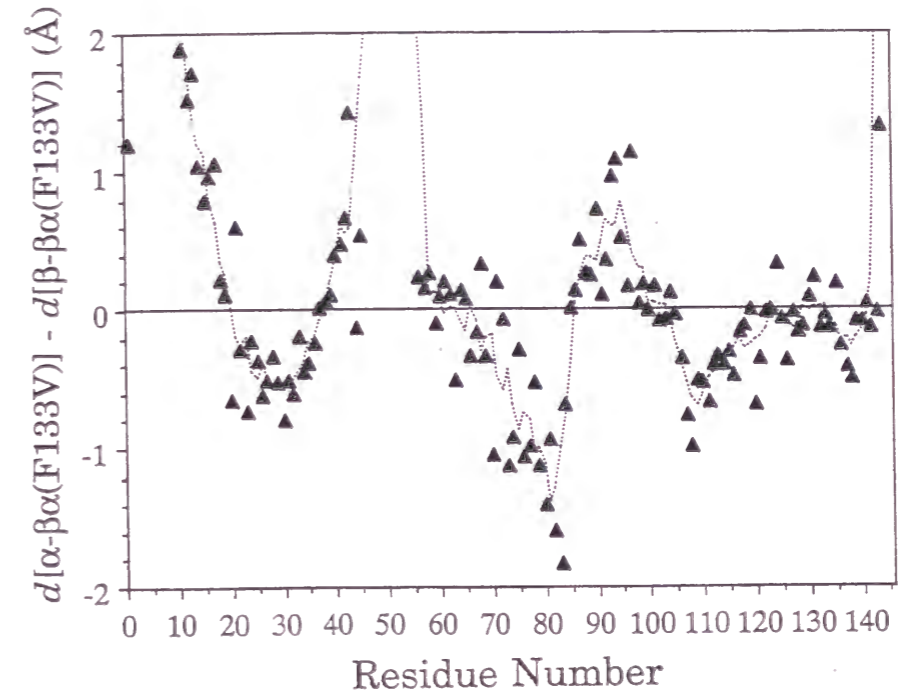


Fig. 4 Structural Comparisons between the α - and chimeric $\beta\alpha(\text{F133V})$ -subunits and between the β - and chimeric $\beta\alpha(\text{F133V})$ -subunits. A horizontal axis demonstrates residue number of the subunits. The perpendicular axis represents the difference in the distance between one C^α atom of the α -subunit and the corresponding one of the $\beta\alpha(\text{F133V})$ -subunit, $d[\alpha - \beta\alpha(\text{F133V})]$, and the distance between the C^α atom of the β -subunit and the corresponding one of the $\beta\alpha(\text{F133V})$ -subunit, $d[\beta - \beta\alpha(\text{F133V})]$. Large positive value in the region at the residue number of 45-55 corresponds to the defect of D-helix only in the α -subunit.

be reasonable that the M4 substitution involving exchange of G-helix altered the back-bone structure in this segment into the α -subunit type. Sequentially, this structural alteration might lead to the effects on the region from 70 to 85 contained in the E-helix and EF-corner through the B/E helix packing. Thus, the present comparison among the back-bone structures of the α -, β -, and $\beta\alpha(\text{F133V})$ -subunits indicate that the module M4 significantly determines its own structure for itself, but the module substitution induces substantial transformation in some parts through the helix packings.

Subunit Interface Structure of $\beta\alpha(\text{F133V})$ -subunit - Fig. 5 shows the tetramer structures of the β - and $\beta\alpha(\text{F133V})$ -subunits. As clearly illustrated in this figure, the tetramer structure of the $\beta\alpha(\text{F133V})$ -subunit is quite similar to that of the β -subunit. Such similarity in the quaternary structures of the β - and $\beta\alpha(\text{F133V})$ -subunits indicates that interaction sites between the $\beta\alpha(\text{F133V})$ -subunits almost corresponds to those between the β -subunits. However, since the $\beta\alpha(\text{F133V})$ -subunit formed a stable tetramer even below sample concentration of 1 μM (data not shown) where the β_4 tetramer dissociates completely to monomers (25), the subunit interface in the $[\beta\alpha(\text{F133V})]_4$ must be more tightly packed than that in the β_4 tetramer. To exactly compare the interfaces of the β - and $\beta\alpha(\text{F133V})$ -subunits, the close subunit contacts are listed in Tables II and III. In the Tables II, the number of the $\beta\alpha(\text{F133V})_1$ - $\beta\alpha(\text{F133V})_2$ close contacts, which corresponds to the α_1 - β_1 contacts in hemoglobin tetramer, is not remarkably different from that of the corresponding β_1 - β_2 ones (12), but it is to be noted that there are two strong hydrogen bonds between 122Phe and 30Arg and between 127His and 30Arg in the $\beta\alpha(\text{F133V})_1$ - $\beta\alpha(\text{F133V})_2$ interface as shown in Fig. 6. Such strong interactions were not observed in the β_1 - β_2 interface (12). Although it is difficult to assign free energies to these different subunit contacts, these two hydrogen bonds are probably the main reason for the increased $\beta\alpha(\text{F133V})_1$ - $\beta\alpha(\text{F133V})_2$ interactions relative to the β_1 - β_2 ones.

Interestingly, the formation of the hydrogen bond between 127His and 30Arg in the $\beta\alpha(\text{F133V})_1$ - $\beta\alpha(\text{F133V})_2$ interface would be also reflected in the NMR spectra in the hydrogen bonded proton region (Fig. 7). While no exchangeable proton signals were observed in the downfield region from 10 to 15 ppm for the isolated carbonmonoxy β -subunits, a broad proton signal at 12.5 ppm was detected for the $\beta\alpha(\text{F133V})$ -subunit. This peak disappeared in 100 % D_2O (data not shown). Such an exchangeable proton signal in the downfield region is also encountered for carbonmonoxy Hb A, which has been assigned to

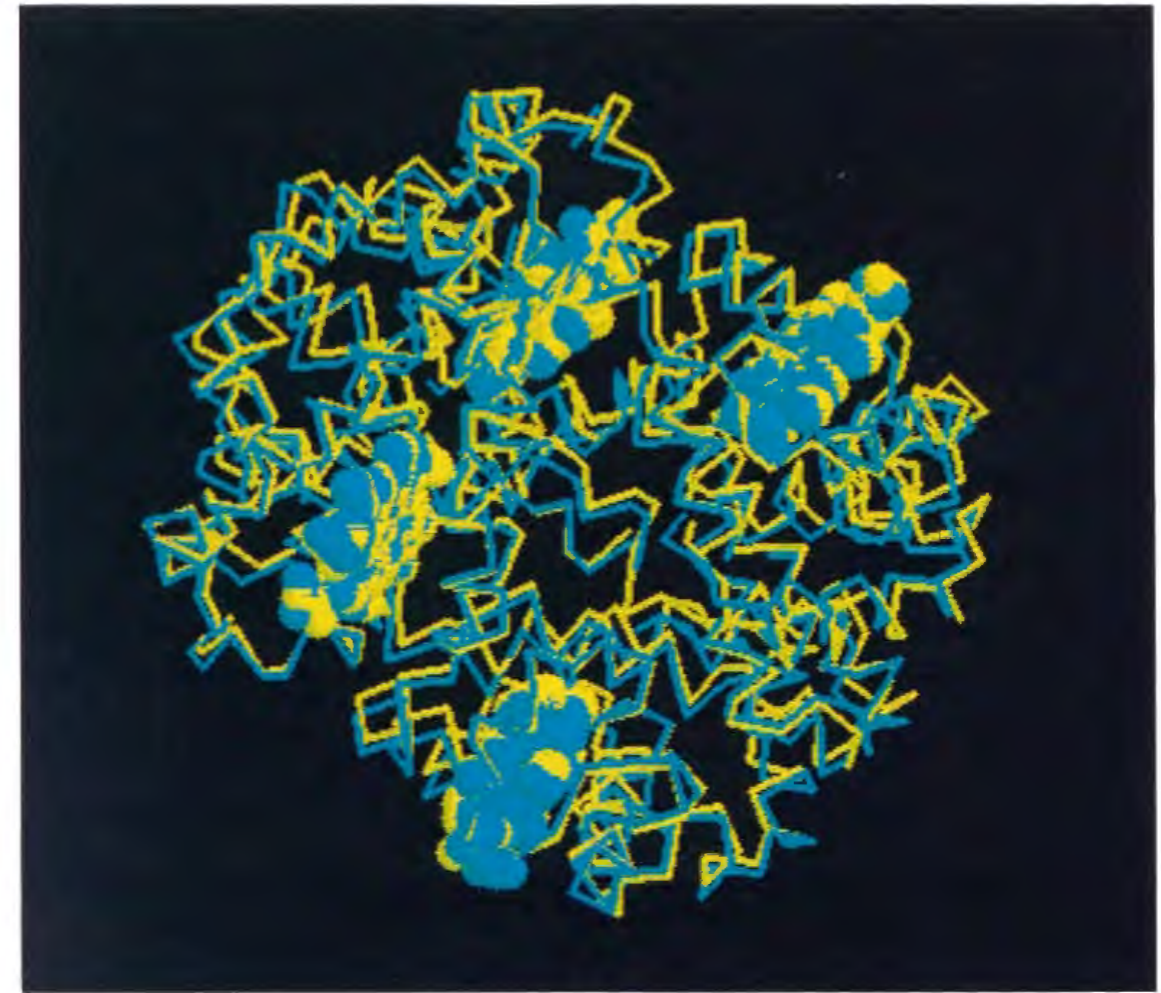


Fig. 5 Quaternary structures of the β_4 - and $\beta\alpha(\text{F133V})_4$ -tetramers. Heme molecules are expressed by a space filling model. Colors correspond to the β -subunit (yellow) and $\beta\alpha(\text{F133V})$ -subunit (blue).

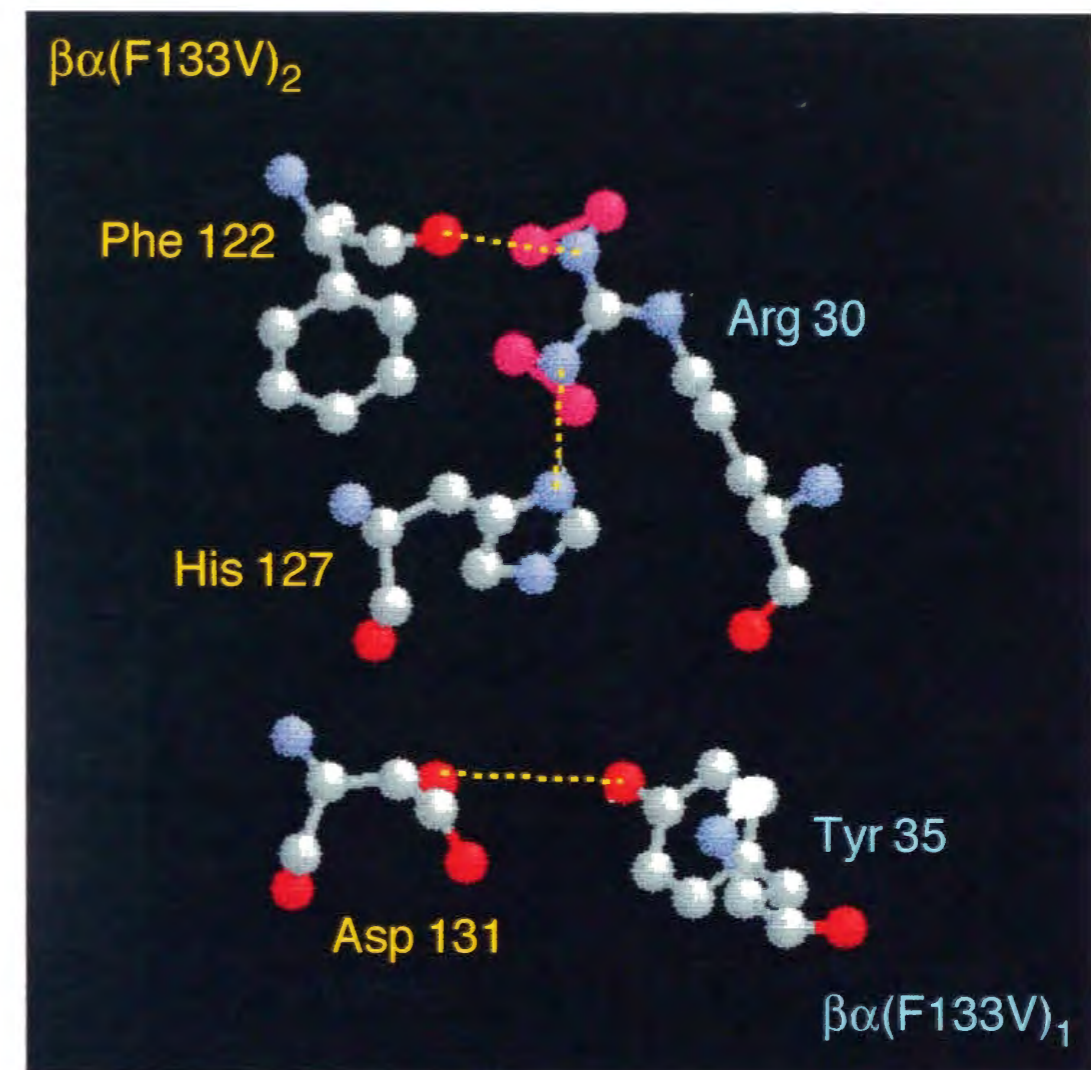


Fig. 6 $\beta\alpha(\text{F133V})_1$ - $\beta\alpha(\text{F133V})_2$ interface structure of $\beta\alpha(\text{F133V})_4$ -tetramers. The $\beta\alpha(\text{F133V})_1$ - $\beta\alpha(\text{F133V})_2$ interface corresponds to α_1 - β_1 interface in hemoglobin. Dotted lines represent a hydrogen bond in the interface.

Table II Subunit-subunit contacts of the $\beta\alpha(\text{F133V})_1$ - $\beta\alpha(\text{F133V})_2$ interface of the $[\text{CO-}\beta\alpha(\text{F133V})]_4$ and the corresponding β_1 - β_2 interface of the $[\text{CO-}\beta_4]^*$

| $\beta\alpha(\text{F133V})_1$ | | $\beta\alpha(\text{F133V})_2$ | | | | β_1 | | β_2 | | | |
|-------------------------------|----------|-------------------------------|-------------------|-------------|----------|-----------|----------|-------------------|-------------------|-------------|----------|
| residues | residues | Atoms | | Distance(Å) | | residues | residues | Atoms | | Distance(Å) | |
| 30Arg | 127His | N $_{\eta}$ | N $_{\delta}$ | 3.09 | H | 30Arg | 127Gln | N $_{\eta}$ | O $_{\epsilon 1}$ | 2.78 | H |
| 30Arg | 122Phe | N $_{\eta 1}$ | O | 2.93 | H | 30Arg | 122Phe | N $_{\eta}$ | O | 2.81 | H |
| 33Val | 124Pro | C $_{\gamma}$ | O | 3.59 | | | | | | | |
| 35Tyr | 131Asp | O $_{\eta}$ | O $_{\epsilon 2}$ | 3.81 | | 35Tyr | 131Gln | O $_{\eta}$ | N $_{\epsilon 2}$ | 3.54 | |
| 55Met | 124Pro | S $_{\delta}$ | C $_{\epsilon}$ | 3.63 | | | | | | | |
| 108His | 108His | N $_{\epsilon}$ | N $_{\delta}$ | 3.29 | H | | | | | | |
| 115Ala | 112Val | C $_{\beta}$ | O | 3.60 | | 115Ala | 112Cys | C $_{\beta}$ | O | 3.59 | |
| 115Ala | 116Ala | O | C $_{\alpha}$ | 3.52 | | 115Ala | 116His | O | C $_{\alpha}$ | 3.50 | |
| 116Ala | 115Ala | C $_{\alpha}$ | O | 3.32 | | 116His | 115Ala | C $_{\alpha}$ | O | 3.40 | |
| 116Ala | 119Pro | O | C $_{\beta}$ | 3.34 | | 116His | 119Gly | N $_{\epsilon 2}$ | O | 2.73 | H |
| | | | | | | 116His | 120Lys | N $_{\epsilon 2}$ | N | 3.70 | |
| | | | | | | 116His | 122Phe | N $_{\epsilon 2}$ | O | 3.42 | |
| 119Pro | 116Ala | C $_{\beta}$ | O | 3.47 | | 119Gly | 116His | O | N $_{\epsilon 2}$ | 3.12 | H |
| 122Phe | 30Arg | O | N $_{\eta 1}$ | 2.11 | H | 122Phe | 30Arg | O | N $_{\eta 1}$ | 2.75 | H |
| 127His | 30Arg | N $_{\delta}$ | N $_{\eta 1}$ | 2.06 | H | 127Gln | 30Arg | O $_{\epsilon 1}$ | N $_{\eta}$ | 2.79 | H |
| 127His | 34Val | N $_{\delta}$ | N $_{\eta 1}$ | 3.89 | | | | | | | |

*Borgstahl et al. (1994)

Interface contacts are defined using a 3.9 Å cutoff. **H**: hydrogen bond

the hydrogen bonds in the subunit interface (26, 27). Since it can be thought that ^{127}His causes the downfield shift of the hydrogen bonded proton because of the ring current effect by π -orbital electrons on its side chain, the unique resonance at 12.5 ppm for $\beta\alpha(\text{F133V})$ -subunit can be assignable to a hydrogen bond between ^{127}His and ^{30}Arg at the $\beta\alpha(\text{F133V})_1$ - $\beta\alpha(\text{F133V})_2$ interfaces. This speculation is reassured by the experimental result that the homotetramer of the β -subunit mutant of Q127H also showed an exchangeable proton resonance at 12.5 ppm just as did the $[\beta\alpha(\text{F133V})]_4$ (28).

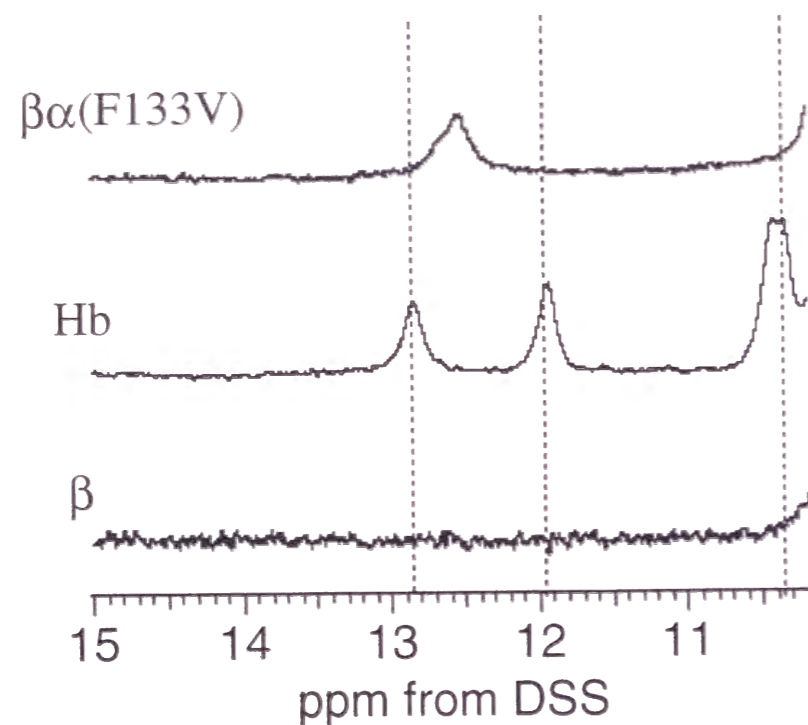


Fig. 7 NMR spectra in the hydrogen bonded proton region for carbonmonxygenated globins Proton resonance peaks for Hb at 10.4, 11.9 and 12.8 ppm are assigned to the hydrogen bonded protons between Asp-94 α_1 and Asn-102 β_2 (27), His-103 α_1 and Asn-108 β_1 (26), and Asp-126 α_1 and Tyr-35 β_1 (27). Experimental conditions were as follows: 50 mM Na-Phosphate, 0.1 M NaCl, pH 7.4, at 290 K. Sample concentration was 600 μM on the heme basis.

In addition to the $\beta\alpha(\text{F133V})_1$ - $\beta\alpha(\text{F133V})_2$ interface, we have investigated the $\beta\alpha(\text{F133V})_1$ - $\beta\alpha(\text{F133V})_3$ interface, which is corresponding to α_1 - β_2 interface in hemoglobin. Since α_1 - β_2 interactions serve as a regulator of equilibrium between $\alpha\beta$ dimer and $\alpha_2\beta_2$ tetramer in hemoglobin (29, 30), the relationship of the $\beta\alpha(\text{F133V})_1$ - $\beta\alpha(\text{F133V})_3$ interface structure with the formation of the stable tetramer $[\beta\alpha(\text{F133V})]_4$ should be also noticed. In Table III, the $\beta\alpha(\text{F133V})_1$ -

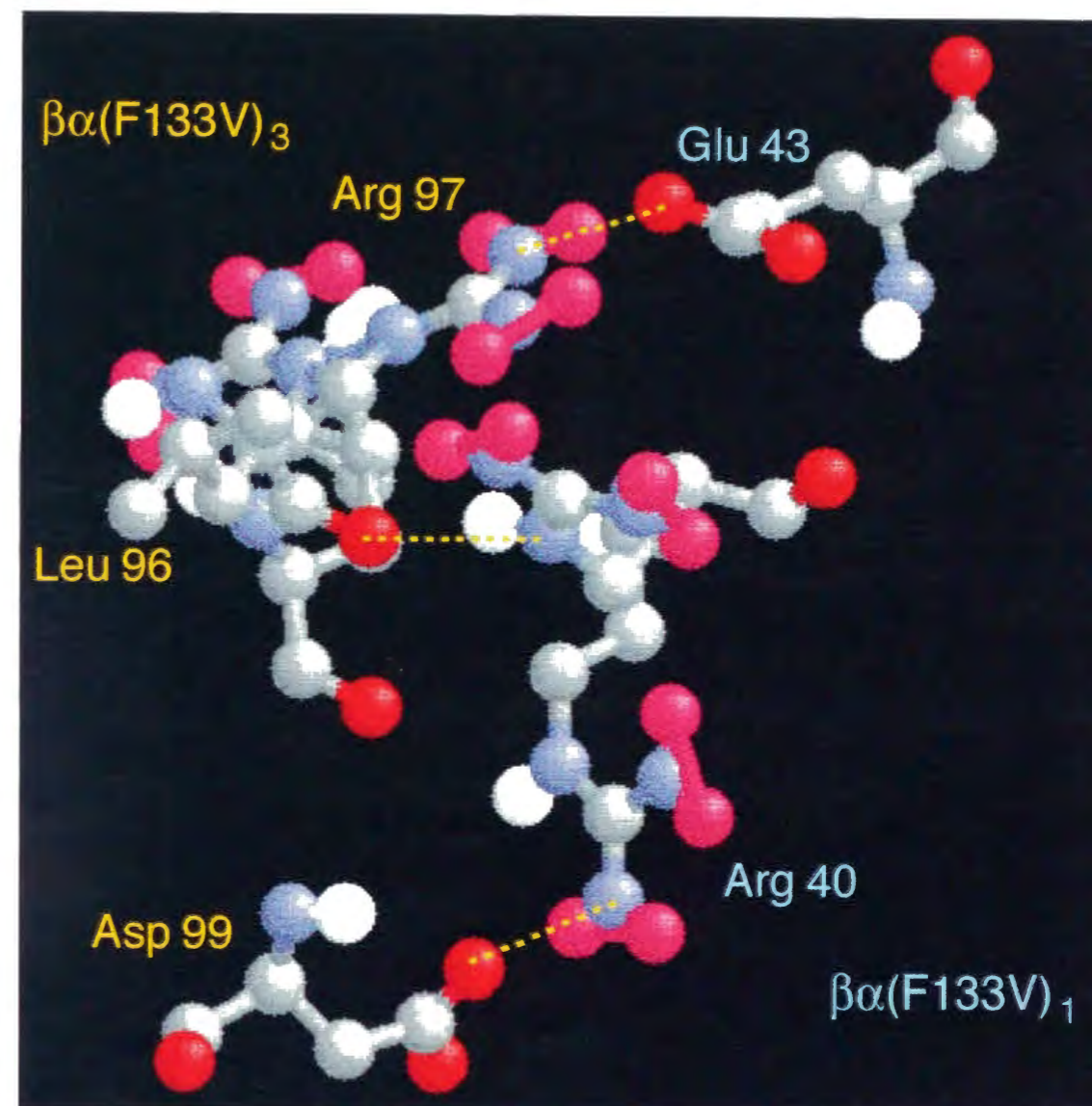


Fig. 8 $\beta\alpha(\text{F133V})_1$ - $\beta\alpha(\text{F133V})_3$ interface structure of $\beta\alpha(\text{F133V})_4$ -tetramers. The $\beta\alpha(\text{F133V})_1$ - $\beta\alpha(\text{F133V})_3$ interface corresponds to α_1 - β_2 interface in hemoglobin. Dotted lines represent a hydrogen bond or salt bridge in the interface.

Table III Subunit-subunit contacts of the $\beta\alpha(\text{F133V})_1$ - $\beta\alpha(\text{F133V})_3$ interface of the $[\text{CO-}\beta\alpha(\text{F133V})]_4$ and the corresponding β_1 - β_3 interface of the $[\text{CO-}\beta_4]^*$

| $\beta\alpha(\text{F133V})_1$ | | $\beta\alpha(\text{F133V})_3$ | | | | β_1 | | β_3 | | | |
|-------------------------------|----------|-------------------------------|-----------------|-------------|-----------|-----------|----------|-----------------|-----------------|-------------|-----------|
| residues | residues | Atoms | | Distance(Å) | | residues | residues | Atoms | | Distance(Å) | |
| 37Trp | 97His | C $_{\beta}$ | O | 3.82 | | 37Trp | 97His | C $_{\beta}$ | O | 3.41 | |
| 37Trp | 99Asp | N $_{\epsilon}$ | O $_{\delta 2}$ | 3.00 | H | 37Trp | 99Asp | C $_{\delta 1}$ | C $_{\delta 2}$ | 3.27 | |
| 37Trp | 99Asp | C $_{\delta 1}$ | C $_{\delta 2}$ | 3.38 | | 37Trp | 100Pro | C $_{\delta 2}$ | C $_{\delta}$ | 3.56 | |
| 37Trp | 100Pro | C $_{\delta 2}$ | C $_{\delta}$ | 3.69 | | | | | | | |
| 39Gln | 97Arg | N $_{\epsilon}$ | N $_{\eta 1}$ | 3.36 | H | | | | | | |
| 40Arg(1) | 41Phe | C $_{\zeta}$ | C $_{\zeta}$ | 3.32 | | 40Arg(1) | 41Phe | C $_{\zeta}$ | C $_{\zeta}$ | 3.19 | |
| | | | | | | 40Arg(1) | 97His | N $_{\epsilon}$ | O | 3.02 | H |
| 40Arg(1) | 99Asp(1) | N $_{\eta 1}$ | C $_{\delta}$ | 2.88 | SB | 40Arg(1) | 99Asp(1) | N $_{\eta 1}$ | C $_{\delta}$ | 2.70 | SB |
| 40Arg(2) | 96Leu | N $_{\eta 1}$ | O | 2.96 | H | 40Arg(2) | 96Leu | N $_{\eta}$ | O | 2.79 | H |
| 41Phe | 40Arg(2) | C $_{\zeta}$ | C $_{\zeta}$ | 3.27 | | 41Phe | 40Arg(2) | C $_{\zeta}$ | C $_{\zeta}$ | 3.24 | |
| 96Leu | 40Arg(1) | O | N $_{\eta 1}$ | 2.73 | H | 96Leu | 40Arg(1) | O | N $_{\eta 1}$ | 3.34 | H |
| 97Arg | 37Trp | O | C $_{\beta}$ | 3.65 | | 97His | 37Trp | O | C $_{\beta}$ | 3.45 | |
| 97Arg | 40Arg(2) | O | N $_{\epsilon}$ | 3.42 | H | 97His | 40Arg(2) | O | N $_{\epsilon}$ | 3.09 | H |
| 97Arg | 43Glu | N $_{\eta 1}$ | O $_{\delta 1}$ | 3.04 | SB | | | | | | |
| 99Asp(1) | 37Trp | O $_{\delta 2}$ | O $_{\delta 2}$ | 3.46 | | 99Asp(1) | 37Trp | O $_{\delta 2}$ | O $_{\delta 2}$ | 3.24 | |
| | | | | | | 99Asp(1) | 102Asn | O $_{\delta 2}$ | N $_{\delta 2}$ | 2.73 | H |
| 102Asn | 99Asp(1) | N $_{\delta 2}$ | O $_{\delta 2}$ | 3.02 | H | 102Asn | 99Asp(1) | N $_{\delta 2}$ | O $_{\delta 2}$ | 2.73 | H |

*Borgstahl et al. (1994)

Interface contacts are defined using a 3.9 Å cutoff. **H**: hydrogen bond **SB**: salt bridge

(1) Main conformer (2) Alternate conformer

$\beta\alpha(\text{F133V})_3$ close contacts are compiled and compared with the corresponding β_1 - β_3 ones of the β_4 tetramer. As found in this table, number of hydrogen bonds and van der Waals interactions in the $\beta\alpha(\text{F133V})_1$ - $\beta\alpha(\text{F133V})_3$ interface is almost the same as that in the β_1 - β_3 interface (11). Of particular interest is that there is a salt bridge between ^{97}Arg and ^{43}Glu as well as between ^{99}Asp and ^{40}Arg in the $\beta\alpha(\text{F133V})_1$ - $\beta\alpha(\text{F133V})_3$ interface as clearly shown in Fig. 7. Just as the ^{40}Arg and ^{99}Asp salt bridge introduces ionic interactions that should strengthen the β_4 homo-tetramer (12), these two salt bridges would be essential for the tetramer formation of the $\beta\alpha(\text{F133V})$ -subunit. Here, it should be noted that there are alternate conformers for the side chains of the ^{40}Arg and ^{97}Arg in the $\beta\alpha(\text{F133V})_1$ - $\beta\alpha(\text{F133V})_3$ interface (Fig. 8). Such alternate conformers were also observed for ^{40}Arg and ^{99}Asp in the β_1 - β_3 interface of the β_4 tetramer, which is the result of steric conflicts that prevent both $^{40}\text{Arg}(\beta_1)$ - $^{99}\text{Asp}(\beta_3)$ and $^{99}\text{Asp}(\beta_1)$ - $^{40}\text{Arg}(\beta_3)$ salt bridges from forming simultaneously (12). As well, $^{40}\text{Arg}(\beta\alpha(\text{F133V})_1)$ - $^{99}\text{Asp}(\beta\alpha(\text{F133V})_3)$ and $^{99}\text{Arg}(\beta\alpha(\text{F133V})_1)$ - $^{40}\text{Asp}(\beta\alpha(\text{F133V})_3)$ salt bridges are considered not to form simultaneously because of the steric hindrance. Thus, the dual conformations in the subunit interface were also observed in the $[\beta\alpha(\text{F133V})]_4$, revealing that the local structure around these salt bridges in the $\beta\alpha(\text{F133V})_1$ - $\beta\alpha(\text{F133V})_3$ interface is almost conserved upon the substitution of the module M4. This result is consistent with the present finding that the tertiary structure of the $\beta\alpha(\text{F133V})$ -subunit is similar to that of the β -subunit in the regions of the residue number 38-55 and 85-102 (Fig. 4).

Heme Environmental Structure of $\beta\alpha(\text{F133V})$ -subunit - Since oxygen binding property of globin proteins is very sensitive to the heme environmental structure (30-33), it is important to analyze the heme vicinity of the $\beta\alpha(\text{F133V})$ -subunit in detail. Fig. 9 demonstrates the heme environmental structures of the β - and $\beta\alpha(\text{F133V})$ -subunits and reveals no remarkable difference in the dispositions of their heme surrounding residues. However, there are some slight but significant disparities in their structures. As shown in Fig. 9, the distance between proximal histidyl N_ϵ and heme iron of the $\beta\alpha(\text{F133V})$ -subunit is 2.18 Å, whereas that of the β -subunit is 2.04 Å. The elongation of the distance by 0.14 Å corresponds to the larger deviation of the heme iron from the heme plane in the $\beta\alpha(\text{F133V})$ -subunit than in the β -subunit. In general, the larger the deviation of the heme iron from the heme plane, the lower the oxygen affinity of globins (31, 32), which is reflected in oxygen binding properties for the β - and $\beta\alpha(\text{F133V})$ -subunits. Here it is noteworthy that although the oxygen equilibrium curve for the $\beta\alpha(\text{M4})$ -subunit could not be measured because of the rapid autoxidation in the previous study (3), the introduction of the mutation of

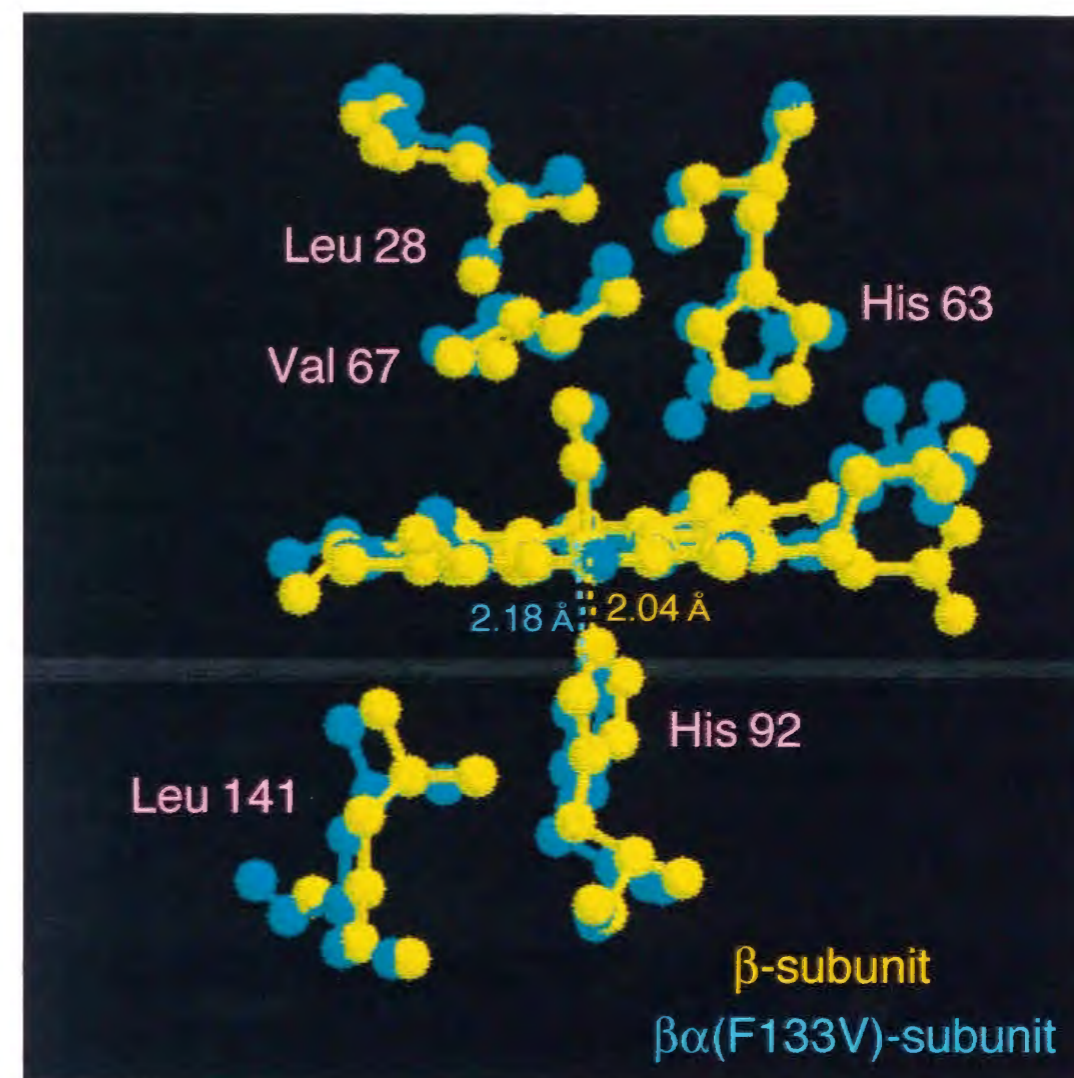


Fig. 9 Heme distal structures of of the β - and $\beta\alpha(\text{F133V})$ -subunits. Colors correspond to the β -subunit (yellow) and $\beta\alpha(\text{F133V})$ -subunit (blue).

F133V suppressed the autoxidation, resulting in success in the measurement. Fig. 10 shows oxygen equilibrium curves of the β - and $\beta\alpha(\text{F133V})$ -subunits, and the oxygen equilibrium parameters are compiled in Table IV. The P_{50} value for the $\beta\alpha(\text{F133V})$ -subunit is 1.61 mmHg, which is much higher than that of the β -subunit (0.37 mmHg). This result indicates that oxygen affinity for the $\beta\alpha(\text{F133V})$ -subunit is considerably low compared to the β -subunit. On the basis of the correlation between oxygen affinity and deviation of the heme iron from the heme plane addressed above, the lower oxygen affinity for the $\beta\alpha(\text{F133V})$ -subunit is consistent with the present finding that the distance between proximal histidyl N_{ϵ} and heme iron of the $\beta\alpha(\text{F133V})$ -subunit is surely longer than that of the β -subunit, leading to the larger deviation of the heme iron from the heme plane.

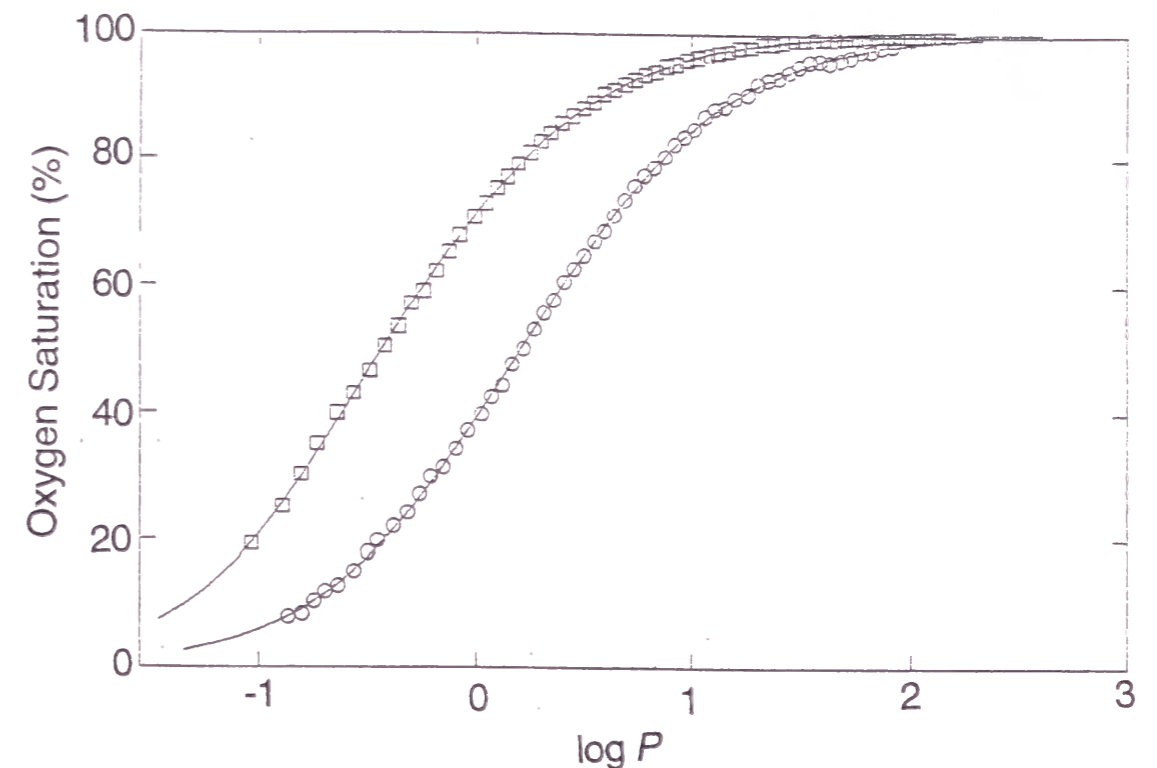


Fig. 10 Oxygen equilibrium curves for the β - and $\beta\alpha(\text{F133V})$ -subunits. Signals correspond to the β -subunit (\square) and $\beta\alpha(\text{F133V})$ -subunit (\circ). Experimental conditions were as follows: 50 mM Tris, 0.1 M NaCl, pH 7.4, at 25°C. Sample concentration was 60 μM on the heme basis.

Table IV Oxygen Equilibrium Parameters for the β - and $\beta\alpha(\text{F133V})$ -subunits

| | P_{50} [mmHg] | n_{max} |
|-----------------------------|-----------------|------------------|
| β | 0.37 | 0.97 |
| $\beta\alpha(\text{F133V})$ | 1.61 | 1.01 |

In addition to the heme proximal site, we have investigated the heme distal structure. Table V lists the distances between heme iron and the heme distal residues such as Leu28, His63 and Val67 in the β - and $\beta\alpha$ (F133V)-subunits. Here it is not negligible that the dispositions of their side chains are locally altered by the substitution of the module M4. In particular, the δ 1- and δ 2-methyls of the ^{28}Leu in the $\beta\alpha$ (F133V)-subunit is deviated from that in the β -subunit, suggesting that the M4 substitutions substantially perturbs the local environment around ^{28}Leu . This inspection is reasonable based on the structural comparison between the β - and $\beta\alpha$ (F133V)-subunits in Fig. 4, where B-helix including ^{28}Leu of the $\beta\alpha$ (F133V)-subunit is not superimposed on that of the β -subunit. Thus, the present x-ray crystallographic study has elucidated the structural changes in the heme vicinity cause by the substitution of the module M4. Consequently, it was concluded that the module substituted β -subunit almost retained the heme environmental structure of the parent β -subunit as suggested by the previous study (3), but structural perturbations by the module substitution was transmitted to the heme vicinity probably through the interactions between modules.

Table V Distance (\AA) between Heme Iron and Heme Surrounding Residues in the β - and $\beta\alpha$ (F133V)-subunits

| | $\beta\alpha$ (F133V) | β |
|-------------------------------------|-----------------------|---------|
| Fe - His(F8) N_ϵ | 2.18 | 2.04 |
| Fe - His(E7) N_ϵ | 4.36 | 4.37 |
| Fe - His(E7) $\text{C}_{\delta 2}$ | 5.40 | 5.13 |
| Fe - Val(E11) $\text{C}_{\gamma 1}$ | 5.03 | 4.87 |
| Fe - Val(E11) $\text{C}_{\gamma 2}$ | 6.01 | 5.81 |
| Fe - Leu(B10) $\text{C}_{\delta 1}$ | 7.15 | 6.42 |
| Fe - Leu(B10) $\text{C}_{\delta 2}$ | 8.53 | 7.33 |
| Fe - Leu(H19) $\text{C}_{\delta 1}$ | 6.68 | 6.20 |
| Fe - Leu(H19) $\text{C}_{\delta 2}$ | 7.07 | 6.82 |

CONCLUSIONS

As discussed above, we have succeeded in crystallization of the module substituted β -subunit by introducing the mutation of F133V for removal of the steric hindrance within the subunit. The back-bone structure of the $\beta\alpha$ (F133V)-subunit was rather close to that of the α -subunit in the region of the module M4, strongly suggesting that the module M4 is a quasi-independent structural unit in globin structure. However, the substitution of the module

M4 simultaneously caused more or less structural perturbations on some regions through the modular interactions, resulting in remarkable change in globin functions such as subunit assembly and oxygen binding. Thus, the present study confirmed that the globin structure and function are regulated by combination of structural property of the modules themselves and significant interactions between the modules.

ACKNOWLEDGEMENTS

We thank Drs. M. Suzuki, N. Watanabe and N. Sakabe for their help in data collection at the Photon Factory. A part of computational work was done at the CAD facility of Nagoya University Venture Business Laboratory. This work was partly supported by Grant-in-Aid for Encouragement of Young Scientists (No. 08780618) from the Ministry of Education, Science, Sports and Culture of Japan.

REFERENCES

1. Go, M. (1981) *Nature* 291:90-92
2. Go, M. (1983) *Proc. Natl. Acad. Sci. U.S.A.* **80**, 1964-1968
3. Wakasugi, K., Ishimori, K., Imai, K., Wada, Y., Morishima, I. (1994) *J. Biol. Chem.* **269**, 18750-18756
4. Brünger, A.T. X-PLOR. (1992) Version 3.1. A system for X-ray crystallography and NMR. Yale University Press, New Haven, 125-127.
5. Wada, Y., Fujita, T., Hayashi, A., Sakurai, T., and Matsuo, T. (1989) *Biomed. Environ Mass Spectrom.* **18**, 563-565
6. Nagai, K., and Thøgerson, H.C. (1984) *Nature* **309**, 810-812
7. Nagai, K., and Thøgerson, H.C. (1987) *Methods Enzymol.* **153**, 461-481
8. Nagai, K., Perutz, M. F., and Poyart, C. (1985) *Proc. Natl. Acad. Sci. U.S.A.* **82**, 7252-7257
9. Inaba, K., Wakasugi, K., Ishimori, K., Konno, T., Kataoka, M., and Morishima, I. (1997) *J. Biol. Chem.* **272**, 30054-30060
10. Jancarik, J., Kim, S.-H. (1991) *J. Appl. Cryst.* **24**, 409-411
11. Otwinowski, Z. (1993) In "Proceedings of the CCP4 Study Weekend." Sawyer, L., Isaacs, N., Bailey, S., eds. SERC Daresbury Laboratory, England, 56-62.
12. Borgstahl, G.O.E., Rogers, P.H., Arnone, A. (1994) *J. Mol. Biol.* **236**, 817-830
13. Borgstahl, G.O.E., Rogers, P.H., Arnone, A. (1994) *J. Mol. Biol.* **236**, 831-843
14. Cambillau, C. (1992) Turbo-FRODO, *Molecular Graphics Program for Silicon Graphics IRIS 4D Series, Ver 3.0*. Bio-graphics, Marseille, France
15. Serk (1994) *Acta Crystallogr.* **D50**, 760-763
16. Imai, K. (1981) *Methods. Enzymol.* **76**, 438-449

17. Imai, K. (1982) *Allosteric Effect in Haemoglobin*, Cambridge University Press, London
18. Imai, K., Morimoto, H., Kotani, M., Watari, H., Hitata, W. and Kuroda, M. (1970) *Biochem. Biophys. Acta* **200**, 189-196
19. Hayashi, A., Suzuki, T. and Shin, M. (1973) *Biochem. Biophys. Acta* **310**, 309-316
20. Lynch, R. E., Lee, G. R. and Cartwright, G. E. (1976) *J. Biol. Chem.* **251**, 1015-1019
21. Winterbourn, C. C., McGrath, B. M. and Carrell, R. W. (1976) *Biochem. J.* **155**, 493-502
22. Imai, K. (1994) *Methods. Enzymol.* **232**, 559-576
23. Fauchere, J. L. and Pliska, V. (1983) *Eur. J. Med. Chem.* **18**, 369-375
24. Lesk, A. M. and Chothia, C. (1980) *J. Mol. Biol.* **136**, 225-270
25. Valdes, R. Jr., and Ackers, G. K. (1977) *J. Biol. Chem.* **252**, 74-81
26. Fung, L. W. M. and Ho, C. (1975) *Biochemistry* **14**, 2526-2535
27. Russu, I. M., Ho, N. T. and Ho, C. (1987) *Biochim. Biophys. Acta.* **914**, 40-48
28. Kondo et al., *submitted for publication*
29. Ishimori, K., Hashimoto, M., Imai, K., Fushitani, K., Miyazaki, G., Morimoto, H., Wada, Y. and Morishima, I. (1994) *Biochemistry* **33**, 2546-2553
30. Perutz, M. F. (1970) *Nature* **228**, 726-739
31. Nagai, K and Kitagawa, T. (1980) *Proc. Natl. Acad. Sci. U.S.A.* **77**, 2033-2037
32. Nagai, K., Kitagawa, T. and Morimoto, H. (1980) *J. Mol. Biol.* **136**, 271-289
33. Nagai, K., La Mar, G. N., Jue, T. and Bunn, F. (1982) *Biochemistry* **21**, 842-847

FOOTNOTE

¹The crystal of the hemo-tetramer of the carbonmonoxy $\beta\alpha(\text{F133V})$ -subunit is called as $[\text{CO-}\beta\alpha(\text{F133V})]_4$.

PART III

EFFECTS OF PSEUDO-MODULE SUBSTITUTION ON GLOBIN STRUCTURE AND FUNCTION

Chapter 3

Substitution of pseudo-module PM3 in hemoglobin α -
and β -subunits ($\beta\alpha(\text{PM3})$ -subunit)

ABSTRACT

Functional and structural significance of the "module" in proteins have been investigated for globin proteins. Our previous studies have revealed that some modules in globins are responsible for regulating the subunit association and heme environmental structures, whereas the module substitution often induces fatal structural destabilization, resulting in failure of functional regulation. In this paper, in order to gain further insight into functional and structural significance of the modular structure in globins, we focused upon "pseudo-module" in globin structure of which boundaries are located at the center of modules. Although the pseudo-module has been supposed not to retain a compactness, the $\beta\alpha(\text{PM3})$ -subunit, in which one of the pseudo-module, the F1-H6 region, of the α -subunit is implanted into the β -subunit, conserved stable globin structure and its association property was converted into that of the α -subunit, as does the module substituted globin, the $\beta\alpha(\text{M4})$ -subunit. These results suggest that modules are not unique structural and functional units for globins. Interestingly, however, the recent reconsideration of the module boundary indicates that the modules in globins can be further divided into two small modules and one of the boundaries for the new small modules coincides with that of the pseudo-module we substituted in this study. Although it would be premature to conclude the significance of the modular structure in globins, it can be safely said that we have found new structural units in globin structure, probably new modules.

Recent structural studies of proteins have revealed that many protein structures are constructed by the compact structural unit, "modules", which correspond to the exons on the gene structure (1, 2). The gene of globin is made up of three exons interrupted by two introns and the exons 1, 2 and 3 correspond to the modules M1, M2 + M3 and M4, respectively. The correlation of globin structure and function with its modular structure was exemplified by the observation that specific functions of globins are attributed to the specific modules (3). As found in Fig. 1A, the amino acid residues associated with the heme contacts and the $\alpha 1-\beta 2$ contacts are concentrated in the module M2 + M3, whereas the $\alpha 1-\beta 1$ contact cluster is located in the module M4.

To gain insights into the structural and functional significance of the "module" in globins, we have prepared a variety of the "module"-substituted globins (4-6). The module M4 substituted hemoglobin β -subunit [$\beta\alpha(M4)$ -subunit], in which the module M4 was replaced by that of the α -subunit, exhibited the native β -subunit-like heme environmental structure, while it preferentially associated with the native β -subunit, not with the α -subunit (4). These findings indicate that the module substitution can convert the association property of the hemoglobin subunit without substantial structural changes in the heme vicinity, suggesting that the module is a structural and functional unit (4). However, the counterpart chimeric globin, the $\alpha\beta(M4)$ -subunit, of which module M4 was derived from that of the β -subunit, was quite unstable and the association property was not affected by the module substitution (5). Such destabilization in globin structure was also encountered for other module substituted globins (6), which leads us to reconsider the structural and functional significance of the modular structures in globins and examine effects of "non-module substitution" on globin structure and function to compare with those of the module substitution.

In the present study, we have focused upon the "pseudo-module" in globin structure. The pseudo-module is defined as a segment starting at a center of one module and ending at the center of the adjacent module (Figs. 1) and supposed not to form a compact structural unit (7). Since the pseudo-modules do not statistically coincide with exons (8), they would have neither evolutionary nor functional meanings (9, 10). Herewith, we have prepared a "pseudo-module" substituted globin, the $\beta\alpha(PM3)$ -subunit, as illustrated in Fig. 2 and compared its structural and functional properties with those of the corresponding stable module substituted globin, $\beta\alpha(M4)$ -subunit. We are concerned here with the effects of the pseudo-module substitution on the globin structure. Furthermore, we have paid attention to the association property of the chimeric globins, since the amino acid residues contributing to the $\alpha 1-\beta 1$

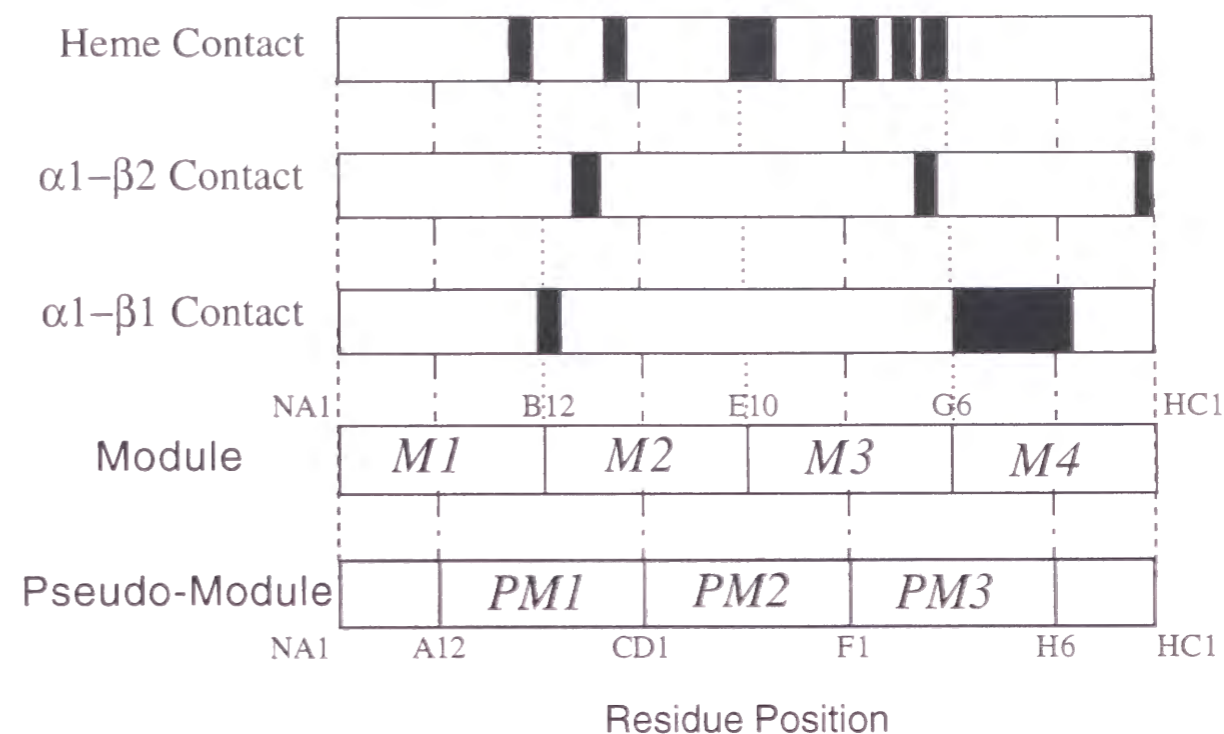


Fig. 1 Module- and pseudo-module boundaries and residues with well defined functional roles in hemoglobin subunits proposed by Eaton (1980)

contact are concentrated in the pseudo-module PM3 as well as in the module M4 (Fig. 1). The heme environmental structure and oxygen affinity for the chimeric globin have been also examined by using various spectroscopic methods to describe the functional and structural effects of the pseudo-module substitution in globins.

EXPERIMENTAL PROCEDURES

Expression Vector Construction – The expression vectors of the $\beta\alpha(M4)$ - and $\beta\alpha(PM3)$ -subunits were constructed as illustrated in Fig. 2. The N-terminal valine residue was replaced by a methionine to initiate the peptide elongation for the module and pseudo-module substituted subunits. To obtain the genes of the $\beta\alpha(PM3)$ -subunit, *Kpn* I (GGTACC) and *Mlu* I sites (ACGCGT) were introduced at the start and end of the PM3, respectively, by polymerase chain reaction with silent mutation.

Protein Preparation – All of the module and pseudo-module substituted subunits were purified as previously reported for recombinant Hb (4, 11-13). We confirmed the correct expression of the desired subunits by fast atom bombardment mass spectroscopy (data not shown) (14) and no additional mutations were detected. We also synthesized "wild-type" β -subunit¹ which

has a methionine residue at the N-terminal instead of the valine residue as a reference and confirmed that the structural properties of the "wild-type" β -subunit are virtually the same as those of "native" β -subunit isolated from human red blood cell.

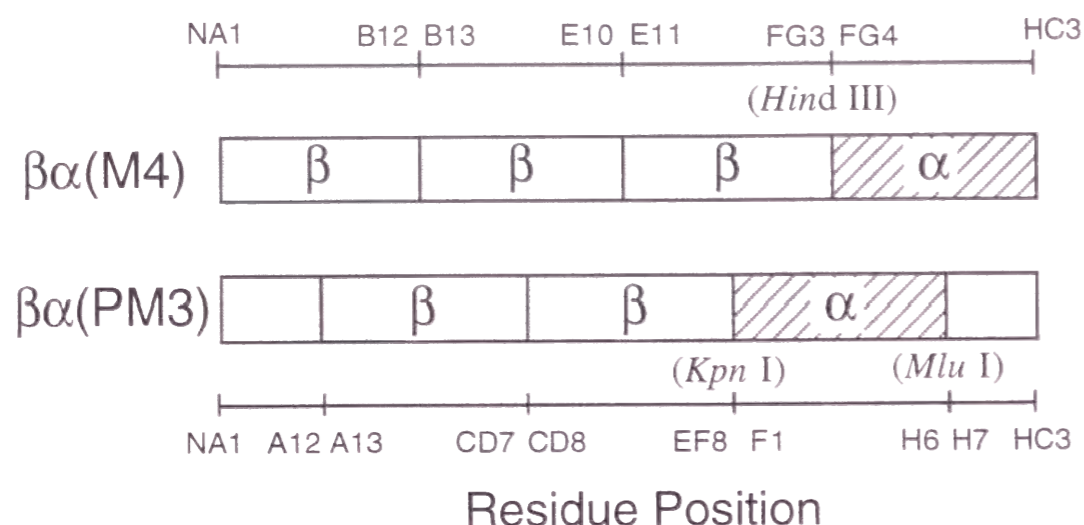


Fig. 2 Novel globin subunits synthesized in this study Restriction enzyme sites used in these preparation are noted in a parenthesis.

Circular Dichroism Spectra—CD spectra of the cyano-met subunits in far UV region were measured with Jasco J-760. Concentration of the samples was 5 μ M and the light path of the cell was 1 mm. The buffer used in the measurements was 20 mM Na-phosphate containing 0.1 M NaCl and 5 mM NaCN, pH 7.4 at room temperature.

Urea Denaturation Curves - Reaction solutions contained 20 mM Tris (pH 7.4), 1 mM NaCN and various concentrations of urea. Sample concentration was 5 μ M. The ellipticity at 222 nm was monitored by Jasco J-760 CD spectrometer after ~10 hours equilibration at room temperature. Cyanomet derivatives are used for the measurements to avoid aggregation of heme and reduce the irreversible denaturation² (15). The fractional denatured population (f_D) for various urea concentrations was estimated by the following equation (I);

$$f_D = ([\theta]_{222, N} - [\theta]_{222}) / ([\theta]_{222, N} - [\theta]_{222, D}) \quad (I)$$

where $[\theta]_{222, N}$, $[\theta]_{222, D}$ and $[\theta]_{222}$ represent ellipticities at 222 nm in the native and denatured states and in each urea concentration, respectively. The free energy of denaturation, ΔG , was calculated by the following equation (II) (15):

$$\Delta G = -RT \ln(f_D / (1 - f_D)) \quad (II)$$

When ΔG varied linearly with urea concentration, $[\text{urea}]$, ΔG_{H_2O} , extrapolated ΔG at $[\text{urea}] = 0$, can be estimated by the following equation:

$$\Delta G = \Delta G_{H_2O} - m_{\text{urea}} [\text{urea}] \quad (III)$$

where m_{urea} is the slope of the linear relation between ΔG and $[\text{urea}]$.

Gel Chromatogram - Gel filtration measurements were performed by using a Sephacryl S-200 HR column (0.8 cm-d x 62 cm-l) at 4 °C. The buffer used for the chromatography was 50 mM Tris, in the presence of 0.1 M NaCl, and 1 mM Na₂EDTA, pH 7.4 and the flow rate was 7 ml/h. The eluted fractions were monitored by absorption at the Soret band (16, 17). Dimer-tetramer dissociation constant of the samples was determined by concentration dependence of the centroid elution volume over the range from 0.5 to 200 μ M (16, 17). The following functional dependence of the elution volume (V_e) versus protein concentration (C_T) allows us to determine the dimer-tetramer equilibrium constants for the samples (16):

$$V_e = \sum_j j V_j (m_j) / C_T \quad (IV)$$

where V_j are elution volumes for the individual species pertaining to the various aggregates (j -mers), and the (m_j) term represents molar concentrations for the respective species.

NMR Spectra - ¹H NMR spectra at 500 MHz were recorded on BRUKER Avance DRX 500. We used a Water Gate pulse sequence for the diamagnetic region to minimize the water signal in the sample. For the measurements of the hyperfine-shifted proton resonances, we utilized a LOSAT pulse sequence. The probe temperature was controlled at 290 \pm 0.5 K by a temperature control unit of the spectrometer. The volume of the NMR sample was 500 μ l and the concentration was 600 μ M on the heme basis. Proton shifts were referenced with respect to the proton resonance of 2, 2,-dimethyl-2-silapentane-5-sulfonate (DSS).

Oxygen Equilibrium Curves and Analysis - Oxygen equilibrium curves were measured by using an improved version (18, 19) of an auto-oxygenation apparatus (20). The wavelength of the detection light was 560 nm and the protein concentration was 60 μ M on the heme basis. The temperature of the sample in the oxygenation cell was constant within \pm 0.05 °C. The hemoglobin reductase system (21) was added to the sample before each measurement to reduce oxidized subunits. To minimize the autoxidation of the sample during the measurements, catalase and superoxide dismutase were added to the sample and the concentration was 0.1 μ M (22, 23). The oxygenation data were acquired by use of a micro-computer (model PC-98XA, Nippon Electric Co., Tokyo), which was interfaced to the oxygenation apparatus (24).

RESULTS

Circular Dichroism Spectra - As reported by our previous studies (5,6), the module substitutions often induced severe destabilization in globin structure, which is characterized by the prominent decrease of the negative ellipticities at 222 and 208 nm in the CD spectra (5). In Fig. 3, however, the pseudo-module substituted globin, $\beta\alpha(\text{PM3})$ -subunit, exhibits two broad and large negative peaks around 222 and 208 nm characteristic of the α -helical structure. These negative peaks were also observed for the module substituted $\beta\alpha(\text{M4})$ -subunit and native hemoglobin (25), indicating that the secondary structure for the β -subunit is almost insensitive to the substitution of the pseudo-module PM3 as the case for the M4 substitution.

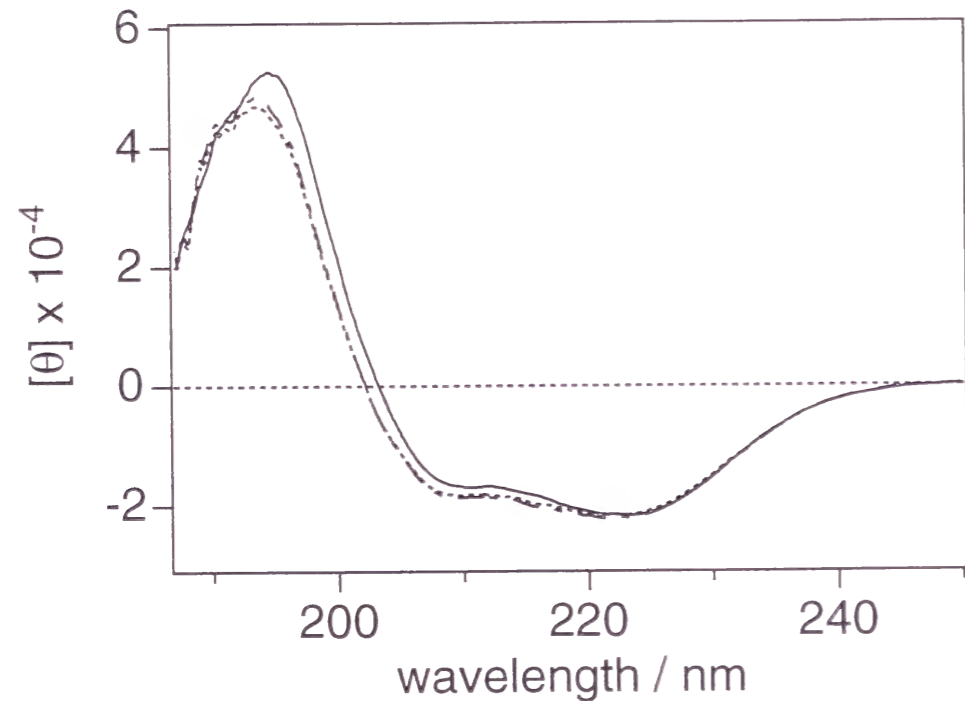


Fig. 3 CD spectra in far UV region of the cyano-met native, module and pseudo-module substituted globin subunits Lines correspond to hemoglobin (—), $\beta\alpha(\text{M4})$ -subunit (- - -), $\beta\alpha(\text{PM3})$ -subunit (- · - ·).

Urea Denaturation Curves - Alterations in equilibrium stability upon the module and pseudo-module substitutions were quantified by urea-induced denaturation experiment. As clearly delineated in Fig. 4A, the transition curve for the urea denaturation in the $\beta\alpha(\text{PM3})$ -subunit is quite similar to that

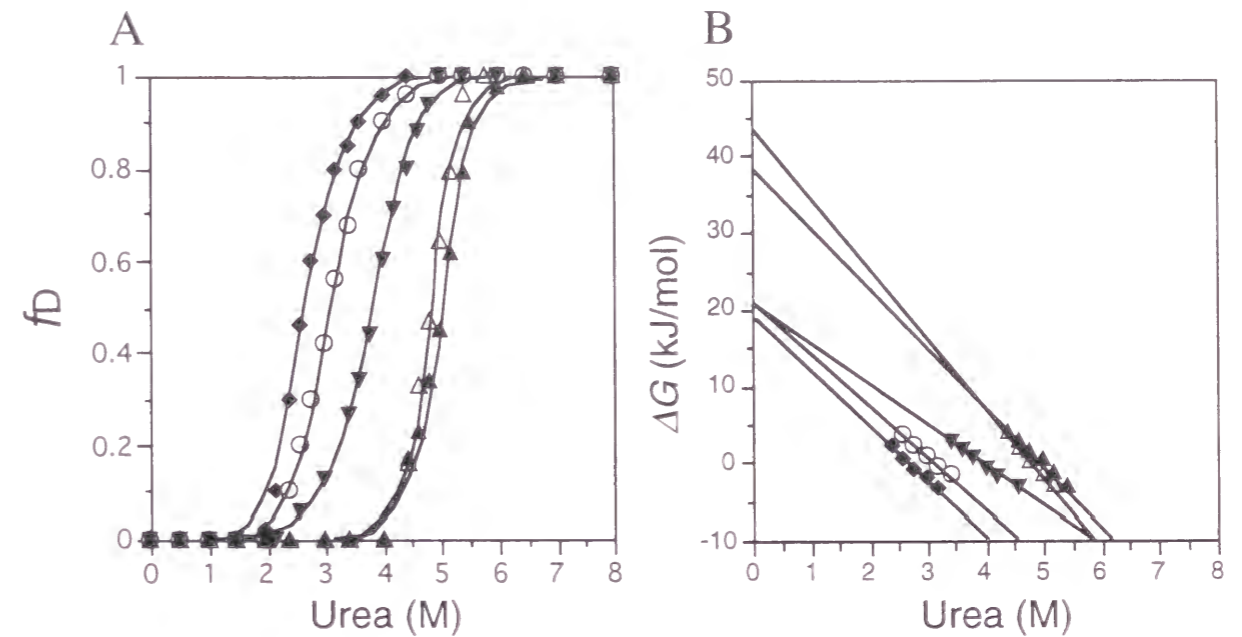


Fig. 4(A) Urea-induced denaturation curves for hemoglobin (▲), α -subunit (▼), β -subunit (◆), $\beta\alpha(\text{M4})$ -subunit (△) and $\beta\alpha(\text{PM3})$ -subunit (○). Molecular ellipticities in the native and completely denatured states are normalized to 0 and 1, respectively. Experimental conditions were as follows: 20 mM Tris, 0.1 M NaCl, 5mM NaCN, pH 7.4, at 290 K. Sample concentration was 5 μM on the heme basis. **(B) Relationship between ΔG and [Urea] for hemoglobin (▲), α -subunit (▼), β -subunit (◆), $\beta\alpha(\text{M4})$ -subunit (△) and $\beta\alpha(\text{PM3})$ -subunit (○).** They were calculated from the respective urea denaturation curves in (A).

Table I Parameters of urea denaturation for tetrameric Hb, isolated α -, β -, $\beta\alpha(\text{PM3})$ - and $\beta\alpha(\text{M4})$ -subunits

$\Delta G_{\text{H}_2\text{O}}$ and m_{urea} were determined by fitting the ΔG -[urea] relations to equation (III).

| | $\Delta G_{\text{H}_2\text{O}}$ (kJ / mol) | m_{urea} (kJ / mol per M) |
|---------------------------|--|------------------------------------|
| Hb | 37.8 | -7.54 |
| α | 20.2 | -5.22 |
| β | 17.8 | -6.65 |
| $\beta\alpha(\text{PM3})$ | 20.3 | -6.52 |
| $\beta\alpha(\text{M4})$ | 43.1 | -8.91 |

for the native β -subunit, indicating that the globular structure of the $\beta\alpha(\text{PM3})$ -subunit is as stable as that of the native β -subunit. For the $\beta\alpha(\text{M4})$ -subunit, the denaturation curve was shifted to the right side from that of the β -subunit and almost superimposed on that of tetrameric native hemoglobin. In Fig. 4B, the free energy of denaturation (ΔG) was plotted against urea concentrations and a

linear fitting procedure by using equation (III) determined the extrapolated ΔG in the absence of urea, ΔG_{H_2O} , and the slope of the linear relation (*ie* $d\Delta G / d[\text{urea}]$), m_{urea} (Table I). Although the substitution of the module M4 increases ΔG_{H_2O} by about 25 kJ/mol and m_{urea} by 2.3 kJ/mol per M (M: urea concentration), the corresponding parameters for the substitution of the pseudo-module PM3 are almost unchanged from those for the β -subunit. The effects of the pseudo-module PM3 substitution on the protein stability of the β -subunit are minimal, compared to those of the module M4.

Association Properties – However, the association property of the pseudo-module substituted globin, $\beta\alpha(\text{PM3})$ -subunit, clearly differs from that of the wild-type β -subunit. Fig. 5A illustrates gel chromatogram of the carbonmonoxy chimeric globins in the presence and absence of the native subunits and the centroid elution volumes of the samples as a function of protein concentration (16, 17) are shown in Fig. 5B. Under the condition employed here, the mixture of native α - and β -subunits forms a tetramer, whereas the isolated α -subunit remains in a monomer (17). The wild-type β -subunit is in the equilibrium between monomers and tetramers (17). The position of the elution peak for the $\beta\alpha(\text{PM3})$ -subunit is also between those of a tetramer and a monomer, but the peak position at 22.5 ml was significantly deviated from that of the wild-type β -subunit at 22.0 ml. Since this elution peak was independent of the sample concentration from 5 to 80 μM (Fig. 5B), the $\beta\alpha(\text{PM3})$ -subunit forms a stable homo-dimer, not an equilibrium state between tetramers and dimers or monomers. In the chromatogram for the mixture of the $\beta\alpha(\text{PM3})$ - and α -subunits, two peaks were observed, each of which coincides with the peak for the isolated $\beta\alpha(\text{PM3})$ - and α -subunits, indicating no association of the $\beta\alpha(\text{PM3})$ -subunit with the α -subunit. On the other hand, the peak for the mixture of the $\beta\alpha(\text{PM3})$ - and β -subunits showed a single broad peak and the elution pattern for the mixture was not a simple addition of those of the corresponding isolated subunits. These elution patterns imply that the $\beta\alpha(\text{PM3})$ -subunit preferentially binds to the β -subunit, not to the α -subunit, and the association property of the $\beta\alpha(\text{PM3})$ -subunit corresponds to that of the α -subunit as the case for the $\beta\alpha(\text{M4})$ -subunit (4). It should be noted here that the elution peak for the mixture was detected at the middle of those for tetrameric native Hb A and dimeric $\beta\alpha(\text{PM3})$ -subunits, suggesting that the complex of the $\beta\alpha(\text{PM3})$ - and β -subunits is in the equilibrium between a hetero-dimer [$\beta\alpha(\text{PM3})$] β and a hetero-tetramer [$\beta\alpha(\text{PM3})$] β $_2$. As shown in Fig. 5B, the elution peak for the mixture of the $\beta\alpha(\text{PM3})$ - and β -subunits depends on the protein concentration and the fitting curve of the mixture shifts to the right side, compared to that of native hemoglobin tetramer, indicating that the

dissociation into dimers was enhanced in the complex of the $\beta\alpha(\text{PM3})$ - and β -subunits. The tetramer-dimer dissociation constants, K_D , were estimated as 1.4 (16) and 11 μM for Hb A and the complex of the $\beta\alpha(\text{PM3})$ - and β -subunits, respectively.

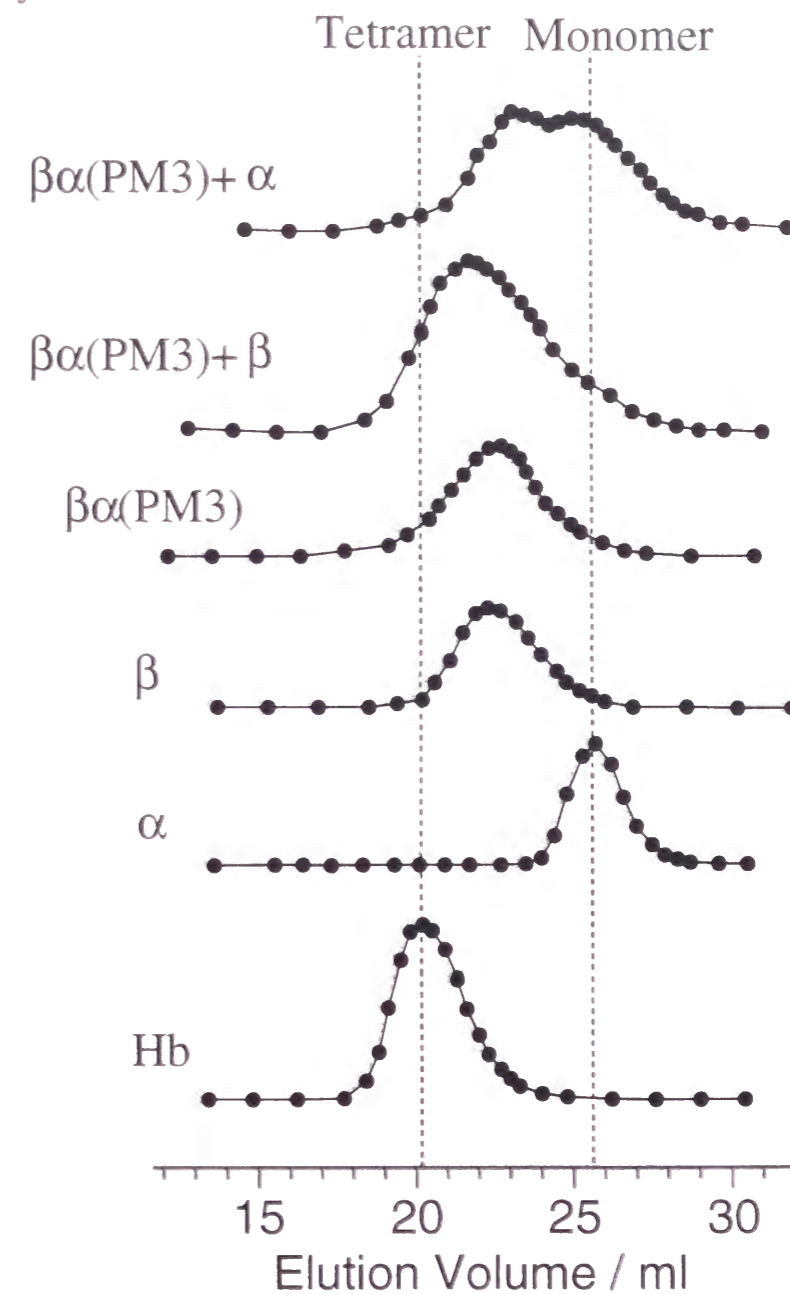


Fig. 5(A) Chromatography of carbonmonoxy form of the $\beta\alpha(\text{PM3})$ -subunit on a sephacryl S-200 HR column Experimental conditions were as follows: 50 mM Tris, 0.1 M NaCl, pH 7.4, at 277 K. Sample concentration was 20 mM on the heme basis.

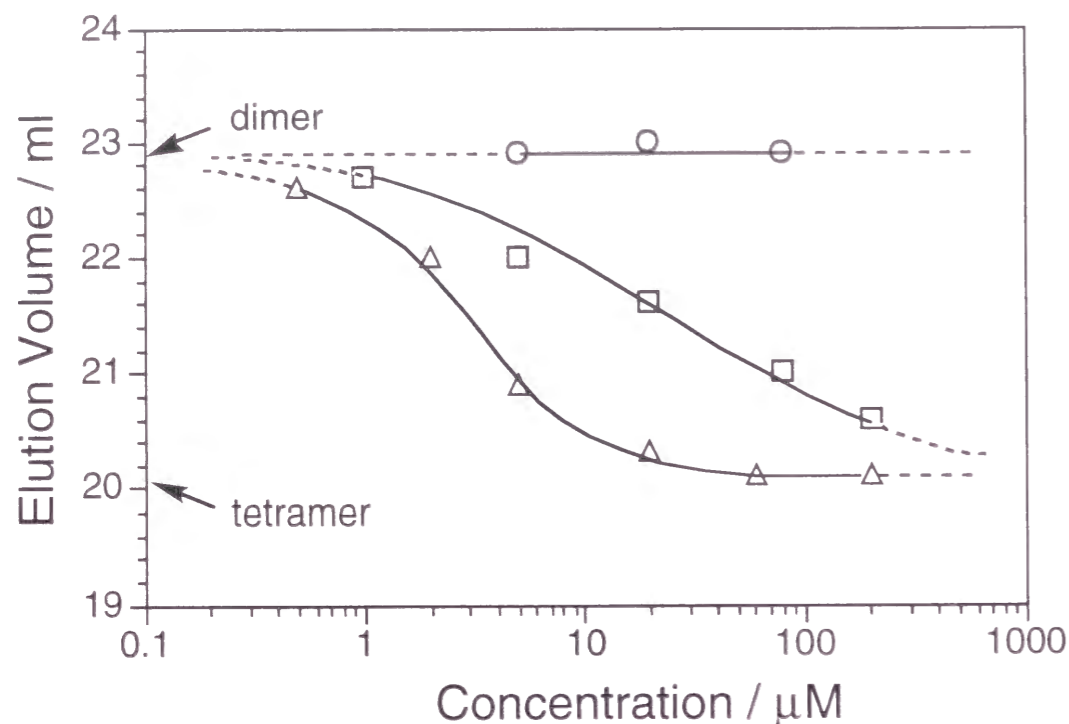


Fig. 5(B) Centroid elution volumes of hemoglobin, the isolated $\beta\alpha(\text{PM3})$ -subunit and the mixture of the β - and $\beta\alpha(\text{PM3})$ -subunits as a function of protein concentration Symbols correspond to hemoglobin (▲), $\beta\alpha(\text{PM3})$ -subunit (○) and the mixture of the β - and $\beta\alpha(\text{PM3})$ -subunits (□). Experimental conditions were as follows: 50 mM Tris, 0.1 M NaCl, pH 7.4, at 277 K.

Subunit Interface Structures – In order to gain further insights into the subunit interface structure for the pseudo-module substituted globins and its complex of the $\beta\alpha(\text{PM3})$ - and β -subunits, we have measured the ^1H NMR spectra in the hydrogen-bonded proton region for the carbonmonoxy and deoxy forms (Figs. 6A and 6B). While no exchangeable proton signals were observed in the downfield region from 10 to 15 ppm for the isolated carbonmonoxy β -subunits, a broad proton signal at 12.4 ppm was detected for the $\beta\alpha(\text{PM3})$ -subunit. This peak disappeared in 100 % D_2O (data not shown). Such an exchangeable proton signal in the downfield region was also encountered for carbonmonoxy Hb A, which has been assigned to the hydrogen bonds in the subunit interface (26-28). Similarly, the resonance at 12.4 ppm can be assignable to the hydrogen bond at the subunit interfaces of the homo-dimer, $[\beta\alpha(\text{PM3})]_2$. In the presence of the native β -subunit, another exchangeable proton resonance appeared at 10.4 ppm (Fig. 6A), which would also originate from a hydrogen bonded proton in the subunit interface of the complex of the $\beta\alpha(\text{PM3})$ - and β -subunits.

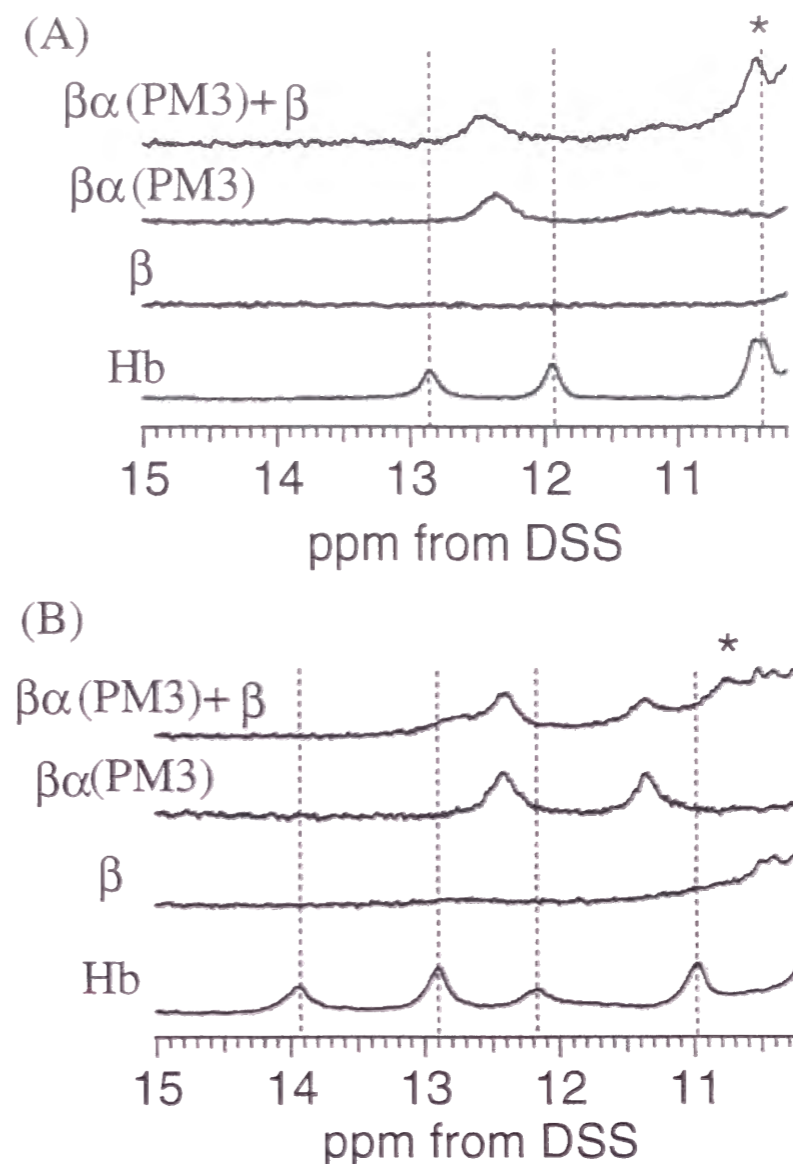


Fig. 6(A) NMR spectra in the hydrogen bonded proton region for carbonmonoxygenated subunits Proton resonance peaks for Hb at 10.4, 11.9 and 12.8 ppm have been assigned to the hydrogen bonded protons between Asp-94 α_1 and Asn-102 β_2 (27), His-103 α_1 and Asn-108 β_1 (28), and Asp-126 α_1 and Tyr-35 β_1 , respectively (28). An asterisk represents a novel resonance peak which appears upon the mixture of the β - and $\beta\alpha(\text{PM3})$ -subunits. Experimental conditions were as follows: 50 mM Na-Phosphate, 0.1 M NaCl, pH 7.4, at 290 K. Sample concentration was 600 μM on the heme basis. **(B) NMR spectra in the hydrogen bonded proton region for deoxygenated subunits** Proton resonance peaks for Hb at 11.0, 12.2, 12.9 and 13.9 ppm have been assigned to the hydrogen bonded protons between Asp-94 α_1 and Trp-37 β_2 (27, 30), His-103 α and Asn-108 β (28), Asp-126 α and Tyr-35 β (28), and Tyr-42 α_1 and Asn-99 β_2 , respectively (27). An asterisk represents a novel resonance peak which appears upon the mixture of the β - and $\beta\alpha(\text{PM3})$ -subunits. Experimental conditions were as in (A).

Structural alterations in the subunit interface by the pseudo-module substitution are also evident in the NMR spectra of the deoxygenated state of the chimeric globin. By the dissociation of the ligands from Hb A, the rearrangements in the α_1 - β_2 subunit interface are induced (29), which is reflected in the NMR spectra in the downfield region. For deoxy Hb A, the characteristic T-state marker resonances were observed at 13.9 and 11.0 ppm (Fig. 6B) (27, 30), whereas, in the $\beta\alpha$ (PM3)-subunit, these marker signals were not detected and a new peak appeared at 11.3 ppm by deoxygenation. Although the appearance of the resonance at 11.3 ppm by deoxygenation suggests the rearrangements in the hydrogen bonds at the subunit interface in the pseudo-module substituted globin, its spectral pattern is quite different from that of hemoglobin. In addition to the resonance peaks at 11.4 and 12.4 ppm, the complex of the $\beta\alpha$ (PM3)- and β -subunits in the deoxy state exhibited an exchangeable proton signal at 10.7 ppm (Fig. 6B), which was not observed for the isolated deoxygenated subunits. The spectral features for the complex are still quite different between the carbonmonoxy and deoxy states, but the resonance positions for the complex are not identical with those for hemoglobin. This implies that the quaternary structural changes accompanied by deoxygenation for the complex would not fully correspond to those for native Hb A. *Heme Environmental Structures* - The structural perturbation was also manifested in the heme environmental structure, as revealed by ^1H NMR spectra of the carbonmonoxy and deoxy form of the chimeric globins (Figs. 7 and 8). In the carbonmonoxy isolated subunits (Panel A), a peak from the γ_1 -methyl proton of Val (E11) appeared at -2.0 and -2.2 ppm for the α - and β -subunit, respectively, which has served as a marker for the tertiary structure in the heme vicinity (31, 32). The corresponding signal for the $\beta\alpha$ (PM3)-subunit was detected at the same position as that of the native β -subunit, implying that the heme environmental structure near Val(E11) residue was not so perturbed by the pseudo-module substitution (33). However, the resonance peak for the $\beta\alpha$ (PM3)-subunit is significantly broadened and asymmetric, suggesting conformational changes in the heme vicinity upon the pseudo-module substitution. Such conformational changes in the heme distal site are supported by the spectral changes in the spectrum between -0.5 and -1.4 ppm.

Here, noteworthy is that the spectral pattern for the complex of the $\beta\alpha$ (PM3)- and β -subunits is a simple addition of that for the corresponding isolated subunits, regardless of rather stable complex formation of these two subunits. The association of the $\beta\alpha$ (PM3)- and β -subunits would not affect the heme

distal structure of the counterpart subunit, which is in sharp contrast to the complex formation of the native α - and β -subunits.

Fig. 8 shows the ^1H NMR spectra for the deoxy state of the chimeric and native globins. In the NMR spectra of the isolated native α - and wild type β -subunits, an exchangeable proton resonance was observed at 78 and 88 ppm in the far downfield hyperfine shifted region (Fig. 8A), respectively, which have been assigned to the N_δH proton of the proximal histidine (F8) (34, 35). A couple of hyperfine shifted resonances in the region between 12 and 28 ppm (Fig. 8II) originated from the protons of heme peripheral groups including heme methyl groups (36). By the substitution of the pseudo-module PM3 in the β -subunit, the resonance position of the proximal N_δH proton was obviously shifted to the position for the α -subunit. The spectral pattern for the resonances of the heme peripheral group is also highly perturbed by the substitution of the pseudo-module PM3. These prominent spectral changes suggest that the substitution of the pseudo-module PM3 alters the heme proximal structure of the β -subunit and converts the coordination structure of the β -subunit into that of the α -subunit like. On the other hand, the substitution of the module M4 induced much smaller upfield shift for the resonance of the proximal histidine $\text{N}_\delta\text{H}^4$, although the spectral pattern for the heme peripheral groups are rather close to that of the pseudo-module substituted subunit.

In addition to the isolated native and chimeric subunits, we have measured the NMR spectra for the complex of the $\beta\alpha$ (PM3)- and β -subunits in the deoxy state. As shown in Fig. 8, native hemoglobin subunits show a large upfield shift of the proximal histidyl N_δH proton by formation of the $\alpha_2\beta_2$ tetramer, indicating that significant structural changes are induced by the tetramer formation of the native subunits. The resonance positions of the heme peripheral groups in the NMR spectra of tetrameric hemoglobin are quite different from those of the two isolated subunits, supporting the structural changes by formation of the functional tetrameric hemoglobin (36). However, such remarkable spectral changes were not accompanied by the association of the $\beta\alpha$ (PM3)- and β -subunits. Only a slight downfield shift of the proximal histidyl N_δH proton resonance was detected for the $\beta\alpha$ (PM3) subunit. Such a small shift for the resonance positions of the proximal histidines implies that the subunit association of the $\beta\alpha$ (PM3)- and β -subunits does not induce the large structural rearrangements around their heme vicinity.

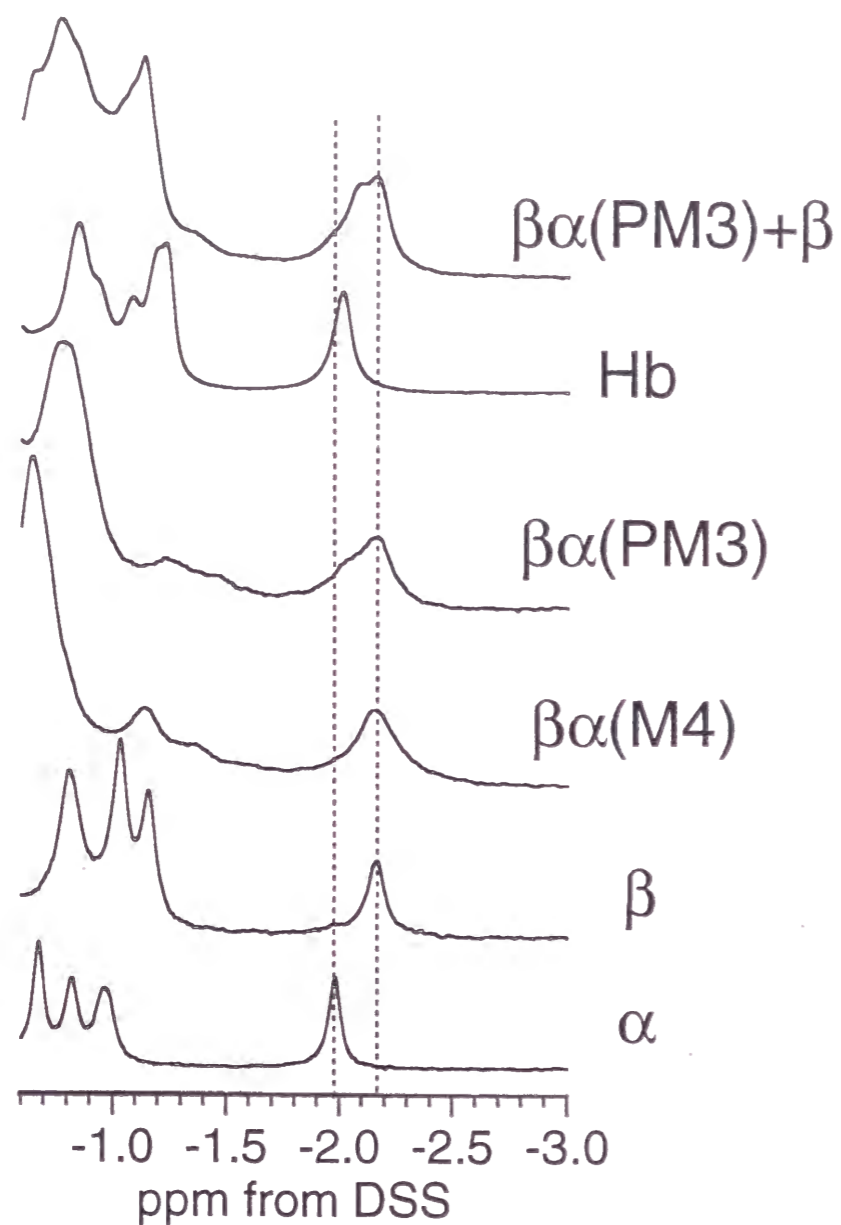


Fig. 7 Proton NMR spectra (500 MHz) for carbonmonoxygenated subunits Experimental conditions were as follows: 50 mM Na-Phosphate, 0.1 M NaCl, pH 7.4, at 290 K. Sample concentration was 600 μ M on the heme basis. The resonance peak around -2.0 ppm has been assigned to γ 1-methyl protons of Val (E11). The signals for the α -subunit at -0.9, -0.7 and -0.6 ppm are from the δ_2 -methyl of Leu(B10), δ_1 -methyl of Leu(FG3) and δ_1 -methyl protons of Leu(B10) [Schaeffer et al., (1988) *Eur. J. Biochem.* **173**, 317-325]. The signals for the β -subunit at -1.2, -1.0 and -0.8 ppm are from the δ_1 and δ_2 -methyls of Leu(H19) and δ_2 -methyl of Leu(B10) [Craescu and Mispelter (1988) *Eur. J. Biochem.* **176**, 171-178].

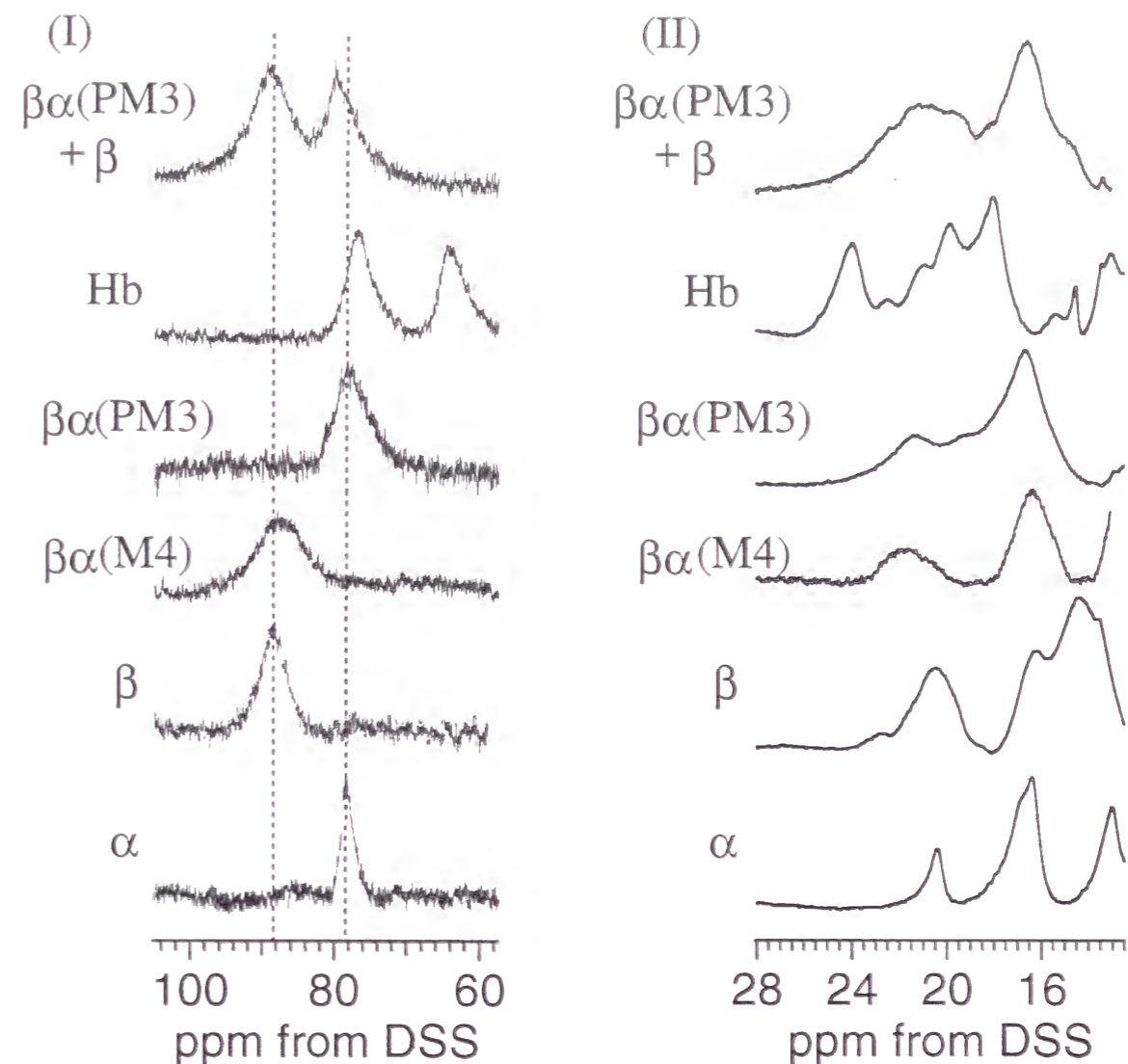


Fig. 8 Proton NMR spectra (500 MHz) for deoxygenated subunits Experimental conditions were as follows: 50 mM Na-Phosphate, 0.1 M NaCl, pH 7.4, at 290 K. Sample concentration was 600 μ M on the heme basis. (I) hyperfine-shifted proton resonances of proximal His $N_{\delta}H$. (II) hyperfine-shifted proton resonances of heme methyl groups

Oxygen Binding Property of the $\beta\alpha$ (PM3)-Subunit – To evaluate the effects of the pseudo-module substitution on the oxygen affinity and cooperativity for the oxygen binding of globins, oxygen equilibrium curves for the chimeric and native globins were examined. Fig. 9 delineates the oxygenation curves, expressed by saturation versus log P plots. The P_{50} value of the $\beta\alpha$ (PM3)-subunit was estimated to be 1.37 mmHg, corresponding to the lower affinity than that for the isolated wild type β -subunit (Table II).

For the complex of the β - and $\beta\alpha$ (PM3)-subunits, the P_{50} value is 0.97 mmHg, which is middle of those of the isolated subunits. Since the oxygen

curve for the complex of the β - and $\beta\alpha(\text{PM3})$ -subunits was not biphasic, the difference of the oxygen affinities of $\beta\alpha(\text{PM3})$ - and β -subunits in the complex are indistinguishable (37). The n_{max} value for the complex is unity, implying that it does not show any cooperative oxygen binding as the case for the isolated chimeric and native α - and β -subunits (Table II).

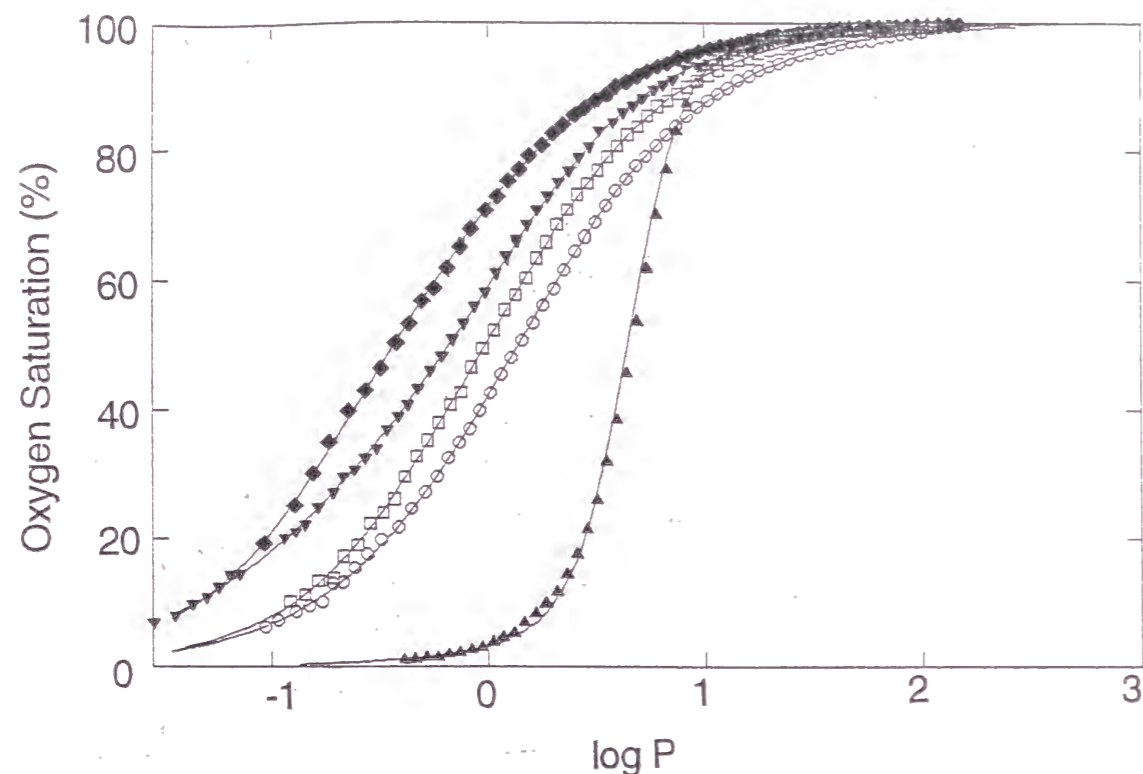


Fig. 9 Y versus log P plots of oxygen equilibrium curves Symbols correspond to hemoglobin (▲), β -subunit (◆), α -subunit (▼), $\beta\alpha(\text{PM3})$ -subunit (○) and the mixture of the β - and $\beta\alpha(\text{PM3})$ -subunits (□). Experimental conditions were as follows: 50 mM Tris, 0.1 M NaCl, pH 8.4, at 25°C. Sample concentration was 60 μM on the heme basis.

Table II Oxygen equilibrium parameters for tetrameric Hb, isolated α -, β -, $\beta\alpha(\text{PM3})$ -subunits and mixture of the β - and $\beta\alpha(\text{PM3})$ -subunits

| | P_{50} (mmHg) | n_{max} |
|---------------------------------|-----------------|------------------|
| Hb | 2.30 | 2.99 |
| α | 0.53 | 1.00 |
| β | 0.37 | 0.97 |
| $\beta\alpha(\text{PM3})$ | 1.37 | 1.01 |
| $\beta\alpha(\text{PM3})+\beta$ | 0.97 | 1.00 |

DISCUSSION

Effects of Pseudo-module Substitution on Structure and Function of Globins - As illustrated in the CD spectra, the pseudo-module substituted subunit, $\beta\alpha(\text{PM3})$ -subunit, can be folded to a stable globin structure as observed for native globins. These minimal effects of the pseudo-module substitution on the protein structure were also supported by the urea denaturation curve for the chimeric subunits (Table I). The free energy change ($\Delta G_{\text{H}_2\text{O}}$) for the denaturation of the $\beta\alpha(\text{PM3})$ -subunit was little affected by the substitution of the pseudo-module PM3. These findings clearly indicate that the replacement of the pseudo-module PM3 in hemoglobin β -subunit with that of the α -subunit did not perturb the globin structure of the native protein.

However, the effects of the pseudo-module substitution on the heme environmental structure were prominent. The characteristic features of the heme environment for the $\beta\alpha(\text{PM3})$ -subunit is that the resonance of the proximal N_δH proton for the deoxy $\beta\alpha(\text{PM3})$ -subunit was observed at the position for the isolated α -subunit. For the module substituted $\beta\alpha(\text{M4})$ -subunit, the coordination structure of the proximal His is still a β -like structure as shown in Fig. 8A (4). Since the pseudo-module PM3 share the amino acid residues from FG4 to H6 with the module M4, this different coordination structure between the two chimeric subunits would originate from the region from F1 to FG3 which is included in PM3, not in M4. In fact, the amino acid sequence from F1 to FG3 constructs most parts of the heme proximal structure and includes the proximal histidine, which strongly suggests that this segment regulates the heme coordination structure.

Contrary to the coordination structure, the structure of the heme distal site of the chimeric $\beta\alpha(\text{PM3})$ -subunits is rather close to the β -subunit. The NMR resonance from methyl group of Val E11 in the carbonmonoxy form appeared at the position for the native β -subunit as found for the module substituted $\beta\alpha(\text{M4})$ -subunit, although minor conformational changes around Val E11 were detected in the NMR spectrum. Based on the amino acid sequences for the β -subunit, the distal cavity of globins is formed by the B, C, D and E-helices which are not involved in the pseudo-module PM3 or module M4. Thus, we can conclude that the substantial structural changes induced by the pseudo-module PM3 substitution are rather localized in the proximal site.

The subunit association is another property which depends on the pseudo-module PM3. As Fig. 5A shows, the $\beta\alpha(\text{PM3})$ -subunit can associate with the β -subunit, but not with the α -subunit, which also resembles that of the native α -subunit. Such a conversion of the association property was also experienced for the module substituted subunit, $\beta\alpha(\text{M4})$ -subunit (4). As depicted in Fig. 2,

the common region in the pseudo-module PM3 and the module M4 is from FG4 to H6 in the amino acid sequence and these amino acid residues would play key roles in the subunit association of hemoglobin. Inspection of the X-ray crystal structure also supports the functional role of this region, since most parts of the $\alpha 1\beta 1$ subunit interface dominating subunit assembly in hemoglobin consists of these residues as revealed in Fig. 1A.

In contrast to the effects of the PM3 substitution on the coordination structure of the proximal histidine and on the association property of the subunits, the oxygen binding properties for $\beta\alpha(\text{PM3})$ -subunit are not so simple to interpret. As found in Fig. 9, the isolated $\beta\alpha(\text{PM3})$ -subunit shows a lower oxygen affinity than the isolated β -subunit. The NMR spectra of its deoxygenated state (Fig. 8) also support the lower oxygen affinity of the $\beta\alpha(\text{PM3})$ -subunit: the upfield bias of the proximal His N_δH resonance corresponds to the increased strain of the iron-histidyl bond, which would be responsible for the decreased oxygen affinity (35). However, the oxygen affinity of the $\beta\alpha(\text{PM3})$ -subunit is still lower than that of the α -subunit in which the resonance position of the proximal histidine N_δH is the same as that in the $\beta\alpha(\text{PM3})$ -subunit. Such an unexpected low oxygen affinity for the $\beta\alpha(\text{PM3})$ -subunit suggests that some other factors such as the heme distal structures affecting the oxygen affinity in globins might be subtly perturbed by the pseudo-module substitution.

On the other hand, the oxygen affinity of the complex of the $\beta\alpha(\text{PM3})$ - and β -subunits was much higher than that of Hb A, and allosteric cooperativity was not detected for the complex. As revealed by the NMR spectrum for the hydrogen bonded region, the hydrogen bonds in the subunit interface of the complex is quite different from that of native Hb A, and the spectral feature characteristic of the T state was missing for the complex. The NMR spectrum in the hyperfine shifted region at 12-28 ppm is also suggestive of absence of the specific interactions between these two subunits (36). On the basis of X-ray structural studies, two sliding contact regions, C2-CD1 and FG3-G7, are essential for the allostericity in hemoglobin A (16, 39-45). However, the C2-CD1 region of the $\beta\alpha(\text{PM3})$ -subunit remains to be β -subunit type upon the pseudo-module substitution. The incomplete adjustment of the $\alpha 1\beta 2$ subunit interface would reduce the subunit interactions in the complex of the β - and $\beta\alpha(\text{PM3})$ -subunits, resulting in non-cooperative oxygen binding.

Structural and Functional Significance of the Pseudo-module PM3 in Globins. In this study, we have shown that the substitution of the structural segment other than the module can also produce a stable "chimeric" globin, which leads us to re-examine the structural and functional significance of the

modular structure in globins. Comparison of the "chimeric" property of the $\beta\alpha(\text{PM3})$ -subunits with that of the native and the module substituted subunit can reinforce the structural and functional significance of the pseudo-module PM3. One of the possible reasons for formation of the stable and functional chimeric globin by the pseudo-module substitution would be high structural homology between the α - and β -subunits. Although the amino acid sequence homology is not so high between the two subunits (~40 %), their globin structures are quite similar except for the deletion of the D-helix in the α -subunit. However, our previous study on the module substituted $\alpha\beta(\text{M4})$ -subunit, in which the module M4 of the β -subunit was implanted into the α -subunit, showed that the globin structure of the $\alpha\beta(\text{M4})$ -subunit is highly perturbed and destabilized probably due to loss of the stable intramolecular helix packing (5), concluding that the structural similarity is not enough to produce a stable chimeric protein. It is thus likely that the PM3 substitution would not accompany substantial failures in the helix packings. According to the previous study by Jennings and Wright, the packing between the A- and H-helices is formed in the first step of the folding process in apo-myoglobin and these helices are crucial for protein folding of globins (46). Since the pseudo-module PM3 contains only a part of H-helix as shown in Fig. 1 and most of the A- and H-helices are derived from the parent β -subunit, the PM3 substitution would not substantially perturb the helix packing.

The stable structure and functional conversion for the $\beta\alpha(\text{PM3})$ -subunit suggest that the pseudo-module PM3 might have some structural significance in the globin structure like the modules, which leads us to re-examine boundary of the module in globins. It should be noted here that the modules in globins, which have been defined on the basis of the diagonal plots of the inter- C_α atom distances for the main chain (1), are much larger in size than those in other proteins (47). That is, the modules in globins consist of 30 - 40 amino acid residues (1), whereas the numbers of the amino acid residues for the modules in most of other proteins are 10 - 25 (7, 47). Such a large modular structure in globins may allow us to infer that the current modules in globin are not minimal unit for the structure and function of globin and can be further divided into some "sub"-modules. In fact, this speculation is strongly supported by the recent revised module assignment with a centripetal profile (7) which indicates that each of the modules in globins can be decomposed into the two "small" modules and, consequently, globins has eight "small" modules (48). Interestingly, the new identified module boundaries in the modules M3 and M4 almost coincide with the boundaries of the pseudo-module PM3. In other words, the substitution of the pseudo-module PM3 might be a kind of the

module substitution. Although it is still premature to conclude that the pseudo-module PM3 is a combination of the two "small" modules, it can be safely said that the pseudo-module PM3 of globins has some structural and functional significance.

In summary, the substitution of the pseudo-module PM3 which is originally supposed to have no structural and functional significance can retain the structural stability comparable to the native globins. Moreover, the structural and functional properties of the PM3 substituted subunit were "chimeric" between the parent subunits. The coordination structure of the proximal histidine and the association property for the $\beta\alpha$ (PM3)-subunit was rather close to that for the α -subunit, while the structure of the distal site was still β -subunit like. These findings strongly suggest that the pseudo-module has some structural and functional significance. Together with the structural and functional properties of the native and module substituted subunits, we can propose that the former half of the pseudo-module PM3 and the latter one would correspond to the "sub"-modules regulating the heme proximal structure and subunit assembly, respectively. In order to strengthen our argument on structural and functional significance of the "sub"-module in globins, the preparation and characterization of the novel chimeric globin subunits in which one of these "sub"-modules is replaced by that of the partner subunit are now in progress.

ACKNOWLEDGMENT

Grateful acknowledgment is dedicated to Dr. Yoshinao Wada for fast atom bombardment mass spectrometry. Furthermore, we are indebted to the reviewers' suggestions very much.

REFERENCES

1. Go, M. (1981) *Nature*, **291**, 90-92
2. Go, M. (1983) *Proc. Natl. Acad. Sci. USA* **80**, 1964-1968
3. Eaton, W. A. (1980) *Nature* **284**, 183-185
4. Wakasugi, K., Ishimori, K., Imai, K., Wada, Y. and Morishima, I. (1994) *J. Biol. Chem.* **269**, 18750-18756
5. Inaba, K., Wakasugi, K., Ishimori, K., Konno, T., Kataoka, M. and Morishima, I. (1997) *J. Biol. Chem.* in press
6. Wakasugi, K., Ishimori, K. and Morishima, I. (1997) *Biophys. Chem.* in press.
7. Noguti, T., Sakakibara, H. and Go, M. (1993) *Proteins* **16**, 357-363

8. Go, M. and Noguti, T. (1995) *Tracing Biological Evolution in Protein and Gene Structures* (eds. Go, M. and Scimmel, P.) 229-235
9. Gilbert, W. (1978) *Nature* **271**, 501
10. Blake, C. C. F. (1979) *Nature* **277**, 598
11. Nagai, K and Thøgerson, H. C. (1984) *Nature* **309**, 810-812
12. Nagai, K., Perutz, M. F., and Poyart, C. (1985) *Proc. Natl. Acad. Sci. U.S.A.* **82**, 7252-7257
13. Nagai, K., and Thøgerson, H.C. (1987) *Methods Enzymol.* **153**, 461-481
14. Wada, Y., Fujita, T. Hayashi, A., Sakurai, T., and Matsuo, T. (1989) *Biomed. Environ Mass Spectrom.* **18**, 563-565
15. Konno, T. and Morishima, I., (1993) *Biochem. Biophys. Acta* **1162**, 93-98
16. Ishimori, K., Hashimoto, M., Imai, K., Fushitani, K., Miyazaki, G., Morimoto, H., Wada, Y. and Morishima, I. (1994) *Biochemistry* **33**, 2546-2553
17. Valdes, R., Jr. and Ackers, G. K. (1977) *J. Biol. Chem.* **252**, 74-81
18. Imai, K. (1981) *Methods. Enzymol.* **76**, 438-449
19. Imai, K. (1982) *Allosteric Effect in Haemoglobin*, Cambridge University Press, London
20. Imai, K., Morimoto, H., Kotani, M., Watari, H., Hitata, W. and Kuroda, M. (1970) *Biochem. Biophys. Acta* **200**, 189-196
21. Hayashi, A., Suzuki, T. and Shin, M. (1973) *Biochem. Biophys. Acta* **310**, 309-316
22. Lynch, R. E., Lee, G. R. and Cartwright, G. E. (1976) *J. Biol. Chem.* **251**, 1015-1019
23. Winterbourn, C. C., McGrath, B. M. and Carrell, R. W. (1976) *Biochem. J.* **155**, 493-502
24. Imai, K. (1994) *Methods. Enzymol.* **232**, 559-576
25. Beychok, S., Tyuma, I., Benesch, R. E., and Benesch, R. E. (1967) *J. Biol. Chem.* **242**, 2460-2462
26. Asakura, T., Adachi, K., Wiley, J. S., Fung, L. W. -M., Ho, C., Kilmartin, J. V. and Perutz, M. F. (1976) *J. Mol. Biol.* **104**, 185-195
27. Fung, L. W. M. and Ho, C. (1975) *Biochemistry* **14**, 2526-2535
28. Russu, I. M., Ho, N. T. and Ho, C. (1987) *Biochem. Biophys. Acta* **914**, 40-48
29. Perutz, M. F. (1970) *Nature* **228**, 726-739
30. Ishimori, K., Imai, K., Miyazaki, G., Kitagawa, T., Wada, Y., Morimoto, H. and Morishima, I. (1992) *Biochemistry* **31**, 3256-3262
31. Lindstrom, T. R., Nore, I. B. E., Charashe, S., Lehmann, H., and Ho, C. (1972) *Biochemistry* **11**, 1677-1681
32. Dalvit, C. and Ho, C. (1985) *Biochemistry* **24**, 3398-3407

33. Shulman, R. G., Wuthrich, K., Yamane, T., Patel, D. and Blumberg, W. E. (1970) *J. Mol. Biol.* **53**, 143
34. Takahashi, S., Lin, A. K. -L. C. and Ho, C. (1980) *Biochemistry* **19**, 5196-5202
35. Nagai, K., La Mar, G. N., Jue, T. and Bunn, H. F., (1982) *Biochemistry* **21**, 842-847
36. Ho, C. (1992) *Advan. Protein Chem.* **43**, 153-312
37. Barrick, D., Ho, N. T., Simplaceanu, V., Dahlquist, F. W. and Ho, C. (1997) *Nature Struct. Biol.* **4**, 78-83
38. Springer, B. A., Sligar, S. G., Olson, J. S. and Phillips Jr. G. N. (1994) *Chem. Rev.* **94**, 699-714
39. Nagai, M., Nishibu, M., Sugita, Y., Yoneyama, M., Jones, R. T. and Gordon, S. (1975) *J. Biol. Chem.* **250**, 3169-3173
40. Weatherall, D. J., Clegg, J. B., Callender, S. T., Wells, R. M. G., Gale, R. E., Huehns, E. R., Perutz, M. F., Viggiano, G. and Ho, C. (1977) *J. Haemat.* **35**, 177-191
41. Thillet, J., Arous, N. and Rosa, J. (1981) *Biochem. Biophys. Acta* **670**, 260-264
42. Rochette, J., Poyart, C., Varet, B. and Wajcman, H. (1984) *FEBS Letters*, **166**, 8-12
43. Imai, K., Fushitani, K., Miyazaki, Z., Ishimori, K., Kitagawa, T., Wada, Y., Morimoto, H., Morishima, I., Shih, D. T. and Tame, J. (1991) *J. Mol. Biol.* **218**, 769-778
44. Hashimoto, M., Ishimori, K., Imai, K., Miyazaki, G., Morimoto, H., Wada, Y. and Morishima, I. (1993) *Biochemistry* **32**, 13688-13695
45. Perutz, M. F. (1989) *Quart. Rev. Biophys.* **22**, 139-236
46. Jennings, P. A. and Wright, P. E. (1993) *Science* **262**, 892-896
47. Yura, K. and Go, M. (1995) *Tracing Biological Evolution in Protein and Gene Structures* (eds. Go, M. and Scimmell, P.) 187-195
48. Go, M. et. al submitted for publication (Nature)

FOOTNOTES

¹"Wild type" subunit represents the protein expressed in *Escherichia coli* and a methionine residue is located at the N-terminal. "Native" subunit corresponds to the protein purified from human red blood cell. In the "wild type" β -subunit, we confirmed that the mutation of Val to Met does not seriously perturb the globular structure and heme environmental structure of the β -subunit. The CD and NMR spectra for the "wild typr" β -subunit were virtually same as those of the "native" β -subunit.

²We have also tried to carry out the urea denaturation experiment in the absence of the heme group. However, the apo chimeric $\beta\alpha(\text{PM3})$ - and $\beta\alpha(\text{M4})$ -subunits are extremely unstable to aggregate under the following condition: pH 7.4, urea concentration of below 2 M, sample concentration of 5 μM . Therefore, we cannot exactly measure molar ellipticity at 222 nm and estimate equilibrium stability for the apo-globins.

³We confirmed the homogeneity of the purified $\beta\alpha(\text{PM3})$ -subunit by native and SDS PAGE gel electrophoresis. Thus, the spectral change would not be due to inhomogeneous preparation.

⁴The line-width for the resonance from the $\beta\alpha(\text{M4})$ -subunit was broad compared to the one for other globins [Johnson, M. E., Fung, L. W. and Ho, C. (1977) *J. Am. Chem Soc.* **99**, 1245-1250). Such a line broadening was also observed for the native isolated subunit in high pH region due to the enhanced exchange rate of the N_δH of the proximal histidine [La Mar, G. N. and Jue, T. (1984) *J. Mol. Biol.* **178**, 929-939]. Although the reasons for the line broadening in the chimeric globin has not yet been clear, some structural changes around the proximal histidine induced by the module substitution might affect the exchange rate of the N_δH of the proximal His.

Chapter 4

Substitution of pseudo-module PM3 in hemoglobin α -subunit and myoglobin (Mb α (PM3)-subunit)

ABSTRACT

Our recent study for the pseudo-module substitution in hemoglobin α - and β -subunits proposed that the pseudo-module PM3, the region from the center of the module M3 to the center of M4, might be a new structural/functional unit regulating heme proximal structure and subunit assembly. To gain further insights into the structural and functional significance of the PM3, we have prepared the Mb α (PM3)-subunit, in which the pseudo-module PM3 of myoglobin was replaced by that of the α -subunit, and compared its structure and function with those of the module M4 substituted myoglobin, Mb α (M4)-subunit. Structural and functional analysis with NMR spectroscopy and gel chromatogram revealed that the heme proximal structure and the association property of the Mb α (PM3)-subunit were not converted into the α -subunit type. Such failure of the structural and functional conversion for the Mb α (PM3)-subunit indicates that the heme proximal structure and the association property of globin proteins are not determined only by the pseudo-module PM3. On the other hand, CD spectra clearly indicated that globin structure of the Mb α (M4)-subunit was drastically disordered compared to that of the Mb α (PM3)-subunit. Considering that the substitution of the module M4 including the H-helix inevitably accompanies substantial perturbations on the A-H helix packing, such structural disorders in the Mb α (M4)-subunit confirms significance of the A-H helix interaction in globin folding.

Globin structure is composed of four compact structural units, modules M1-M4, which are encoded by the exons on the gene structure (1). The previous study on the module substituted globins experimentally suggested that the module is a structural and functional unit regulating subunit assembly and heme environmental structure in hemoglobin (2). However, we have recently proposed that the pseudo-module¹, which is defined as a segment from the center of one module to the center of the following one, is another structural/functional unit dominant in association property and heme proximal structure in hemoglobin.

| Module | ←M4----- | | |
|---------------|------------------------------------|-------|------------------------------|
| Pseudo-Module | ←PM3----- | | |
| Helix | F | FG | G |
| number | 1.....10 | 1...5 | 1.....19 |
| α-subunit | LSALS <u>DLH</u> *A | HKLRV | DPVNFKLL <u>SH</u> CLLVTLAAH |
| myoglobin | LKPLA <u>QSH</u> *AT | KHKI | PIKYLEFISEAIIHVLHSR |

| Module | -----M4→ | | |
|---------------|----------------------|--|--------|
| Pseudo-Module | -----PM3→ | | |
| Helix | GH | H | HC |
| number | 1..... | 1.....26 | 1..... |
| α--subunit | LP <u>AEF</u> | <u>TPAVHASL</u> DKFL ASVSTVLT SKYR | |
| myoglobin | HP <u>GDF</u> | <u>GADAQ</u> AMNKAL QLFRKDIA AKYK | ELGYQG |

Fig. 1. Amino acid sequence for myoglobin and hemoglobin α- and β-subunits in the pseudo-module PM3 and the module M4 The identical residues are expressed in bold style. The underlines imply the residues contributing to A-H helix packing. The proximal histidine (F8) is marked by an asterisk.

In our recent work, we have prepared the pseudo-module substituted β-subunit, βα(PM3)-subunit, where the pseudo-module PM3 from the center of the module M3 to that of the M4 (Fig. 1) was implanted from the α-subunit into the β-subunit (3). According to the functional analysis with gel chromatogram, the βα(PM3)-subunit preferentially bound to the β-subunit, not to the α-subunit, which implies that the PM3 substitution almost converted the association property of the β-subunit into the α-subunit type. In addition, structural analysis by the NMR measurement revealed that the heme proximal structure of the β-subunit is altered to be α-subunit like upon the implantation of the PM3 from the α-subunit (3). Such structural and

functional conversions by the pseudo-module substitution leads us to infer that the pseudo-module PM3 might have some structural/functional significance in the globin structure like the modules.

In the present study, to gain further insights into the structural and functional roles of the pseudo-module PM3, we have also prepared the Mbα(PM3)-subunit, in which the pseudo-module PM3 of myoglobin is replaced by that of the α-subunit (Fig. 2) and compared its structure and function with those of the module M4 substituted myoglobin, the Mbα(M4)-subunit (Fig. 2). Here, our great interest is whether or not the heme proximal structure and the association property of the Mbα(PM3)-subunit are converted into the α-subunit ones as the case for the the βα(PM3)-subunit. Since the amino acid sequence is substantially different among hemoglobin α-, β-subunits and myoglobin in spite of high similarity of their tertiary structures, the implantation of the pseudo-module PM3 from the α-subunit into myoglobin would cause other effects on the globin structure and function than the implantation into the β-subunit. Therefore, the study for the Mbα(PM3)-subunit as well as the βα(PM3)-subunit would provide more general informations on structural/functional significance of the pseudo-module PM3.

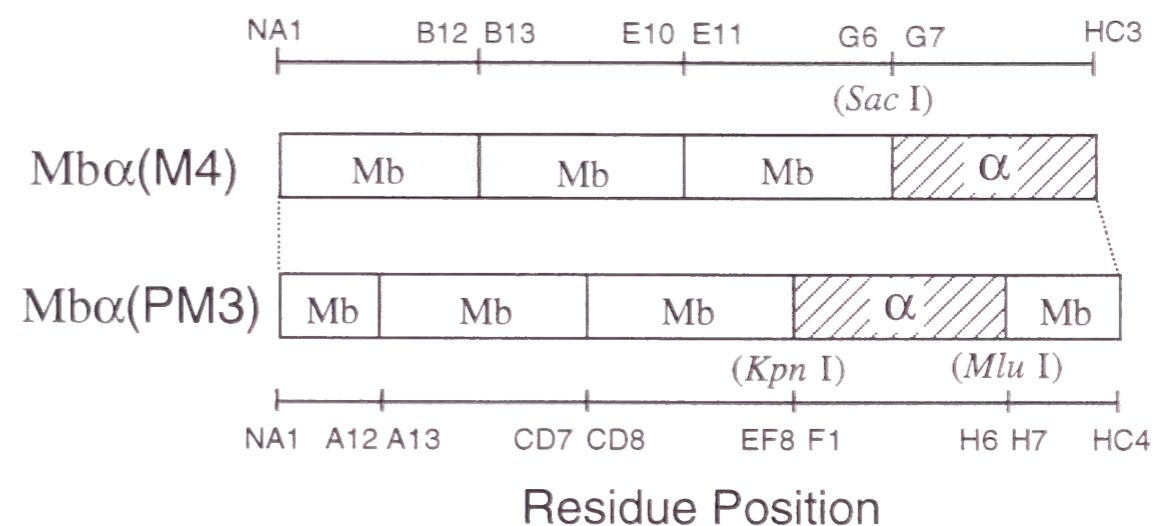


Fig. 2 Novel globins synthesized in this study. Restriction enzyme sites we have used here are written in a parenthesis.

EXPERIMENTAL PROCEDURES

Expression Vector Construction – We have used T7 expression vector to express the Mbα(M4)- and Mbα(PM3)-subunit. Their expression vectors were constructed as illustrated in Fig. 2. A methionine residue was substituted for valine at the N-terminal to initiate the peptide elongation for the present

module and pseudo-module substituted subunits. For the Mb α (M4)-subunit, a *Sac* I site (GAGCTC) was introduced on the boundary between the modules M3 and M4. To construct the genes for the Mb α (PM3)-subunit, *Kpn* I (GGTACC) and *Mlu* I sites (ACGCGT) were implanted by polymerase chain reaction with the mutations from Ala(EF7) and Glu(EF8) to Gly and Thr, respectively. Since the pseudo-module substitution is equivalent to the drastic replacement of as many as 40 amino acid residues, and neither Ala(EF7) nor Glu(EF8) contribute to subunit contact and heme contact (4), we have ignored these two mutations.

Protein Preparation – The prepared gene encoding the chimeric globins were transformed into an *Escherichia coli* strain (BL21), which was grown at 37 °C in 2xTY culture containing ampicillin (100 μ g/ml) overnight. This culture was centrifuged at 5,000 rpm, and the cell pellets were lysed with lysozyme (100 mg per 10 g of pellets) to get the crude chimeric subunits. The module and pseudo-module substituted subunits were purified as previously reported for recombinant Hb (5-7). We confirmed the correct expression of the desired subunits by fast atom bombardment mass spectroscopy (data not shown) (8) and no additional mutations were detected.

Circular Dichroism Spectra - CD spectra of the chimeric and native subunits in far UV region were measured with JASCO J-760 spectrometer at 20 °C. Concentration of the sample was 10 μ M and the buffer was 20 mM Na-phosphate, 0.1 M NaCl and 10 mM NaCN, pH 7.4. The path length for the measurements was 1 mm.

Urea Denaturation Curves – Reaction solutions contain 20 mM Tris (pH 7.4), 1 mM NaCN and various concentrations of urea. Sample concentration was 10 μ M. Changes in the ellipticity at 222 nm were monitored by Jasco J-760 CD spectrometer after ~10 hours equilibration at 20 °C. Cyanomet derivatives were used for the measurements to avoid aggregation of heme and conserve the reversibility between native and denatured states (9)². The fractional denatured population (f_D) under each condition was estimated by the following equation;

$$f_D = ([\theta]_{222, N} - [\theta]_{222}) / ([\theta]_{222, N} - [\theta]_{222, D}) \quad (\text{eq. 1})$$

where $[\theta]_{222, N}$, $[\theta]_{222, D}$ and $[\theta]_{222}$ represent ellipticities at 222 nm in the native, denatured state and under each urea concentration, respectively. The free energy of denaturation, ΔG , was calculated by the following equation:

$$\Delta G = -RT \ln(f_D / (1 - f_D)) \quad (\text{eq. 2})$$

When ΔG varied linearly with urea concentration, [urea], ΔG_{H_2O} , extrapolated ΔG at [urea] = 0, can be estimated by the following equation:

$$\Delta G = \Delta G_{H_2O} - m_{\text{urea}} [\text{urea}] \quad (\text{eq. 3})$$

where m_{urea} is the slope of the linear relation between ΔG and [urea].

Tryptophan Fluorescence Spectra – Tryptophan fluorescence spectra were measured by Perkin Elmer LB50 emission spectrometer at room temperature. The samples were excited at 280 nm, and the emission spectra were measured between 300 and 400 nm (10). We used a crystal cuvette for the fluorescence measurements and the path length was 10 mm. The concentration of the samples was 5 μ M on the heme basis, and the buffer was the same as used in the CD measurements.

NMR Spectra - ¹H NMR spectra at 500 MHz were recorded on BRUKER Avance DRX 500 spectrometer equipped with the Indy workstation (silicon Graphics). In order to measure proton resonances in the diamagnetic region, we used a water gate pulse sequence with 50 ms pulse and 33 K data points over 13-kHz spectral width and minimized the water signal in the sample. The hyperfine-shifted proton resonances were obtained by using a LOSAT pulse sequence with a 65 K data transform of 150 kHz and a 8.5 μ s 90 ° pulse. The probe temperature was controlled at 290 \pm 0.5 K by a temperature control unit of the spectrometer. The volume of the NMR sample was 500 μ l and the concentration was 600 μ M on the heme basis. Proton shifts were referenced with respect to the proton resonance of 2, 2,-dimethyl-2-silapentane-5-sulfonate (DSS).

Gel Chromatogram – Gel filtration measurements were performed by using a Sephacryl S-200 HR column (0.8 cm-d x 62 cm-l) at 4 °C. The buffer used for the chromatography was 50 mM Tris, in the presence of 0.1 M NaCl, and 1 mM Na₂EDTA, pH 7.4 and the flow rate was 7 ml/h (11). The eluted fractions were monitored by absorption at the Soret band (420 nm). Sample volume was 1 ml, and the sample concentration was 20 μ M on the heme basis.

RESULTS

Circular Dichroism Spectra - To examine the effects of the module M4 or pseudo-module PM3 substitution on the globin structure, we have measured far-UV CD spectra of the myoglobin and chimeric globins. As shown in Fig. 3, native myoglobin exhibited two negative broad peaks around 222 and 208 nm (12), which are characteristic of α -helical structure. In the CD spectrum for the Mb α (PM3)-subunit, the molar ellipticity at 222 nm is almost identical to that of myoglobin, but the negative peak at 208 nm increases and a positive peak at 197 nm substantially decreases compared to those of myoglobin. On the other hand, CD curve of the Mb α (M4)-subunit is largely different from that of myoglobin, where the negative ellipticity around 222 nm is quite low and a new

negative peak appears around 206 nm. On the basis of the deconvolution method by Greenfield and Fasman (13), the α -helical content of the Mb α (PM3)-chimeric subunit was approximately estimated as 60 %, which is similar to that of myoglobin (70%), whereas the Mb α (M4)-subunit showed much lower α -helical content (35%). This result clearly indicates that the pseudo-module PM3 substitution causes much less perturbation on the globin structure than the module M4 substitution.

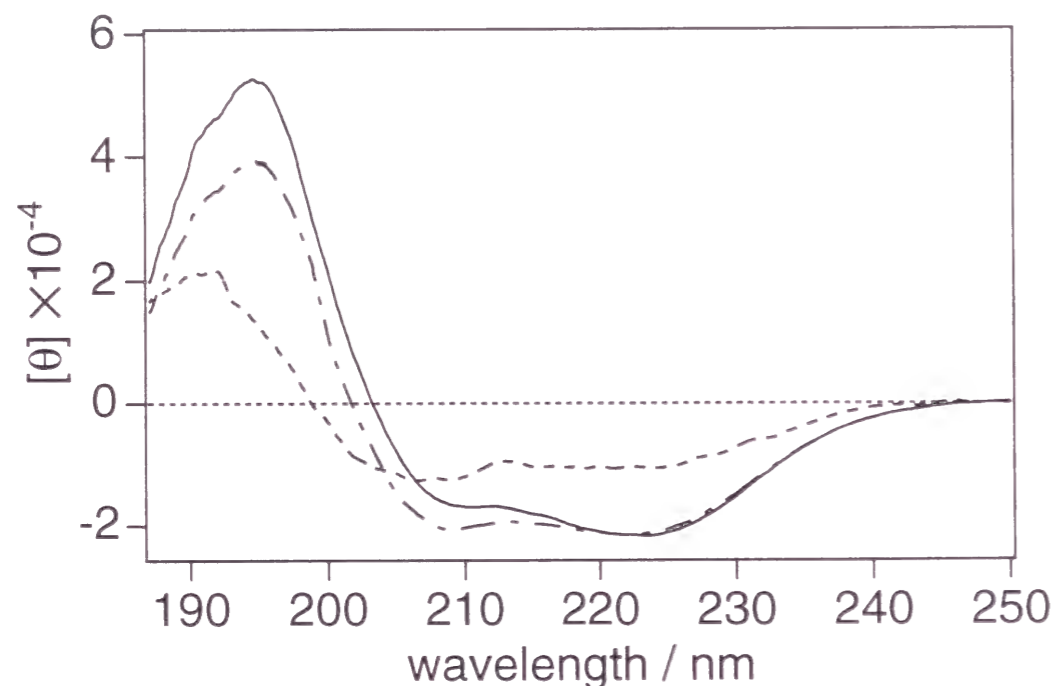


Fig. 3 CD spectra in far UV region of the cyano-met globins. Lines correspond to myoglobin (—), Mb α (M4) (- -)-subunit, and Mb α (PM3)-subunit (- · -). Experimental conditions were as follows: 20 mM Tris, 0.1 M NaCl, 5mM NaCN, pH 7.4, at 290 K. Sample concentration was 5 mM on the heme basis.

Urea Denaturation Curves - Alterations in equilibrium stability upon the pseudo-module and module substitutions were quantified by urea-induced denaturation experiment. The denaturation of the native and chimeric globins was monitored by using the molar ellipticity at 222 nm as a probe of equilibrium stability. As clearly delineated in Fig. 4A, the transition curve for the urea denaturation of the Mb α (PM3)-subunit is largely shifted to the left side from that of myoglobin but exhibits its cooperative denaturation. On the other hand, the Mb α (M4)-subunit did not experience any co-operative denaturation, which implies that the Mb α (M4)-subunit is already in a partly unfolded state in the absence of denaturant. In Fig. 4B, the free energy of denaturation (ΔG) was plotted against urea concentration, and a linear fitting procedure by using eq. 3 determined the extrapolated ΔG in the absence of urea, ΔG_{H_2O} , and the slope of

the linear relation (*ie* $d\Delta G / d[\text{urea}]$), m_{urea} (9). As listed in Table I, ΔG_{H_2O} for myoglobin and the Mb α (PM3)-subunit are 52.8 and 19.9 kJ/mol respectively, and the substitution of the pseudo-module PM3 decreases the equilibrium stability of myoglobin by more than 30 kJ/mol. For the Mb α (M4)-subunit, the parameters of denaturation could not be determined, since its denaturation process cannot be treated as a two states transition model (14). But, it can be safely said that the globin structure of the Mb α (M4)-subunit is much more destabilised compared to that of the Mb α (PM3)-subunit.

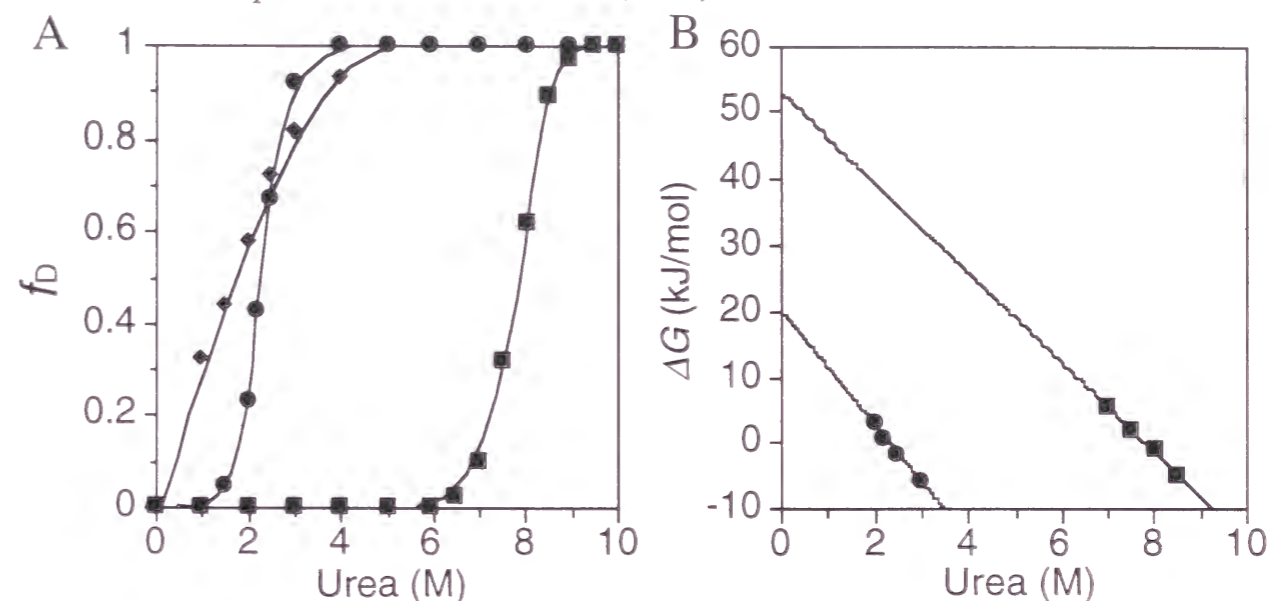


Fig. 4(A) Denaturation curves of the cyano-met globins by urea. Symbols correspond to myoglobin (■), Mb α (M4)-subunit (◆), Mb α (PM3)-subunit (●). Molar ellipticities at 222 nm in the native and completely denatured states were calibrated to 0 and 1, respectively. Experimental conditions were as follows: 20 mM Tris, 0.1 M NaCl, 5mM NaCN, pH 7.4, at 290 K. Sample concentration was 5 μ M on the heme basis. **(B)** Relationship between ΔG and [Urea] for myoglobin (■), and Mb α (PM3)-subunit (●). They were calculated from the respective urea denaturation curves in (A), except for the Mb α (M4)-subunit.

Table I Parameters of urea denaturation for myoglobin, Mb α (PM3)- and Mb α (M4)-subunits. ΔG_{H_2O} and m_{urea} were determined by fitting the ΔG -[urea] relation to eq. 3.

| | ΔG_{H_2O} (kJ/mol) | m_{urea} (kJ/mol per M) |
|-------------------|----------------------------|----------------------------------|
| Mb | 52.8 | 6.85 |
| Mb α (PM3) | 19.9 | 8.64 |
| Mb α (M4) | N. D. | N. D. |

Tryptophan Fluorescence Spectra – In order to investigate local structure as well as global one, we have measured tryptophan fluorescence spectra of Mb and the chimeric subunits. All the globins have two tryptophans, ^7Trp (A5) and ^{14}Trp (A12). Since the emission of Trp (A5) is strongly quenched not only by the heme but also by the nearby Lys (EF2), the main origin for the emission of myoglobin is ^{14}Trp (A12) (15). In Fig. 5, the fluorescence peak (F_{max}) for the Mb α (PM3)-subunit was observed at 335 nm, which is almost identical with that for native myoglobin (337 nm). This result reveals that its local environment around ^{14}Trp remains to be hydrophobic upon the implantation of the pseudo-module PM3 from the α -subunit into myoglobin (16). However, the fluorescence intensity is larger than that for myoglobin, implying that the distances between tryptophan residues and some quenchers become larger to decrease the quenching upon the PM3 substitution (17). On the other hand, the Mb α (M4)-subunit remarkably exhibits a red-shift of a fluorescence peak (F_{max}) and an increase in peak intensity. Such spectral change for the Mb α (M4)-subunit suggest that the local structure around ^{14}Trp is substantially disordered upon the substitution of the module M4 and its local environment become hydrophilic.

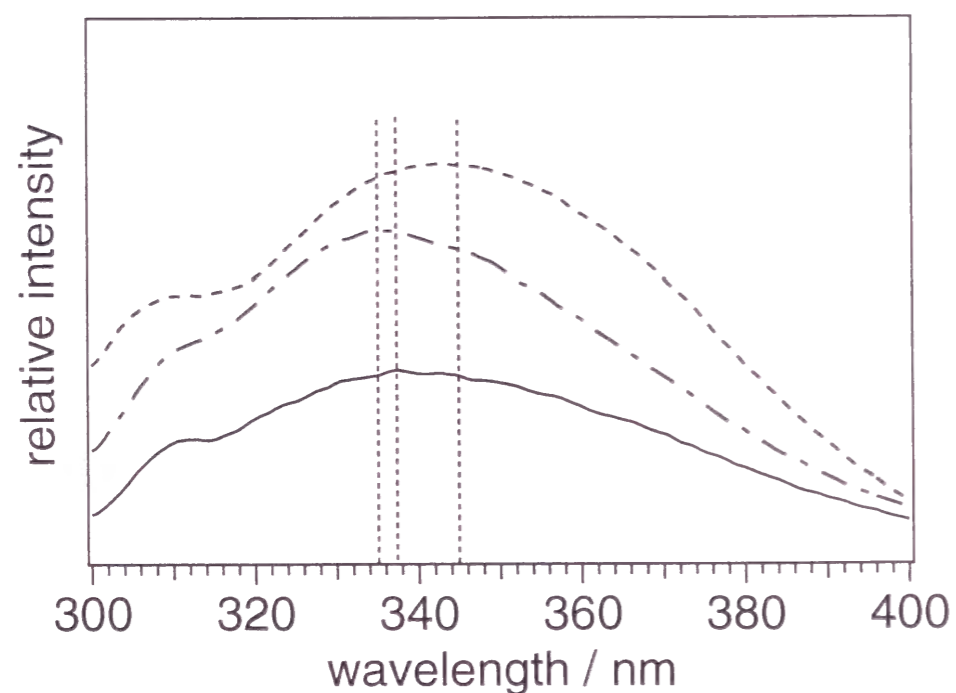


Fig. 5 Tryptophan fluorescence spectra Lines correspond to myoglobin (—), Mb α (M4)-subunit (- - -), Mb α (PM3)-subunit (- · -). Experimental conditions were as follows: 20 mM Tris, 0.1 M NaCl, 5mM NaCN, pH 7.4, at 290 K. Sample concentration was 5 μM on the heme basis. Perpendicular dotted lines demonstrate the peak position for each subunit.

NMR Measurements – By utilizing ^1H NMR spectroscopy, we have examined the effects of the pseudo-module substitution on the heme environmental structure as well as on the local structure around ^{14}Trp (Fig. 6). In the carbonmonoxy form (Panel A), a peak from the γ_1 -methyl proton of Val (E11) was observed at -2.0 and -2.6 ppm for the α -subunit and myoglobin, respectively, which has served as a marker for the tertiary structure in the heme vicinity (18). The corresponding signal for the Mb α (PM3)-subunit appeared at the intermediate position between the two peaks (-2.3 ppm), and the resonance peak is clearly broadened and asymmetric. Moreover, the signals observed in the upfield region at -0.5 to -1.5 ppm (19), which are assignable to a methyl group of Val (A15), Leu (B10) and Val (E11), were largely different between the Mb α (PM3)-subunit and myoglobin, although these residues are commonly conserved in them. Such spectral changes for the Mb α (PM3)-subunit imply that the pseudo-module substitution caused substantial perturbations on its heme distal structure (20).

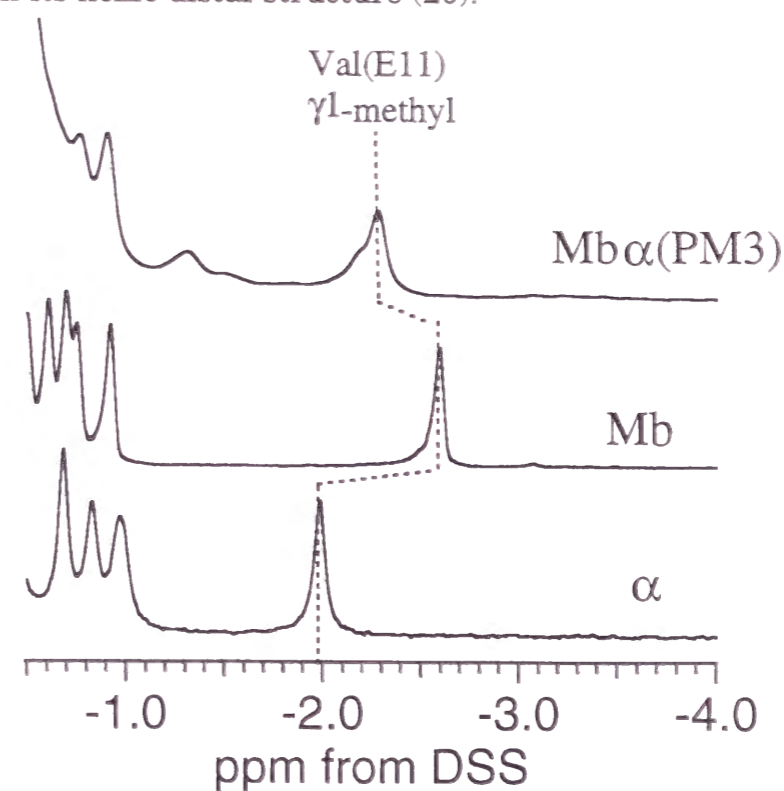


Fig. 6(A) Proton NMR spectra (500 MHz) for the carbonmonoxy hemoglobin α -subunit, myoglobin and the Mb α (PM3)-subunits The resonances from the γ_1 -methyl group of Val(E11) in the carbonmonoxy derivative are shown at -2.0 to -2.6 ppm. Experimental conditions were as follows: 50 mM Na-Phosphate, 0.1 M NaCl, pH 7.4, at 290 K. Sample concentration was 600 μM on the heme basis.

The NMR spectra of the deoxygenated form are shown in Fig. 6B. In a far-downfield region, one exchangeable proton peak was observed, which was assigned to the $N_{\delta}H$ proton of the proximal histidine (F8) (21, 22). In the deoxygenated form, the exchangeable resonance peak was observed at 78 and 83 ppm for the α -subunit and myoglobin, respectively, whereas the deoxy $Mb\alpha(PM3)$ -subunit showed a slight upfield shift of the peak from myoglobin (82 ppm). This slight upfield bias means little change in the interaction between the heme iron and the proximal histidine upon the PM3 substitution (23). However, in Fig. 6B which shows the hyperfine shifted resonances of the heme peripheral group, the spectral feature for the $Mb\alpha(PM3)$ -subunit is largely different from that for myoglobin. The remarkable increase in the resonance peaks in the spectra of the $Mb\alpha(PM3)$ -subunit indicates that its heme environmental structure is substantially perturbed by the implantation of the PM3 from the α -subunit.

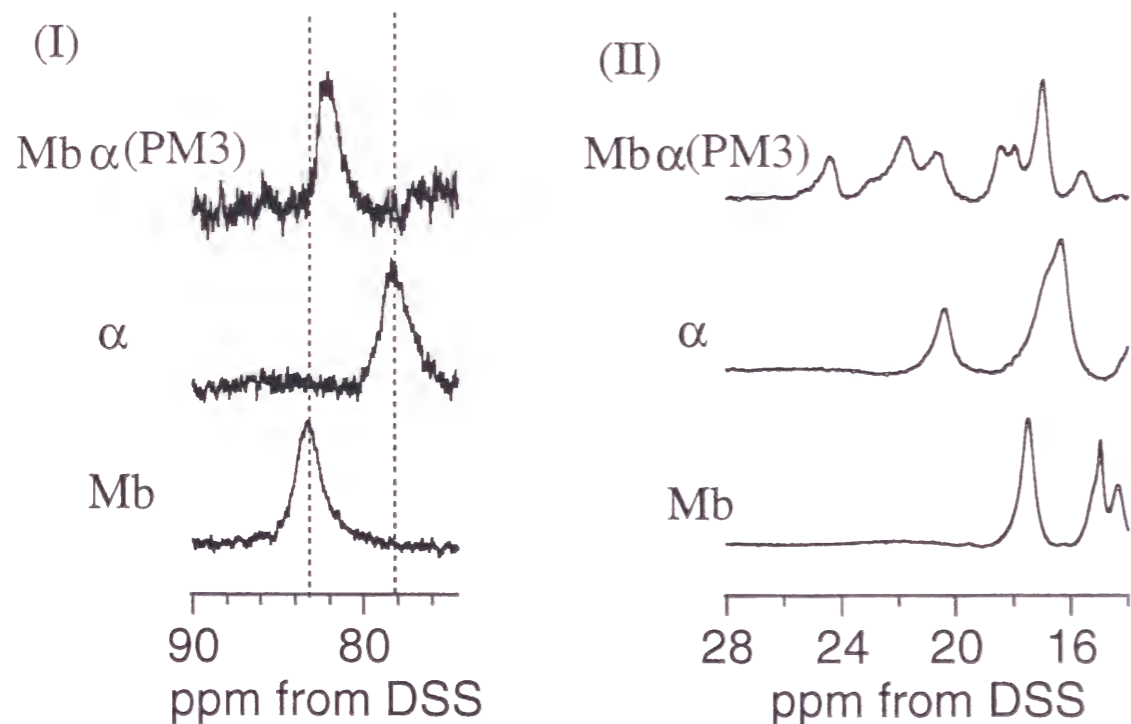


Fig. 6(B) Proton NMR spectra (500 MHz) for the deoxy hemoglobin α -subunit, myoglobin and the $Mb\alpha(PM3)$ -subunits. (I) hyperfine-shifted proton resonance of proximal histidine $N_{\delta}H$. Perpendicular dotted lines demonstrate the resonance peak positions for the α -subunit and myoglobin. (II) Hyperfine shifted proton resonances of heme peripheral groups. Experimental conditions were as follows: 50 mM Na-Phosphate, 0.1 M NaCl, pH 7.4, at 290 K. Sample concentration was 600 μ M on the heme basis.

On the other hand, both the carbonmonxygenated and deoxygenated $Mb\alpha(M4)$ -subunits exhibited no resonance signals characterizing the heme environmental structure, which was the same case for the molten-globule state myoglobin (24). Such disappearance of the resonance peaks from the heme surrounding residues suggest that the heme vicinity of the $Mb\alpha(M4)$ -subunit is still more disordered than that of the $Mb\alpha(PM3)$ -subunit.

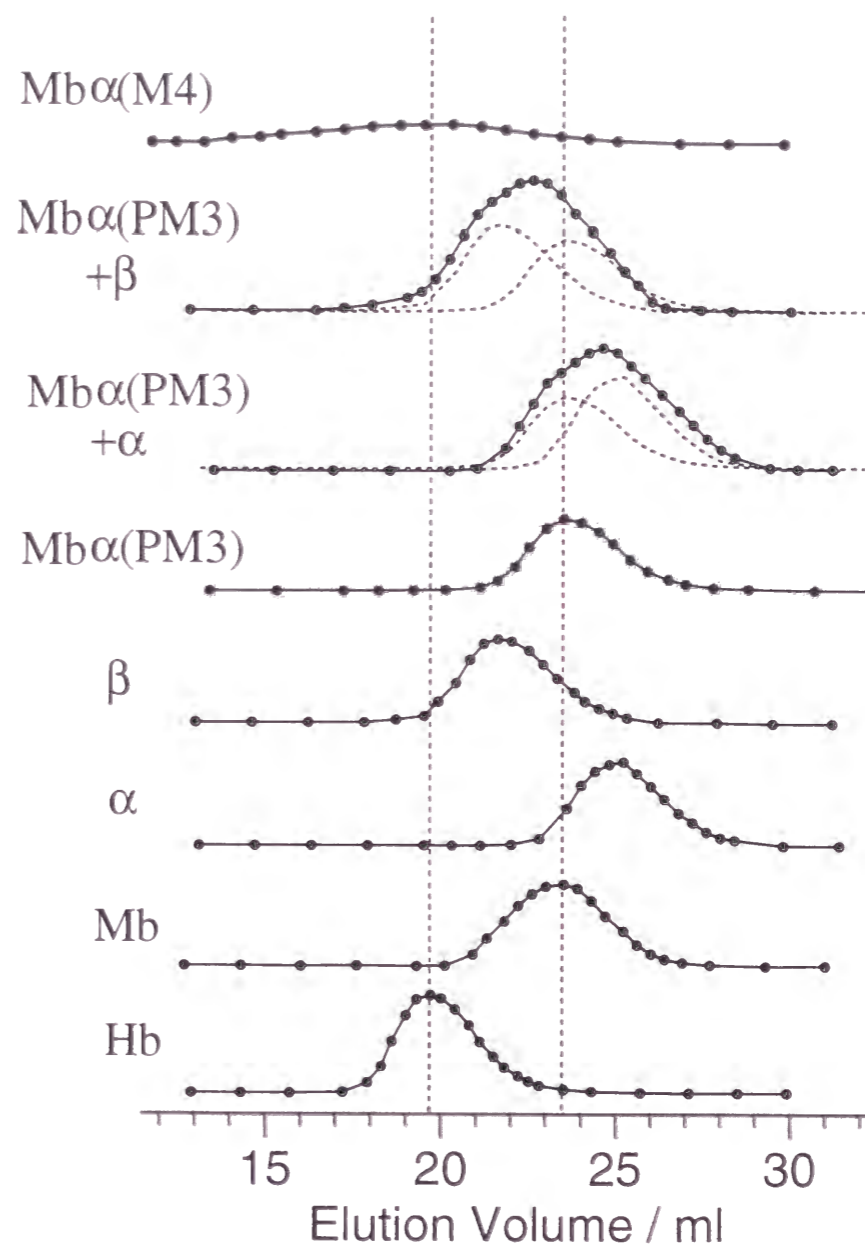


Fig. 7 Chromatography of carbonmonoxy forms of native hemoglobin, myoglobin, hemoglobin α - and β -subunits, the $Mb\alpha(PM3)$ -subunit, the mixtures of the $Mb\alpha(PM3)$ -subunit and hemoglobin subunits, and $Mb\alpha(M4)$ -subunits on a sephacryl S-200 HR column Broken curves in the mixtures of the $Mb\alpha(PM3)$ -subunit and hemoglobin subunits represent elution peaks of the corresponding isolated subunits. Experimental conditions were as follows: 50 mM Tris, 0.1 M NaCl, pH 7.4, at 277 K. Sample concentration was 20 μ M on the heme basis.

Subunit Assembly - To access effects of the pseudo-module or module substitution on subunit assembly of globins, we have performed gel chromatogram of the carbonmonoxy chimeric globins (Fig. 7). Under the sample concentration of 20 μ M, the hemoglobin forms a tetramer, whereas myoglobin is in a monomer (11). As shown in Fig. 7, the elution peak for the Mb α (PM3)-subunit was detected at the same position as native myoglobin. This elution pattern was independent of the protein concentration (data not shown), which reveals that the pseudo-module substituted myoglobin forms a monomer structure. For the mixture of the Mb α (PM3)- and hemoglobin α -subunits, the elution peak was not split, but that is completely superimposed on a simple addition those of the isolated subunits. This is the same case with the mixture of the Mb α (PM3)- and hemoglobin β -subunits. Eventually, no associations were detected between the Mb α (PM3)- and hemoglobin α - or β -subunits.

On the other hand, the Mb α (M4)-subunit showed much broader and weaker elution peak around the tetramer peak than myoglobin, which suggests the existence of many kinds of oligomers bigger than a tetramer or elongated components. In addition, some components of the Mb α (M4)-subunit would not be eluted in the column because of aggregation. This peak feature for the Mb α (M4)-subunit did not change upon the addition of the α - and β -subunits (data not shown), implying that the Mb α (M4)-subunit does not associate with the α - nor β -subunits just as does the Mb α (PM3)-subunit.

DISCUSSION

Structural significance of pseudo-module PM3 in globin proteins - In our previous study, the association property and the heme proximal structure of the β -subunit were converted into the α -subunit type by the implantation of the pseudo-module PM3 from hemoglobin α -subunit into the β -subunit. These results suggested that the pseudo-module PM3 might correspond to a new structural/functional unit regulating the heme proximal structure and the association property (3). In the present work for the Mb α (PM3)-subunit, however, the heme proximal structure and the association property were not converted into the α -subunit type in sharp contrast to the $\beta\alpha$ (PM3)-subunit. In Fig. 6B, the resonance peak from the N δ H proton of the proximal histidine for the Mb α (PM3)-subunit was almost identical to that for myoglobin, not to that for the α -subunit. This suggests that the substitution of the pseudo-module PM3 could not alter the coordination structure of the proximal histidine in myoglobin into the α -subunit one. Thus, the present study does not confirm

that the pseudo-module PM3 is a structural unit regulating the heme proximal structure.

Here, it is quite interesting that the heme proximal structure of the Mb α (PM3)-subunit did not show characters of the α -subunit in contrast to that of the $\beta\alpha$ (PM3)-subunit, although both the chimeric subunits contain the pseudo-module PM3 from the α -subunit. One of the possible reasons would be that structural perturbations by the PM3 substitution on the heme vicinity are more substantial in the Mb α (PM3)-subunit than in the $\beta\alpha$ (PM3)-subunit. The NMR spectral feature at 14-28 ppm for the deoxy Mb α (PM3)-subunit are quite different from those of myoglobin and the α -subunit (Fig. 6B). Furthermore, the resonance position of the γ_1 -methyl protons in the Val(E11) for the carbonmonoxy Mb α (PM3)-subunit was observed at the intermediate position between those for myoglobin and the α -subunit. These spectral patterns indicate that heme environmental structure of the Mb α (PM3)-subunit is neither myoglobin nor the α -subunit like. On the contrary, the $\beta\alpha$ (PM3)-subunit exhibited the resonance peak from γ_1 -methyl protons of Val(E11) at the same position as the β -subunit (3), suggesting that the heme distal site of the $\beta\alpha$ (PM3)-subunit would be well conserved compared to that of the Mb α (PM3)-subunit. That is, in the $\beta\alpha$ (PM3)-subunit the pseudo-module PM3 could be a block constituting the heme proximal site, whereas structural perturbations by the PM3 substitution are so substantial in the Mb α (PM3)-subunit that functional role of the PM3 would not be optimized. In fact, since homology of amino acid sequence between myoglobin and the α -subunit (\sim 20 %) is much lower than that between the α - and β -subunits (\sim 40 %), it is fully plausible that the structural perturbations in the Mb α (PM3)-subunit are more considerable than those in the $\beta\alpha$ (PM3)-subunit.

On the other hand, the Mb α (PM3)-subunit did not bind to the β -subunit as indicated by the gel chromatogram (Fig. 7), revealing that the association property of the Mb α (PM3)-subunit was not converted into the α -subunit type in sharp contrast to that of the $\beta\alpha$ (PM3)-subunit. Consequently, we could not re-assure functional significance of the PM3 for regulation of the association property of globin proteins. Here, inspections on the subunit interactions within the hemoglobin $\alpha_2\beta_2$ tetramer and the β_4 tetramer (25, 26) would provide plausible explanations on the different association properties of the Mb α (PM3)- and $\beta\alpha$ (PM3)-subunits. As shown in Fig. 8, there are approximately four interaction patterns between hemoglobin α - and β -subunits (α - β interaction) and between β - and β -subunits (β - β interaction). In the complex of the $\beta\alpha$ (PM3)- and β -subunits, it can be predicted that there would be two α - β interactions and two β - β ones. That is, besides the residues included in the

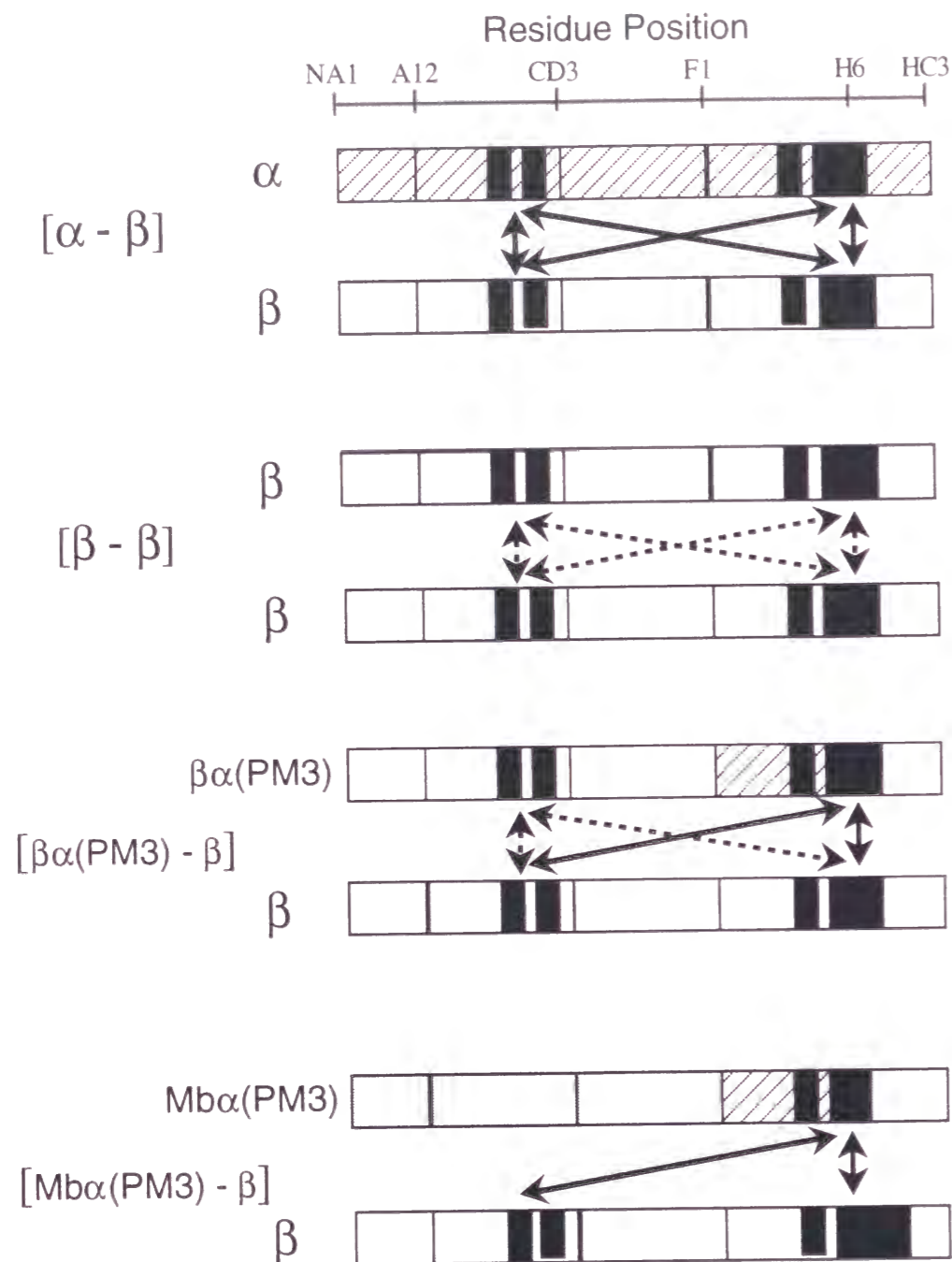


Fig. 8 (Predicted) Interactions between the α - and β -subunits, between the β - and β -subunits, between the $\beta\alpha(\text{PM3})$ - and β -subunits and between the $\text{Mb}\alpha(\text{PM3})$ - and β -subunits (Predicted) α - β (solid line) and β - β (dotted line) interactions are represented by arrows. Black boxes denote the residues contributing to the subunit interactions.

PM3, the B12-CD2 region would also contribute to the association of the $\beta\alpha(\text{PM3})$ -subunit with the β -subunit, which would stabilize the hetero-tetramer structure of the $\beta\alpha(\text{PM3})_2\beta_2$. Nevertheless, as found in Fig. 8, the B12-CD2 region in the $\text{Mb}\alpha(\text{PM3})$ -subunit is derived from myoglobin and contains many hydrophilic residues, which would interrupt the association with the β -subunit. Thus, the functional conversion only in the $\beta\alpha(\text{PM3})$ -subunit revealed that the pseudo-module PM3 is not a unique region dominant in subunit assembly and the other regions are also considerably relevant to the regulation of association property in globin proteins.

Effect of Module M4 and Pseudo-module PM3 Substitution on Globin Structure - It is also notable that the substitution of the pseudo-module PM3 caused much less disorders in the globin and heme environmental structure of myoglobin than the module M4 substitution, although both of the modules involve about 40 amino acid residues. One of the prominent differences between the pseudo-module PM3 and module M4 on globin structure is that the module M4 contains the complete H-helix and C-terminal region (Figs. 1). According to the previous studies with the hydrogen exchange method, it has been revealed that amino acid residues on the H-helix interact with the A-helix to form the inter-helix packing as an initial step for globin folding (27), confirming a crucial role of the A-H helix interaction in stable globin structure. Moreover, it was observed that the mutation at ^{130}Ala (H7) or ^{131}Met (H8) in the H-helix prevents formation of the intermediate states of the folding process in apomyoglobin (28, 29). On the basis of these experimental results, the replacement of several amino acid residues in this region accompanied by the substitution of the module M4 (Fig. 1) would cause substantial perturbation on the inter-helix packing between the A- and H-helices and eventually result in destabilization of the globin structure. On the other hand, the substitution of the pseudo-module PM3 does not include the mutation of these residues as found in Fig. 1, which would lead to little perturbations on the A-H-helix packing. The formation of the A-H-helix packing in the $\text{Mb}\alpha(\text{PM3})$ -subunit is also supported in the tryptophan fluorescence spectra. Its fluorescence peak position similar to that of myoglobin implies that substantial structural alterations are not induced in the micro-environment around ^{14}Trp in A-helix by the implantation of the pseudo-module PM3 of the α -subunit, suggestive of no large structural disorder in the A-helix.

In addition to the substantial perturbations on the A-H helix packing by the M4 substitution, it is also to be noted that the number of the residues in the C-terminal region for the $\text{Mb}\alpha(\text{M4})$ -subunit is shorter by six than for the $\text{Mb}\alpha(\text{PM3})$ -subunit (Fig. 1). These deleted six residues contain two Glys'

constituting the "Schellman motif" in myoglobin, which has been considered to be essential for the stabilization of the α -helical structure in the C-terminal region (30, 31). On the contrary, the Mb α (PM3)-subunit still retains most of the H-helix and the complete length of the C-terminal region from myoglobin. The formation of the stable H-helix with recourse to the Schellman motif would lead to the conservation of the A-H packing, resulting in the higher stability for the Mb α (PM3)-subunit than the Mb α (M4)-subunit. It is, therefore, concluded that the deletion and mutations of the H-helix and C-terminal region by the substitution of the module M4 cause destabilization of the H-helix, which leads to the large structural change in the Mb α (M4)-subunit. In other words, the crucial roles of the Gly^s constituting region in the globin fold were confirmed by comparison of the protein stability between the module and pseudo-module substituted chimeric myoglobins.

CONCLUSION

In the present study, the heme proximal structure and the association property of myoglobin were not converted into the α -subunit type upon the implantation of the pseudo-module PM3 from the α -subunit into myoglobin, which was in sharp contrast to the case for the implantation into the β -subunit. No structural conversion for the Mb α (PM3)-subunit would be attributed to substantial structural perturbations on its heme vicinity by the PM3 substitution. Moreover, no alteration of the association property for the Mb α (PM3)-subunit lead us to infer that the B12-CD2 region besides the pseudo-module PM3 plays crucial roles in regulation of subunit assembly of globin proteins. On the other hand, the large structural difference between the Mb α (PM3)- and Mb α (M4)-subunits confirm that the A-H helix packing and the C-terminal "Schellman Motif" play crucial roles in constructing stable globin structure. Thus, the structural and functional comparisons among some kinds of module or pseudo-module substituted globins provide many insights into regulation mechanism of globin structure and function.

REFERENCES

1. Go, M. (1981) *Nature*, **291**, 90-92
2. Wakasugi, K., Ishimori, K., Imai, K., Wada, Y. and Morishima, I. (1994) *J. Biol. Chem.* **269**, 18750-18756
3. Inaba, K., Ishimori, K., Imai, K. and Morishima, I. *Submitted for publication* (J. Biol. Chem.)
4. Eaton, W. A. (1980) *Nature* **284**, 183-185
5. Nagai, K and Thøgerson, H. C. (1984) *Nature* **309**, 810-812

6. Nagai, K., Perutz, M. F., and Poyart, C. (1985) *Proc. Natl. Acad. Sci. U.S.A.* **82**, 7252-7257
7. Nagai, K., and Thøgerson, H.C. (1987) *Methods Enzymol.* **153**, 461-481
8. Wada, Y., Fujita, T. Hayashi, A., Sakurai, T., and Matsuo, T. (1989) *Biomed. Environ Mass Spectrom.* **18**, 563-565
9. Konno, T. and Morishima, I., (1993) *Biochem. Biophys. Acta* **1162**, 93-98
10. Burstein, E. A., Vedekina, N. S. and Ivkova, M. N. (1973) *Photochem. Photobiol.* **18**, 263-279
11. Valdes, R., Jr. and Ackers, G. K. (1977) *J. Biol. Chem.* **252**, 74-81
12. Beychok, S., Tyuma, I., Benesch, R. E., and Benesch, R. E. (1967) *J. Biol. Chem.* **242**, 2460-2462
13. Greenfield, N. and Fasman, G. D. (1969) *Biochemistry* **8**, 4108-4116
14. Tanford, C. (1970) *Adv. Protein Chem.* **25**, 1-95
15. Postikova, B. G., Komarov, E. Y. and Yumakova, M. E. (1991) *Eur. J. Biochem.* **198**, 233-239
16. Burstein, E. A., Vedenkina, N. S. and Ivkova, M. N. (1973) *Photochem. Photobiol.* **18**, 263-279
17. Stryer, L. (1978) *Annu. Rev. Biochem.* **47**, 819
18. Lindstrom, T. R., Nore, I. B. E., Charashe, S., Lehmann, H., and Ho, C. (1972) *Biochemistry* **11**, 1677-1681
19. Dalvit, C. and Wright P. E. (1987) *J. Mol. Biol.* **194**, 313-327
20. Shulman, R. G., Wuthrich, K., Yamane, T., Patel, D. and Blumberg, W. E. (1970) *J. Mol. Biol.* **53**, 143
21. Goff, H. M. and La Mar, G. N. (1977) *J. Am. Chem. Soc.* **99**, 6599-6606
22. La Mar, G. N., Budd, D. L. and Goff, H. M. (1977) *Biochem. Biophys. Res. Commun.* **77**, 104-110
23. Nagai, K., La Mar, G. N., Jue, T. and Bunn, H. F., (1982) *Biochemistry* **21**, 842-847
24. Loh, S. N., Kay, M. S. and Baldwin, R. L. (1995) *Proc. Natl. Acad. Sci. USA* **92**, 5446-5450
25. Perutz, M. F. (1970) *Nature* **228**, 726-739
26. Borgstahl, G. E. O., Rogers, P. H. and Arnone, A. (1994) *J. Mol. Biol.* **236**, 817-830
27. Wright, P. E. and Jenningth, P. A. (1993) *Science* **262**, 892-895
28. Hughson, F. M., Barrick, D. and Baldwin, R. L. (1991) *Biochemistry* **30**, 4113-4118
29. Kay, M. S. and Baldwin, R. L. (1996) *Nature Structural Biology* **3**, 439-445
30. Aurora, R., Srinivasan, R. and Rose, G. D. (1994) *Science* **264**, 1126-1130
31. Viguera, A. R. and Serrano, L. (1995) *J. Mol. Biol.* **251**, 150-160

FOOTNOTE

¹The pseudo-modules are defined as a segment starting at a center of one module and ending at the center of the following one and do not form a compact structural unit in sharp contrast to the modules as predicted from their correspondence to the region from a peak to the adjacent one in the centripetal profile [Noguti et al., (1993) *Proteins* **16**, 357-363]. Moreover, since the pseudo-modules do not statistically coincide with exons, they would not have evolutionary or functional meanings unlike the modules [Go and Noguti, (1995) *Tracing Biological Evolution in Protein and Gene Structures* (eds. Go, M. and Scimmel, P.) 229-235].

²In this denaturation experiment, we used cyano-met derivatives of the samples to prevent aggregation of dissociated heme for the reversible denaturation. Under this condition, the reversibility was about 90% for myoglobin. For the Mb α (M4)-subunit and Mb α (PM3)-subunit, however, only 50% of the reversibility was detected, probably due to irreversible loss of heme. Such incomplete reversibility was also encountered for the previous study on the denaturation of myoglobin mutants (15).

PART IV

EFFECTS OF SUB-MODULE SUBSTITUTION ON GLOBIN STRUCTURE AND FUNCTION

Chapter 5

Substitution of sub-module m6 in hemoglobin α -
subunit and myoglobin (Mb α (HBM))

ABSTRACT

To investigate the structural and functional significance of the newly proposed structural unit in globins, the "heme binding module", we synthesized a "heme binding module"-substituted chimeric globin and characterized its function and structure. In our previous study [Inaba, et al., submitted], we proposed that the "heme binding module" corresponding to the segment from Leu(F1) to Lys(G6) in hemoglobin α -subunit plays a key role in constructing the heme proximal structure in globins. The replacement of the heme binding module in myoglobin with that of hemoglobin α -subunit converted the absorption spectra characteristic of myoglobin into that of the α -subunit, and in the resonance Raman spectra the vibration mode characteristic of myoglobin completely disappeared by the replacement. While the deviations of the resonance positions of the NMR signals from the amino acid residues located in the distal site were subtle, the hyperfine-shifted NMR resonances for the cyanide bound forms of the module substituted globin indicated that the orientation of the axial histidine is close to that of the α -subunit rather than that of myoglobin, supporting the preferential structural alteration in the heme proximal site. The present finding for the structural alteration by the substitution of the "heme binding module" experimentally revealed that the heme binding module can be a structural segment regulating the heme proximal structure in globin proteins.

Understanding the manner in which the heme environmental structure provided by the apoprotein dictates the ligand binding and catalytic properties of hemoproteins remains to be one of the fundamental objects of research concerning this family of proteins. One of the most significant and prominent structural characteristics of such proteins is the coordination environment of the heme iron, and the substitutions of the axial ligands of the heme iron in hemoproteins have recently been examined by our and other groups (1-3), which revealed the primary roles of the axial ligands in the function and structure of heme proteins. However, the substitution of the axial ligands was sometimes accompanied with destabilization of the protein structure to exert the fatal functional impairments (1, 2). Some interactions formed by amino acid residues near the axial ligands of the heme iron as well as the axial ligand itself play crucial roles in stable heme binding and regulating activity of the heme.

In this study, we have focused on the "heme binding module" the protein segment regulating the heme proximal structure in globin family. The "module" has been defined as a compact structural unit on the protein structure, which consists of 10 - 40 amino acid residues (4, 5). In globins, the protein structure was originally divided into four modules (M1 - M4), each of which corresponds to the exon on the gene structure (4). Our extensive examination of the modular structure of globin by replacement of the specific modules in one globin with those in other globins have shown that some module has structural and functional significance in the protein structure, supporting the modules as structural and functional units in globins (6). However, the substitution of the "pseudo-module"¹, of which boundaries are located in the middle of the modules (Fig. 1) and supposed not to correspond to exons on the gene structure (7), also successfully produced some stable and functional globins, which allows us to conclude that the originally defined module might not be a minimum structural unit, but can be further divided into small structural unit, "sub-module" (8). On the basis of the comparative studies of the functional and structural properties of several module and pseudo-module substituted chimeric globins, we proposed that one of such "sub-modules" located in the heme proximal side can regulate the heme proximal structure of hemoproteins and is referred to as the "heme binding module".

The "heme binding module" of myoglobin we have suggested in this study consists of 21 amino acid residues from F1 to G6, including the axial ligand ⁹³His of the heme. As clearly shown in Fig. 1, most of the residues constructing the heme proximal structure are concentrated in this sub-

module, and it is expected that the heme coordination structure and heme electronic state are determined by this heme binding module. Our previous work on the substitution of the pseudo-module PM3, where the C-terminal fragment of the half of the module M3 and N-terminal-half of the module M4 of the β -subunit was replaced by that of the α -subunit, revealed that the heme environmental structures were affected by the pseudo-module substitution and the resultant structure was close to that of the α -subunit rather than to that of the β -subunit (8), while the M4 substitution did not cause such structural changes and its heme environmental structure still maintained the β -subunit-like structure (6). These results strongly suggest that the N-terminal-half of the PM3, which is not overlapped on the module M4, may regulate the heme coordination structure of the proximal histidine.

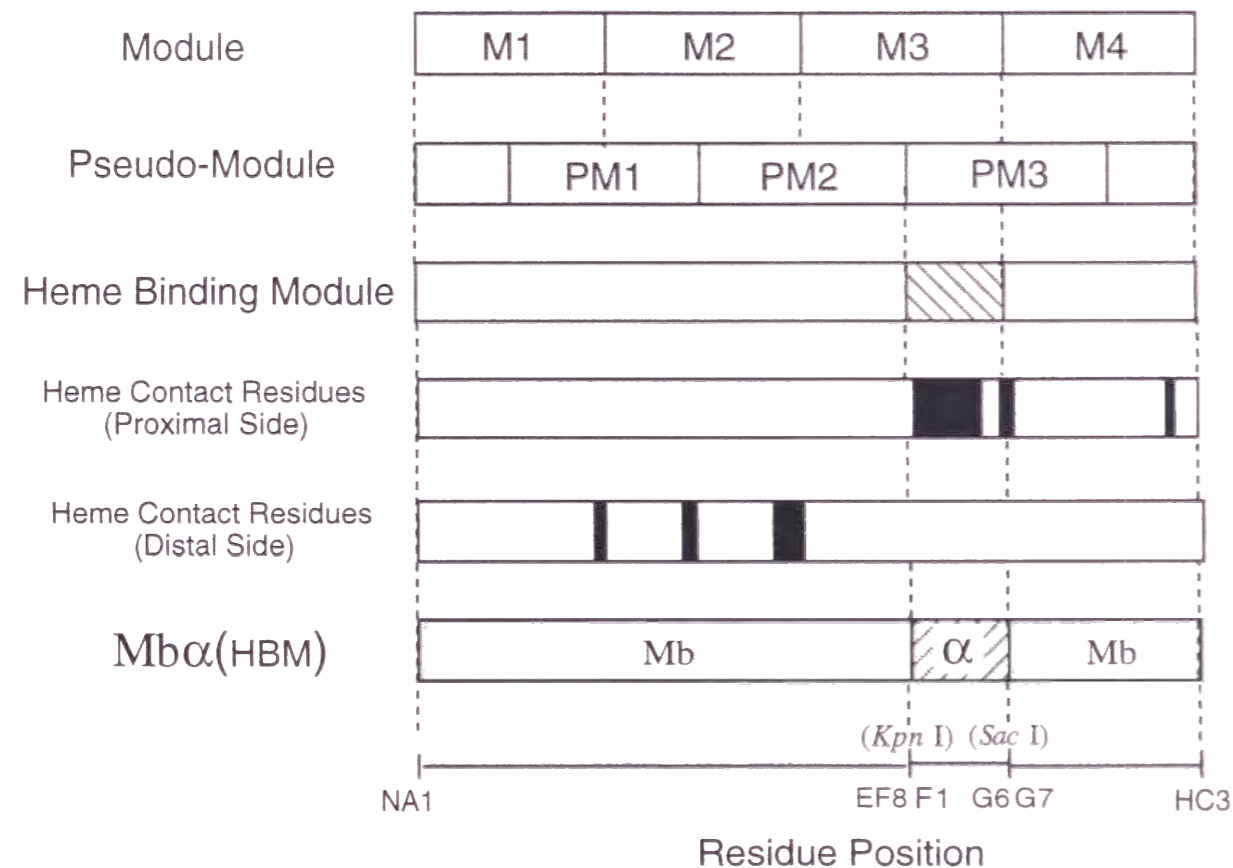


Fig. 1 Boundaries of the conventional module (M1-M4), pseudo-module and heme binding module, heme contacting residues, and Mb α (HBM) synthesized in this study. Restriction enzyme sites used in this preparation are noted in a parenthesis. Black boxes represent heme contacting residues.

| Helix | NA | A | AB | B |
|--|--|------------------------------------|---|---------------------------|
| number | 12 | 1.....16 | 1 | 1.....16 |
| α-subunit | VL | SPADKTNVKA AWGKVG | A | HAGEY GAEALERMFLS |
| myoglobin | VL | SDGEWQLVLNV WGKVE | A | DIPGH GQEV LIRLFKS |
| | | | | |
| C | CD | D | E | EF |
| 1.....7 | 1.....8 | 1.....7 | 1.....20 | 1..... |
| F P T T KTY | F P H F DLSH | H----HG | S AQ V K G H G K K V A D A L T N A V A | H V D D |
| H P E T L G K | F D K F K H L K | S E D E M K A | S E D L K K H G A T V L T A L G G I L K | K K G H |
| | | | | |
| <---HEME BINDING MODULE---> | | | | |
| | F | FG | G | G |
| | | | | GH |
| | 1.....10 | 1.....5 | 1.....19 | 1.....5 |
| M P N A | L S A L S D L H * A | H K L R V | D P V N F K L L S H C L L V T L A A H | L P A E F |
| H E A E | L K P L A Q S H * A T | K H K I | P I K Y L E F I S E A I I H V L H S R | H P G D F |
| | | | | |
| H | | | CH | |
| 1.....26 | | | 1.....4 | |
| T P A V H A S L D K F L A S V S T V L T S K Y R | | | | |
| G A D A Q G A M N K A L Q L F R K D I A A K Y K E L | | | G Y Q G | |

Fig. 2A Amino acid sequence for hemoglobin α -subunit and myoglobin. The identical residues are expressed in bold style. The proximal histidine (F8) is marked by an asterisk.

To examine the structural and functional significance of the "heme binding module", we replaced the heme binding module of myoglobin with that of the α -subunit and characterized the structure and function of the "heme binding module" substituted chimeric globin, Mb α (HBM) (Fig. 1). As is delineated in Figs. 2A and 2B, homology of amino acid sequence in the heme binding modules of myoglobin and the α -subunit is less than 20% (4/21), and the spatial arrangements of heme peripheral substituents are significantly different between these two globins. Moreover, the angle between the porphyrin N₂-N₄ vector and the projection of the proximal imidazole plane onto the heme plane in the α -subunit are substantially larger than that in myoglobin (Fig. 2C). Whether these structural differences are attributed to the heme binding module is our most interest. Accordingly, we focus on the structural changes in the proximal and distal sites of the globins and examine the structural significance of the heme binding module. In the present work,

we utilized several spectroscopies including CD, resonance Raman, and one- and two dimensional NMR spectroscopies to reveal the structural changes in the heme environments induced by the substitution of the heme binding module. Comparing its heme proximal structure with those of myoglobin and the α -subunit would provide new insights into structural and functional significance of the heme binding module.

EXPERIMENTAL PROCEDURES

Construction of Expression Vector - We have used the T7 vector to express the Mb α (HBM). The methionine residue was substituted for valine at the N-terminal to initiate the peptide elongation for the module substituted myoglobin². To construct the gene for the Mb α (HBM), *Kpn* I (GGTACC) and *Sac* I sites (GAGCTC) were introduced at the boundaries of the heme binding module by polymerase chain reaction (Fig. 1). The introduction was inevitably accompanied with the mutations from Ala(EF7), Glu(EF8) and Lys(G6) to Gly, Thr and Glu, respectively. Construction of the desired expression vector was verified by double-stranded DNA sequence analysis (373 DNA sequencer, Applied Biosystems).

Protein Preparation - The prepared gene encoding the Mb α (HBM) was transformed into an *Escherichia coli* strain (BL21), which was grown at 37 °C in 18 L of 2xTY culture containing ampicilin (100 μ g/ml) overnight. This culture was centrifuged by 5,000 r.p.m. for 20 min. and the cell pellets were thawed and suspended in 80 ml of 50 mM Tris-HCl, pH 8.0, 25% sucrose (w/v) 1 mM EDTA and lysed with lysozyme (100 mg per 10 g of pellets) to get the crude chimeric subunits. Then, MgCl₂, MnCl₂ and DNase I were added to final concentrations of 10 mM, 1 mM and 10 μ g/ml, respectively. After 30 min of incubation, 200 ml of 0.2 M NaCl, 1% deoxycholic acid, 1.6 % Nonidet P-40 (v/v), 20 mM Tris-HCl, pH 7.5 and 2 mM EDTA were added to the lysate, which was then centrifuged by 18,000 r.p.m. for 20 min. Then, the pellet was suspended in 0.5% Triton X-100, 1 mM EDTA and centrifuged. This procedure was repeated until a tight pellet was obtained. The protein pellet was dissolved in 8 M urea, 20 mM Tris-HCl, pH 5.2, 1 mM EDTA and loaded onto CL-6B column equilibrated with the same solution (9-11). By eluting the protein attached to the column with 8 M urea, 20 mM Tris-HCl, pH 5.2, 1 mM EDTA, 0.2 M NaCl, we obtained pure chimeric subunit as confirmed on SDS gels. The solubilized denatured protein solution was diluted 16-fold by 20 mM Na₂B₄O₇, pH 12.0. To the supernatant at 4 °C was added 1.1 equivalent of biscyano form of protohemin and the solution was left to stand for 30 min at 4 °C. The reconstituted protein was concentrated into 10 ml and loaded onto a 5 x 30 cm

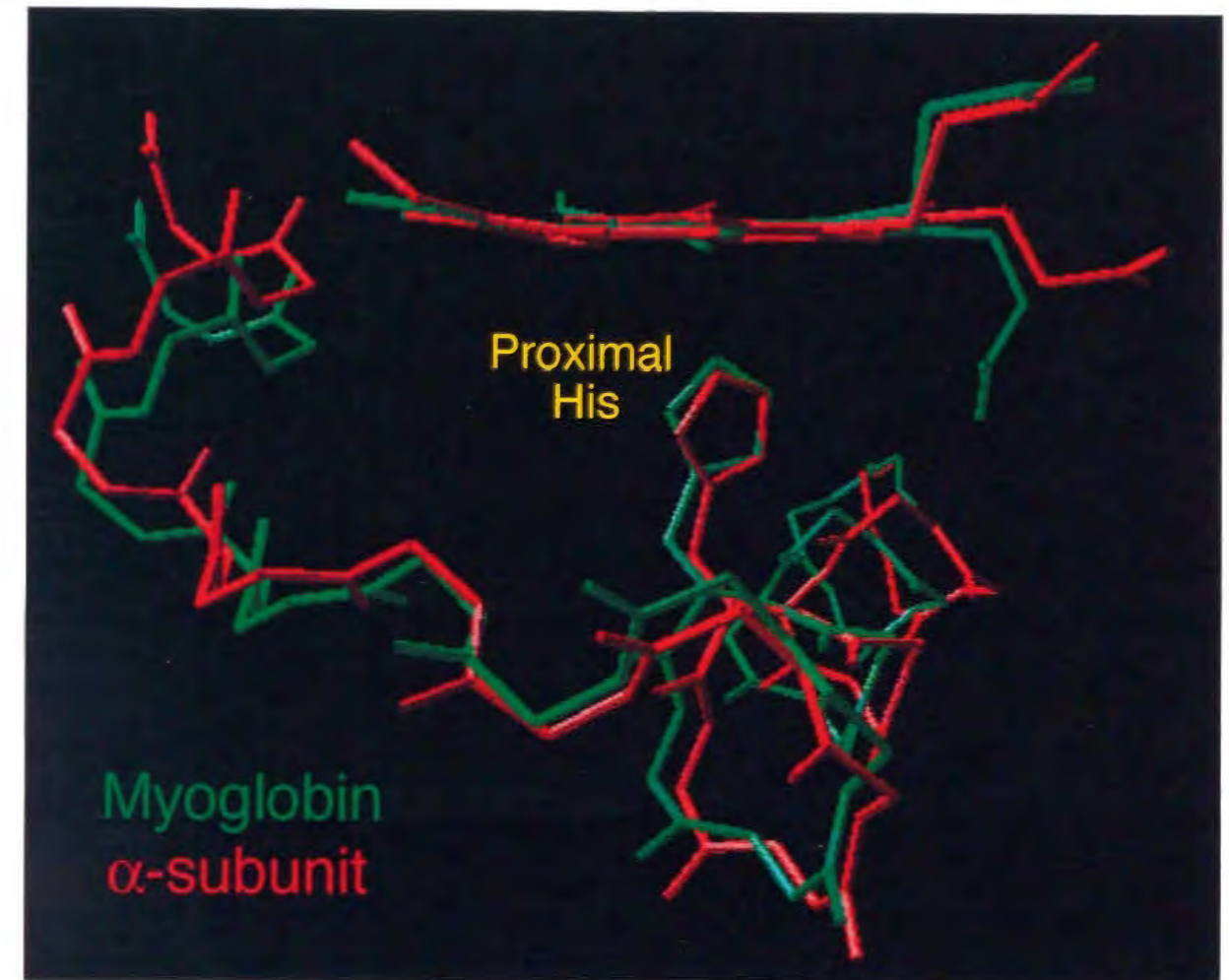


Fig. 2B Side-view of a protohemin and a heme binding module in myoglobin and hemoglobin α -subunit

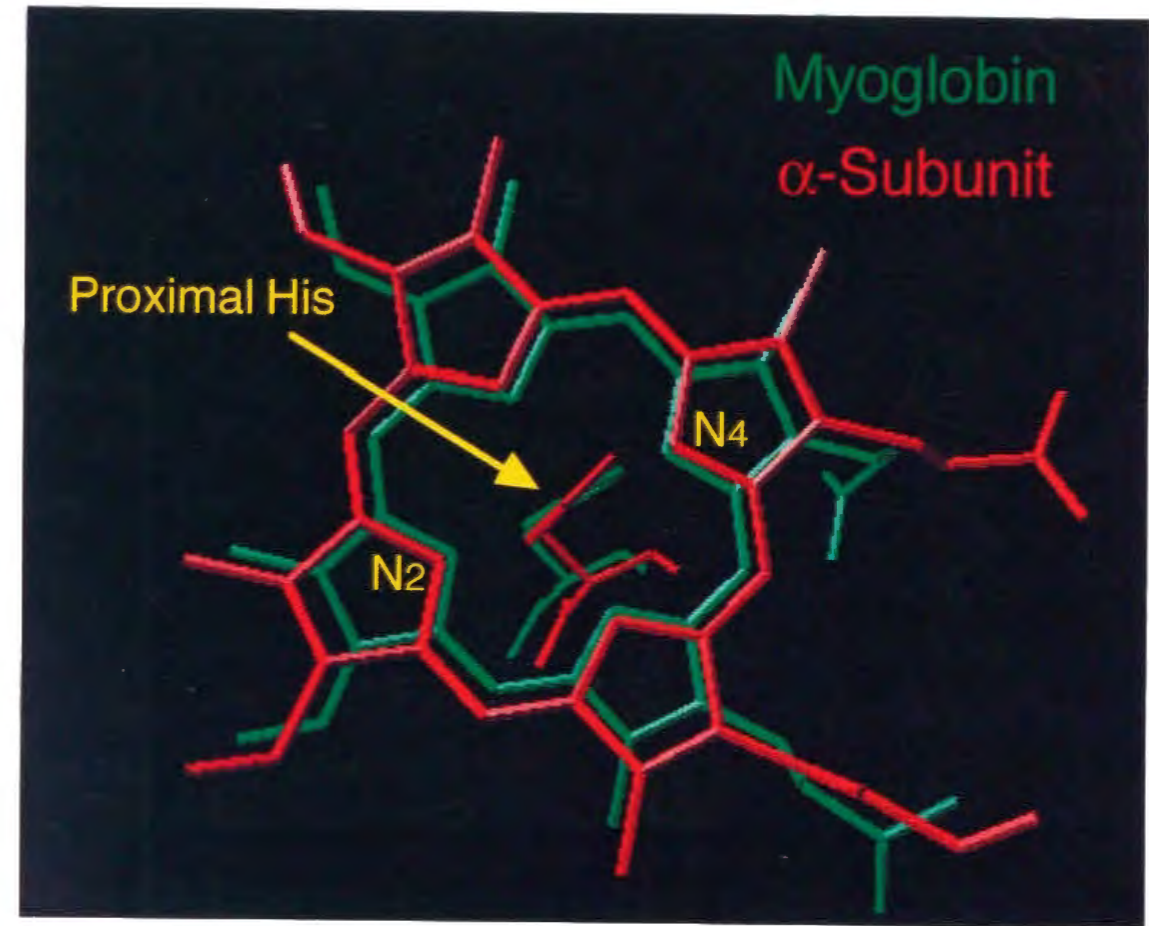


Fig. 2C Top-view of a protohemin and a proximal histidine in myoglobin and hemoglobin α -subunit

G-25 column equilibrated with 20 mM Tris-HCl, 5 mM NaCN, pH 7.4 for buffer exchange. Finally, the cyanomet globin was loaded onto a 3 x 20 cm CM52 column and eluted with 20 mM Tris-HCl, 5 mM NaCN, pH 7.4. The carbon monoxide derivative was prepared by adding minimal amounts of sodium dithionite to the ferric chimeric subunits under CO atmosphere. The globin solution was deoxygenated by repeated evacuation and flushing with N₂ gas under gentle shaking and complete deoxygenation was achieved by addition of minimal amounts of sodium dithionite.

Spectral Measurements - Electronic absorption spectra were recorded at room temperature on Hitachi U-3210. The buffer was 20 mM Tris-HCl, 5 mM NaCN, pH 7.4 for the cyanomet form and 20 mM Tris-HCl, pH 7.4 for carbonmonoxy one. Sample concentration was 10 μ M. Extinction coefficients were calculated on the basis of the protein concentration determined by the pyridine-hemochrome method (12).

CD spectra of the cyanomet chimeric and native subunits in far UV region were measured at room temperature with a Jasco J-760 spectrometer. Concentration of the sample was 10 μ M. The path length for the measurements was 1 mm.

One and two dimensional ¹H NMR spectra at 500 MHz were recorded on BRUKER Avance DRX 500. For the measurements of the hyperfine-shifted proton resonances in the cyanomet and deoxy derivatives, we utilized a LOSAT pulse sequence. The probe temperature was controlled at 290 \pm 0.5 K by a temperature control unit of the spectrometer. The volume of the NMR sample was 600 μ L and the concentration was 1 mM on the heme basis. Proton shifts were referenced with respect to the proton resonance of 2, 2,-dimethyl-2-silapentane-5-sulfonate (DSS). Phase sensitive NOESY spectrum for the cyanomet Mb α (HBM) was obtained as followed by the standard pulse sequence (13). The mixing time (τ_m) was 40 millisecond. On the other hand, phase sensitive NOESY spectra for the carbonmonoxy form were acquired with the standard pulse sequence (14, 15). The mixing time (τ_m) was 80 millisecond, which is enough to avoid problems of spin diffusion (16, 17).

Resonance Raman scattering for the deoxy derivatives was excited at 441.6 nm with a He/Ca laser (Kinmon Electronics, CDR80SG) and detected at room temperature by a JEOL-400D Raman spectrometer equipped with a cooled HTV-943-02 photomultiplier. The frequencies of the Raman spectrometer were calibrated with indene. Sample concentration was 40 μ M on the heme basis.

FT-IR spectra for carbonmonoxy derivative were obtained at 1 cm⁻¹ resolution on a Bio-Rado FTS-30 spectrophotometer at room temperature. The

sample concentration was about 1 mM. We have used a CaF₂ cell with 0.1 mm path length.

Oxygen Equilibrium Curves and Analysis – Oxygen equilibrium curves were measured by using an improved version (18, 19) of an auto-oxygenation apparatus (20). The wavelength of the detection light was 560 nm. The temperature of the sample in the oxygenation cell was constant at 25 ± 0.05 °C. The volume of the sample was 6 mL and the concentration was 60 μM on the heme basis. The hemoglobin reductase system (21) was added to the sample before each measurement to reduce oxidized subunits. To minimize the autoxidation of the sample during the measurements, catalase and superoxide dismutase were added to the sample and the concentration was 0.1 μM (22, 23). The oxygenation data were acquired by use of a micro-computer (model PC-98XA, Nippon Electric Co., Tokyo), which was interfaced to the oxygenation apparatus (24).

RESULTS

CD Spectra - To examine effects of the substitution of the heme binding module on globin structure, we have measured CD spectra in far UV region for the Mbα(HBM) and myoglobin (data not shown). The CD curve of the Mbα(HBM) was completely superimposed on that of myoglobin, and the ellipticity at 222 nm was also identical to that of myoglobin, indicating that the substitution of the "heme binding module" did not perturb the secondary structure of globins.

Electronic Absorption Spectra - By measuring the absorption spectrum of the chimeric protein, we have accessed the effects of the "heme binding module" on the electronic state of the heme (Figs. 3A and 3B). In Fig. 3A, the absorption spectra of carbonmonoxy derivatives of myoglobin, hemoglobin α-subunit and their chimeric globin are illustrated. Although all the carbonmonoxy globins exhibit strong Soret bands around 420 nm and two small peaks in the visible region, some small but significant spectral differences were observed between myoglobin and the hemoglobin α-subunit. The Soret peak for carbonmonoxy myoglobin appeared at 422 nm, while that of the α-subunit was detected at 419 nm. Also, two small peaks in the visible region for myoglobin were deviated from those of the α-subunit. These spectral deviations have been attributed to the difference in the coordination structure of myoglobin and hemoglobin α-subunit as depicted in Figs. 1B and 1C. In the "heme binding module" substituted myoglobin, Mbα(HBM), the Soret peak appeared at 419 nm, which corresponds to that of the α-subunit.

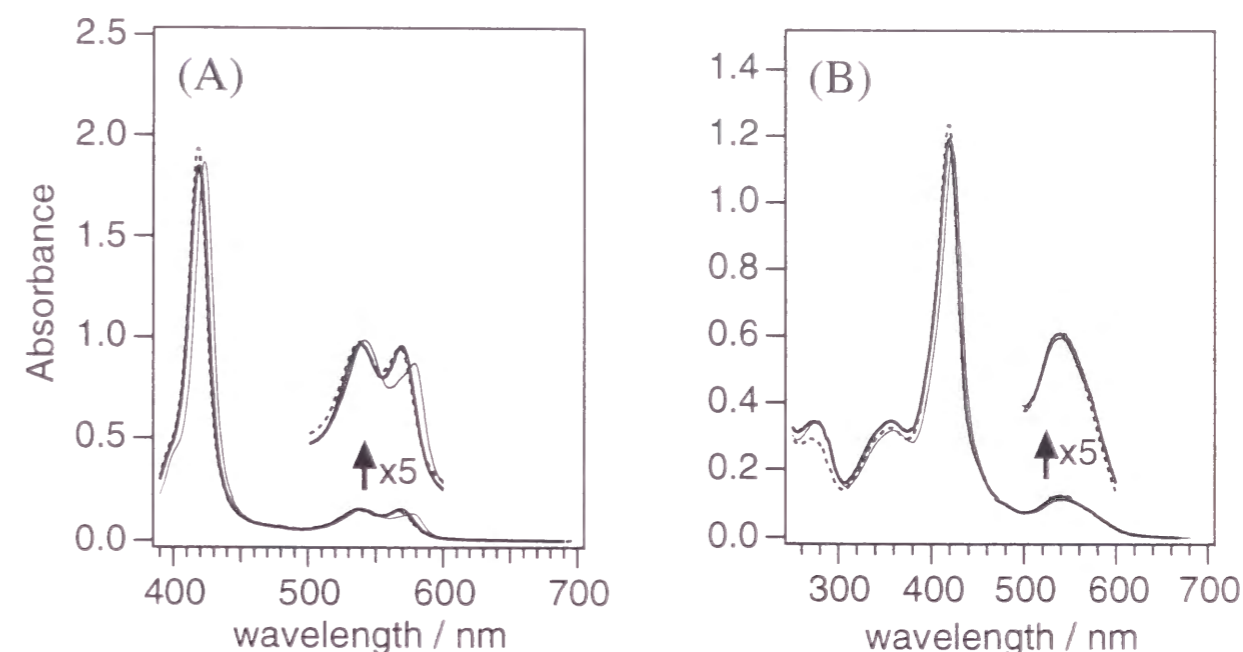


Fig. 3 Electron absorption spectra of a carbon monoxide form (A) and a cyanomet form (B). Concentration of each subunit was 10 μM. Lines correspond to wild-type myoglobin (—), hemoglobin α-subunit (---), and the Mbα(HBM) (—), respectively. The Q bands from 500 to 600 nm are enlarged by five times on the perpendicular axis.

Table I Wavelength (Extinction Coefficients [$\text{mM}^{-1} \text{cm}^{-1}$]) of Absorption Maxima in Optical Absorption Spectra for Carbonmonoxy and Cyanomet Globins

| | WT Mb | | Hb α | | Mbα(HBM) | |
|-----------------|--------------|-----------------------------|--------------|-----------------------------|--------------|-----------------------------|
| | Soret | visible | Soret | visible | Soret | visible |
| CO | 422 (187) | 542 (14.0) 579 (12.2) | 419 (191) | 540 (13.6) 569 (13.4) | 419 (185) | 540 (13.5) 570 (13.4) |
| CN ⁻ | 422 (116) | 540 (11.3) | 419 (124) | 540 (12.5) | 419 (119) | 540 (12.5) |

For the visible region, the spectral pattern of the chimeric globin is quite similar to that of the α-subunit rather than to that of parent globin, myoglobin. Such spectral similarities between the α-subunit and Mbα(HBM) are also encountered for the ferric low spin state. For the cyanomet forms of the globins, the Soret band and one broad peak are observed around 420 nm and in the visible region, respectively. As clearly shown in Fig. 3B, the Soret peaks for both of the α-subunit and Mbα(HBM) were detected at 419 nm, while myoglobin

showed its Soret peak at 422 nm. The peak positions of the prominent bands are compiled in Table I. As clearly shown in Fig. 3 and Table I, the wavelengths and extinction coefficients of absorption maxima for the Mb α (HBM) are almost the same as those of the α -subunit, implying that the implantation of the heme binding module from the α -subunit into myoglobin converts the heme electronic state of myoglobin into that of the α -subunit.

Resonance Raman Spectra of the Deoxy Form - The different coordination structure of the heme iron in globins was also manifested in the resonance Raman spectra. Fig. 4 shows the low-frequency region of the Raman spectra for the globins we examined here. In this region are observed several vibration modes of the porphyrin backbone and the stretching band between the heme iron and the axial histidine (25). Although the iron - His stretching

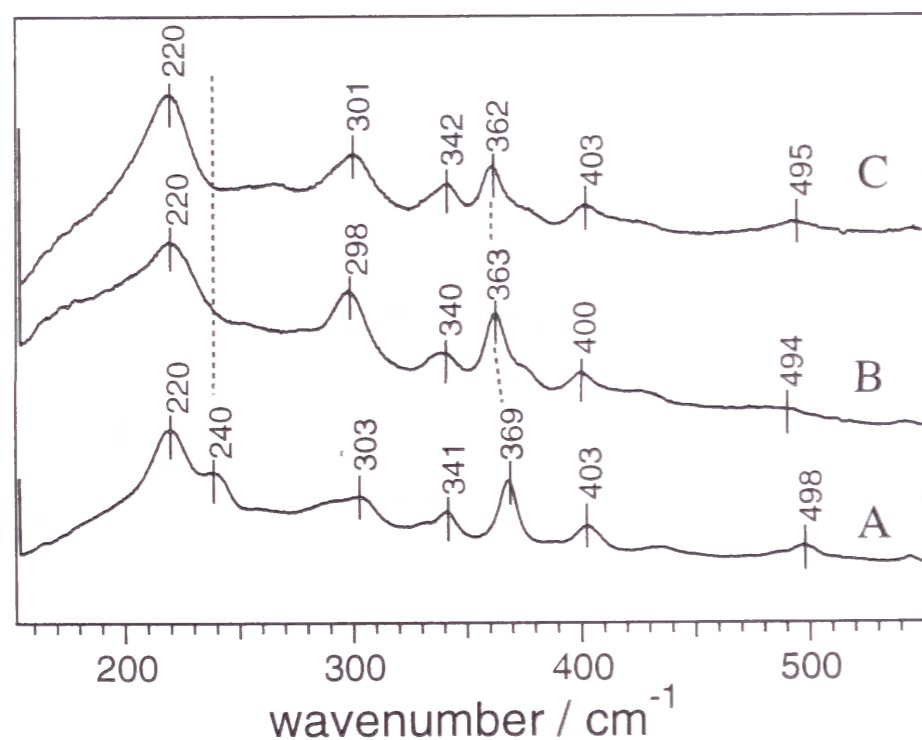


Fig. 4 Resonance Raman spectra for deoxy myoglobin (A), α -subunit (B) and Mb α (HBM) (C) excited by He/Cd laser (441.6 nm). The spectra were measured at room temperature and pH 7.4. The sample concentration was 50 μ M.

mode is almost identical to that for myoglobin, there are a few distinct differences between these two globins. One of the characteristic features of myoglobin is appearance of the bending mode $\delta(C_{\beta}C_1)$ coupled with $\delta(C_{\beta}$ -propionate) and $\delta(C_{\beta}$ -methyl) at 240 cm^{-1} (25). This band was not detected in the spectrum of the hemoglobin α -subunit. In the spectrum of Mb α (HBM), the bending mode completely disappeared, suggesting the porphyrin of the Mb α (HBM) being in some α -subunit characters. The porphyrin vibration

Table II Raman Frequencies (cm^{-1}) for Deoxy Globins

| mode | WT-Mb | Hb α | Mb α (HBM) |
|-----------------------------|-------|-------------|-------------------|
| $\nu_{\text{Fe-His}}$ | 220 | 220 | 220 |
| $\delta(C_{\beta}C_1)$ | 240 | — | — |
| $\chi(C_{\beta}C_1)$ | 303 | 298 | 301 |
| $\delta(\text{pyr deform})$ | 341 | 340 | 342 |
| $\delta(C_{\beta}C_cC_d)$ | 369 | 363 | 362 |
| $\delta(C_{\beta}C_aC_b)_4$ | 403 | 400 | 403 |
| $\chi(\text{pyr swivel})$ | 498 | 494 | 495 |

modes characteristic of the α -subunit are also noticed in the position of the porphyrin-propionate bending mode, $\delta(C_{\beta}C_cC_d)$. Myoglobin exhibited the porphyrin-propionate bending band at 369 cm^{-1} , whereas the position of the bending modes for the α - and Mb α (HBM)s are at 363 and 362 cm^{-1} , respectively. These spectral features for the Mb α (HBM) are characteristic of the α -subunit, suggesting that the local structure around the heme substituents in the Mb α (HBM) is also α -subunit like. The assignments for some of the scattering peaks in this region are listed in Table II (25).

^1H NMR Spectra of the Heme Binding Module Substituted Globin - To gain further insight into the heme environmental structure of the module substituted globin, we examined the NMR spectra of deoxy, carbonmonoxy and cyanide-bound forms of the globins. As shown in Fig. 5(I), the hyperfine-shifted resonances from the proximal histidyl N_{δ} protons appear at 83 and 78 ppm for myoglobin and the α -subunit in the deoxy state, respectively (26, 27). By the substitution of the heme binding module, the proximal histidyl $\text{N}_{\delta}\text{H}$ for myoglobin experienced a subtle but significant upfield shift and the position of the resonance was placed at a middle of those of these two globins, showing the coordination structure of the proximal histidine in the Mb α (HBM) being close to that in the α -subunit. However, as shown in Fig. 5(II), the spectral patterns for the hyperfine-shifted proton signals at 12-24 and -2 to -10 ppm which originated from the protons of the heme peripheral groups and nearby protein residues (28) are quite different between the α - and Mb α (HBM)s. Since the spectral patterns in these regions for the Mb α (HBM) are also different from those of myoglobin, it can be inferred that the substitution of the heme-binding module causes substantial perturbations on its heme environmental structure for the deoxy form.

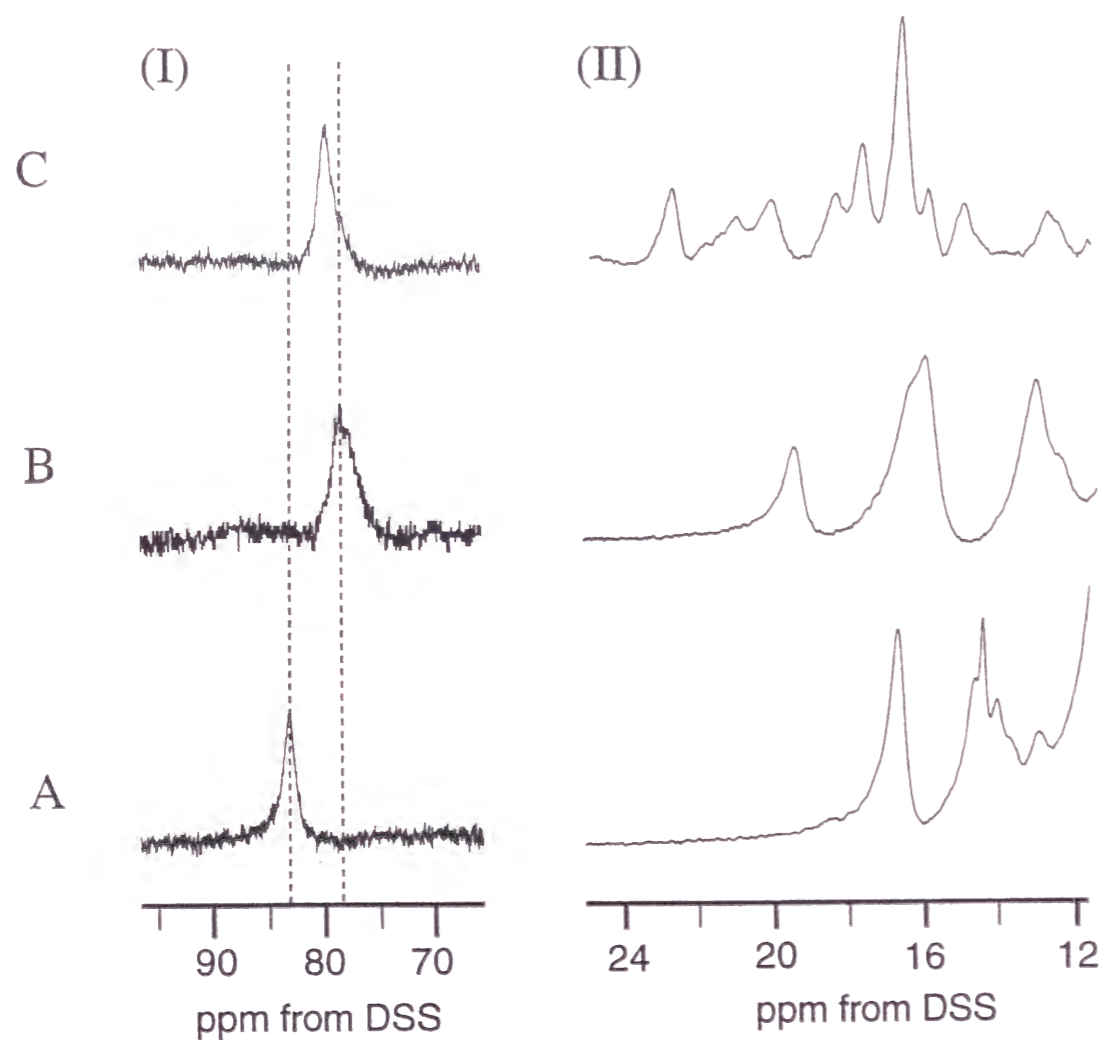


Fig. 5 Proton NMR spectra (500 MHz) for deoxy myoglobin (A), α -subunit (B) and Mb α (HBM) (C) (I) hyperfine shifted proton resonance of proximal histidyl N δ H (II) hyperfine shifted proton resonances of proximal peripheral groups. The spectra were measured in 90% H₂O at 290 K and pH 7.4. The signals around 80 ppm were not detected in 100% D₂O buffer solution.

We also measured the NMR spectra of the liganded forms of the globins as illustrated in Fig. 6. In the upfield region, the prominent peak at -2.5 ppm for myoglobin has been assigned to the methyl group of Val 67 in the distal site. The corresponding signal (Val 62 in the α -subunit) was observed at the -2.1 ppm for the α -subunit. In spite of the substitution of the heme binding module in myoglobin, the peak position for the methyl group of Val 67 was little shifted, indicating that the structural perturbation around the valine residue was extremely small. However, the peak observed around -1.3 ppm for the Mb α (HBM) which was not detected for neither myoglobin nor the α -subunit

would correspond to some structural changes in the amino acid residues located near the porphyrin ring.

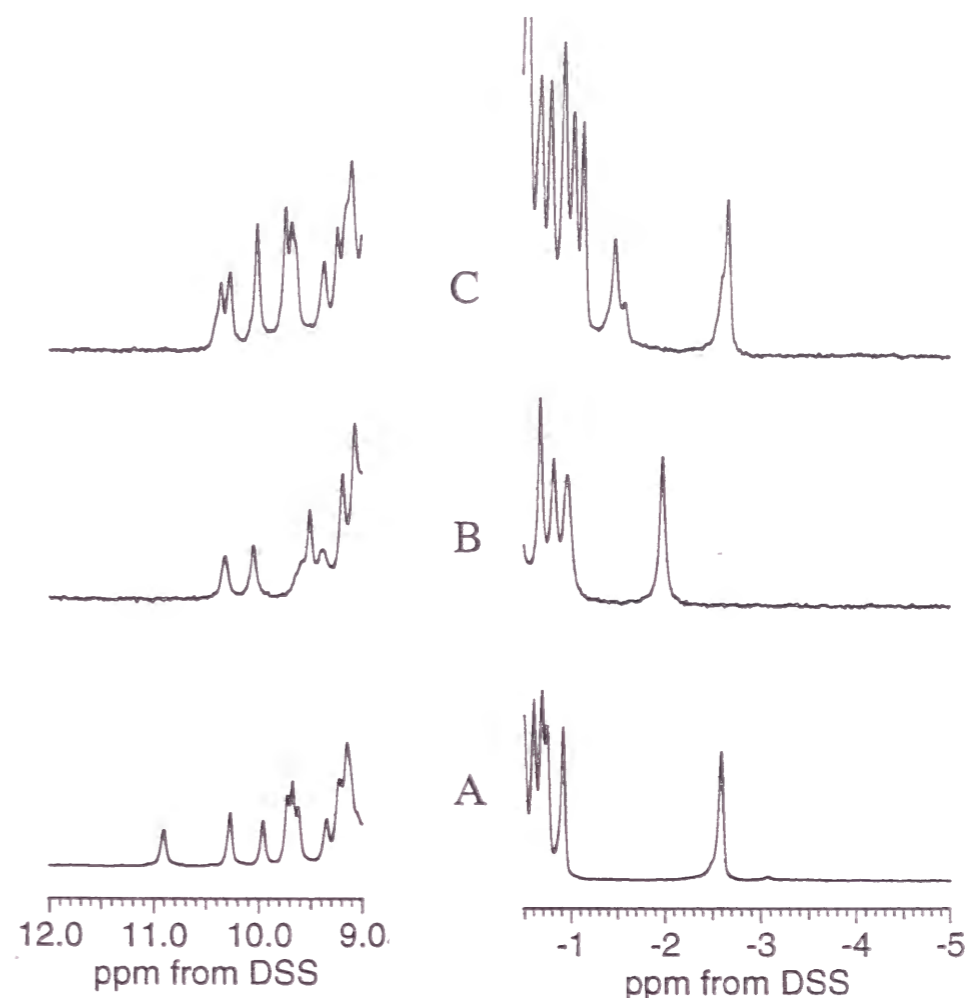


Fig. 6 Proton NMR spectra (500 MHz) for carbonmonoxy myoglobin (A), α -subunit (B) and Mb α (HBM) (C). The spectra were measured in 90% H₂O at 290 K and pH 7.4.

In order to access the structural changes in the distal site, we utilized two-dimensional NMR spectroscopy. In Fig. 7A-7C are illustrated NOESY spectra of carbonmonoxy myoglobin, α - and Mb α (HBM)s showing the cross-peaks from the methyl group of the valine residue (16, 17, 29). The connectivity patterns for the methyl group in the Mb α (HBM) is similar to that of myoglobin. For example, the cross peak between γ 1-methyl protons of Val(E11) and C δ H proton of His(E7) for myoglobin and Mb α (HBM) were observed at almost the same position. The similarity in the NOE connectivities including Val(E11) between myoglobin and Mb α (HBM) also supports the minor structural changes in the heme distal side by the module substitution.

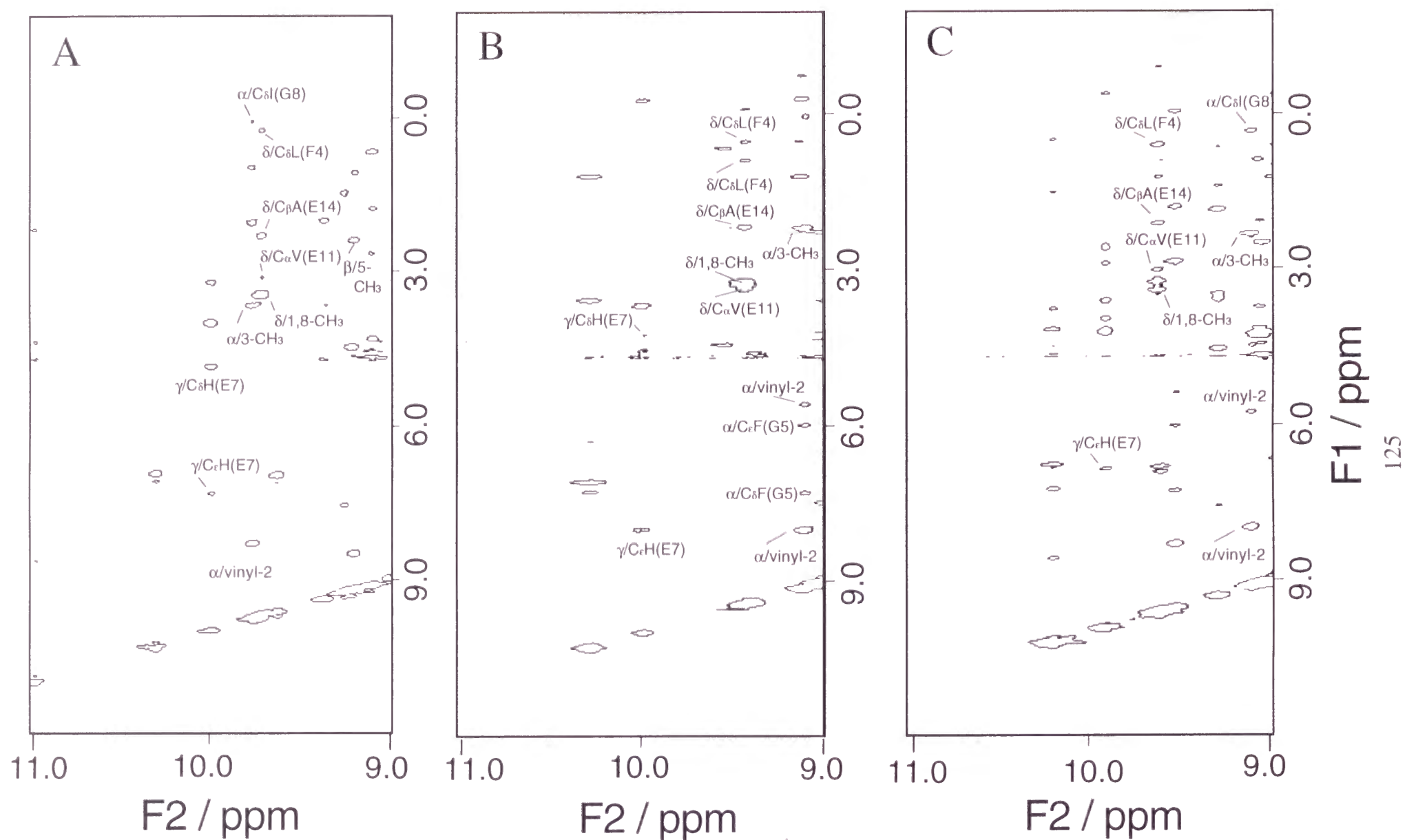


Fig. 8 Region of NOESY spectra for carbonmonoxy myoglobin (A), α -subunit (B) and Mb α (HBM) (C) in 90% H₂O. The NOE cross-peaks from the heme meso proton resonances are indicated. Samples contain 1 mM protein in 50 mM sodium phosphate buffer at pH 7.4. The spectra were measured at 283 K.

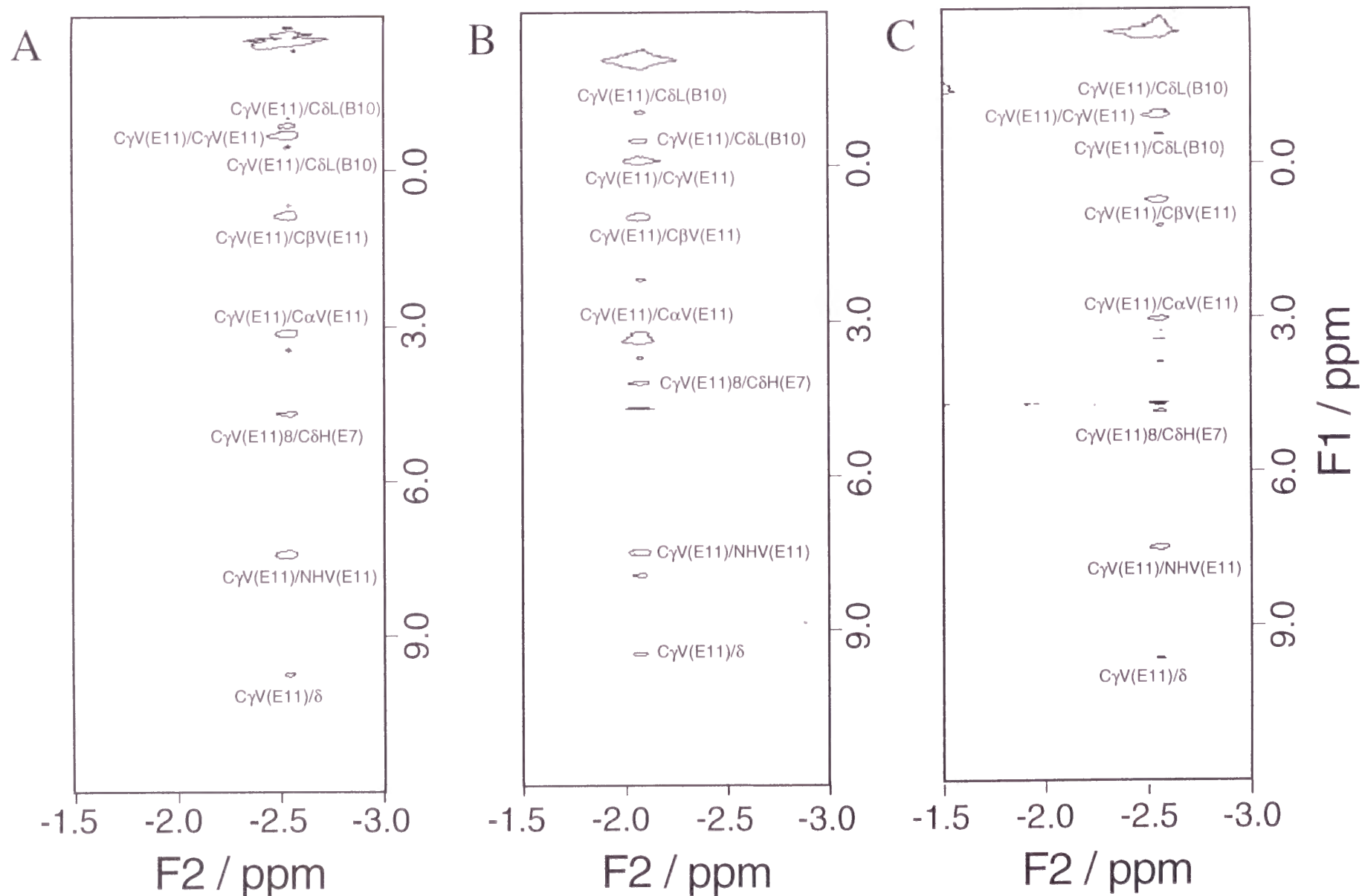


Fig. 7 Region of NOESY spectra for carbonmonoxy myoglobin (A), α -subunit (B) and Mb α (HBM) (C) in 90% H₂O. The NOE cross-peaks from the ring current-shifted proton resonances of the heme surrounding residues in the distal side are indicated. Samples contain 1 mM protein in 50 mM sodium phosphate buffer at pH 7.4. The spectra were measured at 283 K.

Table III Assignment of ^1H NMR Signals of the Carbonmonoxy Globins (ppm from DSS) at 10 °C and pH 7.4

| | WT-Mb | Hb α | Mb α (HBM) |
|------------------------------------|--------------|--------------|-------------------|
| Heme α -meso | 9.77 | 9.11 | 9.11 |
| Heme β -meso | 9.21 | 9.00 | — |
| Heme γ -meso | 9.99 | 10.00 | 9.91 |
| Heme δ -meso | 9.71 | 9.43 | 9.62 |
| Heme 1-methyl | 3.45 | 3.20 | 3.26 |
| Heme 3-methyl | 3.65 | 2.18 | 2.25 |
| Heme 5-methyl | 2.39 | 2.25 | 2.32 |
| Heme 8-methyl | 3.45 | 3.28 | 3.42 |
| Heme 2-Vinyl C α H | 8.05 | 8.02 | 8.00 |
| C β H | — | 5.59 | 5.60 |
| Leu(B10) C δ H ₃ | -0.88, -0.45 | -1.05, -0.49 | -0.99, -0.55 |
| His(E7) C δ H | 4.68 | 4.19 | 4.83 |
| C ϵ H | 7.32 | 8.02 | 6.86 |
| Val(E11) C α H | 3.11 | 3.36 | 3.02 |
| C β H | 0.85 | 0.99 | 0.72 |
| C γ H ₃ | -2.54, -0.70 | -2.07, -0.11 | -2.56, -0.92 |
| NH | 7.43 | 7.48 | 7.48 |
| Ala(E14) C β H ₃ | 2.30 | 2.10 | 2.13 |
| Leu(F4) C δ H ₃ | 0.50 | 0.52, 0.88 | 0.60 |
| Phe(G5) C δ H ₂ | — | 7.31 | — |
| C ϵ H ₂ | — | 5.99 | — |
| Ile(G8) C δ H ₃ | 0.07 | — | -0.05 |

On the other hand, in the downfield region, the meso protons of the porphyrin ring are key resonances to examine the heme environmental structure. Although one-dimensional spectra of the carbonmonoxy forms did not give any characteristic signals as depicted in Fig. 6, the NOE connectivities in the two-dimensional spectra provide us with more detailed structural characterization for the globins. In Fig. 8, the resonance position of the α -meso proton and its connectivities is shown as one of the characteristic differences between myoglobin and α -subunit. The resonance position of the α -meso proton is 9.77 ppm for myoglobin, which is 0.66 ppm downfield from that of the α -subunit. Also, the cross peaks between the α -meso proton and Phe(G5) appear in the spectrum of the α -subunit, but not in that of myoglobin. Instead of this cross peak, the NOE to Ile(G8) was found in myoglobin. For the Mb α (HBM), the position and connectivities of the α -meso proton were chimeric between these two parent globins. The resonance from the α -meso proton appeared at 9.11 ppm with the resonance position identical to that of the α -subunit, whereas the cross peak to Ile(G8) was detected but the one to Phe(G5) was missing, characteristic of myoglobin. The signal assignments by NOESY spectra are summarized in Table III.

In addition to the NMR spectra of the deoxy and carbonmonoxy forms of the globins, we also utilized the hyperfine-shifted resonances of the cyanomet forms, which have served as markers for the heme environmental structures in the liganded forms of globins. As depicted in Fig. 9A, several prominent hyperfine-shifted signals from the heme peripheral groups were observed for cyanide bound forms of globins (13, 30-33). In myoglobin, three methyl groups attached to the porphyrin ring experienced large hyperfine-shifts, and resonance positions for 5-, 1- and 8- methyl groups were 28.1, 18.9, and 13.3 ppm, respectively (13). In the α -subunit, the heme methyl resonances were less downfield shifted as shown in Fig. 9A. The resonance from the 5-, and 1-methyl group appeared at 23.1 and 17.0 ppm (33), respectively, and the peak from the 8-methyl group was hidden in the diamagnetic region. The 2-vinyl C α H proton signal of myoglobin was more downfield shifted, compared with the α -subunit. On the basis of theoretical analysis of the hyperfine-shifted spectra and comparison of the X-ray structure, the dispersion of the positions of the heme peripheral groups has been considered to primarily depend on the orientation of the axial histidine (34).

For the Mb α (HBM), several hyperfine-shifted NMR resonances assignable to the heme peripheral groups were also detected. We have assigned the heme methyl group signals of the cyanomet Mb α (HBM) by analogy with the spectral pattern of cyanomet myoglobin and α -subunit and NOEs between the heme

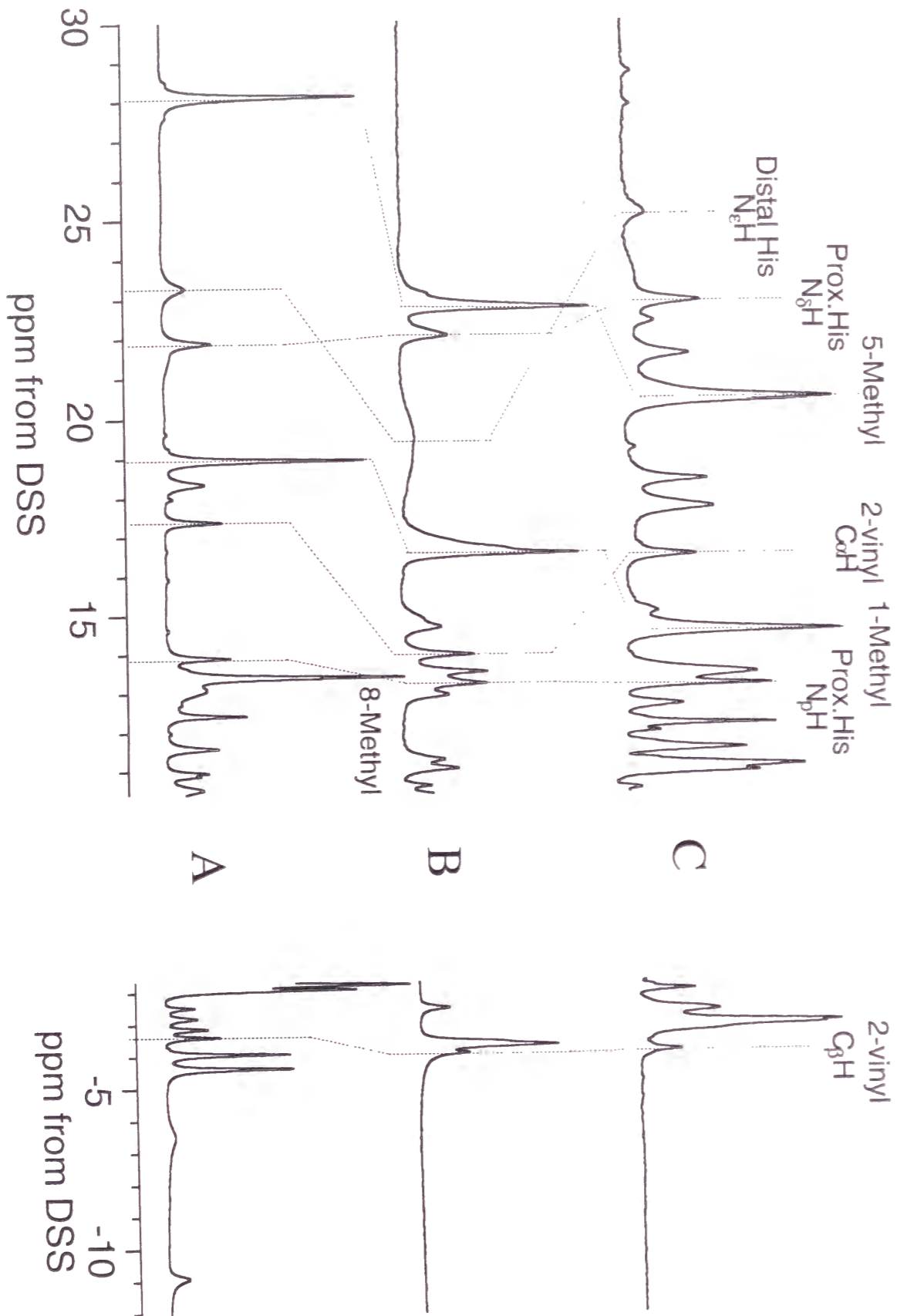


Fig. 9A Proton NMR spectra (500 MHz) for cyanomet myoglobin (A), α -subunit (B) and Mb α (HBM) (C). The spectra were measured in 90% H₂O at 290 K and pH 7.4

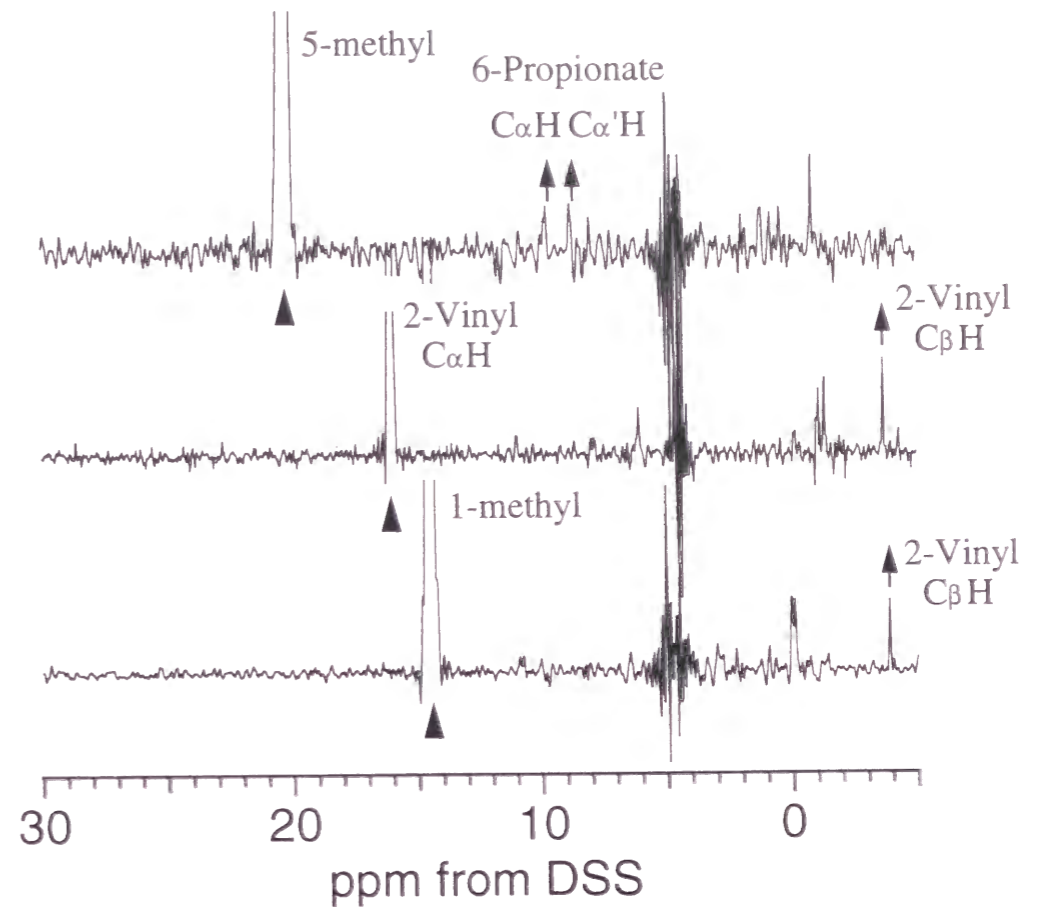


Fig. 9B Cross sections of NOESY spectrum for the cyanomet Mb α (HBM) at 20.7(I), 16.4(II) and 14.7(III) ppm (I) Saturate 5-methyl completely; note NOEs to 6-propionate C α H and C α' H (II) Saturate 2-vinyl C α H completely; note NOE to 2-vinyl C β H (III) Saturate 1-methyl completely; note NOE to 2-vinyl C β H The diagonal peaks are labeled by an arrow. The spectra were measured in 90% H₂O at 290K and pH 7.4.

substituents. A strong NOE was found between the peaks at 14.5 and -3.9 ppm and the irradiation at 16.4 ppm peak also induced a positive NOE at -3.9 ppm as shown in Fig. 9B. These NOEs indicate that the peak at 14.5 ppm can be assigned to the 1-methyl group and the peaks at 16.4 and -3.9 ppm to C α H and C β H of the 2-vinyl group. By irradiation at the peak of 20.7 ppm, two NOE signals were observed at 9.7 and 9.2 ppm, which is characteristic NOE between the 5-methyl group and 6-propionate (13). These assignments are compiled in Table IV.

In addition to the resonances from the heme peripheral groups, those from the amino acid residues located near the heme iron are also useful probes for heme environmental structures (35). In myoglobin and α -subunit, the small exchangeable proton peaks have been assigned to the protons of the

heme surrounding residues (36). We also observed exchangeable proton signals at 25.2, 23.0 and 13.2 ppm for the Mb α (HBM). On the basis of NOE connectivity between the exchangeable protons, we were able to assign the signals at 23.0 and 13.2 ppm to the proximal histidine N δ H and proximal histidine peptide N ρ H, respectively (13). The signal at 25.2 ppm is consequently assignable to the distal histidine N ϵ H. The peak assignments are listed in Table IV. As clearly shown in Fig. 9A and Table IV, the peak positions of these exchangeable protons were shifted by the substitution of the heme binding module, suggesting that the substitution of the heme binding module perturbs both of the heme proximal and distal structures of cyanomet myoglobin.

Table IV Assignment of ^1H NMR Signals of the Cyanomet Globins (ppm from DSS)

| | WT-Mb | Hb α | Mb α (HBM) |
|------------------------|-------|-------------|-------------------|
| 5-CH ₃ | 28.1 | 23.1 | 20.7 |
| 1-CH ₃ | 18.9 | 17.0 | 14.5 |
| 8-CH ₃ | 13.3 | – | – |
| 2-vinyl C α H | 17.3 | 14.0 | 16.4 |
| 2-vinyl C β H | –3.4 | –3.9 | –3.9 |
| His(F8) N δ H | 21.9 | 22.2 | 23.0 |
| His(F8) N ρ H | 13.9 | 13.2 | 13.2 |
| His(E7) N ϵ H | 23.2 | 19.6 | 25.0 |

Fig. 10 FT-IR spectra of CO stretching region for carbonmonoxy wild-type myoglobin (A), α -subunit (B) and Mb α (HBM) (C) The spectra were measured at room temperature and pH 7.4. The sample concentration was about 1 mM on the heme basis.

Infrared Spectra of the CO Form - To investigate the heme distal structures of the Mb α (HBM) in more detail, we have measured infrared spectra in the C-O stretch region (Fig. 10). In myoglobin, the major CO stretching mode was observed at 1945 cm⁻¹, whereas the band appeared at 1951 cm⁻¹ for the α -subunit (37), indicating that heme environment near the liganded carbon monoxide is significantly different between these two globins. The implantation of the heme binding module from the α -subunit into myoglobin induced appearance of two additional bands at 1932 and 1969 cm⁻¹. According to the conventional notation of IR stretch frequency (37), the bands

at 1964 cm⁻¹, 1945 cm⁻¹ and 1932 cm⁻¹ are referred to as A₀, A₁ and A₃, respectively. Since these stretching bands have been assigned to three distinct conformations of the iron bound CO (37), the Mb α (HBM) affords multiple conformations of the liganded carbon monoxide, reflecting the substantial alteration of the electrostatic and steric environment in its heme distal pocket.

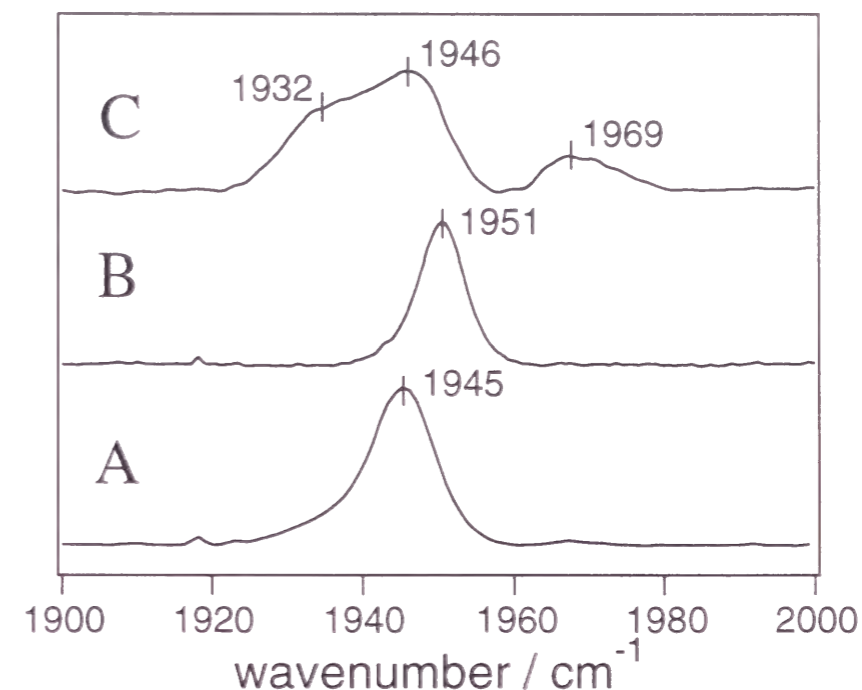


Fig. 10 FT-IR spectra of CO stretching region for carbonmonoxy wild-type myoglobin (A), α -subunit (B) and Mb α (HBM) (C) The spectra were measured at room temperature and pH 7.4. The sample concentration was about 1 mM on the heme basis.

Oxygen Affinity - We have examined functional properties as well as structural ones of the Mb α (HBM) by observing its oxygen affinity. Fig. 11 shows the oxygen equilibrium curves expressed by the Hill plot. Although some deviations are found in the curves, the oxygen binding properties for the Mb α (HBM) are virtually identical to that of the α -subunit or myoglobin. As listed in Table V, the P_{50} values of wild-type myoglobin, α -subunit and Mb α (HBM) are estimated to be 0.73, 0.66 and 0.72 mmHg, respectively. The n_{max} values are also almost unity for all the samples. The replacement of the heme binding module did not induce significant alterations of the oxygen binding properties of globins.

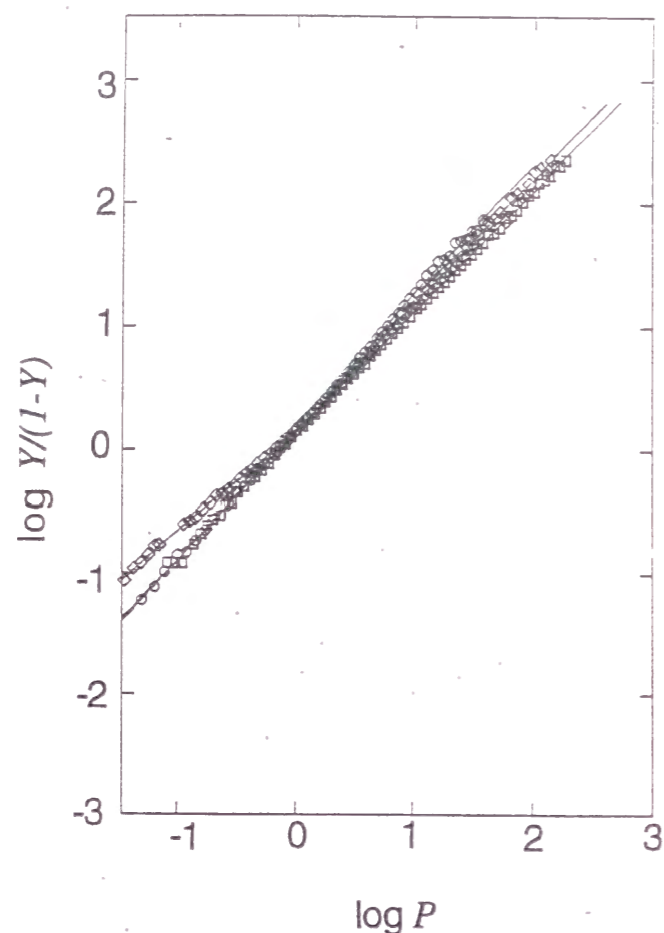


Fig. 11 Oxygen equilibrium curves for wild-type myoglobin (\square), α -subunit (\diamond) and Mb α (HBM) (\circ) Experimental conditions were as follows: 50 mM Tris, 0.1 M NaCl, pH 7.4, at 25°C. Sample concentration was 60 μ M on the heme basis and sample volume was 6 ml.

Table V Oxygen Equilibrium Parameter Values for Globins

| | P_{50} [mmHg] | n_{max} |
|-------------------|-----------------|-----------|
| WT-Mb | 0.73 | 1.04 |
| Hb α | 0.66 | 1.06 |
| Mb α (HBM) | 0.72 | 1.16 |

DISCUSSIONS

Structure of the Mb α (HBM) - As clearly shown in the electronic absorption spectra, the electronic state of the heme of the Mb α (HBM) is similar to that of the α -subunit, not of myoglobin. Since the wavelength and extinction coefficients of absorption maxima are mainly determined by the coordination structure of a proximal ligand and hydrophobicity of the heme environments (1, 38), the spectral similarity between the Mb α (HBM)- and α -subunits implies

that its heme proximal structure is changed into the α -subunit type by the substitution of the heme binding module. Such a crucial roles of the heme binding module in the structure of the proximal site was also evidenced by the NMR spectra of the Mb α (HBM). As shown in Fig. 9A, the hyperfine-shifted resonances from the heme peripheral groups in the Mb α (HBM) experienced substantial upfield bias of the resonance positions from those of myoglobin. It is generally accepted that the hyperfine shifts of the heme methyl proton NMR signals for cyanomet hemoproteins are predominantly governed by the interaction of the p_{π} -orbital of the N_{δ} of His 93 with the iron d_{xz} and d_{yz} orbital where the unpaired electron resides. Previous studies have shown that the chemical shifts (δ) of the heme methyl proton signals of the cyanomet hemoproteins correlate with the angle (Φ) between the projection of the proximal imidazole plane onto the heme plane and the porphyrin N_2 - N_4 vector (34). The angle (Φ) for myoglobin and the α -subunit was respectively estimated as 19° and 24° from their heme methyl resonance positions, which is consistent with the x-ray crystallographic study (Fig. 2C). In the Mb α (HBM), more tilt angle ($\Phi = 26^\circ$) was obtained by the resonance positions of the heme methyl groups, suggesting that its heme coordination structure of the proximal histidine is similar to that of the α -subunit rather than that of myoglobin.

^1H NMR and resonance Raman spectra of the deoxy form also provide further insights into the heme proximal structure. The subtle but significant upfield bias of the $N_{\delta}\text{H}$ proton resonance of the proximal histidine is observed for the deoxy Mb α (HBM) as compared with deoxy myoglobin. Since the hyperfine shifts for the axial imidazole in the deoxy state primarily reflect spin transfer via Fe- N_{ϵ} σ bonding (26, 27), the upfield shift (less downfield hyperfine shift) corresponds to the increased strain imposed on the iron-histidyl bond in the Mb α (HBM), resulting in less electron spin transfer from the heme iron to the proximal His (39). However, the stretching band between the heme iron and axial histidine was shown to be insensitive to the module substitution, and the strain imposed on the Fe - N_{ϵ} bond would not be strengthened in the Mb α (HBM). Although the structural factors affecting the hyperfine shifted histidyl proton have not yet been clear, it can be safely said that the implantation of the heme binding module from the α -subunit into myoglobin affected the heme environmental structure of the proximal side in myoglobin to maintain the α -subunit type heme environmental structure.

The α -subunit character of the heme environmental structure of the Mb α (HBM) is also suggested by some of the heme vibration modes. Most prominent changes in the resonance Raman spectra by the module

substitution are disappearance of a scattering peak around 240 cm^{-1} assigned to $C_{\beta}-C_1$ bending mode [$\delta(C_{\beta}C_1)$] coupled with $\delta(C_{\beta}\text{-propionate})$ and $\delta(C_{\beta}\text{-methyl})$. In addition to the band at 240 cm^{-1} , the substantial shift to low wavenumber of the porphyrin-propionate bending mode [$\delta(C_{\beta}C_cC_d)$] for the Mb α (HBM) was also observed, indicating that the module substitution affected the heme environmental structure around the propionate of the heme. In fact, the propionate in myoglobin forms a hydrogen bond with His(FG2) N ϵ H, whereas the α -subunit does not bear such a hydrogen bond between the propionate and His(FG2) N ϵ H. The missing of the bending mode suggests that the Mb α (HBM) constructs the α -subunit-like heme environmental structure.

In sharp contrast to the substantial structural changes in the proximal site, the structural changes in the distal site were rather small. As illustrated in Fig. 12, the NOE connectivities between the distal residues are conserved among three globins. However, the Mb α (HBM) exhibited subtle but significant shifts of the cross peak positions from those of myoglobin (Table III), which would correspond to alterations in the dispositions of the heme distal residues (40). The increase in the relative proportions of the conformers A $_0$ and A $_3$ as revealed by the IR spectra was also suggestive of the structural changes in the heme environments around the heme ligand. Although the spectral changes in the IR spectrum of the Mb α (HBM) were drastic, similar spectral changes were also encountered for Mb mutants having the mutation sites at His(E7), Val(E11), Phe(CD1), Arg(CD3), Phe(CD4) or Leu(B10) (41), some of which have similar structure to wild type protein except for the mutation sites. It, therefore, follows that the spectral changes in the distal side were not so prominent as those in the proximal site, and the effects of the substitution of the heme binding module on heme environments are localized in the heme proximal site.

Structural and Functional Significance of the Heme Binding Module - Present spectroscopic data clearly show that the structure of the proximal site was preferentially perturbed by the heme binding module substitution and the resultant structure had an α -subunit character, while the perturbations on the distal site were more moderate and the distal structure was still close to that of myoglobin. Such a chimeric structural features were also reported in our previous paper (8). The replacement of the pseudo-module PM3, the amino acid sequence from F1 to H6, in the β -subunit with that of the α -subunit affected the structure of the proximal site, resulting in the α -subunit type structure, whereas the structure of the distal site remains the β -subunit like. Together with the present and previous studies of the module substitutions, we

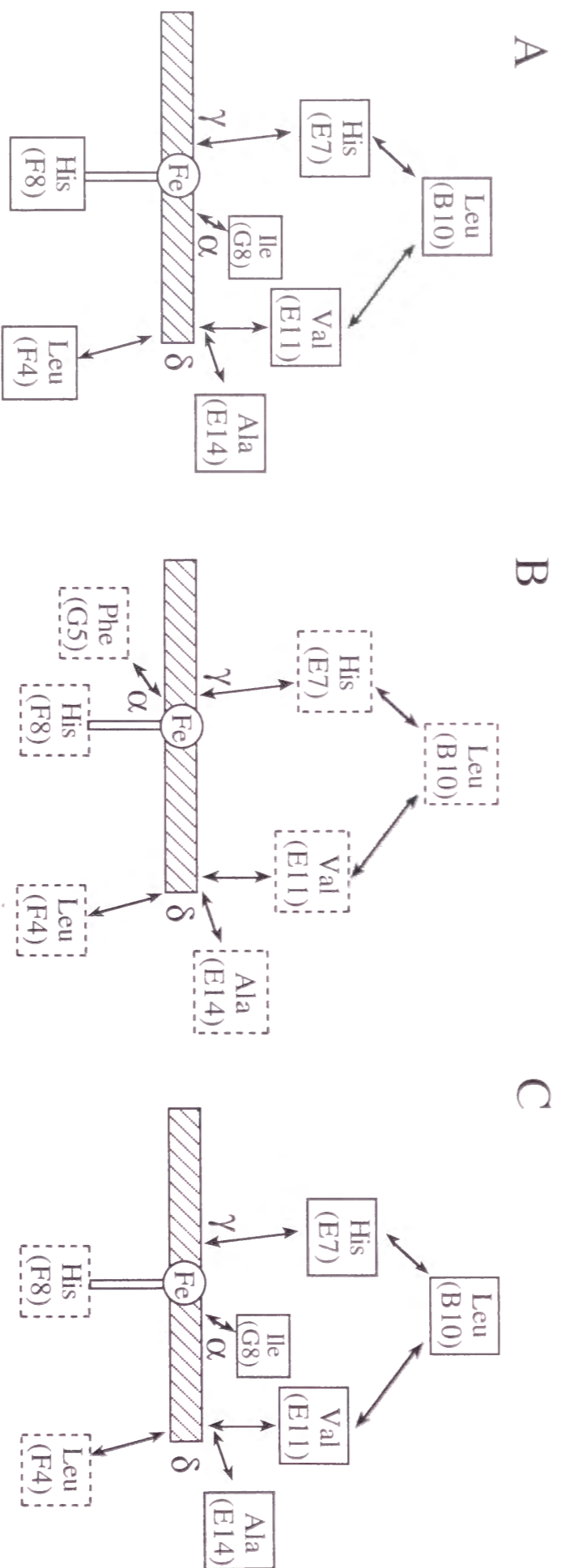


Fig. 12 Schematic diagram showing NOE connectivities between heme and surrounding amino acid residues in Mb (A), α -subunit (B) and Mb α (HBM) (C) Amino acid residues included in the heme binding module from the α -subunit are framed by boxes expressed with broken lines. " α ", " γ " and " δ " in this figure represent α -meso, γ -meso and δ -meso protons of the heme, respectively.

can conclude that the "heme binding module" would be a primary determinant for the proximal structure of globins, but not for the distal structure. In other words, the "heme binding module" can be one of the structural units which regulate the heme proximal structure of hemoproteins.

However, the effects of the substitution of the heme binding module on the structure of the distal site are not negligible. The IR spectrum of the carbonmonoxy Mb(HBM) unambiguously revealed the structural changes in the heme distal site, implying that the structure of the distal site is surely influenced by the structural changes in the proximal site. One of the reasons for the perturbation in the distal site would be that the substitution of the heme binding module affects the intramolecular packing between the module and the other regions. According to the inspection by Lesk and Chothia, the major inter-helix contacts in globin structure are found in A/H, B/E, B/G, F/H and G/H helix packings (42). Since the heme binding module includes the F-helix and a part of the G-helix and homology of the residues in the heme binding module is quite low (4/21) between myoglobin and the α -subunit (Fig. 2A), the substitution would perturb the B/G, F/H and G/H helix packings, resulting in the structural changes in the distal heme environment. Therefore, although the heme binding module is a primary structural factor to regulate the structure of the proximal site in hemoproteins, the inter-helix interactions are also crucial to maintain the other parts of the protein structure.

Summary - As discussed above, the heme proximal structure and heme electronic state of myoglobin was altered into the α -subunit type upon the implantation of the heme binding module from the α -subunit into myoglobin, while the effects of this module substitution on the heme distal structure were subtle. These results demonstrate that the heme binding module corresponds to a structural segment playing crucial roles in regulation of the heme proximal structure and heme electronic state in globin proteins. It is also to be noted that other hemoproteins such as cytochrome b₅ or c₅₅₁ also contain a heme binding segment structurally similar to the module in globin proteins (43, 44). The conservation of heme binding module in various hemoproteins would have some significance of the molecular evolution in hemoproteins. In addition, the substitution of the heme binding module might be a cue for design of the new functional hemoproteins, since this substitution can preferentially affect the structure of the heme proximal site without severe structural disorders.

ACKNOWLEDGEMENT

We are grateful to Mr. Haruyuki Harada (Kyoto University) and Dr. Kiyohiro Imai (Osaka University) for measurements of NOESY spectra and oxygen equilibrium curves, respectively. Furthermore, we are indebted to Dr. Satoshi Takahashi and Dr. Teizo Kitagawa for resonance Raman spectral measurement.

REFERENCE

1. Adachi, S., Nagano, S., Ishimori, K., Watanabe, Y., and Morishima, I. (1991) *Biochem. Biophys. Res. Commun.* **180**, 138-144
2. Adachi, S., Nagano, S., Ishimori, K., Watanabe, Y., Eagawa, T., Kitagawa, T., Makino, R. and Morishima, I. (1993) *Biochemistry* **32**, 241-252
3. Hildebrand, D. P., Burk, D. L., Maurus, R., Ferrer, J. C., Brayer, G. D. and Mauk, A. G. (1995) *Biochemistry*, **34**, 1997-2005
4. Go, M. (1981) *Nature*, **291**, 90-92
5. Go, M. (1983) *Proc. Natl. Acad. Sci. USA* **80**, 1964-1968
6. Wakasugi, K., Ishimori, K., Imai, K., Wada, Y. and Morishima, I. (1994) *J. Biol. Chem.* **269**, 18750-18756
7. Noguti, T., Sakakibara, H. and Go, M. (1993) *Proteins* **16**, 357-363
8. Inaba, K., Ishimori, K., Imai, K. and Morishima, I. Submitted for publication (J. Biol. Chem.)
9. Nagai, K and Thøgerson, H. C. (1984) *Nature* **309**, 810-812
10. Nagai, K., Perutz, M. F., and Poyart, C. (1985) *Proc. Natl. Acad. Sci. U.S.A.* **82**, 7252-7257
11. Nagai, K., and Thøgerson, H.C. (1987) *Methods Enzymol.* **153**, 461-481
12. Paul, K. G., Theorell, H. and Akesson, A. (1953) *Acta Chem. Scand.* **7**, 1284-1287
13. Emerson, S. D. and La Mar, G. N. (1990) *Biochemistry* **29**, 1545-1556
14. Jeener, J., Meier, B. H. Bachmann, P. and Ernst, R. R. (1979) *J. Chem. Phys.* **71**, 4546-4553
15. Bodenhausen, G., Kogler, H. and Ernst, R. R. (1984) *J. Magn. Res.* **58**, 370
16. Dalvit, C. and Wright P. E. (1987) *J. Mol. Biol.* **194**, 313-327
17. Dalvit, C. and Wright P. E. (1987) *J. Mol. Biol.* **194**, 329-339
18. Imai, K. (1981) *Methods. Enzymol.* **76**, 438-449
19. Imai, K. (1982) *Allosteric Effect in Haemoglobin*, Cambridge University Press, London
20. Imai, K., Morimoto, H., Kotani, M., Watari, H., Hitata, W. and Kuroda, M. (1970) *Biochem. Biophys. Acta* **200**, 189-196

21. Hayashi, A., Suzuki, T. and Shin, M. (1973) *Biochem. Biophys. Acta* **310**, 309-316
22. Lynch, R. E., Lee, G. R. and Cartwright, G. E. (1976) *J. Biol. Chem.* **251**, 1015-1019
23. Winterbourn, C. C., McGrath, B. M. and Carrell, R. W. (1976) *Biochem. J.* **155**, 493-502
24. Imai, K. (1994) *Methods. Enzymol.* **232**, 559-576
25. Hu, S., Smith, K. M. and Spiro, T. G. (1996) *J. Am. Chem. Soc.* **118**, 12638-12646
26. Goff and La Mar (1977) *J. Am. Chem. Soc.* **99**, 6599-6606
27. La mar, G. N., Budd, D. L. and Goff, H. (1977) *Biochem. Biophys. Res. Commun.* **77**, 104-110
28. Busse, S. C. and Jue, T. (1994) *Biochemistry* **33**, 10934-10943
29. Adachi, S., Sunohara, N., Ishimori, K. and Morishima, I. (1992) *Biochemistry* **267**, 12614-12621
30. La Mar, G. N. and Krishnamoorthi, R. (1983) *Biophys. J.* **44**, 177-183
31. Emerson, S. D. and La Mar, G. N. (1990) *Biochemistry* **29**, 1556-1566
32. Lambright, D. G., Balasubramanian, S. and Boxer, S. G. (1989) *J. Mol. Biol.* **207**, 289-299
33. La Mar, G. N., Jue, T., Nagai, K., Smith, K. M., Yamamoto, Y., Kauten, R. J., Thanabal, V., Langry, K. C., Pandey, R. K. and Leung, H. K. (1988) *Biochim. Biophys. Acta* **952**, 131-141
34. Yamamoto, Y., Nanai, N., Chujo, R. and Suzuki, T. (1990) *FEBS Lett.* **264**, 113-116
35. Shulman, R. G., Glarum, S. H. and Karplus, M (1971) *J. Mol. Biol.* **57**, 93-115
36. Varadarajan, R., Labright, D. G. and Boxer, S. G. (1989) *Biochemistry* **28**, 3771-3781
37. Ansari, A., Berendzen, J., Braustein, D., Cowen, B. R., Frauenfelder, H., Hong, M. K., Iben, I. E. T., Johnson, J. B., Ormos, P., Sauke, T. B., Scholl, R., Schulte, A., Steinbach, P. J., Vittitow, J., and Young, R. D. (1987) *Biophys. Chem.* **26**, 337-355
38. Shiro, Y., Iizuka, T., Marubayashi, K., Ogura, T., Kitagawa, T., Balasubramanian, S. and Boxer, S. (1994) *Biochemistry* **33**, 14986-14992
39. Nagai, K., La Mar, G. N., Jue, T. and Bunn, H. F., (1982) *Biochemistry* **21**, 842-847
40. Shulman, R. G., Wuthrich, K., Yamane, T., Patel, D. and Blumberg, W. E. (1970) *J. Mol. Biol.* **53**, 143
41. Li, T., Quillin, M. L., Phillips, G. N. Jr. and Olson, J. N. (1994) *Biochemistry* **33**, 1433-1446

42. Lesk, A. M. and Chothia, C. (1980) *J. Mol. Biol.* **136**, 225-270
43. Argos, P. and Mathews, F. S. (1975) *J. Biol. Chem.* **250**, 747-751
44. Detlefsen, D. J., Thanabal, V., Pecorano, V. L. and Wagner, G. (1991) *Biochemistry* **30**, 9040-9046

FOOTNOTE

¹The pseudo-modules are defined as a segment starting at a center of one module and ending at the center of the following one and do not form a compact structural unit in sharp contrast to the modules as predicted from their correspondence to the region from a peak to the adjacent one in the centripetal profile [Noguti et al., (1993) *Proteins* **16**, 357-363]. Moreover, since the pseudo-modules do not statistically coincide with exons, they would not have evolutionary or functional meanings unlike the modules [Go, M. and Noguti, T. (1995) *Tracing Biological Evolution in Protein and Gene Structures* (eds. Go, M. and Scimmel, P.) 229-235].

²In this paper, we expressed the chimeric subunit in *Escherichia coli* without cII protein. That is, the subunit used here has a methionine residue at the N-terminal instead of a valine residue. However, we have in parallel confirmed that the mutation of Val to Met causes no affects on globular structure and heme environmental structure of myoglobin by using CD, NMR, resonance Raman and IR spectroscopies. Therefore, there are no problems in using the methionine-initiated chimeric subunit.

Chapter 6

Substitution of sub-module m6 and m7 in hemoglobin α -
and β -subunits ($\beta\alpha(m6)$ - and $\beta\alpha(m7)$ -subunits)

ABSTRACT

In the present study, we have focused upon the sub-modules m1-m8 in hemoglobin subunits, which structurally correspond to a half of the conventional modules M1-M4. In particular, since the sub-modules m6 and m7 respectively contain many residues contributing to heme contact and subunit contact, their functional roles should be noted. Herewith, we have prepared novel chimeric globins, $\beta\alpha(m6)$ - and $\beta\alpha(m7)$ -subunits, where each of the sub-modules m6 and m7 in hemoglobin β -subunit is replaced by that of the α -subunit. Gel chromatogram showed that the $\beta\alpha(m7)$ -subunit did not bind to the α - nor β -subunits, whereas the $\beta\alpha(m6)$ -subunit preferentially bound to the α -subunit. That is, the $\beta\alpha(m6)$ -subunit conserves the association property of the β -subunit type in contrast to the $\beta\alpha(m7)$ -subunit. Their different association properties strongly suggest that the sub-module m7 has one of essential factors to determine association property of hemoglobin subunits. On the other hand, NMR and resonance Raman spectroscopies revealed that the heme environmental structure of the $\beta\alpha(m7)$ -subunit, in which the sub-module m6 is derived from the β -subunit, was rather close to that of the β -subunit. However, the $\beta\alpha(m6)$ -subunit in the complex with the α -subunit exhibited structural character identical to the β -subunit in hemoglobin in spite of the implantation of the m6 from the α -subunit. These results imply that heme proximal structure depends on the subunit interactions as well as the sub-module m6. Thus, the present study for the substitution of the sub-modules m6 and m7 provides many insights not only into their structural and functional significance but also into regulation mechanism of structure and function in hemoglobin.

It has been accepted that globin structure is made up of four modules M1, M2+M3 and M4, which are corresponding to the exons 1, 2 and 3 on the gene structure, respectively (1). Inspection on the relationship between these three coding sequences and function in hemoglobin has suggested that the central module, M2+M3, constructs the heme environmental structure, while subunit contacting residues are concentrated in the module M4 (2). Our previous studies for the module substitutions in hemoglobin α - and β -subunits also experimentally supported the correspondence of the modules to hemoglobin function (3).

However, it has been proposed in our recent work for the pseudo-module¹ substitution that the modules M3 and M4 in globin proteins could be further divided into two sub-modules at the center of each module. The $\beta\alpha(\text{PM3})$ -subunit, where the pseudo-module PM3, the segment from the center of the module M3 to that of the module M4, was implanted from the α -subunit into the β -subunit, exhibited the association property of the α -subunit, just as did the module M4-substituted β -subunit, $\beta\alpha(\text{M4})$ -subunit (4). This result allows us to infer that the common region of the pseudo-module PM3 and the module M4, the former half of the module M4 (Fig. 1), might correspond to a new functional unit regulating the association property of hemoglobin subunits. Moreover, the heme coordination structure of the proximal histidine in the $\beta\alpha(\text{PM3})$ -subunit was converted into the α -subunit type, whereas the $\beta\alpha(\text{M4})$ -subunit has the β -subunit one, implying that the region included only in the pseudo-module PM3, the latter half of the module M3 (Fig. 1), might be a functional unit dominant in the heme proximal structure. Such decomposition of the conventional modules in hemoglobin subunits is strengthened by the recent automatical module assignment (5), which states that the conventional modules M1-M4 in globins can be further divided into two sub-modules, m1-m8 (Fig. 1) (6). Based on this new module assignment in globin proteins, the sub-modules m6 and m7 correspond to the latter half of the module M3 and the former one of the module M4, and many residues contributing to heme contact and subunit contact are concentrated in the sub-modules m6 and m7, respectively (Fig. 1).

In the present study, to confirm structural and functional roles of these sub-modules m6 and m7, we have synthesized novel chimeric subunits, $\beta\alpha(\text{m6})$ - and $\beta\alpha(\text{m7})$ -subunits, where only one of the sub-modules m6 and m7 of the β -subunit is replaced by that of the α -subunit (Fig. 2). On the basis of the functions of the sub-modules m6 and m7 inferred above, we have especially focused upon whether or not the heme proximal structure of the $\beta\alpha(\text{m6})$ -subunit and the association property of the $\beta\alpha(\text{m7})$ -subunit are altered into the

α -subunit ones. The present study describes the effects of the sub-module substitutions on hemoglobin structure and function, which would provide many insights into significance of the newly assigned sub-modules.

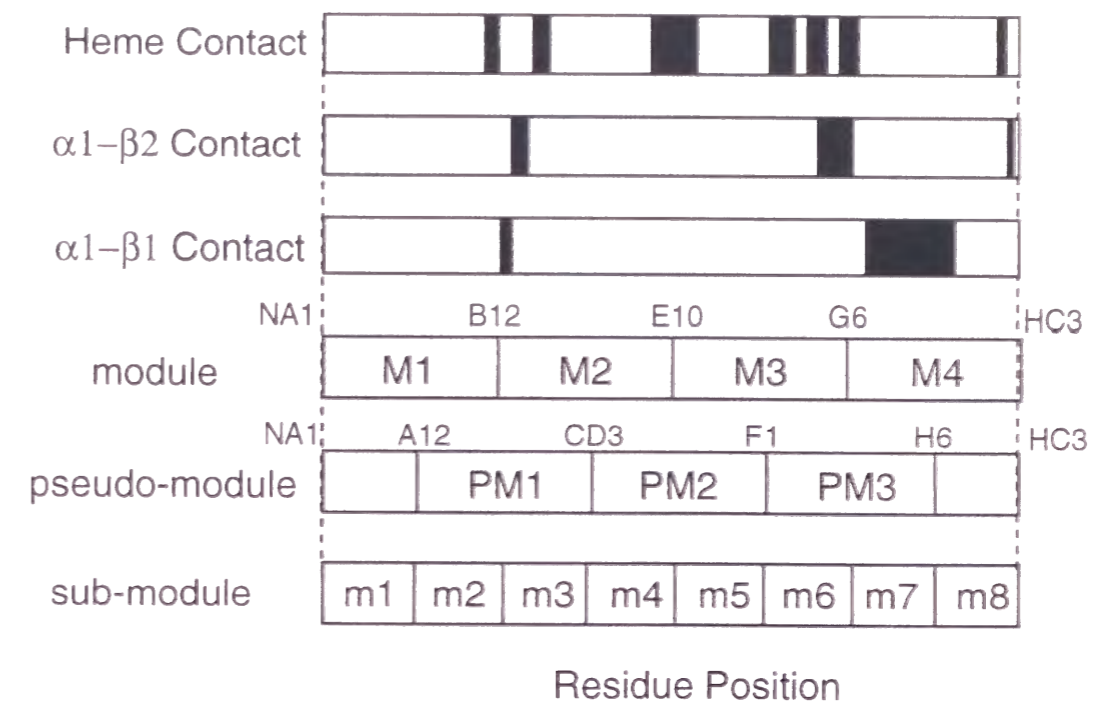


Fig. 1 Boundaries of the conventional module (M1-M4), pseudo-module (PM1-PM3) and recently proposed sub-modules (m1-m8), and residues with well defined functional roles in hemoglobin subunits (2).

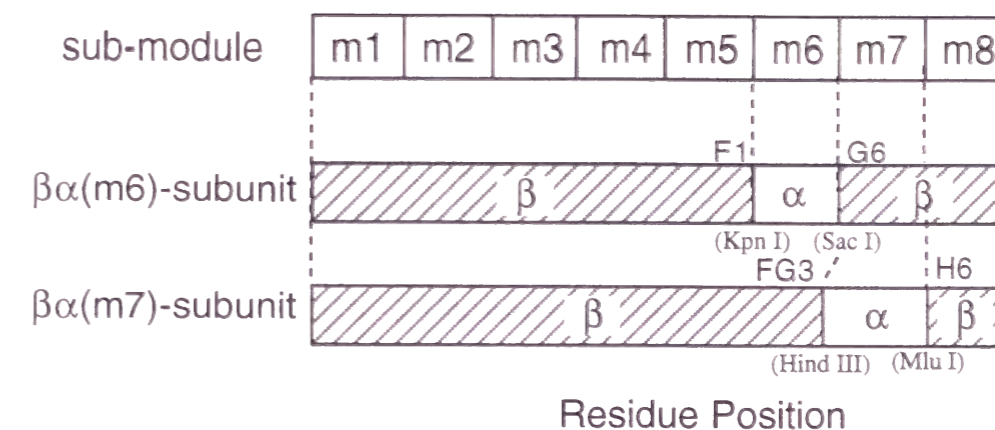


Fig. 2 $\beta\alpha(\text{m6})$ - and $\beta\alpha(\text{m7})$ -subunits synthesized in this study. Restriction enzyme sites used in this preparation are noted in a parenthesis.

EXPERIMENTAL PROCEDURES

Construction of Expression Vector - The expression vectors of the $\beta\alpha(m6)$ - and $\beta\alpha(m7)$ -subunits were constructed as illustrated in Fig. 2. The methionine residue was substituted for valine at the N-terminal to initiate the peptide elongation for the globins. To construct the gene for the chimeric subunits, *Kpn* I (GGTACC), *Sac* I (GAGCTC), *Hind* III and *Mlu* I (ACGCGT) sites were introduced at the boundaries of the modules m6 and m7 by polymerase chain reaction, accompanied with the mutation from Lys(G6) to Glu. The *Kpn* I - *Sac* I and *Hind* III - *Mlu* I fragments of the α -subunit amplified by PCR are respectively implanted into the T7 expression vector encoding the β -subunit. Construction of the desired expression vector was verified by double-stranded DNA sequence analysis (373 DNA sequencer, Applied Biosystems).

Protein Preparation - The prepared genes encoding the $\beta\alpha(m6)$ - and $\beta\alpha(m7)$ -subunits were transformed into an *Escherichia coli* strain (BL21), which was grown at 37 °C in 2xTY culture containing ampicillin (100 μ g/ml) overnight. This culture was centrifuged by 5,000 r.p.m. for 20 min. and the cell pellets were thawed and suspended in 80 ml of 50 mM Tris-HCl, pH 8.0, 25% sucrose (w/v) 1 mM EDTA and lysed with lysozyme (100 mg per 10 g of pellets) to get the crude chimeric subunits. Then, MgCl₂, MnCl₂ and DNase I were added to final concentrations of 10 mM, 1mM and 10 μ g/ml, respectively. After 30 min of incubation, 200 ml of 0.2 M NaCl, 1% deoxycholic acid, 1.6 % Nonidet P-40 (v/v), 20 mM Tris-HCl, pH 7.5, 2mM EDTA was added to the lysate, which was then centrifuged by 18,000 r.p.m. for 20 min. Then, the pellet was suspended in 0.5% Triton X-100, 1 mM EDTA and centrifuged. This procedure was repeated until a tight pellet was obtained. The protein pellet was dissolved in 8 M urea, 20 mM Tris-HCl, pH 5.2, 1 mM EDTA and loaded onto a 2.5 x 15 cm CL-6B column equilibrated in the same solution (7-9). Through eluting the protein attached to the column with 8 M urea, 20 mM Tris-HCl, pH 5.2, 1 mM EDTA, 0.2 M NaCl, we obtained chimeric subunit purity as confirmed on SDS gels. The solubilized denatured protein solution was diluted 16-fold by 20 mM Na₂B₄O₇, pH 12.0. To the supernatant at 4 °C was added 1.1 equivalent of biscyano form of protohemin and the solution was left to stand for 30 min at 4 °C. The reconstituted protein was concentrated into 10 ml and loaded onto a 5 x 30 cm G-25 column equilibrated with 20 mM Tris-HCl, 5 mM NaCN, pH 7.4 for buffer exchange. Finally, the cyanomet globin was loaded onto a 3 x 20 cm CM52 column and eluted with 20 mM Tris-HCl, 5 mM NaCN, pH 7.4. The carbon monoxide derivative was prepared by adding minimal amounts of sodium dithionite to the ferric chimeric subunits under CO atmosphere. The

globin solution was deoxygenated by repeated evacuation and flushing with N₂ gas under gentle shaking and complete deoxygenation was achieved by addition of minimal amounts of sodium dithionite.

Gel Chromatogram - Gel filtration measurements were performed by using a Sephacryl S-200 HR column (0.8 cm-d x 62 cm-l) at 4 °C. The buffer used for the chromatography was 50 mM Tris, in the presence of 0.1 M NaCl, and 1 mM Na₂EDTA, pH 7.4 and the flow rate was 7 ml/h. The eluted fractions were monitored by absorption at the Soret band (420 nm) (10). Dimer-tetramer dissociation constant of the samples was determined by concentration dependence of the centroid elution volume in FPLC over the range from 0.5 to 800 μ M (10, 11). The following dependence of the elution volume (V_e) versus protein concentration (C_T) allows us to determine the dimer-tetramer equilibrium constants for the samples (10):

$$V_e = \sum_j V_j(m_j) / C_T \quad (\text{Eq. 1})$$

where V_j are elution volumes for the individual species pertaining to the various aggregates (j -mers), and the (m_j) term represents molar concentrations for the respective species.

Spectral Measurements - CD spectra of the chimeric and native subunits in far UV region were measured at room temperature with a Jasco J-760 spectrometer. Concentration of the sample was 10 μ M, and the buffer was 20 mM Na Phosphate, 0.1 M NaCl, 5 mM NaCN and 1 mM Na₂EDTA, pH 7.4. The path length for the measurements was 1 mm.

¹H NMR spectra at 500 MHz were recorded on BRUKER Avance DRX 500 spectrometer equipped with the Indy workstation (silicon Graphics). In order to measure proton resonances in the diamagnetic region, we used a water gate pulse sequence with 50 ms pulse and 33 K data points over 13-kHz spectral width and minimized the water signal in the sample. The hyperfine-shifted proton resonances were obtained by using a LOSAT pulse sequence with a 65 K data transform of 150 kHz and a 8.5 μ s 90 ° pulse. The probe temperature was controlled at 290 \pm 0.5 K by a temperature control unit of the spectrometer. The volume of the NMR sample was 600 μ l and the concentration was 1 mM on the heme basis. The buffer was 20 mM Na Phosphate, 0.1 M NaCl, pH 7.4. Proton shifts were referenced with respect to the proton resonance of 2, 2,-dimethyl-2-silapentane-5-sulfonate (DSS).

Resonance Raman scattering was excited at 441.6 nm with a He/Ca laser (Kinmon Electronics, CDR80SG) and detected by a JEOL-400D Raman spectrometer equipped with a cooled HTV-943-02 photomultiplier. The frequencies of the Raman spectrometer were calibrated with indene. Sample

concentration was 40 μM on the heme basis. The buffer was 20 mM Na Phosphate, 0.1 M NaCl, pH 7.4.

Oxygen Equilibrium Curves and Analysis – Oxygen equilibrium curves were measured by using an improved version (12, 13) of an auto-oxygenation apparatus (14). The wavelength of the detection light was 560 nm. The buffer was 50 mM Tris, 0.1 M NaCl, pH 7.4. The temperature of the sample in the oxygenation cell was constant at 25 ± 0.05 °C. Sample volume was 6 ml and concentration was 100 μM on the heme basis. The hemoglobin reductase system (15) was added to the sample before each measurement to reduce oxidized subunits. To minimize the autooxidation of the sample during the measurements, catalase and superoxide dismutase were added to the sample and the concentration was 0.1 μM (16, 17). The oxygenation data were acquired by use of a micro-computer (model PC-98XA, Nippon Electric Co., Tokyo), which was interfaced to the oxygenation apparatus (18).

RESULTS

CD Spectra - To examine effects of the substitution of the sub-module m6 or m7 on globin structure, we have measured CD spectra in far UV region. The CD curves of both the $\beta\alpha(\text{m6})$ - and $\beta\alpha(\text{m7})$ -subunits were superimposed on those of native subunits, and the ellipticity at 222 nm was identical among the subunits (data not shown). These results revealed that the secondary structure for the β -subunit is almost insensitive to the sub-module substitution.

Association Properties – Confirming no drastic disorders in the secondary structure of the $\beta\alpha(\text{m6})$ - and $\beta\alpha(\text{m7})$ -subunits by the CD measurements, we have investigated their association property by gel chromatogram. Fig. 2A illustrates gel chromatograms of the carbonmonoxy chimeric globins in the presence and absence of the native subunits. Under the condition employed here, the mixture of native α - and β -subunits forms tetramers, whereas the isolated α -subunit remains in a monomer (10). The β -subunit is in the equilibrium between monomers and tetramers (10). As shown in Fig. 2A, the elution peak for the isolated $\beta\alpha(\text{m7})$ -subunit is completely identical with that of hemoglobin, which indicates that the $\beta\alpha(\text{m7})$ -subunit forms a homo-tetramer $[\beta\alpha(\text{m7})]_4$ by self-association. In the presence of the α -subunit, two peaks were observed, each of which coincided with those of the isolated α - and $\beta\alpha(\text{m7})$ -subunits. Moreover, the mixture of the β - and $\beta\alpha(\text{m7})$ -subunits exhibits a remarkable shoulder on the right side of the peak at 19.6 ml. This peak feature for the mixture also correspond to a simple addition of the peaks for the isolated subunits. These elution patterns reflect that the $\beta\alpha(\text{m7})$ -subunit neither associates with the α - nor β -subunits.

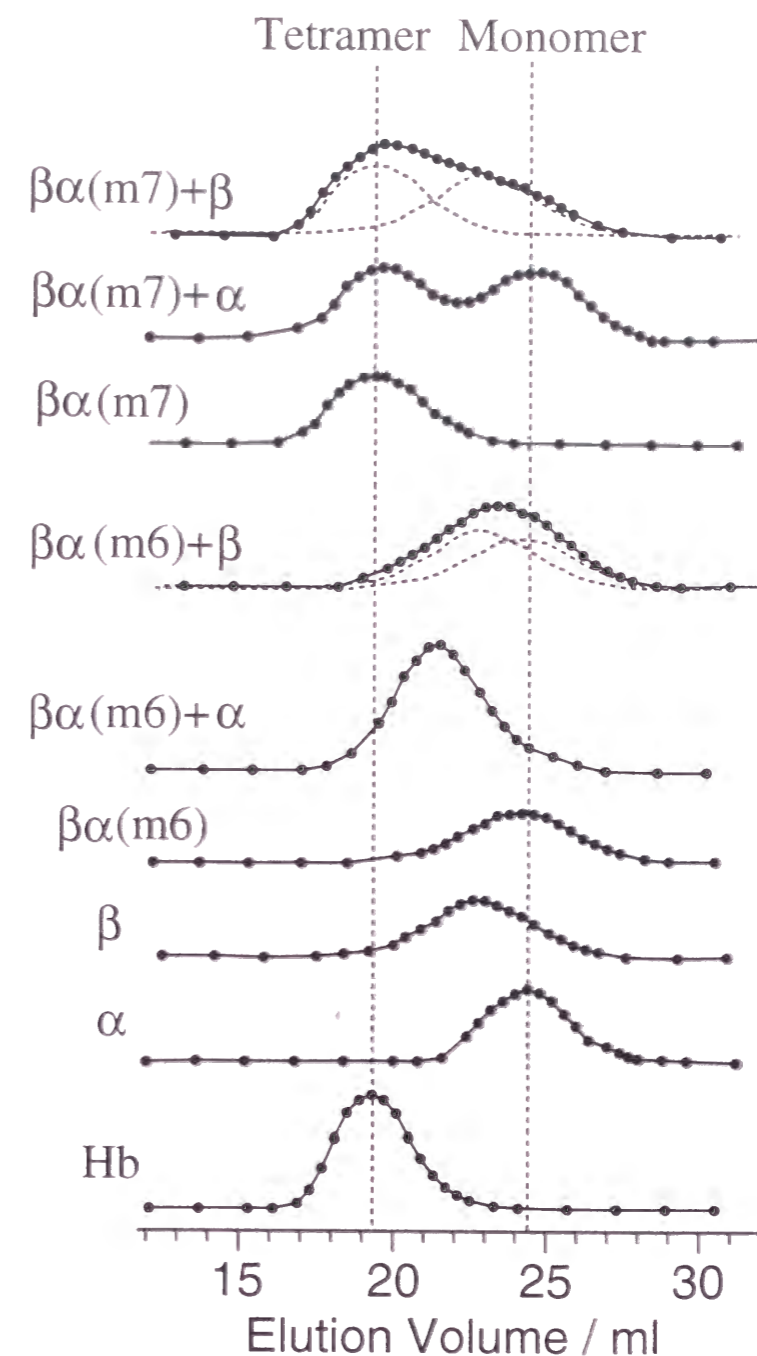


Fig. 3(A) Gel Chromatogram of carbonmonoxy forms of the $\beta\alpha(\text{m6})$ - and $\beta\alpha(\text{m7})$ -subunits on a sephacryl S-200 HR column Experimental conditions were as follows: 50 mM Tris, 0.1 M NaCl, pH 7.4, at 277 K. Sample concentration was 10 μM on the heme basis. Broken curves in the mixtures of the $\beta\alpha(\text{m6})$ - and β -subunits and the $\beta\alpha(\text{m7})$ - and β -subunits represents elution peaks of the corresponding isolated subunits.

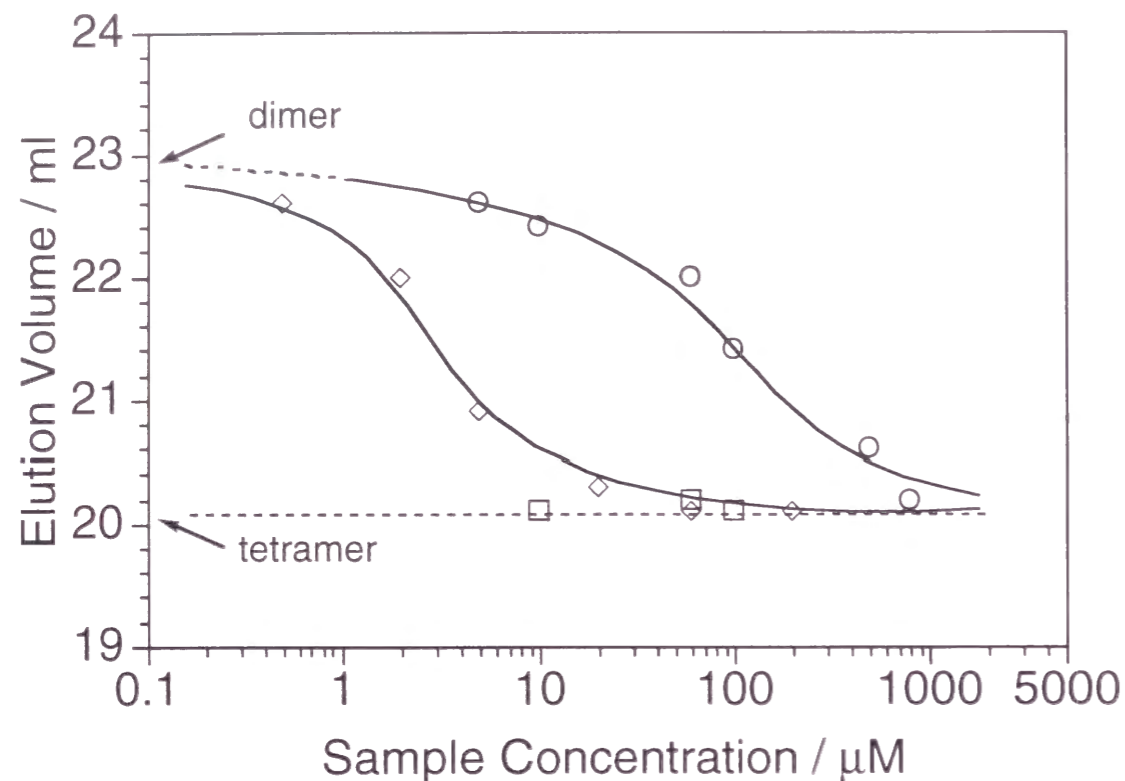


Fig. 3(B) Centroid elution volumes of Hemoglobin, the isolated $\beta\alpha(m7)$ -subunit, the complex of the native α - and $\beta\alpha(m6)$ -subunits in FPLC as a function of protein concentration Symbols correspond to hemoglobin (\diamond), $\beta\alpha(m7)$ -subunit (\square) and the complex of the α - and $\beta\alpha(m6)$ -subunits (\circ). The fitting curves were determined by the analysis method described in EXPERIMENTAL PROCEDURES. Experimental conditions were as follows: 50 mM Tris, 0.1 M NaCl, pH 7.4, at 277 K.

On the other hand, the position of the elution peak for the $\beta\alpha(m6)$ -subunit is superimposed on that of the α -subunit, revealing its monomer structure. In the chromatogram for the mixture of the $\beta\alpha(m6)$ - and β -subunits, a single broad peak was observed, but this elution pattern can be simulated by a simple addition of those of the isolated subunits. On the other hand, the mixture of the $\beta\alpha(m6)$ - and α -subunits also showed a single broad peak, which is clearly shifted to the lower elution volume by 3 ml from those of the isolated ones. These elution patterns imply that the $\beta\alpha(m6)$ -subunit preferentially binds to the α -subunit, not to the β -subunit. That is, the association property of the $\beta\alpha(m6)$ -subunit remains to be the β -subunit one upon the m6 substitution. It should be noted here that the elution peak for the mixture was dependent on the sample concentration. Fig. 3B shows the centroid elution volumes of the samples as a function of protein concentration (10, 11), where the fitting curve

of the complex of the $\beta\alpha(m6)$ - and α -subunits obtained by the Eq. 1 exhibits that the complex is in the equilibrium between a hetero-dimer $[\beta\alpha(m6)]\alpha$ and a hetero-tetramer $[\beta\alpha(m6)_2]\alpha_2$. The tetramer-dimer dissociation constants, K_D , were estimated as 1.4 and 40 μ M for Hb A and the complex of the $\beta\alpha(m6)$ - and α -subunits, respectively. Since the sub-module m6 contains the residues contributing to $\alpha 1$ - $\beta 2$ contact and its substitution inevitably accompanies structural perturbations in the $\alpha 1$ - $\beta 2$ subunit interface of the complex, such an increase in the dissociation constant for the $[\beta\alpha(m6)_2]\alpha_2$ into the $[\beta\alpha(m6)]\alpha$ would be reasonable.

Subunit Interface Structure - In order to gain further insights into the quaternary structure of the homo-tetramer $[\beta\alpha(m7)]_4$ and the complex of the $\beta\alpha(m6)$ -subunit with the α -subunit, we have analysed their subunit interface structures by measuring the ^1H NMR spectra in the hydrogen-bonded proton region for the carbonmonoxy and deoxy forms (Figs. 4A and 4B). While no exchangeable proton signals were observed in the downfield region from 10 to 15 ppm for the isolated carbonmonoxy β -subunits, two broad proton signals were detected at 12.4 and 10.4 ppm for the $\beta\alpha(m7)$ -subunits (Fig. 4A). These peaks disappeared in 100 % D_2O (data not shown). Such an exchangeable proton signal in the down field region was also encountered for carbonmonoxy Hb A, which has been assigned to the hydrogen bonds in the subunit interface as described in figure legend (19, 20). Similarly, the resonances at 12.4 and 10.4 ppm can be assignable to hydrogen bond at the subunit interfaces of the homo-tetramer, $[\beta\alpha(m7)]_4$. On the other hand, the spectral feature in this region for the complex of the $\beta\alpha(m6)$ - and α -subunits is very similar to that of hemoglobin. Three resonance peaks at 12.8, 12.0 and 10.4 ppm for the complex, which would correspond to the hydrogen bonds in the subunit interface of hemoglobin, strongly suggest that the quaternary structure of the complex is quite similar to that of hemoglobin.

By the dissociation of the ligands from Hb A, the rearrangements in the $\alpha 1$ - $\beta 2$ subunit interface are induced (19-22), which is reflected in the NMR spectra for the downfield region. For deoxy Hb A, exchangeable proton resonances were observed at 13.9 and 11.0 ppm besides at 12.2 and 12.9 ppm (Fig. 4B), which have been also assigned to the hydrogen bonds between ^{42}Tyr and ^{99}Asn and between ^{94}Asp and ^{37}Trp (19, 22). On the other hand, an additional peak appeared at 10.8 ppm in the deoxy $\beta\alpha(m7)$ -subunit. The peak at 10.8 ppm was not found in the carbonmonoxy state, suggesting the rearrangement in its interface structure upon the deoxygenation. The complex of the $\beta\alpha(m6)$ - and α -subunits in the deoxy derivative also exhibited the NMR spectrum in the

hydrogen-bonded region different from that in the carbonmonoxy one, where two new peaks appeared at 14.0 and 11.0 ppm instead of a peak at 10.4 ppm as found in Hb (Fig. 4B). Such spectral change would correspond to a structural rearrangement of the intersubunit hydrogen bonds in the complex upon deoxygenation. Since the spectral patterns for hemoglobin and the complex are quite similar, the quaternary structural change accompanied by the deoxygenation for the complex would be almost equivalent to that for native Hb A.

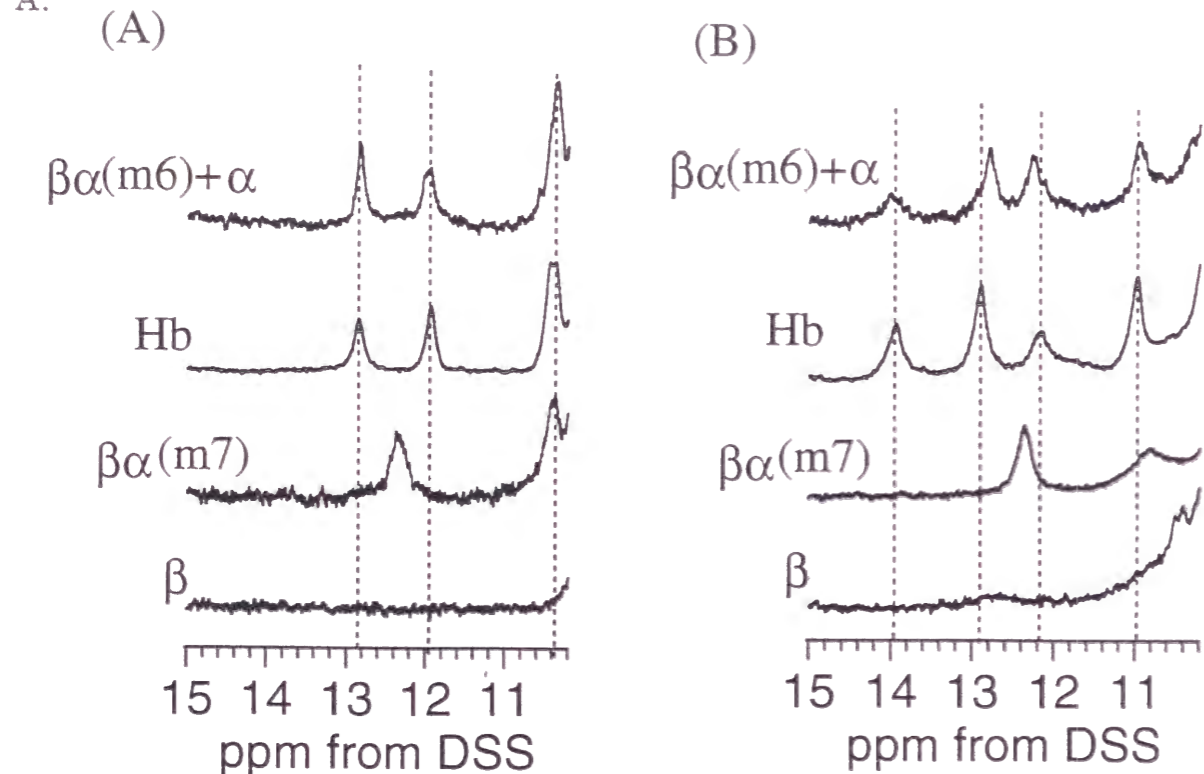


Fig. 4(A) NMR spectra in the hydrogen bonded proton region for carbonmonoxygenated subunits. Proton resonance peaks for Hb at 10.4, 11.9 and 12.8 ppm are assigned to the hydrogen bonded protons between Asp-94 α_1 and Asn-102 β_2 (Fung and Ho, 1975), His-103 α_1 and Asn-108 β_1 (Russu et al., 1987), and Asp-126 α_1 and Tyr-35 β_1 (Russu et al., 1987). Experimental conditions were as follows: 50 mM Na-Phosphate, 0.1 M NaCl, pH 7.4, at 290 K. Sample concentration was 600 μ M on the heme basis. **(B) NMR spectra in the hydrogen bonded proton region for deoxygenated subunits.** Proton resonance peaks for Hb at 11.0, 12.2, 12.9 and 13.9 ppm are assigned to the hydrogen bonded protons between Asp-94 α_1 and Trp-37 β_2 (Fung and Ho, 1977; Ishimori et al., 1992), His-103 α and Asn-108 β (Russu et al., 1987), Asp-126 α and Tyr-35 β (Russu et al., 1987), and Tyr-42 α_1 and Asn-99 β_2 (Fung and Ho, 1977). Experimental conditions were as in (A).

¹H NMR Spectra of the Cyanide Form - In addition to the association properties for the sub-module substituted globins, their heme environmental structures are also to be noted. Since contact shifts in low-spin ferric hemoproteins contain many structural informations on the heme vicinity (23), we have measured NMR spectra for cyanomet forms. As illustrated in Fig. 5, the 5-, 1-methyl and 2-vinyl C α proton signals are assigned for the α -, β -

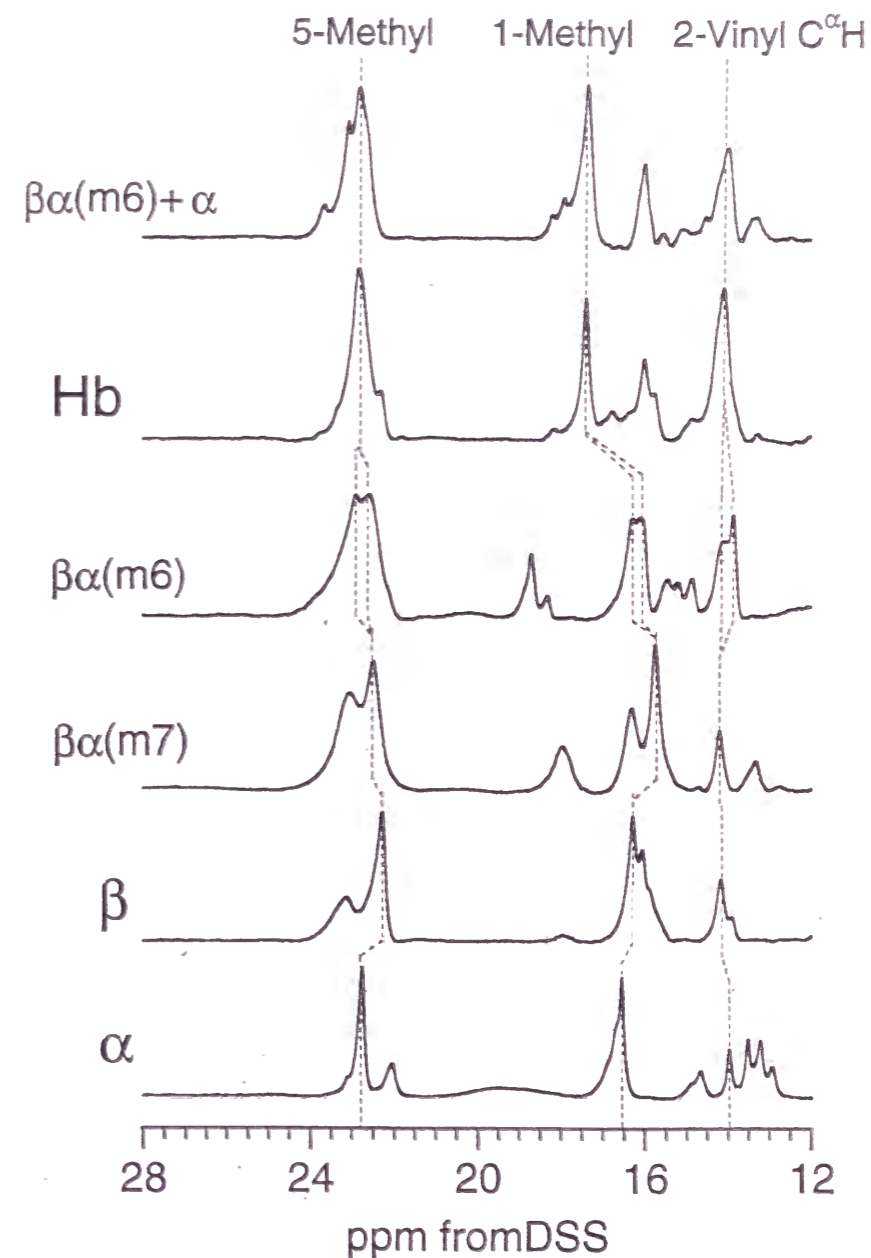


Fig. 5 Proton NMR spectra (500 MHz) for the cyanomet globins Experimental conditions were as follows: 50 mM Na-Phosphate, 0.1 M NaCl, 5 mM NaCN, pH 7.4, at 290 K. Sample concentration was 600 μ M on the heme basis.

subunits and hemoglobin (24). These signal positions in the $\beta\alpha(m7)$ -subunit are almost identical to those in the β -subunit except for the slight shift of 1-methyl signal, revealing that structural perturbation by the m7 substitution on the heme vicinity is not substantial. On the other hand, the resonance peaks for the $\beta\alpha(m6)$ -subunit are remarkably splitted, which was time-independent (data not shown). These results suggested that there are two kinds of heme orientations in the isolated $\beta\alpha(m6)$ -subunit (25, 26). That is, the substitution of the sub-module m6 induced substantial decrease in the control of the heme orientation. However, such split of the resonance peaks was little observed for the complex of the $\beta\alpha(m6)$ - and α -subunits, and its spectral feature is quite similar to that of hemoglobin. This result implies that the association of the $\beta\alpha(m6)$ -subunit with the α -subunit recovered specific interactions between the globin and heme and that the heme environmental structure of the $\beta\alpha(m6)$ -subunit in the complex corresponds to that of the β -subunit in hemoglobin tetramer.

¹H NMR Spectra of the Carbonmonoxy Form - The heme environmental structure for the subunits could be analysed by ¹H NMR spectra for the carbonmonoxy form as well as the cyano-met form. A peak from the γ_1 -methyl proton of Val (E11) appeared at -2.0 and -2.2 ppm for the carbonmonoxy α - and β -subunits as shown in Fig. 6, which has served as a marker for the tertiary structure in the heme vicinity (27, 28). The corresponding signal for the $\beta\alpha(m7)$ -subunit was shifted by about 0.5 ppm from that of the β -subunit, implying that the disposition of Val(E11) residue against heme was slightly removed by the m7 substitution (29). Moreover, a shoulder peak can be also found on the right side of the main peak, which indicates that there is a minor conformation in its heme vicinity. Such a shoulder peak of the γ_1 -methyl proton of Val (E11) was more remarkably observed for the carbonmonoxy $\beta\alpha(m6)$ -subunit. Besides, the signals from other heme surrounding residues of the $\beta\alpha(m6)$ -subunit at -0.5 to -1.5 ppm were drastically different from those of the β -subunit. These spectral changes reflect substantial disorder in the heme environmental structure of the $\beta\alpha(m6)$ -subunit. On the other hand, the shoulder peak of the γ_1 -methyl protons disappeared upon its association with the α -subunit, which would correspond to a single conformation of the Val (E11). This result suggests that the association of the $\beta\alpha(m6)$ -subunit with the α -subunit stabilizes its heme environmental structure into a specific conformer.

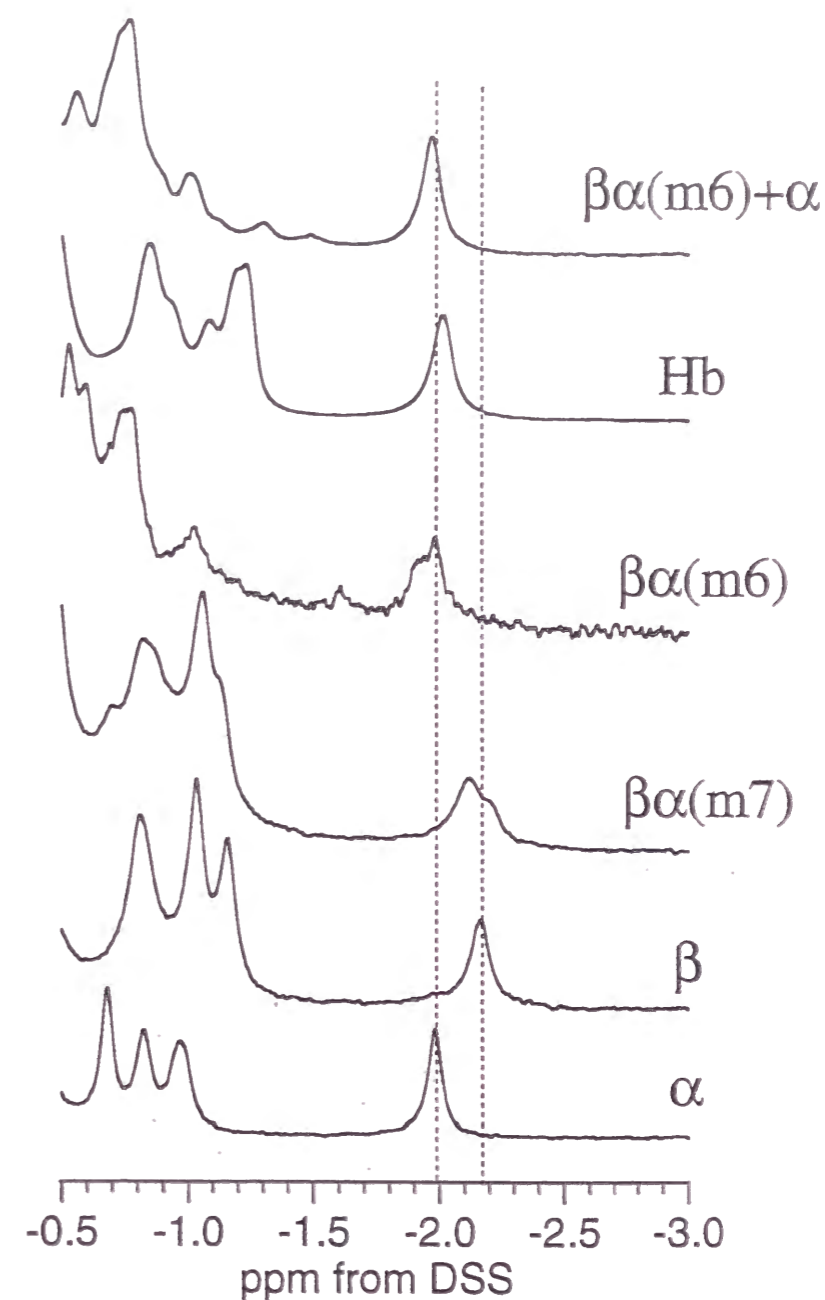


Fig. 6 Proton NMR spectra (500 MHz) for the carbonmonoxy globins Experimental conditions were as follows: 20 mM Na-Phosphate, 0.1 M NaCl, pH 7.4, at 290 K. Sample concentration was 600 μ M on the heme basis. The resonance peak around -2.0 ppm is assigned to γ_1 -methyl protons of Val (E11). The signals for the α -subunit at -0.9, -0.7 and -0.6 ppm are from the δ_2 -methyl of Leu(B10), δ_1 -methyl of Leu(FG3) and δ_1 -methyl protons of Leu(B10) [Schaeffer et al., (1988) *Eur. J. Biochem.* **173**, 317-325]. The signals for the β -subunit at -1.2, -1.0 and -0.8 ppm are from the δ_1 and δ_2 -methyls of Leu(H19) and δ_2 -methyl of Leu(B10) [Craescu and Mispelter (1988) *Eur. J. Biochem.* **176**, 171-178].

¹H NMR Spectra of the Deoxy Form - We have obtained more detailed informations on the heme environmental structure by the measurement of ¹H NMR spectra in the deoxy form. As shown in Fig. 7(I), the α - and β -subunits exhibit a proximal histidyl N_δH proton resonance at 78 and 87 ppm, respectively (30). In native hemoglobin, significant structural transitions are induced by the tetramer formation of the α - and β -subunits, which

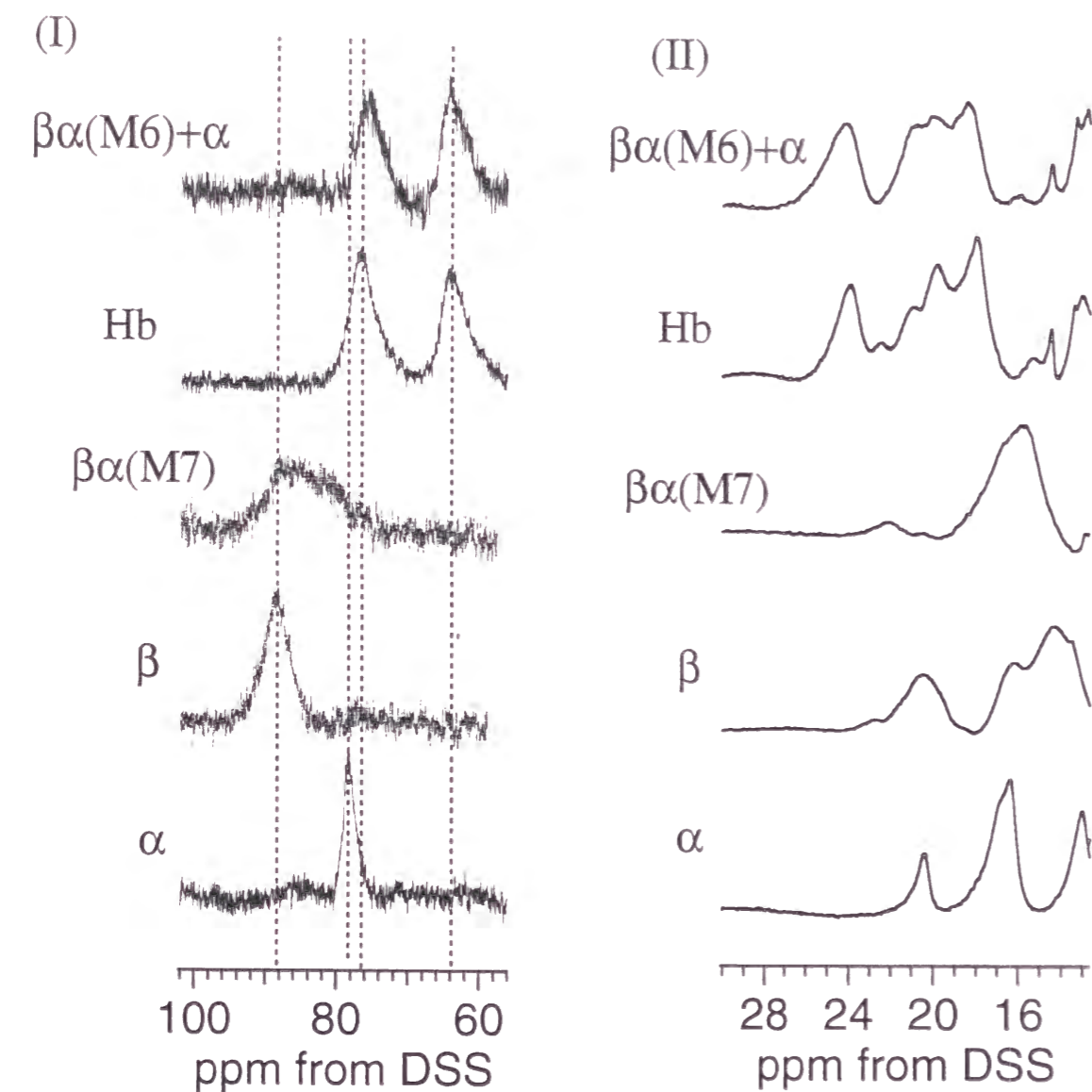


Fig. 7 Proton NMR spectra (500 MHz) for the deoxy globins (I) hyperfine-shifted proton resonances of proximal His N_δH. (II) hyperfine shifted proton resonances of heme methyl groups. Experimental conditions were as follows: 20 mM Na-Phosphate, 0.1 M NaCl, pH 7.4, at 290 K. Sample concentration was 600 μ M on the heme basis.

accompanies a large upfield shift of their proximal histidyl N_δH protons. For the $\beta\alpha$ (m7)-subunit, the main peak is positionally superimposed on that of the β -subunit at 87 ppm, but this peak is asymmetric like as the peak from the γ 1-methyl proton of Val (E11) in the carbonmonoxy form (Fig. 6), which would reflect existence of a minor conformation in its heme vicinity. On the other hand, the NMR spectrum for the deoxygenated $\beta\alpha$ (m6)-subunit could not be measured because of its rapid autoxidation and considerable aggregation. Nevertheless, the complex of the $\beta\alpha$ (m6)- and α -subunits could form a stable deoxy derivative and exhibited the N_δH proton resonances at almost the same positions as hemoglobin. Thus, the coincidence of the N_δH proton resonances in the complex and hemoglobin demonstrates that the heme coordination structure of the proximal His in the complex is very similar to that in hemoglobin.

Fig. 7(II) illustrates the hyperfine-shifted proton signals at 12-30 ppm which come from the protons of the heme (31). The spectral feature of the $\beta\alpha$ (m7)-subunit is quite different from that of the β -subunit, which indicates that the heme electronic state of the β -subunit is substantially affected by the substitution of the sub-module m7. Here, it should be noted that the complex of the $\beta\alpha$ (m6)- and α -subunits showed a quite similar spectral pattern to hemoglobin in the region at 12-30 ppm as well as 55-80 ppm. That is, the implantation of the module m6 from the α -subunit did little affect the heme vicinity of the β -subunit in its complex with the α -subunit.

Resonance Raman Spectra of the Deoxy Form - In order to gain further insights into the heme coordination structure of the proximal histidine, we have also measured the resonance Raman spectra of the globins in the deoxy form. Fig. 8 shows the low-frequency region of the Raman spectra measured with a 1.00 cm^{-1} resolution. As clearly illustrated in Fig. 7, the stretching mode of Fe-His bond (ν (Fe-His)) for both the $\beta\alpha$ (m7)- and β -subunits was observed at 222 cm^{-1} , revealing that the steric bond strength did not alter upon the substitution of the sub-module m7 in the α - and β -subunits. On the other hand, the peak position of the ν (Fe-His) in Hb was shifted by 7 cm^{-1} to the low wavenumber from that in the isolated β -subunit, corresponding to the transition in the heme coordination structure of the proximal histidine upon the association of the α - and β -subunits. As the case for hemoglobin, the stretching mode of Fe-His bond for the complex of the $\beta\alpha$ (m6)- and α -subunits was observed at 215 cm^{-1} , which indicates that the bond strength in the complex is identical to that in hemoglobin.

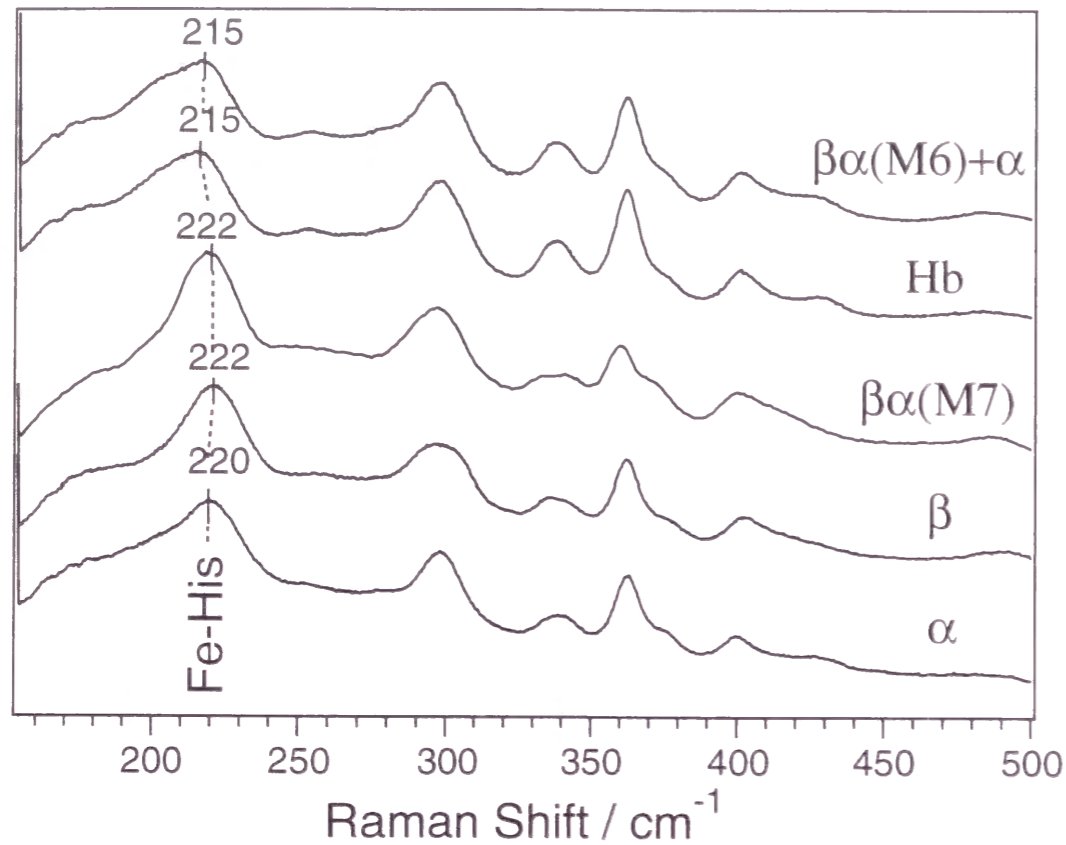


Fig. 8 Resonance Raman spectra for the deoxy globins excited by He/Cd laser (441.6 nm) Experimental conditions were as follows: 50 mM Na-Phosphate, 0.1 M NaCl, pH 7.4, at room temperature. The sample concentration was 50 μ M on the heme basis.

Oxygen Affinity - On the basis of the correlation between function and structure in globin proteins, we are also interested in the oxygen binding properties for the sub-module substituted subunits. Fig. 9 shows the oxygen equilibrium curves expressed by the Hill plot. As listed in Table I, the P_{50} and n_{max} values of the isolated $\beta\alpha(m7)$ -subunit are estimated to be 0.50 mmHg and 1.00, respectively. These values delineate high oxygen affinity and no cooperative oxygen binding for the $\beta\alpha(m7)$ -subunit, which are also encountered for the β -subunit. Therefore, it can be thought that the substitution of the sub-module m7 does not substantially affect oxygen binding property of the β -subunit. For the isolated the $\beta\alpha(m6)$ -subunit, the quantitative analysis has not yet been successful due to its rapid autoxidation and considerable aggregation. Interestingly, the P_{50} and n_{max} values for the complex of the $\beta\alpha(m6)$ - and α -subunits are estimated to be 3.19 mmHg and 1.64, which represents its lower oxygen affinity than the isolated subunits and cooperative oxygen binding, as the case for hemoglobin. That is, the complex did not completely lose the

oxygen binding property of hemoglobin in spite of the implantation of the sub-module m6 from the α -subunit into the β -subunit. This result is consistent with the structural transition in the subunit interface indicated by the NMR spectra in the hydrogen bonded proton region (Fig. 4).

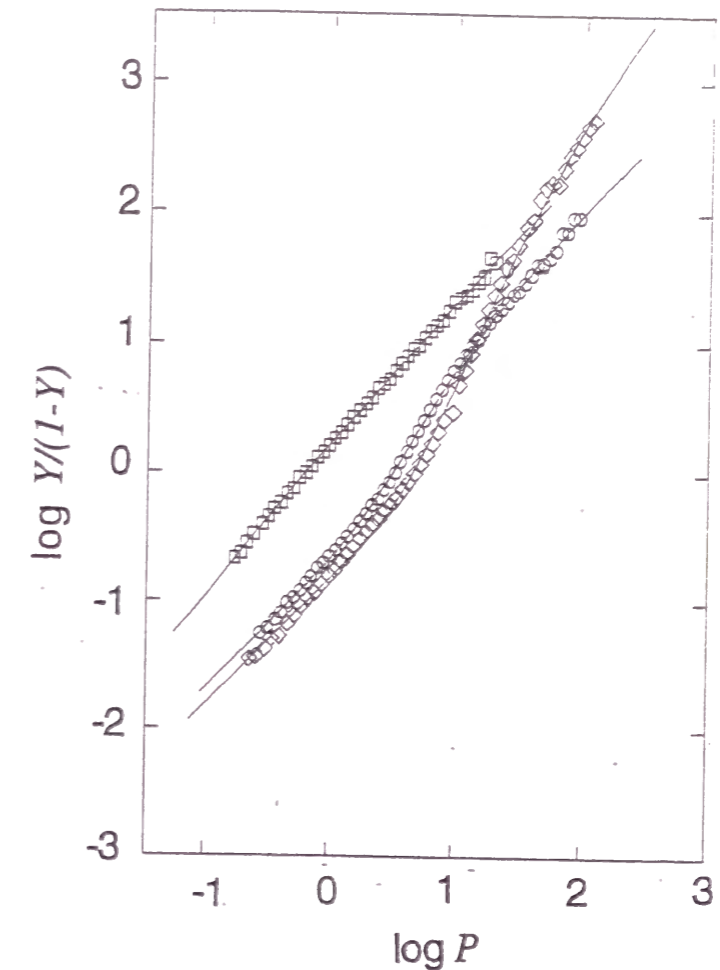


Fig. 9 Oxygen equilibrium curves for hemoglobin (\diamond), isolated $\beta\alpha(m7)$ -subunit (\square) and complex of the α - and $\beta\alpha(m6)$ -subunits (\circ) Experimental conditions were as follows: 50 mM Tris, 0.1 M NaCl, pH 7.4, at 25°C. Sample concentration was 100 μ M on the heme basis.

Table I Oxygen equilibrium parameters for tetrameric Hb, isolated α -, β -, $\beta\alpha(M7)$ -subunits and complex of α - and $\beta\alpha(m7)$ -subunits.

| | P_{50} [mmHg] | n_{max} |
|--------------------------|-----------------|-----------|
| Hb | 3.82 | 2.20 |
| α | 0.53 | 1.00 |
| β | 0.37 | 0.97 |
| $\beta\alpha(m7)$ | 0.50 | 1.00 |
| $\beta\alpha(m6)+\alpha$ | 3.19 | 1.64 |

DISCUSSION

Association Property of the $\beta\alpha(m7)$ - and $\beta\alpha(m6)$ -subunits - As revealed by gel chromatogram and ^1H NMR spectra in hydrogen bonded proton region (Figs. 3 and 4), the $\beta\alpha(m7)$ -subunit formed a homo-tetramer structure and did not bind to the α - nor β -subunits. This result means that the association property of the β -subunit was lost upon the implantation of the sub-module m7 from the α -subunit into the β -subunit, but it was not converted into the α -subunit type in contrast to the case of the substitution of the conventional module M4 or pseudo-module PM3. On the basis of such incomplete conversion of the association property by the m7 substitution, the sub-module m7 is not a unique functional unit regulating the association property of hemoglobin subunits. As shown in Fig. 1, in fact, the sub-modules m6 and m7 besides m7 contains amino acid residues contributing to the $\alpha 1$ - $\beta 1$ and $\alpha 1$ - $\beta 2$ contacts, which would be also crucial for the regulation of the association property.

However, it should be noted here that the $\beta\alpha(m6)$ -subunit could associate with the α -subunit and form a hetero-tetramer $[\beta\alpha(m6)]_2\alpha_2$, although its dissociation constant to the hetero-dimer $[\beta\alpha(m6)]\alpha$ was substantially increased. Considering that the sub-module m7 in the $\beta\alpha(m6)$ -subunit is derived from the β -subunit unlike the $\beta\alpha(m7)$ -subunit, the β -subunit like association property for the $\beta\alpha(m6)$ -subunit strongly suggests functional significance of the sub-module m7 in subunit assembly. Therefore, the different association properties between the $\beta\alpha(m6)$ - and $\beta\alpha(m7)$ -subunits can be interpreted to support the functional roles of the sub-module m7 on subunit assembly in hemoglobin. Eventually, it can be safely said that the sub-module m7 is one of essential factors to determine association property of globin subunits.

Heme Environmental Structure of the $\beta\alpha(m6)$ - and $\beta\alpha(m7)$ -subunits - We are concerned about the heme environmental structure as well as the association property for the chimeric subunits. In the ^1H NMR spectra of the cyanide form (Fig. 5), the resonance peaks of the heme methyl protons for the isolated $\beta\alpha(m6)$ -subunit are time-independently splitted, which suggests two heme orientations in the chimeric subunit (25, 26, 32). Such two heme orientations imply that interactions between the globin and heme cannot control the heme orientation and the heme environmental structure of the $\beta\alpha(m6)$ -subunit is disordered. Thus, the substitution of the sub-module m6 causes drastic perturbations on the heme vicinity. On the other hand, the splitted resonance peaks of the heme methyl groups were remarkably decreased in the complex of the $\beta\alpha(m6)$ - and α -subunits, and its spectral

feature was very similar to that of hemoglobin. This result indicates that the association of the $\beta\alpha(m6)$ -subunit with the α -subunit surely recovers the specific interactions between the globin and heme, which would be equivalent to formation of the stable heme environmental structure in the $\beta\alpha(m6)$ -subunit. Of interest is here that the NMR and resonance Raman spectral features of the complex in the deoxy state almost coincided with those of hemoglobin (Figs. 7 and 8). Since the hyperfine shift of the proximal histidyl N_δH proton and the Fe-His vibrational mode depend on strength of an interaction between heme iron and proximal histidine (33), such coincidence of the spectral features indicate that the heme coordination structure of the complex is quite similar to that of hemoglobin. That is, the heme coordination structure of the $\beta\alpha(m6)$ -subunit in the complex with the α -subunit correspond to that of the β -subunit in hemoglobin. Therefore, the implantation of the sub-module m6 from the α -subunit did not convert the heme proximal structure of the β -subunit into the α -subunit one in the complex. Eventually, we could not confirm that the sub-module m6 is a structural unit independently regulating the heme proximal structure.

Here, it should be also noted that the $\beta\alpha(m7)$ -subunit, containing the sub-module m6 derived from the β -subunit, showed similar spectroscopic characters to the β -subunit. As found in the NMR spectra for the cyano-met form (Fig. 5), signal positions from the heme substituents for the $\beta\alpha(m7)$ -subunit are similar to those for the β -subunit. The resonance Raman peak from the $\nu(\text{Fe-His})$ in the $\beta\alpha(m7)$ -subunit is also identical to that in the β -subunit. Moreover, the $\beta\alpha(m7)$ -subunit exhibited the NMR signals of the $\gamma 1$ -methyl proton of Val(E11) in the carbonmonoxy form and the proximal histidyl N_δH proton in the deoxy form at the positions close to the β -subunit, although existence of minor conformations were observed. These results indicate that the $\beta\alpha(m7)$ -subunit rather conserves the β -subunit like heme environmental structure. Since the $\beta\alpha(m7)$ -subunit contains the sub-module m6 derived from the β -subunit, such conservation of the heme environmental structure reflect structural significance of the sub-module m6.

Thus, it is interesting that structural regulation by the sub-module m6 is not recognized for the the $\beta\alpha(m6)$ -subunit in the complex with the α -subunit, but for the $\beta\alpha(m7)$ -subunit. One of the possible reasons would be their different associated states. The $\beta\alpha(m7)$ -subunit forms a homo-tetramer, $[\beta\alpha(m7)]_4$, whereas the $\beta\alpha(m6)$ -subunit is in a hetero-tetramer, $[\beta\alpha(m6)]_2\alpha_2$. As revealed in the NMR spectra for the carbonmonoxy and deoxy forms (Figs. 6 and 7), the heme environmental structure of the isolated β -subunit is surely

different from that of the β -subunit binding to the α -subunit, which strongly supports that the subunit assembly substantially affect the heme vicinity. Therefore it is likely that the interactions between the $\beta\alpha(m6)$ - and α -subunits might stabilize the heme proximal structure of the $\beta\alpha(m6)$ -subunit into the β -subunit one so that the complex of the $\beta\alpha(m6)$ - and α -subunits formed a quaternary structure identical to hemoglobin. In other words, global interactions such as subunit contacts would be crucial for the regulation of the heme proximal structure in hemoglobin, although the functional roles of the sub-module m6 is not negligible.

Oxygen Affinity of the $\beta\alpha(m6)$ - and $\beta\alpha(m7)$ -subunits - As shown by the oxygen equilibrium curves (Fig. 9), it is quite interesting that slight but significant allosteric cooperativity was observed for the complex of the $\beta\alpha(m6)$ - and α -subunits. Since the sub-module m6 includes many residues requisite for functional $\alpha1$ - $\beta2$ interface structure in the FG3-G4 region (Fig. 1), the m6 substitution would lead to much perturbation on the interface. However, most of the residues in this region, Leu(FG3), Val(FG5), Asp(G1), Pro(G2) and Asn(G4), are common in the α - and β -subunits, which might enable structural transition of the complex upon deoxygenation. Such structural transition of the complex is strongly supported by its NMR spectra in the deoxy form (Figs. 4 and 7), where the exchangeable proton peaks at 11 and 14 ppm from the hydrogen bonds in the $\alpha1$ - $\beta2$ interface were observed for the complex (Fig. 4) and the proximal histidyl $N\delta H$ protons of the complex exhibited the remarkable upfield shift from those of the isolated subunits as the case for hemoglobin (Fig. 7). On the other hand, the $\beta\alpha(m7)$ -subunit demonstrated high oxygen affinity and no cooperative oxygen binding just as did the isolated hemoglobin subunits, implying that the substitution of the sub-module m7 did not substantially affect oxygen binding property of the β -subunit. Since the NMR spectra revealed that the $\beta\alpha(m7)$ -subunit did not experience the structural transition upon the deoxygenation found in hemoglobin (Figs. 4 and 7), its no cooperativity would be reasonable.

Summary - As discussed above, the present finding that the $\beta\alpha(m6)$ -subunit could associate with the α -subunit in sharp contrast to the $\beta\alpha(m7)$ -subunit reflect functional roles of the sub-module m7 on regulation of the association property in hemoglobin. However, the incomplete conversion of the association property for the $\beta\alpha(m7)$ -subunit strongly suggests that only the module m7 is not dominant in this regulation. On the other hand, the heme proximal structure of the $\beta\alpha(m6)$ -subunit in the complex with α -subunit is almost identical to that of the β -subunit in hemoglobin despite of the m6 substitution, whereas the isolated $\beta\alpha(m7)$ -subunit exhibited structural

characters rather close to the β -subunit. This indicates that the subunit interactions as well as the sub-module m6 play crucial roles in regulation of heme environmental structure. Thus, the present study for the substitution of the sub-modules m6 and m7 provides many insights not only into their structural and functional significance but also into regulation mechanism of structure and function in hemoglobin.

Acknowledgment

We are very grateful to Dr. Kiyohiro Imai (Osaka University) for measurements of oxygen equilibrium curves. Furthermore, we are indebted to Dr. Satoshi Takahashi and Dr. Teizo Kitagawa for resonance Raman spectral measurement.

Reference

1. Go, M. (1981) *Nature*, **291**, 90-92
2. Eaton, W. A. (1980) *Nature* **284**, 183-185
3. Wakasugi, K., Ishimori, K., Imai, K., Wada, Y. and Morishima, I. (1994) *J. Biol. Chem.* **269**, 18750-18756
4. Inaba, K., Ishimori, K., Imai, K. and Morishima, I. submitted for publication (J. Biol. Chem.)
5. Noguti, T., Sakakibara, H. and Go, M. (1993) *Proteins* **16**, 357-363
6. Go, M. et al. submitted for publication (Nature)
7. Nagai, K and Thøgerson, H. C. (1984) *Nature* **309**, 810-812
8. Nagai, K., Perutz, M. F., and Poyart, C. (1985) *Proc. Natl. Acad. Sci. U.S.A.* **82**, 7252-7257
9. Nagai, K., and Thøgerson, H.C. (1987) *Methods Enzymol.* **153**, 461-481
10. Valdes, R., Jr. and Ackers, G. K. (1977) *J. Biol. Chem.* **252**, 74-81
11. Ishimori, K., Hashimoto, M., Imai, K., Fushitani, K., Miyazaki, G., Morimoto, H., Wada, Y. and Morishima, I. (1994) *Biochemistry* **33**, 2546-2553
12. Imai, K. (1981) *Methods. Enzymol.* **76**, 438-449
13. Imai, K. (1982) *Allosteric Effect in Haemoglobin*, Cambridge University Press, London
14. Imai, K., Morimoto, H., Kotani, M., Watari, H., Hitata, W. and Kuroda, M. (1970) *Biochem. Biophys. Acta* **200**, 189-196
15. Hayashi, A., Suzuki, T. and Shin, M. (1973) *Biochem. Biophys. Acta* **310**, 309-316
16. Lynch, R. E., Lee, G. R. and Cartwright, G. E. (1976) *J. Biol. Chem.* **251**, 1015-1019
17. Winterbourn, C. C., McGrath, B. M. and Carrell, R. W. (1976) *Biochem. J.* **155**, 493-502
18. Imai, K. (1994) *Methods. Enzymol.* **232**, 559-576
19. Fung, L. W. M. and Ho, C. (1975) *Biochemistry* **14**, 2526-2535
20. Russu, I. M., Ho, N. T. and Ho, C. (1987) *Biochem. Biophys. Acta* **914**, 40-48
21. Asakura, T., Adachi, K., Wiley, J. S., Fung, L. W. -M., Ho, C., Kilmartin, J. V. and Perutz, M. F. (1976) *J. Mol. Biol.* **104**, 185-195
22. Ishimori, K., Imai, K., Miyazaki, G., Kitagawa, T., Wada, Y., Morimoto, H. and Morishima, I. (1992) *Biochemistry* **31**, 3256-3262
23. La Mar (1979) in *Biological Applications of Magnetic Resonances* (Shulman, R. G. Ed.) Academic press, New York, 305-342

24. La Mar, G. N., Jue, T., Nagai, K., Smith, K. M., Yamamoto, Y., Kauten, R. J., Thanabal, V., Langry, K. C., Pandey, R. K. and Leung, H-K. (1988) *Biochim. Biophys. Acta.*, **952**, 131-141
25. Ishimori, K. and Morishima, I. (1988) *Biochemistry* **27**, 4747-4753
26. Yamamoto, Y. and La Mar, G. N. (1986) *Biochemistry* **25**, 5288-5297
27. Lindstrom, T. R., Nore, I. B. E., Charashe, S., Lehmann, H., and Ho, C. (1972) *Biochemistry* **11**, 1677-1681
28. Dalvit, C. and Ho, C. (1985) *Biochemistry* **24**, 3398-3407
29. Shulman, R. G., Wuthrich, K., Yamane, T., Patel, D. and Blumnborg, W. E. (1970) *J. Mol. Biol.* **53**, 143
30. Nagai, K., La Mar, G. N., Jue, T. and Bunn, H. F., (1982) *Biochemistry* **21**, 842-847
31. Ho, C. (1992) *Advan. Protein Chem.* **43**, 153-312
32. La Mar, G. N., Yamamoto, Y., Jue, T., Smith, K. M. and Pandey, R. K. (1985) *Biochemistry* **24**, 3826-3831
33. Nagai, K. and Kitagawa, T. (1980) *Proc. Natl. Acad. Sci.. U.S.A.* **77**, 2033-2037

FOOTNOTE

¹The pseudo-modules are defined as a segment starting at a center of one module and ending at the center of the following one and do not form a compact structural unit in sharp contrast to the modules as predicted from their correspondence to the region from a peak to the adjacent one in the centripetal profile [Noguti et al., (1993) *Proteins* **16**, 357-363]. Moreover, since the pseudo-modules do not statistically coincide with exons, they would not have evolutionary or functional meanings unlike the modules (Go et al., submitted for publication).

PART V

SUMMARY AND GENERAL CONCLUSIONS

In the present thesis, the author aimed to clarify structural and functional significance of the modules by preparing and characterizing a variety of chimeric globins, in which the modules, pseudo-modules or sub-modules were substituted. To achieve this aim, the author has examined effects of these substitutions on globin structure and function by various spectroscopies. The results of the studies are summarized below.

Chapters in Part II are devoted to reveal structural and functional alterations induced by the module substitutions in hemoglobin subunits. In Chapter I, focusing upon the functional significance of the module M4 on the subunit assembly, the author has designed the chimeric $\alpha\beta(\text{M4})$ - and $\beta\alpha(\text{M4})$ -subunits, in which the module M4 was replaced by that of the partner subunit. The association property for the $\beta\alpha(\text{M4})$ -subunit was converted into that of the α -subunit, while the $\alpha\beta(\text{M4})$ -subunit still exhibited the α -subunit type association property. Based on various spectroscopic data and computer modeling, the globin structure of the $\alpha\beta(\text{M4})$ -subunit would substantially collapse, due to the intramolecular steric constraint between ^{14}Trp and ^{125}Tyr , which would lead to the failure in the functional conversion for the $\alpha\beta(\text{M4})$ -subunit. The different structural and functional effects of the module substitution between the $\alpha\beta(\text{M4})$ - and $\beta\alpha(\text{M4})$ -subunits suggest that intramodular interactions in the subunit are crucial to construct stable globin proteins, even if the modules correspond to structural and functional units.

In order to investigate structural alterations induced by the module substitution in more detail, the author have tried to solve the x-ray crystal structure of the $\beta\alpha(\text{M4})$ -subunit in chapter 2. Unfortunately, however, the crystallization of the chimeric subunit has not yet been successful probably due to the unstable helix packing. To avoid the unstable packing, the author substituted ^{133}Phe for Val, which enables us to obtain the crystals for the x-ray diffraction study. The structural analysis of the mutated $\beta\alpha(\text{M4})$ -subunit has revealed that the back-bone structure of the $\beta\alpha(\text{M4})$ -subunit was almost superimposed on that of the β -subunit. However, it should be noted that the local structure of the module M4 in the $\beta\alpha(\text{M4})$ -subunit was close to that of the α -subunit rather than that of the β -subunit, which strongly suggests that the module M4 is a quasi-independent structural unit in globin structure.

In the Chapters in Part III, to gain further insights into structural and functional significance of the modules, the author has examined effects of "non-module" substitution on globin structure and function. In these chapters, the author has focused upon the "pseudo-module", of which boundaries are located at the center of the module and supposed not to retain a compactness, which is in sharp contrast to modules. In Chapter 3, the

pseudo-module PM3 from the α -subunit was implanted into the β -subunit, and the structure and function of the pseudo-module PM3 substituted globin were compared with those of the $\beta\alpha$ (M4)-subunit. As found for the $\beta\alpha$ (M4)-subunit, the $\beta\alpha$ (PM3)-subunit conserved stable globin structure, and its association property was converted into that of the α -subunit. The heme proximal structure of the $\beta\alpha$ (PM3)-subunit were also changed to α -subunit like. Such structural and functional conversions by the substitution of the pseudo-module PM3 allow us to speculate that modules are not unique structural and functional units in globins. That is, the pseudo-module PM3 would have some structural and functional significance just as do the modules. In fact, it should be noted that the recent reconsideration of the module boundary indicates that the modules in globins can be further divided into two small modules ("sub-modules") and one of the boundaries for the new "sub-modules" would coincide with that of the pseudo-module we substituted in this study. Together with the present experimental results and the theoretical reconsideration of the modular structure of globins, it can be concluded that the author might identify new structural units in globin proteins, probably new modules.

To further examine the structural and functional significance of the pseudo-module PM3, the author has also implanted the pseudo-module PM3 from the α -subunit into myoglobin as well as the β -subunit, and compared the structure and function of the PM3 substituted myoglobin, Mb α (PM3), with those of the module M4 substituted myoglobin, Mb α (M4) in Chapter 4. NMR spectroscopy and gel chromatogram revealed that the heme proximal structure and the association property of the Mb α (PM3) were not converted into the α -subunit type as expected from the results of the Mb α (M4)-subunit. However, CD and tryptophan fluorescence spectra clearly indicated that the Mb α (PM3) almost retained native globin structure, whereas that of the Mb α (M4) was drastically perturbed. The structural perturbations induced by the PM3 substitution was much more moderate compared to those by the M4 substitution, concluding that the pseudo-module PM3 has some structural significance and would correspond to new structural units, sub-modules.

In the Chapters in Part IV, therefore, the structural and functional roles of the sub-modules in globin proteins were discussed. One of the sub-modules the author has paid attention to was the "heme binding module", which includes most of the residues constructing the heme proximal site crucial for functions of hemoproteins and corresponds to the N-terminal half of the pseudo-module PM3. To examine functional roles of the heme binding module in the regulation of the heme coordination structure and heme electronic state,

we have prepared Mb α (HBM) in Chapter 5, where the heme binding module of myoglobin was replaced by that of the α -subunit. Various spectroscopic results revealed that the heme electronic state and heme coordination structure of the Mb α (HBM) deviated from those of myoglobin and were rather close to those of the α -subunit. On the other hand, structural alterations in the heme distal site were subtle compared to the proximal site, indicating that the substitution of the heme binding module preferentially converted the heme proximal structure of myoglobin into the α -subunit type. Such structural conversion in the Mb α (HBM) experimentally confirmed that the heme binding module is a structural segment regulating the heme proximal structure in globin proteins.

In Chapter 6, the functional roles of the C-terminal half of the pseudo-module PM3 (sub-module m7) as well as the N-terminal one (sub-module m6 or heme binding module) are examined. Since the implantation of the pseudo-module PM3 from the α -subunit also converted the association property of the β -subunit into that of the α -subunit as found for the implantation of the module M4, the common region of the M4 and PM3, the sub-module m7, can be considered a functional unit responsible for the association property of the hemoglobin subunits. Herewith, to discuss the structural and functional significance of these sub-modules, we have prepared novel chimeric globins, $\beta\alpha$ (m6)-subunit and $\beta\alpha$ (m7)-subunits, in which each of the sub-modules m6 and m7 in hemoglobin β -subunit is replaced by the corresponding sub-modules of the α -subunit. Gel chromatogram showed that the $\beta\alpha$ (m7)-subunit did not bind to the α - nor β -subunits, whereas the $\beta\alpha$ (m6)-subunit preferentially bound to the α -subunit. That is, the $\beta\alpha$ (m6)-subunit conserves the the association property of the β -subunit type in contrast to the $\beta\alpha$ (m7)-subunit. Taking into account that the $\beta\alpha$ (m6)-subunit reserves the segment of the sub-module m7 derived from the β -subunit unlike $\beta\alpha$ (m7)-subunit, their different association properties strongly suggest that the sub-module m7 is one of the determinants to regulate association property of hemoglobin subunits. Consequently, this work for the $\beta\alpha$ (m6)- and $\beta\alpha$ (m7)-subunits strengthens the argument of the functional roles of the sub-module m7 in subunit assembly.

In conclusion, the author has extensively studied structural and functional effects caused by the module, pseudo-module and sub-module substitutions in globins. With recourse to these works, the author has discovered new structural and functional units regulating heme proximal structure and subunit assembly in globin proteins. It can be concluded that some of the globin structure and function are regulated by the specific modules or sub-modules, although intramolecular interactions between the modules

are essential for constructing the stable globin structure. On the basis of the structural and functional advantages of the modules revealed in this thesis and the statistical correspondence of the modules to exons on the gene, the module substitution would be one of the potent mechanism to create new multi-functional proteins in the process of the molecular evolution. Also, there would not be a little possibility that artificial proteins bearing required functions are designed by combinations of the proper modules. Thus, the author believe that the present findings and proposals are sure to contribute to development of the scientific areas including the protein design, molecular evolution of proteins and related protein chemistry.